Dissecting Repulsive Guidance Molecule/ Neogenin function and signaling during neural development

DIANNE M.A. VAN DEN HEUVEL

COLOFON

The research described in this thesis was performed at the Department of Neuroscience and Pharmacology, Rudolf Magnus Institute of Neuroscience, University Medical Center Utrecht, The Netherlands.

Author:	Dianne M.A. van den Heuvel
Layout and cover design:	Netty van Haarlem (netaanzet.net)
Painting used on cover:	Gabriëlle van de Laak
Printing:	Cyron (Cyron.nl)
ISBN:	978-90-393-5919-8

Dissecting Repulsive Guidance Molecule/ Neogenin function and signaling during neural development

Analyse van de functie en signaaltransductie van Repulsive Guidance Molecule/Neogenin tijdens de neuronale ontwikkeling

(met een samenvatting in het Nederlands)

PROEFSCHRIFT

ter verkrijging van de graad van doctor aan de Universiteit Utrecht

op gezag van de rector magnificus, prof.dr. G.J. van der Zwaan, ingevolge

het besluit van het college voor promoties in het openbaar te verdedigen op

donderdag 28 februari 2013

des middags te 2:30 uur

door

Dirgje Maria Adriana van den Heuvel

geboren op 10 september 1983 te Tiel

Promotor: Prof.dr. J.P.H. Burbach

Co-promotor: Dr. R.J. Pasterkamp

Voor mijn ouders

CONTENTS

CHAPTER 1
General introduction

OUTLINE GENERAL INTRODUCTION

Preface

1 The Neogenin receptor and its ligands
1.1 Neogenin
1.2 Repulsive guidance molecules
1.3 Netrins

2 Neogenin functions in the developing nervous system
2.1 Neurogenesis
2.2 Differentiation
2.3 Migration
2.4 Apoptosis
2.5 Axon guidance
2.5.1 The retinotectal system
2.5.2 The supraoptic tract
2.5.3 The entorhinal-hippocampal system

3 Neogenin functions in injury and disease
3.1 Axon regeneration
3.2 Neurological disease
3.2.1 Multiple sclerosis
3.2.2 Alzheimer, Parkinson's disease and epilepsy

4 Neogenin signaling
4.1 Neogenin signaling in repulsive axon guidance
4.1.1 RhoA and Ras GTPase signaling
4.1.2 Neogenin ectodomain shedding
4.2 Transcription regulation
4.3 Apoptosis signaling

5 Aim and outline of this thesis

PREFACE

The development of the mammalian brain into a complex structure comprising millions of neurons and even more neuronal connections is orchestrated by cell signaling mechanisms that control diverse neurodevelopmental processes. Perturbations of these signaling mechanisms can lead to the onset of neurodevelopmental disorders like autism and schizophrenia. Although the transmembrane receptor Neogenin and its repulsive guidance molecule (RGM) ligands have been implicated in diverse neurodevelopmental processes, including neurogenesis, neuronal cell differentiation, migration and apoptosis, their role in neurite outgrowth regulation and axon guidance is best characterized. Activation of Neogenin signaling by RGMs induces growth cone collapse, neurite outgrowth inhibition and axon repulsion. From a clinical perspective RGMs and Neogenin have been implicated in axon regeneration, multiple sclerosis, Alzheimer and Parkinson's disease. Our understanding of the role of RGM-Neogenin signaling in developing brain structures is rather limited and only few components of the Neogenin signaling cascade have been identified so far. This thesis explores the role and signaling mechanisms of Neogenin during neural development by 1) an expression analysis of Neogenin, RGMs and coreceptors of the uncoordinated locomotion-5 (Unc5) family in the developing mouse brain, and 2) *in vitro* and *in vivo* proteomics studies to identify novel Neogenin signaling proteins. The following sections briefly summarize our current knowledge of the molecular properties of Neogenin and its ligands, the function of RGMs and Neogenin during neural development and in disease, and neuronal RGM-Neogenin signaling mechanisms.

1 THE NEOGENIN RECEPTOR AND ITS LIGANDS

1.1 NEOGENIN

Neogenin was originally isolated from embryonic chick brain as a close homologue of the tumor suppressor and axon guidance receptor deleted in colorectal cancer (DCC) (Fearon *et al.* 1990, Keino-Masu *et al.* 1996, Vielmetter *et al.* 1994). Its amino acid sequence and deduced secondary structure characterize Neogenin as a member of the immunoglobulin (Ig) superfamily of cell surface receptors that also includes Down syndrome cell adhesion molecule (DSCAM) and L1 (Moos *et al.* 1988, Vielmetter *et al.* 1994, Yamakawa *et al.* 1998). The extracellular domain of Neogenin contains four immunoglobulin-like (Ig-like) domains followed by six fibronectin type III (FNIII) domains (Figure 1A) (Vielmetter *et al.* 1994). In the Neogenin intracellular domain three regions are recognized (P1-3) that are highly conserved between Neogenin and DCC (De Vries and Cooper 2008, Phan *et al.* 2011, Vielmetter *et al.* 1994).

Neogenin is widely expressed in both neural and non-neural tissues during embryonic development and at postnatal and adult stages in different species (Fitzgerald *et al.* 2006, Gad *et*

al. 1997, Gessert *et al*. 2008, Keeling *et al*. 1997, Mawdsley *et al*. 2004, Wilson and Key 2006). In the mouse brain prominent Neogenin expression has been reported in the olfactory bulb, cortex, hippocampus and cerebellum (Gad *et al*. 1997, Keeling *et al*. 1997). The Neogenin coding region contains four alternatively spliced regions (Keeling *et al*. 1997). Expression analysis studies reveal differential expression of the Neogenin splice variants during development (Keeling *et al*. 1997, Shen *et al*. 2002, Vielmetter *et al*. 1994). Although broad Neogenin expression has been observed in the developing and adult brain, a detailed analysis of Neogenin expression in different brain structures has not been reported. Furthermore, Neogenin expression has predominantly been studied at the RNA level, using *in situ* hybridization, while data on Neogenin protein expression is rather scarce. Neogenin interacts with two families of ligands: the RGMs and Netrins, which both interact with the Neogenin FNIII domains (Geisbrecht *et al*. 2003, Rajagopalan *et al*. 2004, Yang *et al*. 2008). Ligand binding studies indicate that the binding affinity of Netrin-1 to Neogenin is about 10 times lower compared to binding of RGMs to Neogenin (Yamashita *et al*. 2007). The following sections discuss the RGM and Netrin ligand families in more detail.

1.2 REPULSIVE GUIDANCE MOLECULES

The growth cone collapse-inducing activity of RGMs was originally identified in the chick visual system, where RGM expression in the tectum repels Neogenin-expressing temporal retinal axons (Monnier *et al*. 2002, Rajagopalan *et al*. 2004). There are three vertebrate homologs of chick RGM: RGMa, RGMb (Dragon) and RGMc (Hemojuvelin (HJV)) (Schmidtmer and Engelkamp 2004). The RGM homologs arose early in vertebrate evolution through gene duplication and share 40-50% similarity in amino acid sequence (Camus and Lambert 2007, Schmidtmer and Engelkamp 2004, Severyn *et al*. 2009). RGMs are cysteine-rich proteins that contain an Arg-Gly-Asp (RGD) tri-amino acid motif, a partial von Willebrand factor type D (vWF) domain, two hydrophobic domains at the N- and C-termini and a glycosylphosphatidylinositol (GPI)-anchor domain at the C-terminus, which links RGMs to the cell membrane (Figure 1A) (Monnier *et al*. 2002). Autocatalytic cleavage of RGMs generates two separate N- and C-terminal fragments that are kept together by a disulfide bridge (Niederkofler *et al*. 2004, Zhang *et al*. 2005). Further proteolytic processing by the proprotein convertases furin and subtilisin/kexin-like isozyme-1 (SKI-1) has been revealed for RGMa, which generates four C-terminal membrane-bound and three N-terminal soluble forms of RGMa (Tassew *et al*. 2012) (Figure 1B). All cleaved RGMa protein products inhibit neurite growth via Neogenin, through interaction with the Neogenin fibronectin type III domains (Tassew *et al*. 2012).

RGMa and RGMb are predominantly expressed in the central nervous system (CNS). RGMc expression is limited to skeletal muscle, the heart and liver and has a critical role in iron homeostasis (Kuninger *et al*. 2004, Niederkofler *et al*. 2004, Oldekamp *et al*. 2004, Schmidtmer and Engelkamp 2004, Zhang *et al*. 2005). Expression of RGMa and RGMb mRNA has been detected in many different brain areas at embryonic and postnatal stages (Oldekamp *et al*.

2004, Schmidtmer and Engelkamp 2004). However, the analysis of RGM expression in different brain areas is not very detailed and information on RGM protein expression is mostly absent. In the developing nervous system, RGM-Neogenin function has been related to axon guidance, neuron migration, differentiation and survival (Key and Lah 2012). However, how precisely RGMs contribute to the development of specific brain areas is largely unknown.

Apart from being ligands for Neogenin, RGMs also function as coreceptors in bone morphogenetic protein (BMP) signaling (Corradini *et al*. 2009). RGM molecules bind BMP-2 and BMP-4 ligands and associate with type I and type II BMP receptors *in cis*, thereby enhancing BMP signaling (Babitt *et al*. 2005, Babitt *et al*. 2006, Samad *et al*. 2005) (Figure 1C). In BMP signaling regulating iron homeostasis, BMP ligands form a signaling complex with HVJ/RGMc, BMP receptors and Neogenin to induce hepcidin expression (Kuns-Hashimoto *et al*. 2008, Xia *et al*. 2008, Zhang *et al*. 2009). Furthermore, in endochondral bone development, cis interaction of Neogenin with the RGM-BMP receptor complex is required for the localization of this signaling complex to lipid rafts and activation of Smad signaling (Zhou *et al*. 2010). RGM-mediated BMP signaling has not been implicated in neuronal functions yet.

1.3 NETRINS

Netrins are laminin-like molecules that function as guidance cues for migrating cells and axons during neural development (Lai Wing *et al*. 2011, Yurchenco and Wadsworth 2004). In vertebrates, secreted Netrin-1, -2, -3 and -4, and GPI-linked Netrin-Gs have been identified, which contain a laminin-like globular VI domain, three epidermal growth factor (EGF) repeats (domain V), and a C-terminal domain (Figure 1A) (Nakashiba *et al*. 2000, Serafini *et al*. 1994, Wang *et al*. 1999, Yin *et al*. 2000). Netrin-1-4 bind the Ig superfamily receptors DCC (Keino-Masu *et al*. 1996), Unc5A-D (Leonardo *et al*. 1997), Neogenin (Keino-Masu *et al*. 1996, Wang *et al*. 1999) and DSCAM (Ly *et al*. 2008).

Netrins are bifunctional and can either attract or repel growing axons depending on the Netrin receptors present. Axon attraction is mediated by DCC and DSCAM (Keino-Masu *et al*. 1996, Ly *et al*. 2008), while axon repulsion requires signaling through Unc5 homodimers, or Unc5/DCC or Unc5/DSCAM heterodimers (Hong *et al*. 1999, Purohit *et al*. 2012). *In vivo* studies in *Drosophila* support the model that Unc5 homodimers mediate short-range repulsion in response to Netrins, while Unc5 heterodimers might facilitate long-range responses by increasing the sensitivity to relatively low Netrin concentrations (Keleman and Dickson 2001). *In vivo* loss-of-function studies in mice revealed that the major Netrin-1 guidance receptor in the embryonic mammalian brain is DCC. The phenotype of DCC null embryos closely resembles the abnormalities seen in Netrin-1-deficient embryos. Both mutants exhibit severe defects in commissural axon extension towards the floor plate of the embryonic spinal cord and lack several major commissures within the forebrain (Fazeli *et al*. 1997, Serafini *et al*. 1996). So far, a role for Netrin-1-mediated Neogenin signaling in axon guidance has only been revealed in

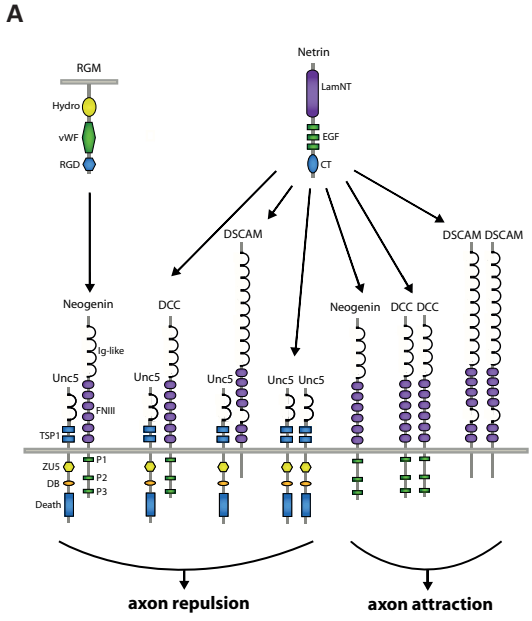

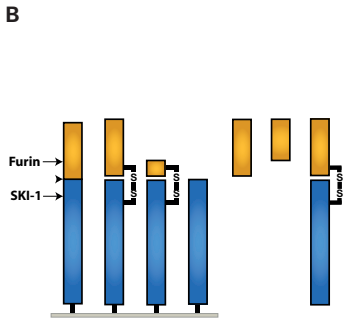

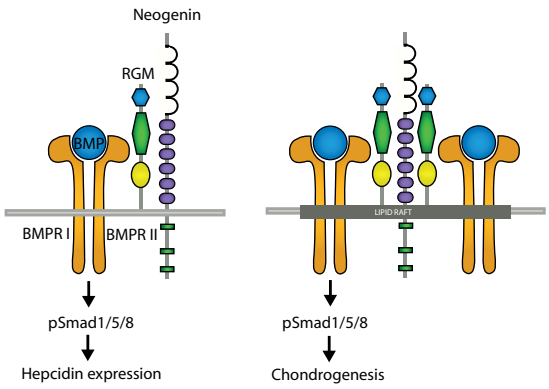

FIGURE 1. Repulsive guidance molecule (RGM) and Netrin receptor signaling in axon guidance. (A) Binding of RGM to Unc5/Neogenin and Netrin to Unc5/DCC or Unc5/Down syndrome cell adhesion molecule (DSCAM) heterodimers or Unc5 homodimers mediates axon repulsion. In contrast, binding of Netrin to Neogenin, DCC or DSCAM mediates axon attraction. Axon attractive Netrin-Neogenin signaling has only been revealed in *Xenopus*. (B) Autocatalytic (arrowhead) cleavage and proteolytic cleavage (black arrows) of RGMa by furin and subtilisin/kexin-like isozyme-1 (SKI-1) generates four C-terminal membrane-bound and three N-terminal soluble forms of RGMa. All cleaved RGMa isoforms inhibit neurite outgrowth through binding and activation of the Neogenin receptor. (C, D) RGM and Neogenin are essential components of the bone morphogenetic protein (BMP)/BMP receptor signaling complex regulating iron homeostasis (C) and bone development (D). CT, C-terminus; DB, DCC-binding; EGF; epidermal growth factor; Hydro, hydrophobic; FNIII; fibronectin type III; Ig; immunoglobulin; LamNT, laminin N-terminal domain; P, conserved cytoplasmic motif; RGD, Arg-Gly-Asp; TSP1, thrombospondin 1; vWF, von Willebrand factor type D; ZU5, ZO-1 and Unc5-like.

Xenopus. Supraoptic axons in the embryonic *Xenopus* forebrain display a Neogenin-dependent chemoattractive response to Netrin-1 (Wilson and Key 2006).

2 NEOGENIN FUNCTIONS IN THE DEVELOPING NERVOUS SYSTEM

A series of *in vitro* and *in vivo* studies during the past decade has revealed diverse roles for RGMs and Neogenin during neural development. The importance of RGM and Neogenin function during early development was revealed by gene knockout or knockdown. RGMa knockout mice show severe defects in neural tube closure and an exencephalic phenotype in approximately 50% of the embryos (Niederkofler *et al*. 2004). Depletion of Neogenin in zebrafish embryos leads to the development of a neural tube that lacks a lumen (Mawdsley *et al*. 2004). Furthermore, in *Xenopus* embryos, loss of either RGMa or Neogenin during neurulation results in defective neural fold elevation and failure of proper neural tube closure (Kee *et al*. 2008). Besides their essential role in neural tube closure in the early embryo, RGM and Neogenin also function in a number of neurodevelopmental processes at later stages. The function of RGMs and Neogenin in neurogenesis, neuronal differentiation, migration, axon guidance and neuronal apoptosis will be discussed in the next paragraphs.

2.1 NEUROGENESIS

At embryonic stages, strong Neogenin expression is detected in neurogenic and gliogenic precursors in the developing mouse brain, like radial glia, neuroblasts and olfactory neuronal progenitors (Fitzgerald *et al*. 2006, Fitzgerald *et al*. 2007, Shoemaker *et al*. 2010). In addition, Neogenin expression was revealed in neural stem cell populations in the adult forebrain subventricular zone (Bradford *et al*. 2010, Fitzgerald *et al*. 2007, Shoemaker *et al*. 2010). To further characterize these Neogenin-positive cells in the mouse brain, immunohistochemistry was combined with flow cytometry (FACS) to isolate the population of Neogenin-expressing cells from mouse embryonic day 11.5 (E11.5), E14.5 and adult forebrain. Cultures enriched for cells with high Neogenin expression levels from embryonic or adult stages revealed a high proliferative and neurogenic potential (Fitzgerald *et al*. 2006, Shoemaker *et al*. 2010). These experiments show that Neogenin is associated with a continuously self-renewing and neurogenic cell population in the embryonic and adult cortex. Although RGMa is also prominently expressed in proliferative zones in the mouse embryo, the role of RGMa in cortical neurogenesis is less well characterized. A subset (about 40%) of the Neogenin-expressing cells isolated from E11.5 cortex expressed RGMa. Further studies are needed to reveal the role of RGM-Neogenin signaling in neurogenesis.

2.2 DIFFERENTIATION

An initial study on Neogenin expression in embryonic chick brains revealed expression in neuronal cell layers in the retina and cerebellum harboring differentiating cells (Vielmetter *et al.* 1994). *In vivo* studies in chick embryos revealed a positive effect of RGM-Neogenin signaling on neuronal differentiation. Overexpression of RGM in the chick embryonic mid- and hindbrain resulted in an increase in differentiated neurons (Matsunaga *et al.* 2006). In these experiments, differentiated neurons were detected in the direct vicinity of RGM-overexpressing cells, indicating that RGM functions as a ligand mediating cell differentiation. In addition, overexpression of Neogenin in embryonic chick brains also enhanced neuronal differentiation (Matsunaga *et al.* 2006). In experiments in which overexpression of RGM was combined with short hairpin-mediated knockdown of Neogenin, no effect on neuronal differentiation was observed. Together, these experiments support the idea that the RGM-Neogenin signaling pathway regulates neuronal differentiation in the chick embryo.

A recent study in *Xenopus* embryos unveils that RGMa can also act cell-autonomously to enhance neuronal differentiation (Lah and Key 2012a). Mosaic overexpression of RGMa induces neuronal differentiation of cells in the neuroepithelium that express RGMa ectopically. In contrast to RGM-Neogenin-mediated neuronal differentiation in the chick mid- and hindbrain, the effect of RGMa overexpression on neuronal differentiation in *Xenopus* was independent of Neogenin. Knockdown of Neogenin did not reduce the increase in neuronal differentiation by RGMa. In all, these studies indicate that both RGM and Neogenin can induce neuronal differentiation, but also show that the RGM signaling mechanisms that mediate neuronal differentiation may differ between neuronal subsets or species.

2.3 MIGRATION

Besides expression of Neogenin in neuroblasts and differentiating cells, Neogenin was also detected in several populations of migrating cells in the developing brain. Expression of Neogenin has been detected on radially migrating postmitotic neuroblasts in the embryonic cortex and on interneuron neuroblasts migrating tangentially from the ganglionic eminence (Fitzgerald *et al.* 2006). In addition, Neogenin-positive neural precursors are present in the rostral migratory stream that originates in the cortical subventricular zone and ends in the olfactory bulb (Bradford *et al.* 2010). In *ex vivo* experiments, Neogenin overexpression in neuroblasts from the ganglionic eminence resulted in reduced migration away from the ventricular zone, revealing a role for Neogenin in migration (Andrusiak *et al.* 2011).

Neogenin expression was also detected in migrating dentate gyrus precursor cells in the mouse hippocampus. Migration of dentate gyrus precursor cells was inhibited by RGMb, indicating that RGMb might set the boundaries of this migrational stream in the dentate gyrus (Conrad *et al.* 2010). In experiments using animal cap explants, consisting of pluripotent stem cells from late-blastula stage *Xenopus* embryos, RGMa overexpression stimulated cell migration from

animal cap explants in a Neogenin-dependent manner (Lah and Key 2012b). Together, these experiments hint at an important role for RGM-Neogenin signaling in neuronal cell migration.

2.4 APOPTOSIS

Neogenin, its close homolog DCC, and Unc5A-D belong to the structurally diverse family of dependence receptors (Bredesen *et al.* 2005, Goldschneider and Mehlen 2010, Llambi *et al.* 2001, Matsunaga *et al.* 2004, Mehlen and Fearon 2004). The absence of ligand induces self-activation of these receptors, resulting in proteolytic processing of the receptor and activation of apoptotic signaling cascades (Bredesen *et al.* 2005, Goldschneider and Mehlen 2010). Therefore, the survival of cells expressing these receptors depends on the presence of their ligands.

In line with its role as dependence receptor, overexpression of Neogenin or depletion of RGM ligand in the embryonic chick neural tube induced apoptosis (Matsunaga *et al.* 2004). In addition, activation of apoptotic signaling by Neogenin overexpression in the chick neural tube could be blocked by coexpression of RGM ligand (Matsunaga *et al.* 2004). Also in the retina, the presence of RGMa promoted survival of rat retinal ganglion cells (RGCs) in *in vitro* retinal cultures (Koeberle *et al.* 2010). In an *in vivo* model of neurodegeneration, intraocular injection of RGMa strongly reduced RGC apoptosis after optic nerve transection in rats.

Overexpression of RGM in the chick neural tube did not affect apoptosis levels (Matsunaga *et al.* 2004). Furthermore, addition of RGMa to *in vitro* cultures of either dorsal root ganglia neurons or PC12 neuroblastoma cells did not affect apoptosis in these cells (Conrad *et al.* 2007). In contrast, overexpression of RGMa in early *Xenopus* embryos induced severe cell death in a Neogenin-dependent manner (Lah and Key 2012a, Shin and Wilson 2008). Together, these experiments hint at the existence of different RGM-Neogenin signaling mechanism regulating apoptosis.

2.5 AXON GUIDANCE

During neural development growing axons are directed to their proper targets by guidance cues in the environment. These cues can be membrane-attached or secreted, and induce either attractive or repulsive signaling through ligand-specific axon guidance receptors (Dickson 2002, Tessier-Lavigne and Goodman 1996). RGM ligands are important axon guidance cues in chick retinotectal map formation, the formation of the *Xenopus* supraoptic tract and the development of the entorhinal-hippocampal system in mice (Brinks *et al.* 2004, Monnier *et al.* 2002, Wilson and Key 2006). In the following paragraphs, the roles of Neogenin, RGMs and also Netrin-1 in axon tract formation in these systems will be summarized and discussed.

2.5.1 THE RETINOTECTAL SYSTEM

A role for RGM-mediated Neogenin signaling in axon guidance was first identified in chicken where RGM-Neogenin signaling is essential for correct mapping of temporal retinal RGC axons

to the anterior tectum (Figure 2A) (Matsunaga *et al.* 2006, Monnier *et al.* 2002, Rajagopalan *et al.* 2004). In the chick retina, Neogenin is expressed in RGC neurons in a nasal-low to temporal-high gradient (Rajagopalan *et al.* 2004). Chick RGM has a graded expression along the anterior-posterior axis of the tectum, with low expression in the anterior tectum and high expression in the posterior tectum (Monnier *et al.* 2002). In *in vitro* experiments, growth cones of temporal RGC axons expressing Neogenin collapsed in response to RGM and axon growth of these neurons was strongly inhibited (Monnier *et al.* 2002, Rajagopalan *et al.* 2004). Furthermore, temporal retinal axons did not grow on a substrate of RGM protein, when offered a choice between membrane coatings of RGM- and mock-transfected cells in a stripe assay (Monnier *et al.* 2002, Rajagopalan *et al.* 2004). The avoidance of RGM-expressing cell membranes by temporal retinal axons was neutralized when Neogenin or RGM function was blocked by specific antibodies or when RGM was removed from the cell membrane by enzymatic cleavage of the GPI-link (Rajagopalan *et al.* 2004). In addition to expression of RGM in the tectum, RGM expression was also revealed on RGC axons (Tassew *et al.* 2008). RGM overexpression or knockdown in either the embryonic chick tectum or the retina resulted in topographic mapping errors of temporal RGC axons in the optic tectum (Matsunaga *et al.* 2006, Tassew *et al.* 2008). Furthermore, intraretinal pathfinding errors of RGC axons were observed. Together these data show that RGM expression in both the chick retina and tectum is important in retinotectal map formation and that RGM-Neogenin signaling guides temporal RGC axons to the anterior tectum. Analysis of *RGMa* knockout mice did not reveal any defects in the axonal projections from RGCs to the superior colliculus, indicating that RGM-Neogenin signaling may not be involved in retinotectal map formation in the mouse (Niederkofler *et al.* 2004).

2.5.2 THE SUPRAOPTIC TRACT

In *Xenopus*, signaling of both RGMa and Netrin-1 through Neogenin is required for proper formation of the supraoptic tract (SOT) (Lah and Key 2012a, Wilson and Key 2006). The SOT is the precursor of the mammalian internal capsule and the earliest dorsoventral pathway connecting the telencephalon and diencephalon in the vertebrate forebrain. Neogenin is expressed by telencephalic neurons that give rise to the SOT and RGMa and Netrin-1 are expressed in the embryonic *Xenopus* forebrain (Figure 2B) (Wilson and Key 2006). A series of *in vivo* gain- and loss-of-function experiments revealed an essential role for RGMa-Neogenin and Netrin-1-Neogenin signaling in the formation of the SOT. Morpholino-induced knockdown of RGMa, Netrin-1 or Neogenin resulted in highly aberrant trajectories of SOT axons (Wilson and Key 2006). In addition, this phenotype was also observed upon mosaic overexpression of RGMa in the embryonic *Xenopus* brain (Lah and Key 2012a). Simultaneous partial knockdown of RGMa and Neogenin or Netrin-1 and Neogenin induced similar defects in SOT formation as observed in knockdown experiments for these genes separately (Wilson and Key 2006). These experiments revealed the involvement of RGMa-Neogenin and Netrin-1-Neogenin signaling in the formation of this axon bundle. During SOT development, the repulsive effect of

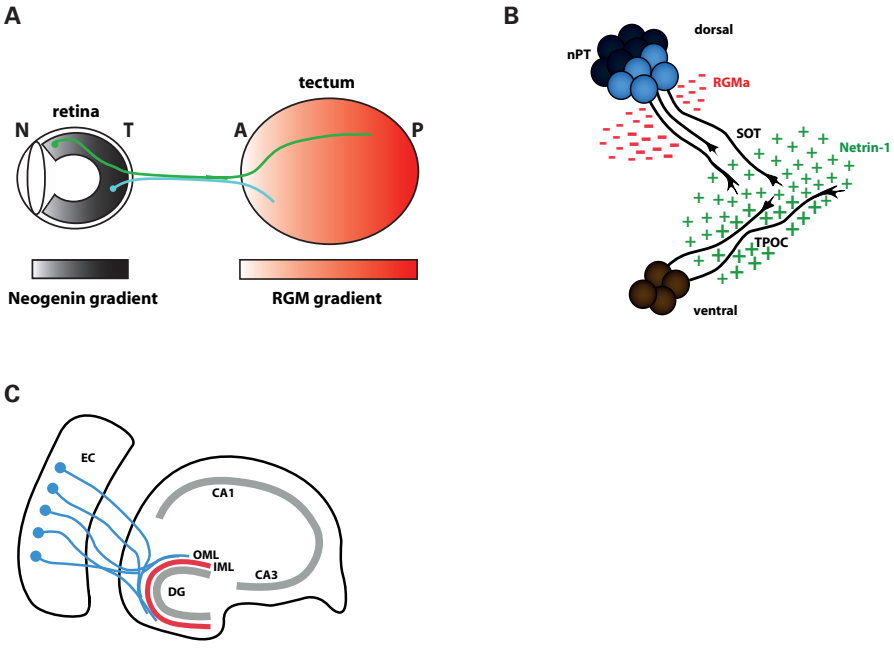

FIGURE 2. RGM and Neogenin-mediated axon guidance.

(A) In chicken, graded expression of Neogenin in the retina and RGM in the tectum restricts the growth of Neogenin-expressing neurites of temporal retinal ganglion cells from the RGM-high posterior tectum. (B) Both RGM- and Netrin-1-mediated Neogenin signaling regulates the formation of the supraoptic tract (SOT), connecting dorsal and ventral brain areas in *Xenopus*. Repulsive RGMa-Neogenin signaling restricts the growth of telencephalic axons into a tight bundle, while a gradient of Netrin-1 expression mediates neurite attraction of these neurons to their target area in the ventral brain. (C) In the mouse, entorhinal cortical (EC) axons project to outer molecular layer of the dentate gyrus (DG), as axon growth into the adjacent inner molecular layer is repelled by RGMa. A, anterior; CA, cornu ammonis; N, nasal; nPT, presumptive nucleus of the telencephalon; P, posterior; T, temporal; TPOC, tract of the post-optic commissures.

RGMa-Neogenin signaling directs Neogenin-positive axons to grow into a tight bundle, while Netrin-1-Neogenin signaling mediates an attractive effect on these axons and stimulates the growth of these axons to their target area in the ventral part of the brain (Figure 2B).

2.5.3 THE ENTORHINAL-HIPPOCAMPAL SYSTEM

In mice, RGMa has a role in axon guidance events in the developing hippocampus (Brinks *et al.* 2004). During hippocampal development, entorhinal cortical neurons project their axons to a specific layer of the dentate gyrus: the outer molecular layer (Figure 2C). Neurite outgrowth experiments and stripe assays reveal a strong repellent effect of RGMa on entorhinal cortical

axons (Brinks *et al*. 2004). RGMa expression is detected in the inner molecular layer of the dentate gyrus, aligning the outer molecular layer. In organotypic hippocampal slice cultures in which RGMa function is blocked by anti-RGMa antibodies or cleavage of RGMa from the cell membrane, the specific termination pattern of entorhinal cortical fibers to the outer molecular layer is abolished. Massive aberrant entorhinal cortical projections are observed that terminate in hippocampal subfields other than the outer molecular layer (Brinks *et al*. 2004). These experiments indicate that RGMa expression in the inner molecular layer of the dentate gyrus repels entorhinal cortical axons to the outer molecular layer (Figure 2C). Expression of Neogenin has been detected in the entorhinal cortex (Gad *et al*. 1997). However, the role of Neogenin in the repulsion of entorhinal axons by RGMa is unknown.

Besides the neurite outgrowth-inhibiting effects of RGMa and RGMb on cortical neurons (Hata *et al*. 2009, Liu *et al*. 2009), RGMa-mediated neurite outgrowth inhibition has also been shown for cerebellar granule and dorsal root ganglia neurons (Conrad *et al*. 2007, Hata *et al*. 2006). Despite these findings and the identification of RGM and Neogenin expression in many other brain areas (Gad *et al*. 1997, Keeling *et al*. 1997, Oldekamp *et al*. 2004, Schmidtmer and Engelkamp 2004), evidence of a role for RGM-mediated axon guidance in neuronal systems in the mouse brain, other than the entorhinal-hippocampal system, is currently lacking. Therefore, future studies are required to elucidate the role of RGM-Neogenin signaling in the development of other axon tracts in the developing mouse brain.

3 NEOGENIN FUNCTIONS IN INJURY AND DISEASE

Besides their essential roles during neural development, there is increasing evidence that RGMs and Neogenin have important functions in disease processes in the adult nervous system. In the adult CNS, neuronal injury-induced RGMa expression contributes to the failure of axon regeneration. Recently, a role for RGMa-Neogenin signaling was revealed in the immune system and RGMa-Neogenin signaling has been implicated in the autoimmune response against myelin in multiple sclerosis. Furthermore, RGMa function has been related to Alzheimer and Parkinson's disease, and a genetic association study revealed a possible relation between RGMa and epilepsy. These roles of RGMa and Neogenin in nervous system disease are discussed in more detail in the following sections.

3.1 AXON REGENERATION

There is only very limited long distance regeneration in the adult CNS. Injury to the adult brain and spinal cord frequently causes permanent neuronal deficits and severe health problems. The neurite outgrowth restrictive environment around CNS lesion sites prohibits large-scale spontaneous regeneration. Nogo, myelin-associated glycoprotein (MAG) and oligodendrocyte-myelin glycoprotein (OMgp) are three potent inhibitors of axon regeneration

that are expressed by myelinated fiber tracts and oligodendrocytes, and show elevated expression upon neuronal injury (Grados-Munro and Fournier 2003, Yamashita *et al.* 2005). Enhanced expression of several repulsive axon guidance molecules, for example semaphorin 3A and ephrin-A3, also contributes to the neurite outgrowth restrictive environment around the lesion site (Irizarry-Ramirez *et al.* 2005, Pasterkamp *et al.* 2001, Yaron and Zheng 2007). Also for RGMa an increase in expression is observed around the lesion site after focal cerebral ischemia or traumatic brain injury in humans and spinal cord injury or optic nerve crush in rats (Doya *et al.* 2006, Hata *et al.* 2006, Schnichels *et al.* 2011, Schnichels *et al.* 2012, Schwab *et al.* 2005). Increased RGMa expression is evident on myelinated fibers, and in neurons, oligodendrocytes, microglia and macrophages. To verify whether blocking RGMa in the injured CNS has a positive outcome on axon regeneration, RGMa function was blocked by neutralizing antibodies (Hata *et al.* 2006). Local administration of antibodies in the injured rat spinal cord for two weeks after injury resulted in pronounced regeneration of axons beyond the lesion site and improved motor function (Hata *et al.* 2006) (Figure 3A). Similar to RGMa, increased RGMb is also detected in the injured rat spinal cord (Liu *et al.* 2009). However, it is unknown whether blocking RGMb leads to enhanced axon regeneration.

In rats a strong increase in RGMa levels was observed after induction of focal cerebral ischemia/reperfusion injury (Jiang *et al.* 2012, Zhang *et al.* 2011). Electrical stimulation of the cerebral cortex has been shown to have a neuroprotective effect following ischemic stroke in humans (Baba *et al.* 2009, Kumar *et al.* 2011, Page *et al.* 2012). However, the underlying mechanisms of this effect are poorly understood. Interestingly, electrical stimulation of the olfactory bulb (Zhang *et al.* 2011) or fastigial nucleus (Jiang *et al.* 2012) after ischemic injury in rats, resulted in a downregulation of RGMa expression and enhanced axon growth in ischemic cortex and improved neurological function. Together, these studies show that reduction of RGMa expression or blockage of RGMa function is a potent therapeutic strategy after CNS injury or focal cerebral ischemia, with possible applications in humans.

3.2 NEUROLOGICAL DISEASE

3.2.1 Multiple sclerosis

Multiple sclerosis (MS) is an autoimmune-mediated demyelinating disease of the CNS, resulting in degeneration of nerve bundles and progressive paralysis (Sospedra and Martin 2005, Trapp and Nave 2008). In MS, $CD4^+$ T cells specific for myelin activate an immune response in the white matter of the brain and spinal cord (Chastain *et al.* 2011). RGMa is expressed by antigen-presenting dendritic cells and its expression levels are increased upon inflammation (Muramatsu *et al.* 2011). Dendritic cells activate antigen-specific $CD4^+$ T cells, which express Neogenin. Activation of $CD4^+$ T cells increases their adhesive properties, thereby facilitating their penetrance into tissue (Figure 3B). *In vitro* exposure of $CD4^+$ T cells to

RGMa enhances their adhesive properties, revealing a regulatory role for RGMa in $CD4^+$ T cell activation (Muramatsu *et al.* 2011).

Interestingly, increased levels of RGMa are observed in dendritic cells in the brain and spinal cord of MS patients (Muramatsu *et al.* 2011). Similarly, in a mouse experimental autoimmune encephalomyelitis (EAE) model of MS, dendritic cells in the spinal cord, lymph nodes and spleen display elevated levels of RGMa (Muramatsu *et al.* 2011). In the EAE mouse model, immunization with myelin antigens causes neurodegenerative symptoms through autoimmune attacks by dendritic cells and activated $CD4^+$ T cells. Treatment with a neutralizing anti-RGMa antibody in this mouse model resulted in decreased immune cell infiltration into the spinal cord and reduced production of inflammatory cytokines by $CD4^+$ T cells (Figure 3B) (Muramatsu *et al.* 2011). Furthermore, treated mice revealed less severe demyelination of spinal axons and paralysis of the hind limbs.

A reduction of inflammatory cytokine production was also observed in blood samples of MS patients upon addition of neutralizing anti-RGMa antibody (Muramatsu *et al.* 2011). These findings are of particular interest, since a genetic association study revealed a relation of RGMa polymorphisms with the incidence of MS and to levels of pro-inflammatory cytokines in the cerebrospinal fluid of MS patients (Nohra *et al.* 2010). Together, these lines of data show that RGMa plays critical roles in the pathogenesis of MS, in particular by activation of autoimmune reactive $CD4^+$ T cells. Treatment with an anti-RGMa antibody suppressed $CD4^+$ T cell response and improved clinical outcome. Therefore, RGMa could be a promising target for the treatment of multiple sclerosis.

3.2.2 Alzheimer, Parkinson's disease and epilepsy

Alzheimer's disease (AD) is the most frequent cause of dementia affecting the elderly population. Key pathological changes are extracellular accumulation of amyloid-β in senile plaques and intracellular accumulation of tau protein in neurofibrillary tangles in the brain (Citron 2010). In AD brains accumulation of RGMa was detected in amyloid plaques (Satoh *et al.* 2012). Although the role of RGMa in the neurodegenerative process of AD is currently unknown, accumulation of RGMa could contribute to the regenerative failure of degenerating axons (DeWitt and Silver 1996, Hoozemans *et al.* 2006, Uchida 2010).

Parkinson's disease (PD), another late-onset neurodegenerative disorder, is characterized by loss of dopaminergic neurons in the substantia nigra (SN) (Fearnley and Lees 1991, Rinne *et al.* 1989). In an expression analysis study, a twofold increase in RGMa expression was identified in the SN of PD patients (Bossers *et al.* 2009). The role of RGMa expression in SN neurons is currently unknown. However, elevated levels of RGMa could result in a more inhibitory environment around dopaminergic neurons. This may have a negative effect on the connectivity and survival of dopaminergic neurons in the SN (Lesnick *et al.* 2007).

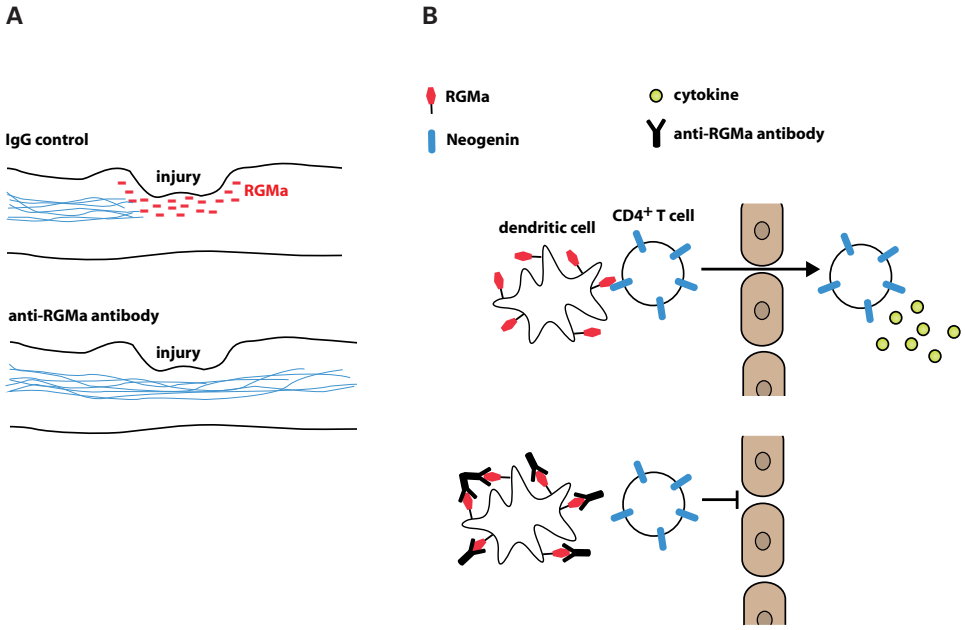

FIGURE 3. RGM and Neogenin function in disease.

RGMa-Neogenin signaling inhibits axon regeneration upon neuronal injury and mediates the autoimmune response to myelin in multiple sclerosis (MS). (A) Upon neuronal injury, RGMa expression around the lesion site is increased and blocks neuronal regeneration. Treatment of rat spinal cord lesions with neutralizing anti-RGMa antibodies resulted in pronounced regeneration of spinal cord axons and improved motor function. (B) RGMa expression in antigen-presenting dendritic cells mediates activation, tissue penetrance and inflammatory cytokine production of Neogenin-expressing $CD4^+$ T cells. A treatment with neutralizing anti-RGMa antibodies in an MS mouse model decreased immune cell infiltration, cytokine production, demyelination of spinal axons and paralysis of the hind limbs.

An association between RGMa and epilepsy comes from a genomic microdeletion identified in a child with epilepsy and mental retardation, comprising the genes for RGMa and chromodomain helicase DNA binding protein 2 (CHD2) (Capelli *et al.* 2012). CHD2 is part of a gene family involved in the negative regulation of gene expression through chromatin remodeling and assembly (Kulkarni *et al.* 2008, Marfella and Imbalzano 2007). Future studies are needed to reveal whether there is a relation between RGMa, epilepsy and mental deficiency.

4 NEOGENIN SIGNALING

Over the last couple of years, a number of studies have begun to elucidate the signaling pathways downstream of Neogenin. An increasing number of studies implicate the small

GTPases RhoA and Ras, several kinases and a number of other signaling proteins in the Neogenin signaling cascade. In addition, recognition sites have been identified in Neogenin for the processing enzymes γ-secretase, caspase-3 and tumor necrosis factor-a converting enzyme (TACE). Cleavage of the Neogenin receptor in the extracellular domain by TACE modulates Neogenin sensitivity to RGMs. Cleavage in the intracellular domain by γ-secretase or caspase-3 is implicated in the Neogenin signaling pathways mediating gene transcription and apoptotic signaling, respectively.

4.1 NEOGENIN SIGNALING IN REPULSIVE AXON GUIDANCE

4.1.1 RhoA and Ras GTPase signaling

Unc5B is an essential coreceptor in the RGMa-activated Neogenin signaling pathway mediating repulsive axon guidance. All Unc5 molecules (Unc5A-D) can interact with Neogenin. However, so far a functional role in Neogenin signaling has only been shown for Unc5B (Hata *et al.* 2009). Unc5B constitutively associates with Neogenin and leukemia-associated Rho guanine-nucleotide exchange factor (LARG), an activator of RhoA GTPase signaling, is associated with Unc5B. RGMs activate Neogenin signaling by direct binding to Neogenin and do not interact with Unc5 molecules. Upon binding of RGMa to Neogenin, focal adhesion kinase (FAK), which is associated with the P3 domain of Neogenin, activates LARG by phosphorylation (Hata *et al.* 2009, Ren *et al.* 2004). Activation of the small GTPase RhoA and its downstream effector Rho kinase by RGMa-Neogenin signaling, induces phosphorylation and activation of myosin II, which mediates F-actin depolymerization and as a consequence growth cone collapse and neurite growth inhibition (Figure 4A) (Conrad *et al.* 2007, Kubo *et al.* 2008)

In addition to activation of RhoA, inhibition of Ras GTPase is essential for RGMa-activated Neogenin signaling during neurite outgrowth inhibition. Under native conditions, Ras-specific GTPase-activating protein p120GAP is associated with FAK, which is phosphorylated at Tyr-397 (Endo and Yamashita 2009, Hecker *et al.* 2004). Upon binding of RGMa to Neogenin, FAK becomes dephosphorylated and p120GAP is released from FAK (Endo and Yamashita 2009). The dissociation of p120GAP from FAK increases its binding to GTP-Ras and induces the inactivation of Ras and its downstream effectors PI3-kinase and Akt (Figure 4A).

4.1.2 Neogenin ectodomain shedding

Another aspect of Neogenin signaling is shedding of the Neogenin extracellular domain following cleavage by TACE, also called ADAM17 (Okamura *et al.* 2011). TACE binds directly to the Neogenin extracellular domain and cuts Neogenin just above the membrane, thereby releasing the extracellular domain. TACE is expressed by embryonic cortical neurons and regulates their sensitivity to RGMa. Depletion of TACE in cultured embryonic cortical neurons increases active Rho levels and enhances growth cone collapse and neurite outgrowth inhibition upon stimulation with RGMa. In contrast, overexpression of TACE inhibits Neogenin

signaling in neurons and reduces their response to RGMa (Okamura *et al*. 2011). Whether neurons endogenously regulate their sensitivity to RGMa by regulating TACE expression levels remains to be shown.

4.2 TRANSCRIPTION REGULATION

The Neogenin intracellular domain (NeoICD) has been identified as a substrate for γ-secretase (Goldschneider *et al*. 2008). γ-Secretase cleavage releases the complete NeoICD, which translocates to the nucleus (Figure 4B) (Goldschneider *et al*. 2008). Specific motifs in the NeoICD sequence were recognized as nuclear localization and nuclear export signals, regulating NeoICD transport in and out of the nucleus. A yeast two-hybrid screen on the NeoICD identified interacting proteins with a nuclear localization and effects in transcription regulation. A chromatin immunoprecipitation experiment revealed that the NeoICD associates with DNA and identified a number of putative target genes which could be transcriptionally regulated by the NeoICD (Goldschneider *et al*. 2008).

A role for Neogenin in transcription regulation was investigated in more detail for two putative target genes: grainyhead-like protein 1 (GRHL1) and cerebral cavernous malformation 2 (CCM2). GRHL1 is a transcription factor implicated in neural development (Cenci and Gould 2005). CCM2 is a scaffold for the p38 mitogen-activated protein kinase (MAPK) signaling cascade, which has been implicated in Netrin-1-mediated axon guidance (Forcet *et al*. 2002). Transcription analysis of CCM2 and GRHL1 in Neogenin-expressing cells revealed that stimulation with RGMa increased the expression levels of CCM2 and GRHL1 (Goldschneider *et al*. 2008).

Together, these experiments show that RGMa-Neogenin signaling regulates gene transcription, which involves cleavage of the NeoICD by γ-secretase. It is currently not known whether activation of the Neogenin receptor by RGMa enhances NeoICD cleavage by γ-secretase. One of the very few signaling proteins that are known to interact with Neogenin; LIM domain only 4 (LMO4), is a transcriptional regulator that interacts with transcription factors (Schaffar *et al*. 2008). Binding of RGMa to Neogenin induces the dissociation of LMO4 from the NeoICD. LMO4 has been shown to be an essential signaling protein in the RGMa-Neogenin pathway inducing neurite outgrowth inhibition (Schaffar *et al*. 2008). The role of RGMa-Neogenin-induced transcription in neurodevelopmental processes, such as neuronal differentiation and axon guidance, is unknown.

4.3 APOPTOSIS SIGNALING

Overexpression of Neogenin or downregulation of RGM ligand in the chick neural tube induces apoptosis (Matsunaga *et al*. 2004). The serine/threonine kinase death-associated protein kinase (DAPK) is an essential signaling protein in the Neogenin pathway inducing apoptosis (Fujita *et al*. 2008). Inactivation of DAPK in the chick neural tube by short hairpin-mediated knockdown or expression of dominant-negative DAPK completely blocks the proapoptotic activity of

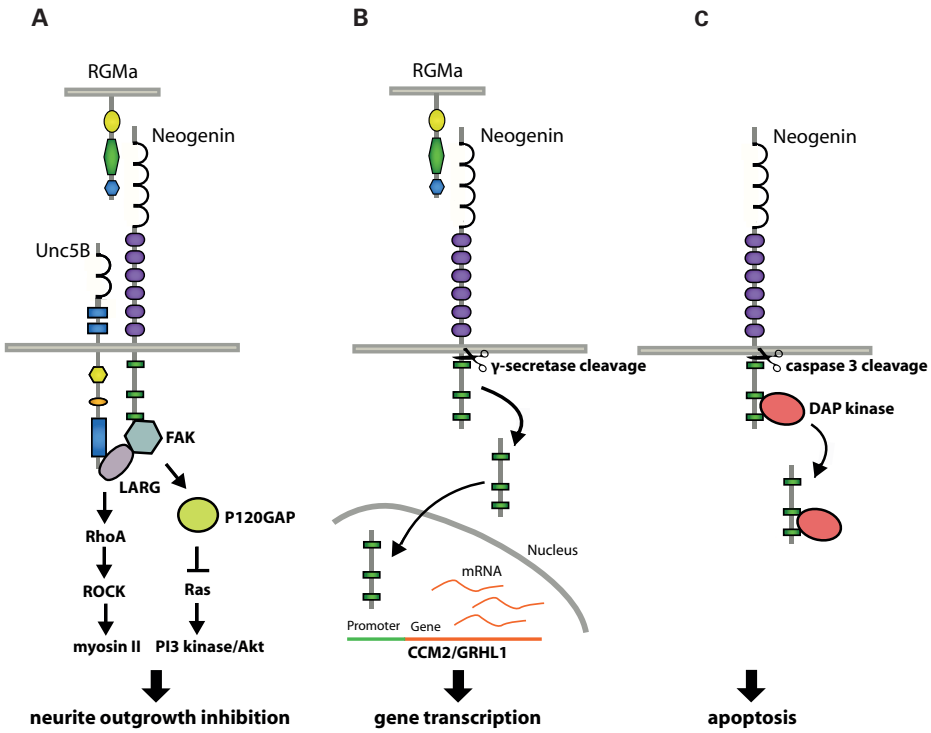

FIGURE 4. Neogenin signaling.

Schematic representation of Neogenin signaling pathways mediating neurite outgrowth inhibition (A), gene transcription (B) and apoptosis(C). (A) In the RGMa-Neogenin signaling cascade mediating growth cone collapse and neurite outgrowth inhibition, focal adhesion kinase (FAK), which is associated with the P3 domain of Neogenin, activates leukemia-associated Rho guanine nucleotide exchange factor (LARG), which is bound to the intracellular domain of the Unc5B coreceptor. LARG mediates activation of RhoA GTPase, Rho kinase and myosin II, leading to F-actin depolymerization. Activation of Neogenin by RGMa, induces dephosphorylation of FAK, which mediates the release of Ras-specific GTPase-activating protein p120GAP from FAK and subsequent inactivation of Ras and PI3 kinase/Akt. (B) The Neogenin intracellular domain (NeoICD) can be released by γ-secretase cleavage, translocate to the nucleus and induce gene transcription. Binding of RGMa to Neogenin enhances the transcription of cerebral cavernous malformation 2 (CCM2) and grainyhead-like protein 1 (GRHL1). (C) Absence of RGMa ligand mediates association of death-associated protein (DAP) kinase to the NeoICD and cleavage of the NeoICD by caspase-3, leading to the activation of apoptotic signaling pathways.

Neogenin. DAPK autophosphorylation on Ser308 is known to inhibit its kinase activity (Shohat *et al.* 2001). Interestingly, upon binding of DAPK to the NeoICD, DAPK autophosphorylation is inhibited and its kinase activity enhanced. However, in the presence of RGMa, DAPK autophosphorylation levels are elevated and kinase activity decreased (Fujita *et al.* 2008). Release of cytochrome c into the cytosol is an early step in apoptotic signaling pathways inducing cell death. Overexpression of Neogenin induces the release of cytochrome c in HEK293 cells, whereas the addition of RGMa or depletion of DAPK in these cells suppresses this release (Fujita *et al.* 2008). Together, these experiments support an essential role for DAPK in Neogenin-mediated apoptosis signaling.

Neogenin overexpression or depletion of RGM in the chick neural tube induces a strong increase in caspase-3 positive cells (Matsunaga *et al.* 2004). A recognition site for caspase-3 was identified in the NeoICD. In the absence of RGMa, the NeoICD is cleaved by caspase-3, generating a proapoptotic domain (Figure 4C). Overexpression of a Neogenin mutant protein in which the caspase-3 cleavage site was mutated, did not induce apoptosis in the chick neural tube, revealing a requirement for caspase-3 cleavage in Neogenin-mediated apoptosis signaling (Matsunaga *et al.* 2004).

In all, the identification of DAPK and caspase-3 function in Neogenin-mediated apoptosis signaling is a first step in the elucidation of the complete Neogenin signaling pathway inducing apoptosis.

5 AIM AND OUTLINE OF THIS THESIS

RGM-Neogenin signaling regulates a wide variety of developmental processes in the nervous system, including axon guidance, neuronal migration, differentiation and apoptosis. Furthermore, RGMa and Neogenin have been implicated in regeneration failure in the adult CNS and contribute to diseases such as multiple sclerosis, Alzheimer and Parkinson's disease. Neogenin signaling during neural development is dependent on the spatiotemporal expression of the Neogenin receptor, the presence of ligands, and the availability of intracellular signaling molecules. Our knowledge of Neogenin, RGM ligand and Unc5 coreceptor expression in the developing brain is very limited. In addition, the Neogenin signal transduction cascade that mediates RGM-induced neurite outgrowth inhibition and other developmental functions remains poorly characterized. The aim of this thesis is to characterize the function and signaling mechanisms of Neogenin during neural development by 1) performing a detailed expression pattern analysis of the Neogenin receptor complex, and of its ligands, during mouse brain development, and 2) through the identification of novel Neogenin signaling proteins using *in vitro* and *in vivo* pull downs and mass spectrometry.

CHAPTER 2: Getting connected in the dopamine system

RGM-Neogenin signaling functions in axon guidance and neuronal network formation. RGMs and Neogenin are broadly expressed in the developing brain, including in the developing mesodiencephalic dopaminergic (mdDA) midbrain. This is intriguing as RGMa levels are selectively increased in mdDA neurons in patients suffering from Parkinson's disease. This chapter presents a detailed overview of the development of the mdDA system, focusing on the molecular and cellular processes that control the development and plasticity of mdDA connectivity.

CHAPTER 3: Spatiotemporal expression of repulsive guidance molecules (RGMs) and their receptor Neogenin in the mouse brain.

Detailed information on the layer- and subset-specific expression of RGMs and Neogenin during neural development is very limited. In this chapter, we performed a detailed analysis of the expression of Neogenin, RGMs and Unc5 coreceptors in a selection of brain areas during mouse brain development. *In situ* hybridization, immunohistochemistry and RGMa section binding revealed differential and layer-specific expression patterns for these proteins. In addition, coexpression of RGMs and/or Neogenin was detected in several brain areas and on several axon bundles. These data suggest important and unexplored roles for RGM-Neogenin signaling during brain development.

CHAPTER 4: The leucine-rich repeat protein Lrig2 binds Neogenin and is required for neurite outgrowth inhibition by RGMa

To further dissect Neogenin signaling pathways, we used *in vitro* and *in vivo* proteomics approaches to identify Neogenin binding partners. In this chapter, an *in vitro* biotin-streptavidin-based pull down of Neogenin signaling complexes was combined with mass spectrometry analysis and led to the identification of many putative novel Neogenin-interacting proteins. The interaction of Neogenin and one of the transmembrane proteins identified in the screen, leucine-rich repeats and immunoglobulin-like domains protein 2 (Lrig2), was studied in more detail using colocalization, *in vivo* co-immunoprecipitation and functional experiments. A functional neurite outgrowth assay showed the requirement of Lrig2 in repulsive RGMa-Neogenin signaling.

CHAPTER 5: *In vivo* proteomics screen using a synapsin I-driven *GFP-Neogenin* transgenic mouse identifies novel Neogenin-interacting proteins

To purify Neogenin complexes from brain tissue *in vivo*, we generated a *Syn-GFP-Neogenin* transgenic mouse. In this mouse the synapsin I promoter drives neuron-specific expression of a GFP-Neogenin fusion protein. An anti-GFP *in vivo* Neogenin pull down on brain lysates of perinatal *Syn-GFP-Neogenin* transgenic mice followed by mass spectrometry analysis revealed a number of putative novel Neogenin-interacting proteins with known functions in cytoskeletal dynamics, neuronal process formation, migration, apoptosis and transcription regulation.

CHAPTER 6: Dock7 binds Neogenin and is required for repulsive RGMa-Neogenin signaling in neurons

The role of one of the Neogenin-interacting proteins identified in the *in vivo* Neogenin pull down (Chapter 5), dedicator of cytokinesis 7 (Dock7), was investigated in Chapter 6. Dock7 is an activator of Cdc42 and Rac GTPases and functions in microtubule cytoskeleton remodeling. Immunohistochemistry and immunoprecipitation experiments revealed the *in vivo* colocalization and interaction of Dock7 and Neogenin in embryonic mouse brains. Functional neurite outgrowth experiments revealed a requirement for Dock7 in RGMa-Neogenin-mediated neurite outgrowth inhibition in cortical neurons.

CHAPTER 7: General discussion

Finally, in Chapter 7 we discuss the results of the work outlined in this thesis in the light of what is known about RGM-mediated Neogenin function and signaling in the developing brain, thereby focusing on its role in axon guidance. The detailed expression analysis of the Neogenin receptor complex during mouse brain development and the novel Neogenin-interacting proteins identified in the proteomics screens are a valuable starting point for future studies on the role and mechanisms of Neogenin signaling during brain development.

REFERENCE LIST

Andrusiak, M. G., K. A. McClellan, D. Dugal-Tessier, L. M. Julian, S. P. Rodrigues, D. S. Park, T. E. Kennedy, and R. S. Slack. 2011. Rb/E2F regulates expression of neogenin during neuronal migration. Mol. Cell Biol. 31:238-247.

Baba, T., M. Kameda, T. Yasuhara, T. Morimoto, A. Kondo, T. Shingo, N. Tajiri, F. Wang, Y. Miyoshi, C. V. Borlongan, M. Matsumae, and I. Date. 2009. Electrical stimulation of the cerebral cortex exerts antiapoptotic, angiogenic, and anti-inflammatory effects in ischemic stroke rats through phosphoinositide 3-kinase/Akt signaling pathway. Stroke 40:e598-e605.

Babitt, J. L., F. W. Huang, D. M. Wrighting, Y. Xia, Y. Sidis, T. A. Samad, J. A. Campagna, R. T. Chung, A. L. Schneyer, C. J. Woolf, N. C. Andrews, and H. Y. Lin. 2006. Bone morphogenetic protein signaling by hemojuvelin regulates hepcidin expression. Nat. Genet. 38:531-539.

Babitt, J. L., Y. Zhang, T. A. Samad, Y. Xia, J. Tang, J. A. Campagna, A. L. Schneyer, C. J. Woolf, and H. Y. Lin. 2005. Repulsive guidance molecule (RGMa), a DRAGON homologue, is a bone morphogenetic protein co-receptor. J. Biol. Chem. 280:29820-29827.

Bossers, K., G. Meerhoff, R. Balesar, J. W. van Dongen, C. G. Kruse, D. F. Swaab, and J. Verhaagen. 2009. Analysis of gene expression in Parkinson's disease: possible involvement of neurotrophic support and axon guidance in dopaminergic cell death. Brain Pathol. 19:91-107.

Bradford, D., R. L. Faull, M. A. Curtis, and H. M. Cooper. 2010. Characterization of the netrin/RGMa receptor neogenin in neurogenic regions of the mouse and human adult forebrain. J. Comp Neurol. 518:3237-3253.

Bredesen, D. E., P. Mehlen, and S. Rabizadeh. 2005. Receptors that mediate cellular dependence. Cell Death. Differ. 12:1031-1043.

Brinks, H., S. Conrad, J. Vogt, J. Oldekamp, A. Sierra, L. Deitinghoff, I. Bechmann, G. Alvarez-Bolado, B. Heimrich, P. P. Monnier, B. K. Mueller, and T. Skutella. 2004. The repulsive guidance molecule RGMa is involved in the formation of afferent connections in the dentate gyrus. J. Neurosci. 24:3862-3869.

Camus, L. M. and L. A. Lambert. 2007. Molecular evolution of hemojuvelin and the repulsive guidance molecule family. J. Mol. Evol. 65:68-81.

Capelli, L. P., A. C. Krepischi, J. Gurgel-Giannetti, M. F. Mendes, T. Rodrigues, M. C. Varela, C. P. Koiffmann, and C. Rosenberg. 2012. Deletion of the RMGA and CHD2 genes in a child with epilepsy and mental deficiency. Eur. J. Med. Genet. 55:132-134.

Cenci, C. and A. P. Gould. 2005. *Drosophila* Grainyhead specifies late programmes of neural proliferation by regulating the mitotic activity and Hox-dependent apoptosis of neuroblasts. Development 132:3835-3845.

Chastain, E. M., D. S. Duncan, J. M. Rodgers, and S. D. Miller. 2011. The role of antigen presenting cells in multiple sclerosis. Biochim. Biophys. Acta 1812:265-274.

Citron, M. 2010. Alzheimer's disease: strategies for disease modification. Nat. Rev. Drug Discov. 9:387-398.

Conrad, S., H. Genth, F. Hofmann, I. Just, and T. Skutella. 2007. Neogenin-RGMa signaling at the growth cone is bone morphogenetic protein-independent and involves RhoA, ROCK, and PKC. J. Biol. Chem. 282:16423-16433.

Conrad, S., F. Stimpfle, S. Montazeri, J. Oldekamp, K. Seid, G. Alvarez-Bolado, and T. Skutella. 2010. RGMb controls aggregation and migration of Neogenin-positive cells *in vitro* and *in vivo*. Mol. Cell Neurosci. 43:222-231.

Corradini, E., J. L. Babitt, and H. Y. Lin. 2009. The RGM/DRAGON family of BMP co-receptors. Cytokine Growth Factor Rev. 20:389-398.

De Vries, M. and H. M. Cooper. 2008. Emerging roles for neogenin and its ligands in CNS development. J. Neurochem. 106:1483-1492.

DeWitt, D. A. and J. Silver. 1996. Regenerative failure: a potential mechanism for neuritic dystrophy in Alzheimer's disease. Exp. Neurol. 142:103-110.

Dickson, B. J. 2002. Molecular mechanisms of axon guidance. Science 298:1959-1964.

Doya, H., T. Ito, K. Hata, M. Fujitani, S. Ohtori, T. Saito-Watanabe, H. Moriya, K. Takahashi, T. Kubo, and T. Yamashita. 2006. Induction of repulsive guidance molecule in neurons following sciatic nerve injury. J. Chem. Neuroanat. 32:74-77.

Endo, M. and T. Yamashita. 2009. Inactivation of Ras by p120GAP via focal adhesion kinase dephosphorylation mediates RGMa-induced growth cone collapse. J. Neurosci. 29:6649-6662.

Fazeli, A., S. L. Dickinson, M. L. Hermiston, R. V. Tighe, R. G. Steen, C. G. Small, E. T. Stoeckli, K. Keino-Masu, M. Masu, H. Rayburn, J. Simons, R. T. Bronson, J. I. Gordon, M. Tessier-Lavigne, and R. A. Weinberg. 1997. Phenotype of mice lacking functional Deleted in colorectal cancer (Dcc) gene. Nature 386:796-804.

Fearnley, J. M. and A. J. Lees. 1991. Ageing and Parkinson's disease: substantia nigra regional selectivity. Brain 114 (Pt 5):2283-2301.

Fearon, E. R., K. R. Cho, J. M. Nigro, S. E. Kern, J. W. Simons, J. M. Ruppert, S. R. Hamilton, A. C. Preisinger, G. Thomas, K. W. Kinzler, *et al.* 1990. Identification of a chromosome 18q gene that is altered in colorectal cancers. Science 247:49-56.

Fitzgerald, D. P., D. Bradford, and H. M. Cooper. 2007. Neogenin is expressed on neurogenic and gliogenic progenitors in the embryonic and adult central nervous system. Gene Expr. Patterns. 7:784-792.

Fitzgerald, D. P., S. J. Cole, A. Hammond, C. Seaman, and H. M. Cooper. 2006. Characterization of neogenin-expressing neural progenitor populations and migrating neuroblasts in the embryonic mouse forebrain. Neuroscience 142:703-716.

Forcet, C., E. Stein, L. Pays, V. Corset, F. Llambi, M. Tessier-Lavigne, and P. Mehlen. 2002. Netrin-1-mediated axon outgrowth requires deleted in colorectal cancer-dependent MAPK activation. Nature 417:443-447.

Fujita, Y., J. Taniguchi, M. Uchikawa, M. Endo, K. Hata, T. Kubo, B. K. Mueller, and T. Yamashita. 2008. Neogenin regulates neuronal survival through DAP kinase. Cell Death. Differ. 15:1593-1608.

Gad, J. M., S. L. Keeling, A. F. Wilks, S. S. Tan, and H. M. Cooper. 1997. The expression patterns of guidance receptors, DCC and Neogenin, are spatially and temporally distinct throughout mouse embryogenesis. Dev. Biol. 192:258-273.

Geisbrecht, B. V., K. A. Dowd, R. W. Barfield, P. A. Longo, and D. J. Leahy. 2003. Netrin binds discrete subdomains of DCC and UNC5 and mediates interactions between DCC and heparin. J. Biol. Chem. 278:32561-32568.

Gessert, S., D. Maurus, and M. Kuhl. 2008. Repulsive guidance molecule A (RGM A) and its receptor neogenin during neural and neural crest cell development of *Xenopus* laevis. Biol. Cell 100:659-673.

Goldschneider, D. and P. Mehlen. 2010. Dependence receptors: a new paradigm in cell signaling and cancer therapy. Oncogene 29:1865-1882.

Goldschneider, D., N. Rama, C. Guix, and P. Mehlen. 2008. The neogenin intracellular domain regulates gene transcription via nuclear translocation. Mol. Cell Biol. 28:4068-4079.

Grados-Munro, E. M. and A. E. Fournier. 2003. Myelin-associated inhibitors of axon regeneration. J. Neurosci. Res. 74:479-485.

Hata, K., M. Fujitani, Y. Yasuda, H. Doya, T. Saito, S. Yamagishi, B. K. Mueller, and T. Yamashita. 2006. RGMa inhibition promotes axonal growth and recovery after spinal cord injury. J. Cell Biol. 173:47-58.

Hata, K., K. Kaibuchi, S. Inagaki, and T. Yamashita. 2009. Unc5B associates with LARG to mediate the action of repulsive guidance molecule. J. Cell Biol. 184:737-750.

Hecker, T. P., Q. Ding, T. A. Rege, S. K. Hanks, and C. L. Gladson. 2004. Overexpression of FAK promotes Ras activity through the formation of a FAK/p120RasGAP complex in malignant astrocytoma cells. Oncogene 23:3962-3971.

Hong, K., L. Hinck, M. Nishiyama, M. M. Poo, M. Tessier-Lavigne, and E. Stein. 1999. A ligand-gated association between cytoplasmic domains of UNC5 and DCC family receptors converts netrin-induced growth cone attraction to repulsion. Cell 97:927-941.

Hoozemans, J. J., R. Veerhuis, J. M. Rozemuller, and P. Eikelenboom. 2006. Neuroinflammation and regeneration in the early stages of Alzheimer's disease pathology. Int. J. Dev. Neurosci. 24:157-165.

Irizarry-Ramirez, M., C. A. Willson, L. Cruz-Orengo, J. Figueroa, I. Velazquez, H. Jones, R. D. Foster, S. R. Whittemore, and J. D. Miranda. 2005. Upregulation of EphA3 receptor after spinal cord injury. J. Neurotrauma 22:929-935.

Jiang, F., H. Yin, and X. Qin. 2012. Fastigial nucleus electrostimulation reduces the expression of repulsive guidance molecule, improves axonal growth following focal cerebral ischemia. Neurochem. Res. 37:1906-1914.

Kee, N., N. Wilson, V. M. De, D. Bradford, B. Key, and H. M. Cooper. 2008. Neogenin and RGMa control neural tube closure and neuroepithelial morphology by regulating cell polarity. J. Neurosci. 28:12643-12653.

Keeling, S. L., J. M. Gad, and H. M. Cooper. 1997. Mouse Neogenin, a DCC-like molecule, has four splice variants and is expressed widely in the adult mouse and during embryogenesis. Oncogene 15:691-700.

Keino-Masu, K., M. Masu, L. Hinck, E. D. Leonardo, S. S. Chan, J. G. Culotti, and M. Tessier-Lavigne. 1996. Deleted in Colorectal Cancer (DCC) encodes a netrin receptor. Cell 87:175-185.

Keleman, K. and B. J. Dickson. 2001. Short- and long-range repulsion by the *Drosophila* Unc5 netrin receptor. Neuron 32:605-617.

Key, B. and G. J. Lah. 2012. Repulsive guidance molecule A (RGMa): a molecule for all seasons. Cell Adh. Migr. 6:85-90.

Koeberle, P. D., A. Tura, N. G. Tassew, L. C. Schlichter, and P. P. Monnier. 2010. The repulsive guidance molecule, RGMa, promotes retinal ganglion cell survival *in vitro* and *in vivo*. Neuroscience 169:495-504.

Kubo, T., M. Endo, K. Hata, J. Taniguchi, K. Kitajo, S. Tomura, A. Yamaguchi, B. K. Mueller, and T. Yamashita. 2008. Myosin IIA is required for neurite outgrowth inhibition produced by repulsive guidance molecule. J. Neurochem. 105:113-126.

Kulkarni, S., P. Nagarajan, J. Wall, D. J. Donovan, R. L. Donell, A. H. Ligon, S. Venkatachalam, and B. J. Quade. 2008. Disruption of chromodomain helicase DNA binding protein 2 (CHD2) causes scoliosis. Am. J. Med. Genet. A 146A:1117-1127.

Kumar, S., C. W. Wagner, C. Frayne, L. Zhu, M. Selim, W. Feng, and G. Schlaug. 2011. Noninvasive brain stimulation may improve stroke-related dysphagia: a pilot study. Stroke 42:1035-1040.

Kuninger, D., R. Kuzmickas, B. Peng, J. E. Pintar, and P. Rotwein. 2004. Gene discovery by microarray: identification of novel genes induced during growth factor-mediated muscle cell survival and differentiation. Genomics 84:876-889.

Kuns-Hashimoto, R., D. Kuninger, M. Nili, and P. Rotwein. 2008. Selective binding of RGMc/hemojuvelin, a key protein in systemic iron metabolism, to BMP-2 and neogenin. Am. J. Physiol Cell Physiol 294:C994-C1003.

Lah, G. J. and B. Key. 2012a. Dual roles of the chemorepellent axon guidance molecule RGMa in establishing pioneering axon tracts and neural fate decisions in embryonic vertebrate forebrain. Dev Neurobiol 72:1458-1470.

Lah, G. J. and B. Key. 2012b. Novel roles of the chemorepellent axon guidance molecule RGMa in cell migration and adhesion. Mol. Cell Biol. 32:968-980.

Lai Wing, S. K., J. P. Correia, and T. E. Kennedy. 2011. Netrins: versatile extracellular cues with diverse functions. Development 138:2153-2169.

Leonardo, E. D., L. Hinck, M. Masu, K. Keino-Masu, S. L. Ackerman, and M. Tessier-Lavigne. 1997. Vertebrate homologues of C. elegans UNC-5 are candidate netrin receptors. Nature 386:833-838.

Lesnick, T. G., S. Papapetropoulos, D. C. Mash, J. Ffrench-Mullen, L. Shehadeh, A. M. de, J. R. Henley, W. A. Rocca, J. E. Ahlskog, and D. M. Maraganore. 2007. A genomic pathway approach to a complex disease: axon

guidance and Parkinson disease. PLoS. Genet. 3:e98.

Liu, X., M. Hashimoto, H. Horii, A. Yamaguchi, K. Naito, and T. Yamashita. 2009. Repulsive guidance molecule b inhibits neurite growth and is increased after spinal cord injury. Biochem. Biophys. Res. Commun. 382:795-800.

Llambi, F., F. Causeret, E. Bloch-Gallego, and P. Mehlen. 2001. Netrin-1 acts as a survival factor via its receptors UNC5H and DCC. EMBO J. 20:2715-2722.

Ly, A., A. Nikolaev, G. Suresh, Y. Zheng, M. Tessier-Lavigne, and E. Stein. 2008. DSCAM is a netrin receptor that collaborates with DCC in mediating turning responses to netrin-1. Cell 133:1241-1254.

Marfella, C. G. and A. N. Imbalzano. 2007. The Chd family of chromatin remodelers. Mutat. Res. 618:30-40.

Matsunaga, E., H. Nakamura, and A. Chedotal. 2006. Repulsive guidance molecule plays multiple roles in neuronal differentiation and axon guidance. J. Neurosci. 26:6082-6088.

Matsunaga, E., S. Tauszig-Delamasure, P. P. Monnier, B. K. Mueller, S. M. Strittmatter, P. Mehlen, and A. Chedotal. 2004. RGM and its receptor neogenin regulate neuronal survival. Nat. Cell Biol. 6:749-755.

Mawdsley, D. J., H. M. Cooper, B. M. Hogan, S. H. Cody, G. J. Lieschke, and J. K. Heath. 2004. The Netrin receptor Neogenin is required for neural tube formation and somitogenesis in zebrafish. Dev. Biol. 269:302-315.

Mehlen, P. and E. R. Fearon. 2004. Role of the dependence receptor DCC in colorectal cancer pathogenesis. J. Clin. Oncol. 22:3420-3428.

Monnier, P. P., A. Sierra, P. Macchi, L. Deitinghoff, J. S. Andersen, M. Mann, M. Flad, M. R. Hornberger, B. Stahl, F. Bonhoeffer, and B. K. Mueller. 2002. RGM is a repulsive guidance molecule for retinal axons. Nature 419:392-395.

Moos, M., R. Tacke, H. Scherer, D. Teplow, K. Fruh, and M. Schachner. 1988. Neural adhesion molecule L1 as a member of the immunoglobulin superfamily with binding domains similar to fibronectin. Nature 334:701-703.

Muramatsu, R., T. Kubo, M. Mori, Y. Nakamura, Y. Fujita, T. Akutsu, T. Okuno, J. Taniguchi, A. Kumanogoh, M. Yoshida, H. Mochizuki, S. Kuwabara, and T. Yamashita. 2011. RGMa modulates T cell responses and is involved in autoimmune encephalomyelitis. Nat. Med. 17:488-494.

Nakashiba, T., T. Ikeda, S. Nishimura, K. Tashiro, T. Honjo, J. G. Culotti, and S. Itohara. 2000. Netrin-G1: a novel glycosyl phosphatidylinositol-linked mammalian netrin that is functionally divergent from classical netrins. J. Neurosci. 20:6540-6550.

Niederkofler, V., R. Salie, M. Sigrist, and S. Arber. 2004. Repulsive guidance molecule (RGM) gene function is required for neural tube closure but not retinal topography in the mouse visual system. J. Neurosci. 24:808-818.

Nohra, R., A. D. Beyeen, J. P. Guo, M. Khademi, E. Sundqvist, M. T. Hedreul, F. Sellebjerg, C. Smestad, A. B. Oturai, H. F. Harbo, E. Wallstrom, J. Hillert, L. Alfredsson, I. Kockum, M. Jagodic, J. Lorentzen, and T. Olsson. 2010. RGMA and IL21R show association with experimental inflammation and multiple sclerosis. Genes Immun. 11:279-293.

Okamura, Y., E. Kohmura, and T. Yamashita. 2011. TACE cleaves neogenin to desensitize cortical neurons to the repulsive guidance molecule. Neurosci. Res. 71:63-70.

Oldekamp, J., N. Kramer, G. Alvarez-Bolado, and T. Skutella. 2004. Expression pattern of the repulsive guidance molecules RGM A, B and C during mouse development. Gene Expr. Patterns. 4:283-288.

Page, S. J., L. Levin, V. Hermann, K. Dunning, and P. Levine. 2012. Longer versus shorter daily durations of electrical stimulation during task-specific practice in moderately impaired stroke. Arch. Phys. Med. Rehabil. 93:200-206.

Pasterkamp, R. J., P. N. Anderson, and J. Verhaagen. 2001. Peripheral nerve injury fails to induce growth of lesioned ascending dorsal column axons into spinal cord scar tissue expressing the axon repellent Semaphorin3A. Eur. J. Neurosci. 13:457-471.

Phan, K. D., L. P. Croteau, J. W. Kam, A. Kania, J. F. Cloutier, and S. J. Butler. 2011. Neogenin may functionally substitute for Dcc in chicken. PLoS. One. 6:e22072.

Purohit, A. A., W. Li, C. Qu, T. Dwyer, Q. Shao, K. L. Guan, and G. Liu. 2012. Down syndrome cell adhesion molecule (DSCAM) associates with uncoordinated-5C (UNC5C) in netrin-1-mediated growth cone collapse. J. Biol. Chem. 287:27126-27138.

Rajagopalan, S., L. Deitinghoff, D. Davis, S. Conrad, T. Skutella, A. Chedotal, B. K. Mueller, and S. M. Strittmatter. 2004. Neogenin mediates the action of repulsive guidance molecule. Nat. Cell Biol. 6:756-762.

Ren, X. R., G. L. Ming, Y. Xie, Y. Hong, D. M. Sun, Z. Q. Zhao, Z. Feng, Q. Wang, S. Shim, Z. F. Chen, H. J. Song, L. Mei, and W. C. Xiong. 2004. Focal adhesion kinase in netrin-1 signaling. Nat. Neurosci. 7:1204-1212.

Rinne, J. O., J. Rummukainen, L. Paljarvi, and U. K. Rinne. 1989. Dementia in Parkinson's disease is related to neuronal loss in the medial substantia nigra. Ann. Neurol. 26:47-50.

Samad, T. A., A. Rebbapragada, E. Bell, Y. Zhang, Y. Sidis, S. J. Jeong, J. A. Campagna, S. Perusini, D. A. Fabrizio, A. L. Schneyer, H. Y. Lin, A. H. Brivanlou, L. Attisano, and C. J. Woolf. 2005. DRAGON, a bone morphogenetic protein co-receptor. J. Biol. Chem. 280:14122-14129.

Satoh, J., H. Tabunoki, T. Ishida, Y. Saito, and K. Arima. 2012. Accumulation of a repulsive axonal guidance molecule RGMa in amyloid plaques: a possible hallmark of regenerative failure in Alzheimer's disease brains. Neuropathol. Appl. Neurobiol.

Schaffar, G., J. Taniguchi, T. Brodbeck, A. H. Meyer, M. Schmidt, T. Yamashita, and B. K. Mueller. 2008. LIM-only protein 4 interacts directly with the repulsive guidance molecule A receptor Neogenin. J. Neurochem. 107:418-431.

Schmidtmer, J. and D. Engelkamp. 2004. Isolation and expression pattern of three mouse homologues of chick Rgm. Gene Expr. Patterns. 4:105-110.

Schnichels, S., P. Heiduschka, and S. Julien. 2011. Different spatial and temporal protein expressions of repulsive guidance molecule a and neogenin in the rat optic nerve after optic nerve crush with and without lens injury. J. Neurosci. Res. 89:490-505.

Schnichels, S., P. Heiduschka, and S. Julien. 2012. RGMA and neogenin protein expression are influenced by lens injury following optic nerve crush in the rat retina. Graefes Arch. Clin. Exp. Ophthalmol. 250:39-50.

Schwab, J. M., P. P. Monnier, H. J. Schluesener, S. Conrad, R. Beschorner, L. Chen, R. Meyermann, and B. K. Mueller. 2005. Central nervous system injury-induced repulsive guidance molecule expression in the adult human brain. Arch. Neurol. 62:1561-1568.

Serafini, T., S. A. Colamarino, E. D. Leonardo, H. Wang, R. Beddington, W. C. Skarnes, and M. Tessier-Lavigne. 1996. Netrin-1 is required for commissural axon guidance in the developing vertebrate nervous system. Cell 87:1001-1014.

Serafini, T., T. E. Kennedy, M. J. Galko, C. Mirzayan, T. M. Jessell, and M. Tessier-Lavigne. 1994. The netrins define a family of axon outgrowth-promoting proteins homologous to C. elegans UNC-6. Cell 78:409-424.

Severyn, C. J., U. Shinde, and P. Rotwein. 2009. Molecular biology, genetics and biochemistry of the repulsive guidance molecule family. Biochem. J. 422:393-403.

Shen, H., H. Illges, A. Reuter, and C. A. Stuermer. 2002. Cloning, expression, and alternative splicing of neogenin1 in zebrafish. Mech. Dev. 118:219-223.

Shin, G. J. and N. H. Wilson. 2008. Overexpression of repulsive guidance molecule (RGM) a induces cell death through Neogenin in early vertebrate development. J. Mol. Histol. 39:105-113.

Shoemaker, L. D., N. M. Orozco, D. H. Geschwind, J. P. Whitelegge, K. F. Faull, and H. I. Kornblum. 2010. Identification of differentially expressed proteins in murine embryonic and postnatal cortical neural progenitors. PLoS. One. 5:e9121.

Shohat, G., T. Spivak-Kroizman, O. Cohen, S. Bialik, G. Shani, H. Berrisi, M. Eisenstein, and A. Kimchi. 2001. The pro-apoptotic function of death-associated protein kinase is controlled by a unique inhibitory autophosphorylation-based mechanism. J. Biol. Chem. 276:47460-47467.

Sospedra, M. and R. Martin. 2005. Immunology of multiple sclerosis. Annu. Rev. Immunol. 23:683-747.

Tassew, N. G., J. Charish, N. G. Seidah, and P. P. Monnier. 2012. SKI-1 and Furin generate multiple RGMa fragments that regulate axonal growth. Dev. Cell 22:391-402.

Tassew, N. G., L. Chestopolava, R. Beecroft, E. Matsunaga, H. Teng, A. Chedotal, and P. P. Monnier. 2008. Intraretinal RGMa is involved in retino-tectal mapping. Mol. Cell Neurosci. 37:761-769.

Tessier-Lavigne, M. and C. S. Goodman. 1996. The molecular biology of axon guidance. Science 274:1123-1133.

Trapp, B. D. and K. A. Nave. 2008. Multiple sclerosis: an immune or neurodegenerative disorder? Annu. Rev. Neurosci. 31:247-269.

Uchida, Y. 2010. Molecular mechanisms of regeneration in Alzheimer's disease brain. Geriatr. Gerontol. Int. 10 Suppl 1:S158-S168.

Vielmetter, J., J. F. Kayyem, J. M. Roman, and W. J. Dreyer. 1994. Neogenin, an avian cell surface protein expressed during terminal neuronal differentiation, is closely related to the human tumor suppressor molecule deleted in colorectal cancer. J. Cell Biol. 127:2009-2020.

Wang, H., N. G. Copeland, D. J. Gilbert, N. A. Jenkins, and M. Tessier-Lavigne. 1999. Netrin-3, a mouse homolog of human NTN2L, is highly expressed in sensory ganglia and shows differential binding to netrin receptors. J. Neurosci. 19:4938-4947.

Wilson, N. H. and B. Key. 2006. Neogenin interacts with RGMa and netrin-1 to guide axons within the embryonic vertebrate forebrain. Dev. Biol. 296:485-498.

Xia, Y., J. L. Babitt, Y. Sidis, R. T. Chung, and H. Y. Lin. 2008. Hemojuvelin regulates hepcidin expression via a selective subset of BMP ligands and receptors independently of neogenin. Blood 111:5195-5204.

Yamakawa, K., Y. K. Huot, M. A. Haendelt, R. Hubert, X. N. Chen, G. E. Lyons, and J. R. Korenberg. 1998. DSCAM: a novel member of the immunoglobulin superfamily maps in a Down syndrome region and is involved in the development of the nervous system. Hum. Mol. Genet. 7:227-237.

Yamashita, T., M. Fujitani, S. Yamagishi, K. Hata, and F. Mimura. 2005. Multiple signals regulate axon regeneration through the Nogo receptor complex. Mol. Neurobiol. 32:105-111.

Yamashita, T., B. K. Mueller, and K. Hata. 2007. Neogenin and repulsive guidance molecule signaling in the central nervous system. Curr. Opin. Neurobiol. 17:29-34.

Yang, F., A. P. West, Jr., G. P. Allendorph, S. Choe, and P. J. Bjorkman. 2008. Neogenin interacts with hemojuvelin through its two membrane-proximal fibronectin type III domains. Biochemistry 47:4237-4245.

Yaron, A. and B. Zheng. 2007. Navigating their way to the clinic: emerging roles for axon guidance molecules in neurological disorders and injury. Dev. Neurobiol. 67:1216-1231.

Yin, Y., J. R. Sanes, and J. H. Miner. 2000. Identification and expression of mouse netrin-4. Mech. Dev. 96:115-119.

Yurchenco, P. D. and W. G. Wadsworth. 2004. Assembly and tissue functions of early embryonic laminins and netrins. Curr. Opin. Cell Biol. 16:572-579.

Zhang, A. S., A. P. West, Jr., A. E. Wyman, P. J. Bjorkman, and C. A. Enns. 2005. Interaction of hemojuvelin with neogenin results in iron accumulation in human embryonic kidney 293 cells. J. Biol. Chem. 280:33885-33894.

Zhang, A. S., F. Yang, J. Wang, H. Tsukamoto, and C. A. Enns. 2009. Hemojuvelin-neogenin interaction is required for bone morphogenic protein-4-induced hepcidin expression. J. Biol. Chem. 284:22580-22589.

Zhang, G., J. H. Zhang, J. Feng, Q. Li, X. Wu, and X. Qin. 2011. Electrical stimulation of olfactory bulb downregulates RGMa expression after ischemia/reperfusion injury in rats. Brain Res. Bull. 86:254-261.

Zhou, Z., J. Xie, D. Lee, Y. Liu, J. Jung, L. Zhou, S. Xiong, L. Mei, and W. C. Xiong. 2010. Neogenin regulation of BMP-induced canonical Smad signaling and endochondral bone formation. Dev. Cell 19:90-102.

CHAPTER 2

Getting connected in the dopamine system

DIANNE M.A. VAN DEN HEUVEL AND
R. JEROEN PASTERKAMP

Department of Neuroscience and Pharmacology, Rudolf Magnus Institute of Neuroscience, University Medical Center Utrecht, Universiteitsweg 100, 3584 CG, Utrecht, The Netherlands

Progress in Neurobiology 85 (2008) 75-93

ELSEVIER

Progress in Neurobiology 85 (2008) 75–93

progress in Neurobiology

www.elsevier.com/locate/pneurobio

Getting connected in the dopamine system

Dianne M.A. Van den Heuvel, R. Jeroen Pasterkamp *

Department of Neuroscience and Pharmacology, Rudolf Magnus Institute of Neuroscience, University Medical Center Utrecht, Universiteitsweg 100, 3584 CG Utrecht, The Netherlands

Received 13 August 2007; received in revised form 30 November 2007; accepted 7 January 2008

Abstract

Dopaminergic neurons located in the ventral midbrain (i.e. mesodiencephalic dopamine, mdDA, neurons) are essential for the control of diverse cognitive and motor behaviors and are associated with multiple psychiatric and neurodegenerative disorders. Three anatomically and functionally distinct subgroups of mdDA neurons have been identified (A8–A10) which give rise to prominent forebrain projections (i.e. the mesostriatal, mesocortical and mesolimbic pathways). The development of mdDA neurons is a complex, multi-step process. It includes early developmental events such as cell fate specification, differentiation and migration, and later events including neurite growth, guidance and pruning, and synapse formation. Significant progress has been made in defining the early events involved in mdDA neuron development [see Smits, S.M., Burbach, J.P., Smidt, M.P., 2006. Developmental origin and fate of meso-diencephalic dopamine neurons. Prog. Neurobiol. 78, 1–16.]. Although later stages of mdDA neuron development are less well understood, recent studies have begun to identify cellular and molecular signals thought to be involved in establishing mdDA neuronal connectivity. The purpose of the present review is to summarize our current understanding of the ontogeny and anatomy of mdDA axon pathways, to highlight recent progress in defining the cellular and molecular mechanisms that underlie the formation and remodeling of mdDA circuits, and to discuss the significance of this progress for understanding and treating situations of perturbed connectivity in the mdDA system.

Keywords: Axon guidance; Development; Drug addiction; Neuronal connectivity; Pruning; Topographic mapping; Parkinson's disease; Plasticity

Contents

Abbreviations: BMP, Bone morphogenetic protein; CNS, Central nervous system; CPu, Caudate putamen; DCC, Deleted in corectal cancer; DM, Dorsal midbrain; EC, External capsule; ES, Embryonic stem; FGF, Fibroblast growth factor; GE, Ganglionic eminence; GDNF, Glial cell line-derived neurotrophic factor; GFAP, Glial fibrillary acidic protein; GPI, Glycophosphatidylinositol; LINGO, leucine-rich repeat Ig-containing; LRRK2, Leucine-rich repeat kinase-2; mdDA, Mesodiencephalic dopamine; MFB, Medial forebrain bundle; NAc, Nucleus accumbens; Pax6, Paired box 6; PD, Parkinson's disease; PFC, Prefrontal cortex; Robo, Roundabout; RRF, Retrorubal field; SHH, Sonic hedgehog; SN, Substantia nigra; SNc, Substantia nigra pars compacta; TH, Tyrosine hydroxylase; VM, Ventral midbrain; VTA, Ventral tegmental area.

* Corresponding author. Tel.: +31 88 7568831; fax: +31 88 7569032.
E-mail address: r.j.pasterkamp@umcutrecht.nl (R.J. Pasterkamp).

0301-0082/$ – see front matter © 2008 Elsevier Ltd. All rights reserved.
doi:10.1016/j.pneurobio.2008.01.003

1. Introduction

Dopaminergic neurons located in the ventral midbrain are essential for the control of cognitive and motor behaviors and are associated with multiple psychiatric and neurodegenerative disorders. Three anatomically and functionally distinct subgroups of mesodiencephalic dopamine (mdDA) neurons have been identified (Carlsson et al., 1962; Dahlström and Fuxe, 1964; Hökfelt et al., 1984). The lateral A9 group corresponds to neurons of the substantia nigra pars compacta (SNc). These neurons have prominent projections to the dorsal striatum (the so-called nigrostriatal or mesostriatal pathway) and are involved in the control of voluntary movement. SNc neurons have been the subject of intense study since their selective degeneration is responsible for the motor defects observed in individuals suffering from Parkinson's disease (PD) (Savitt et al., 2006; Sulzer, 2007). The medial A10 and A8 groups define the ventral tegmental area (VTA) and retrorubal field (RRF), respectively. Neurons in these subgroups prominently innervate the ventromedial striatum and prefrontal cortex (PFC), as part of the mesocorticolimbic system, and are involved in the regulation of emotions and reward. Defective dopaminergic transmission in the limbic system has been implicated in the development of drug addiction, depression and schizophrenia (Nestler, 2000; Robinson and Berridge, 1993). The important link between mdDA neurons and profound neurological and neurodegenerative disorders has triggered an intense study of mdDA neuron function, including of their development. The development of mdDA neurons is a complex, multi-step process. It includes early developmental events such as cell fate specification, differentiation and migration and later events including neurite growth, guidance and pruning, and synapse formation. Significant progress has been made in defining some of the early events. This includes the identification of key transcriptional determinants regulating regional specification and cellular differentiation (Smidt and Burbach, 2007). Although later stages of mdDA neuron development are less well understood, recent studies have begun to identify cellular and molecular signals thought to be important for the establishment of mdDA neuronal connectivity. The purpose of the present review is to summarize our current understanding of the ontogeny and anatomy of mdDA axon projections, to highlight recent progress in defining the cellular and molecular mechanisms that underlie the formation and remodeling of mdDA circuits, and to discuss the significance of this progress for understanding and treating situations of perturbed connectivity in the mdDA system.

2. Ontogeny of mdDA projections

The estimated number of neurons in the adult bilateral mdDA system (A8–A10) ranges from 20,000–30,000 in mice to 400,000–600,000 in human. These neurons give rise to prominent forebrain projections and receive inputs from various other brain regions (Bjorklund and Dunnett, 2007). Work in several different species and employing diverse experimental approaches (e.g. immunohistochemistry, axon tract tracing or XFP-labeled mice) has provided valuable insight into the development of mdDA circuits. Here we summarize our current understanding of the ontogeny of neuronal connectivity in the mdDA system with an emphasis on ascending forebrain projections. We focus on the development of rat mdDA pathways, which have been studied in most detail, unless specified otherwise. In addition, most of what is summarized below is derived from studies using anti-dopamine antibodies to detect mdDA fibers (as well as fibers derived from other dopaminergic nuclei). It should be noted that small discrepancies exist between studies using different markers (e.g. dopamine, tyrosine hydroxylase (TH), dopamine-β-hydroxylase) to examine the ontogeny of dopaminergic fiber outgrowth (see for example discussion in Bjorklund and Dunnett, 2007; Kalsbeek et al., 1988; Voorn et al., 1988).

2.1. Axon growth and guidance

2.1.1. Midbrain and medial forebrain bundle

In rat, the first mdDA neurons are born around E12 and begin to extend processes at E13 (Smidt and Burbach, 2007). These axonal processes initially follow a dorsal trajectory in the midbrain region but then deflect rostrally towards the forebrain (Gates et al., 2004; Nakamura et al., 2000). Following this reorientation, mdDA axons take a ventrorostral course through the diencephalon towards the telencephalon (Gates et al., 2004; Nakamura et al., 2000). Following their exit from the midbrain, individual mdDA axons fasciculate into two large axon bundles, called the medial forebrain bundles (MFBs). The

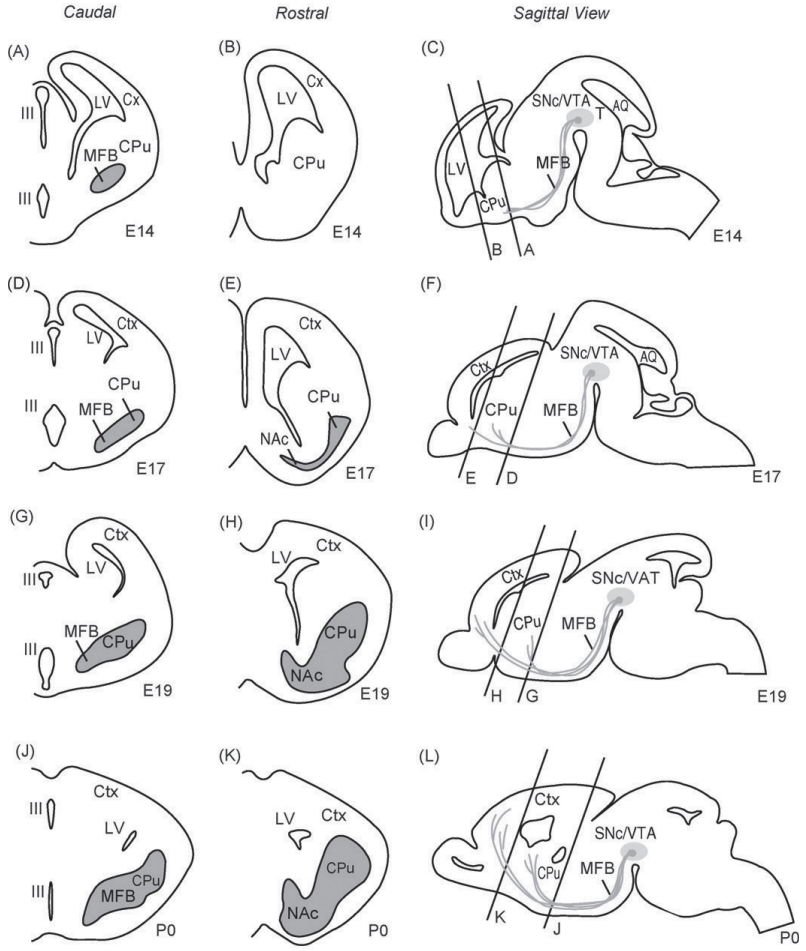

Fig. 1. Ontogeny of mesostriatal projections. Schematic representations illustrating the spatiotemporal distribution of mesodiencephalic dopamine (mdDA) axons in the caudal (A, D, G, and J) and rostral (B, E, H, and K) striatum and in a sagittal view (C, F, I, and L) during development. The rostrocaudal levels represented by panels A, B, D, E, G, H, J, and K are indicated in panels C, F, I and L. (A–C) By E14, mdDA axons reach a region ventrolateral to the developing ganglionic eminence/caudate putamen (CPu) in the caudal forebrain. No mdDA axons can be detected at more rostral levels. (D–F) Over the next few days, mdDA axons continue to accumulate ventrolaterally to the CPu and around E17 mdDA fibers start to innervate the striatum and to extend further rostrally. (G–I) At E19, both caudal and rostral parts of the striatum are heavily innervated by mdDA axons. MdDA innervation is restricted to more lateral regions of the striatum containing differentiated striatal cells. (J–L) At P0, differentiation of the striatum continues and mdDA axons reach more medial parts of the striatum closer to the lateral ventricle (LV). For more details, see corresponding text. III, third ventricle; AQ, aquaduct; Ctx, cortex; MFB, medial forebrain bundle; NAc, nucleus accumbens; SNc/VTA, substantia nigra pars compacta/ventral tegmental area.

MFBs run in the ventrolateral part of the telencephalon and contain mdDA (and non-mdDA) projections to different forebrain regions such as the striatum and cerebral cortex (see Section 2.1.2) (Fig. 1) (e.g. Specht et al., 1981a; Verney, 1999; Voorn et al., 1988; Zhao et al., 2004).

2.1.2. Targets

2.1.2.1. Striatum. The adult striatum is densely innervated by mdDA axons originating from the substantia nigra (SN) and VTA, and to a lesser extent the RRF (Bentivoglio and Morelli, 2005; Bjorklund and Lindvall, 1983). By E14, mdDA fibers in the MFB reach and start to invade the area ventrolateral to the ganglionic eminence (GE) in the rat (Fig. 1A–C). One day later, mdDA fibers in this area become more numerous. In addition, mdDA axons can be found in the primordium of the nucleus accumbens (NAc). At E17, large mdDA axon bundles begin to enter the GE/caudate putamen (CPu) and partially proceed towards the cortex (see Section 2.1.2.2). The majority of mdDA axons are located ventrolaterally in the GE/CPu from where projections extend to the dorsolateral striatum. Interestingly,

the innervation of the GE/CPu by mdDA axons follows a temperospatial gradient that mirrors the pattern of neurogenesis and differentiation of mdDA and striatal neurons, i.e. the most mature dopamine neurons contact the most mature striatal neurons first (Fig. 1D–F) (Specht et al., 1981b; Voorn et al., 1988). At E18, mdDA axons enter the rostral part of the striatum and an intricate network of mdDA fibers emerges at the level of the fornix descending into the septum. At E19, the highest density of mdDA axons in the rostral striatum is found laterally along the external capsule (EC). The EC forms a barrier for the majority of mdDA axons but a subset of fibers passes through to the cortex. At caudal levels, the bulk of mdDA axons are located in the ventromedial striatum. From here, mdDA axons extend into dorsal, medial and lateral directions (Fig. 1G–I). At E20, mdDA axons innervate striatal regions closer to the lateral ventricle (Fig. 1J–L) and the following day patches of mdDA fibers appear in the dorsal followed by the medial striatum. These patches are comprised of extensive ramifications of caudorostrally oriented mdDA axons (Voorn et al., 1988). During the first postnatal week, innervation of striatal regions adjacent to the lateral ventricle increases. In addition, striatal patches become more conspicuous, even in the rostral striatum (Loizou, 1972; Voorn et al., 1988). Intriguingly, by the third week after birth, many patches are replaced by a diffuse innervation of the striatum. In the adult, patches persist in the dorsal and dorsolateral striatum (caudate putamen, CPu) and in the NAc (Ungerstedt, 1971; Voorn et al., 1988).

2.1.2.2. Cortex. In the adult rat, the PFC, perirhinal cortex and cingulate cortex receive a dense dopaminergic input. In addition, widespread but sparse innervation of mdDA fibers can be observed in other cortical regions (Bentivoglio and Morelli, 2005; Bjorklund and Lindvall, 1983). Before E15, no mdDA fibers are present in the cortical anlage. At E15, the first mdDA fibers pass through the developing striatum to the frontal cortex. These early axons are located in the intermediate zone beneath the subplate and the cortical plate (Fig. 2A and B). As the striatum develops, the EC grows into a clear border with a small subset of mdDA fibers traversing through towards the frontal cortex (Kalsbeek et al., 1988). At E16, more axons extend towards the frontal cortex. Most of these fibers are found in the upper part of the intermediate zone and subplate. Some of the most rostral fibers cross the cortical plate to innervate the marginal zone. The next 2 days, mdDA axons extend dorsally in

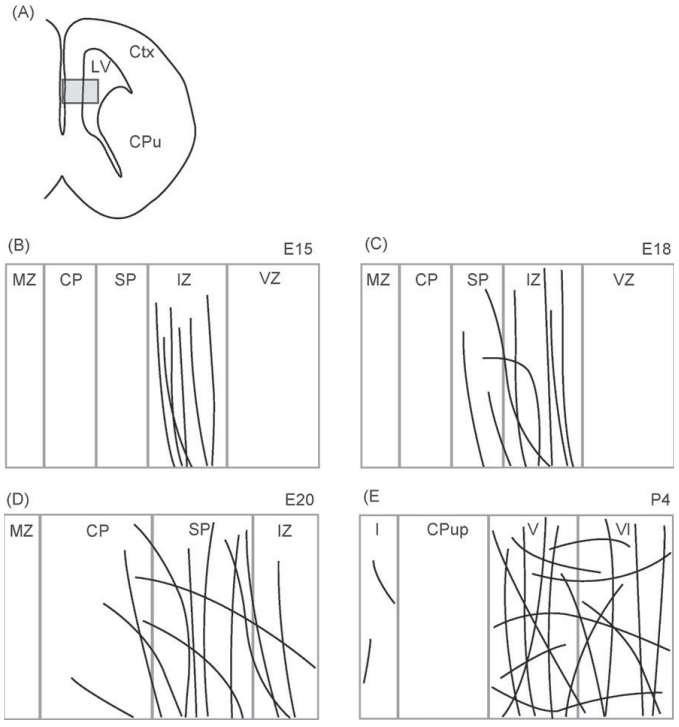

Fig. 2. Ontogeny of mesocortical projections. (A) Schematic representation indicating the region shown in B through E. (B) At E15, mesodiencephalic dopamine (mdDA) axons run in the intermediate zone (IZ) below the subplate (SP) and cortical plate (CP). (C) Over the next few days, mdDA axons extend into the SP but do not enter the CP. (D) At E20, the CP is increasing in size and mdDA axons are extending from the SP into the CP. (E) During postnatal development mdDA innervation and cortical development seem to be correlated, i.e. mdDA axons innervate cortical layers that contain differentiated cells first (starting with layer VI). For more details, see corresponding text. I, layer I; CPu, caudate putamen; CPup, cortical plate upper zone; LV, lateral ventricle; MZ, marginal zone; V, layer V; VZ, ventricular zone.

the subplate of the lateral and medial walls but do not enter the cortical plate (Fig. 2C). Such a ''waiting period'' for mdDA axons in the subplate is also observed in other species including humans (Verney, 1999). At E17, sparse but widespread dopaminergic innervation can be found in other regions of the cerebral cortex such as in somatosensory and occipital cortical areas (Berger et al., 1985; Kalsbeek et al., 1988; Verney et al., 1982). From E20, the cortical plate is increasing in size and the first mdDA axons are extending from the subplate towards the cortical plate (Fig. 2D). During postnatal development, mdDA innervation and cortical development seem to be correlated. MdDA fibers only innervate layers of the cortex that contain differentiated cells (starting with layer VI), while the upper cortical plate with undifferentiated cells is largely devoid of mdDA fiber ingrowth (Fig. 2E). At the end of the first postnatal week, most of the adult characteristics of the topography of mdDA fibers in the PFC can be recognized (Kalsbeek et al., 1988; Van Eden et al., 1987).

2.1.2.3. Other. In addition to the striatum and cortex, a large number of other regions in the adult central nervous system (CNS) are targeted by mdDA fibers including the hippocampus, lateral habenula and amygdala (Bentivoglio and Morelli, 2005). Although several studies note the presence of mdDA fibers in these systems during embryonic development (e.g. Specht et al., 1981b; Voorn et al., 1988) relatively little is known about their precise ontogeny.

2.2. Subset specific wiring

Neurons have often been grouped on basis of neurotransmitter expression or anatomical location. It is becoming increasingly clear, however, that within these neurochemically or anatomically defined neural systems distinct neuronal subsets exist, each displaying unique molecular and functional characteristics (Smits et al., 2006). The selective degeneration of mdDA neurons in the SNc in PD patients confirms the presence of such neuronal subsets within the mdDA system. In addition to neuronal differences between the A8, A9 and A10 groups, neuronal subpopulations with unique anatomical and functional properties exist within each of these groups. For example, in *paired box 6* (*Pax6*) mutant mice most mdDA axons are misrouted dorsorostrally at the p1/p2 border except for a small population of fibers that follows the normal route of the MFB (Vitalis et al., 2000). This observation highlights functional differences between different subsets of mdDA neurons. Furthermore, it has been shown that two largely separate populations of VTA neurons project to the PFC and the NAc (Fallon, 1981; Margolis et al., 2006; Swanson, 1982). The activity of VTA neurons that project to the PFC (mesocortical) but not of those projecting to the NAc (mesolimbic) is influenced by κ opioids (Margolis et al., 2006). This suggests that subsets of VTA mdDA neurons can be independently modulated and supports the idea that they participate in distinct neural circuits within the mdDA system. It is interesting to note that whereas some neuronal subsets are intermixed and scattered throughout the mdDA system, others are concentrated in specific parts of the SN and VTA (Fallon, 1981; Margolis et al., 2006; Swanson, 1982). This complex cellular organization suggests that sophisticated molecular mechanisms must be in place to organize and guide the projections of mdDA neuronal subsets to their specific targets. This idea is supported by recent studies mapping the expression of axon guidance receptors such as deleted in colorectal cancer (DCC) to specific subsets of mdDA neurons. In adult rat, DCC is expressed in a subpopulation of ventral SNc neurons but almost absent from neurons in the dorsal SNc and VTA. In line with this selective pattern of expression, terminal fields in selective parts of SNc projection areas (i.e. the dorsolateral striatum, dorsomedial shell of the NAc, PFC, septum, lateral habenula and ventral pallidum) are labeled for DCC (Osborne et al., 2005). This shows that functionally distinct subsets of mdDA neurons may use specific combinations of axon guidance cues and receptors to establish highly specific projection patterns.

Despite the fact that mdDA neurons in the SNc and VTA have distinct projection targets and functional properties, the population as a whole is often considered to be physiologically and pharmacologically homogeneous. For example, *in vitro* studies using explants or dissociated neurons prepared from early embryonic tissue do often distinguish between SN and VTA. As a result, the results from these studies primarily reflect mdDA cells from VTA, since these cells are in much greater abundance. Therefore, such studies may not provide an accurate reflection of the characteristics of SNc mdDA neurons. In future studies it will be important to consider the distinctions between the SNc and VTA or even between different neuronal subsets within these regions.

2.3. Topographic mapping and axonal pruning

In the adult, SNc mdDA neurons densely innervate the dorsal striatum (the mesostriatal pathway) while VTA mdDA neurons connect to the ventral striatum (the mesolimbic pathway). The mesostriatal pathway is essential for motor functions, while the mesolimbic pathway plays a key role in the motivational aspects of drug addiction as well as in emotion and goal-directed behavior in general. The correlation between the specific functions of different mdDA pathways and their topographic distribution in the striatum suggests that topographic mapping is critical to the functioning of the mdDA system. Interestingly, it has been shown that axonal pruning is essential for the topographic specification of the mesostriatal and mesolimbic pathways (Hu et al., 2004). Pruning is often used to selectively remove exuberant neuronal branches and connections in the immature nervous system to ensure the formation of functional circuitry (Luo and O'Leary, 2005). In contrast to the adult, axon collaterals originating from embryonic VTA and SNc neurons (E15 and E17) do not display a preference for the dorsal or ventral striatum (Fig. 3A). The topographical specificity observed in adulthood is achieved during late embryonic and early postnatal development by the selective elimination of VTA and SNc axon collaterals innervating the dorsal and ventral striatum, respectively (Fig. 3B) (Hu et al., 2004). The molecular signals that regulate

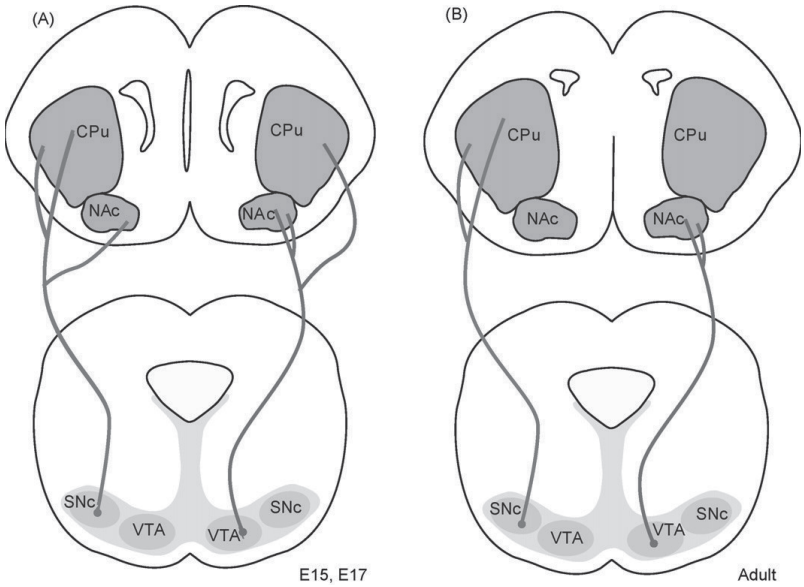

Fig. 3. Axonal pruning. (A) Mesodiencephalic dopamine (mdDA) axon collaterals originating from embryonic substantia nigra pars compacta (SNc) and ventral tegmental area (VTA) neurons (E15 and E17) do not display a preference for the dorsal (caudate putamen (CPu)) or ventral (nucleus accumbens (NAc)) striatum. (B) The topographical specificity of mesostriatal and mesolimbic projections observed in adulthood is achieved during late embryonic and early postnatal development by the selective elimination of VTA and SNc axon collaterals innervating the dorsal and ventral striatum, respectively. Modified from Hu et al. (2004).

the selective pruning of mdDA axon collaterals remain to be identified.

2.4. Adult patterns of connectivity

The organization of axonal projections in the adult mdDA system has been the subject of intense study. In adult rats, the bilateral A8–A10 groups contain ~40,000 TH-positive neurons, with about half of these cells located in the SNc. Interestingly, adult mdDA neurons give rise to complex projections that often do not strictly adhere to the three different mdDA pathways that have been described in literature. For example, although projections from the midbrain to the dorsal striatum are often referred to as nigrostriatal projections, mdDA neurons in the VTA and RRF also project to striatal regions. Similarly, neurons innervating cortical and limbic regions are located not only in the VTA but also in the RRF and SN (Fallon and Moore, 1978; Lindvall and Bjorklund, 1974; Roffler-Tarlov and Graybiel, 1984). Collateralization adds another level of complexity to the organization of adult mdDA pathways. Individual mdDA neurons in the SNc and to a lesser extent in the VTA are believed to project to more than one terminal area (Fallon, 1981; Fallon and Loughlin, 1982; Lindvall and Bjorklund, 1979; Swanson, 1982). It should also be noted that in striking contrast to the mesostriatal, mesolimbic and mesocortical pathways, much less is known about the anatomy and function of mdDA projections to other regions of the adult CNS. For more extensive descriptions and for overviews of adult mdDA pathways in other species, we refer the reader to other recent reviews (Bentivoglio and Morelli, 2005; Bjorklund and Dunnett, 2007).

3. The cellular basis of mdDA axon guidance

Much of what we know today about the molecular and cellular mechanisms regulating neuronal network formation derives from elegant tissue culture experiments. For example, the founding members of several different guidance cue families have been identified on the basis of chemotropic activities observed in co-culture systems that combine projection neurons and their targets (Tessier-Lavigne and Goodman, 1996). Similarly, tissue culture studies have provided a wealth of information on how the cellular environment influences mdDA axon growth and pathfinding. Here, we summarize our current knowledge of the cellular mechanisms that regulate mdDA pathway formation (Fig. 4).

3.1. Midbrain

Embryonic mdDA axons initially follow a dorsal trajectory in the midbrain but then deflect rostrally towards the forebrain. Nakamura et al. (2000) used whole-mount cultures to show that a gradient of directional cues in the dorsal midbrain (DM) contributes to this rostral course. First, they observed that mdDA axons continue to extend towards the rostral pole of the DM following reversal of the rostrocaudal polarity of the DM in

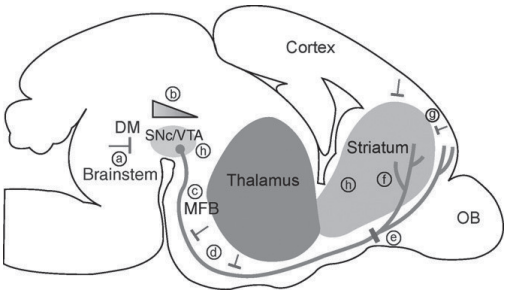

Fig. 4. Cellular influences during mdDA axon outgrowth and pathfinding. Schematic representation illustrating the different brain regions that provide chemotropic information for growing mesodiencephalic dopamine (mdDA) axons during embryonic development. (a) A chemorepulsive activity that emerges from the caudal brainstem has been proposed to guide mdDA axons into a rostral direction towards the telencephalon. (b) A rostral-to-caudal or caudal-to-rostral gradient of axon guidance cues in the dorsal midbrain (DM) instructs mdDA axons to deflect rostrally. (c) The medial forebrain bundle (MFB) region exerts a temporally restricted chemoattractive effect on mdDA axons facilitating their rostral trajectory in the telencephalon. (d) The thalamus is non-permissive for mdDA axon growth and may contribute to the ventrolateral position of the MFB. (e) From E14 to E17 mdDA axons accumulate ventrolaterally to the striatum. Chemorepulsive effects by the overlaying cortex and lack of chemoattractive effects by the striatum may help to enforce this 'waiting period'. (f) Starting at midembryonic stages ganglionic eminence/striatum releases chemoattractive molecules to attract mdDA axons. (g) The cortex has a chemorepulsive influence on mdDA axons which may prevent them from innervating inappropriate cortical areas. (h) In addition to long-distance chemotropic effects, short-range neuron–neuron and neuron–glia interactions are involved in the formation of mdDA connections. OB, olfactory bulb; SNc, substantia nigra pars compacta; VTA, ventral tegmental area. Modified from Gates et al. (2004).

relation to the ventral midbrain (VM) in whole mount preparations. This demonstrates the presence of guidance cues for mdDA axons in the DM. Second, mdDA axons were unable to extend across the border of two caudal or rostral halves of DM. This suggests these guidance cues form a rostrocaudal or caudorostral gradient in the DM (Fig. 4) (Nakamura et al., 2000). In addition to the DM, other structures in close proximity to the mdDA neuron pools may contribute to the initial trajectory of mdDA axons. For example, repulsive cues have been reported to emanate from the caudal brain stem and may repel mdDA axons towards the forebrain (Fig. 4) (Gates et al., 2004). It should be noted, however, that the isthmus and the diencephalon, two other regions neighbouring the region containing developing mdDA neurons, do not influence the growth or guidance of mdDA axons *in vitro* (Nakamura et al., 2000). The molecules that orient mdDA axons in the midbrain towards the forebrain remain to be identified.

3.2. Medial forebrain bundle region

In the forebrain, mdDA axons form two tightly fasciculated longitudinal bundles, the MFBs. Although the molecules that regulate the bundling of mdDA axons are unknown, the MFB region has been shown to exert potent and temporally restricted chemotropic effects on growing mdDA axons *in vitro*. In co-cultures of rat embryonic MFB and midbrain tissue, mdDA axons leave their rostral course and turn to innervate ectopic, caudally positioned medial MFB tissue (Gates et al., 2004). This indicates that the medial MFB region releases a chemoattractant for mdDA axons and may serve as an intermediate target. This idea is consistent with the observation that MFB explants derived from E12 and E15 but not E19 embryos are able to attract mdDA axons (Fig. 4) (Gates et al., 2004). Sustained chemoattraction by the MFB region during late embryogenesis would trap mdDA axons in the MFB and prevent them from innervating their forebrain target regions. In the developing spinal cord it has been shown that the floor plate, an intermediate target for commissural axons, is attractive for pre-crossing but repulsive for post-crossing axons, allowing axons to extend towards and beyond the floorplate but preventing them from accumulating at the midline (Dickson, 2002). Whether similar molecular mechanisms operate in the MFB region is currently unknown.

A characteristic feature of the MFB is its ventrolateral position in the forebrain. Molecular cues emanating from brain regions flanking the presumptive MFB region such as the thalamus and hypothalamus have been postulated to control the ventrolateral course of MFB fibers (see Section 4). Thalamic explants have no long-range chemotropic effects of mdDA axons *in vitro*. However, in contrast to for example striatal tissue mdDA axons fail to enter thalamic explants suggesting the presence of a contact-dependent inhibitor(s) of mdDA axon outgrowth in the thalamus (Fig. 4) (Gates et al., 2004). This idea is further supported by the observation that *Nkx2.1* mutant mice display aberrant midline crossing of MFB fibers and a disorganization of the caudal hypothalamus suggesting that medial brain structures (and the molecules they produce) are involved in maintaining the (ipsi)lateral position of the MFB (Kawano et al., 2003).

3.3. Targets

The robust ingrowth of mdDA axons into the GE/striatum (see Section 2.1.2.1) coincides with the emergence of a potent chemoattractive effect from the embryonic GE/striatum. Both late embryonic and postnatal but not early embryonic GE/striatal explants attract mdDA axons *in vitro* (Fig. 4) (Gates et al., 2004; Johansson and Stromberg, 2003; Ostergaard et al., 1990; Plenz and Kitai, 1996). Thus, axon attraction plays a role at different stages of mdDA neuron development: (1) to guide mdDA axons to the MFB region (E12–E14) (see Section 3.2), and (2) to attract axons from the MFB to the developing striatum (midembryonic and onward). The timing of axon outgrowth through the MFB to the GE/striatum is intriguing. Around E14 in rat, mdDA axons arrive ventral to the GE. Over the subsequent days (until approximately E17) the number of axons in this region increases without notable advance of the projection beyond or into the overlaying striatum (Fig. 4). Such a 'waiting period' is observed in several other neuronal systems, e.g. the spinal cord and the thalamocortical system (Hirata and Fujisawa, 1999; Wang and Scott, 2000). One brain structure that has been proposed to

contribute to this waiting period is the neocortex. The embryonic neocortex exerts chemorepulsive effects on mdDA axons *in vitro* and could both inhibit the rostral progression of mdDA axon growth and prevent fibers from projecting dorsally into the striatal region. The lack of chemoattractive effects from the GE/striatum may also contribute to this waiting period (Gates et al., 2004).

The frontal cortex is another target of mdDA axons (Fig. 4). Remarkably, and as stated above, cortical tissue strongly repels mdDA axons *in vitro* (Gates et al., 2004). However, the cortex is a large and heterogeneous structure and the origin of the cortical explants used in this study was not specified. Other work, employing co-cultures of dissociated mesencephalic and cortical cells, shows that neurons from different cortical regions exert differential effects on the maturation of mdDA neurons (Hemmendinger et al., 1981). These results indicate that characterization of chemotropic influences exerted by (non)-target regions in the cortex on mdDA axons will require microdissection and testing of cortical subregions. Furthermore, it is often difficult to distinguish between the SNc and the VTA at early embryonic stages making it more challenging to assess mdDA subtype-specific chemotropic effects. Neurons in the VTA and SNc are known to innervate distinct brain regions and may respond differentially to different neural tissues. This idea is supported by long-term co-cultures of postnatal explants that show that VTA fibers innervate the cortex, nucleus accumbens and striatum, while axons extending from SN explants only innervate the striatum (Jaumotte and Zigmond, 2005).

The hippocampus receives a minor projection from mdDA neurons and is selectively innervated in midbrain/hippocampal co-cultures suggesting that it is at least permissive for mdDA axon growth. This is in striking contrast to non-target regions such as the cerebellum which is highly non-permissive and repulsive (Jaumotte and Zigmond, 2005; Ostergaard et al., 1990).

3.4. Neuron–neuron and neuron–glia interactions

It is well known that several aspects of neuronal network formation rely on cell–cell interactions. Both neuron–neuron and neuron–glia interactions have been implicated in the wiring of mdDA circuits (Fig. 4).

The terminal fields of mdDA neurons in the striatum and cortex have distinct morphological features. MdDA axons in the striatum form a dense plexus of varicosities while in the frontal cortex single branching axons course through the neuropil and bear infrequent, irregularly shaped varicosities. These specific morphological features can be recapitulated in cultures by combining dissociated mdDA neurons and their target cells. Co-cultures of mesencephalic and striatal cells display a dense axon plexus, while combining cells from the mesencephalon and frontal, but not occipital, cortex leads to the appearance of a punctate network of axonal processes (Hemmendinger et al., 1981). Although in this particular study target-specific effects may have arisen from neuron–glia instead of neuron–neuron interactions (see below), other experiments have confirmed direct effects of target cells on the morphology and function of mdDA neurons (Denis-Donini et al., 1983; di Porzio et al., 1980). For example, neuronal processes of embryonic mdDA axons are significantly shorter in the presence of striatal neurons as compared to non-target cells. In fact, mdDA growth cones even show a tendency to stop when they reach a striatal neuron (Denis-Donini et al., 1983). This together with the observation that striatal membranes and glial cells can promote mdDA neurite outgrowth (Denis-Donini et al., 1983; Tomozawa and Appel, 1986) suggests that neuron–neuron interactions in the striatum may function in target recognition while other striatal cell types (e.g. glia) attract mdDA axons to the developing striatum and/or provide a permissive growth substrate.

Interactions between neurons and glia are essential for the formation of specific neuronal connections (Chotard and Salecker, 2004). In the developing mdDA system, glia and the proteins they produce regulate axon and dendrite growth, pathfinding, branching and targeting (Gates and Dunnett, 2001). The influence of astroglia on mdDA axons is nicely illustrated by co-cultures of ventral mesencephalic and striatal explants in which mdDA axons first use an astroglial bridge to enter the striatal tissue and then continue to extend along an astroglial front within the explant (Gates et al., 1993). Glia are known to exert both negative and positive effects on extending mdDA axons and dendrites through the production of a variety of membrane-bound and soluble proteins including proteoglycans and growth factors. In addition, several of the molecules known to influence mdDA neuron development do so by regulating the morphology and molecular properties of glial cells and their precursors. In a study by Engele and Bohn, for example, the neurotrophic effects of fibroblast growth factor (FGF) on mdDA neurons were found to rely on the increased proliferation of mesencephalic astrocytes in response to FGF (Engele and Bohn, 1991). Glia represent a very heterogenous population of cells and different subpopulations of glial cells can exert divergent effects on extending axons. For example, glial fibrillary acidic protein (GFAP)-positive type II astrocytes support mdDA axon growth and elongation, while S100-positive type I astrocytes promote axonal branching (Johansson and Stromberg, 2002). Furthermore, astrocytes display region-specific effects. For example, mdDA neurons extend a larger number of dendritic processes on mesencephalic as compared to striatal astrocytes (Autillo-Touati et al., 1988). These and other results suggest that subpopulations of astrocytes express region-specific molecular cues that regulate distinct aspects of mdDA pathway formation. Although neurons and glia have been implicated in several different aspects of mdDA pathway formation much remains to be learned about their precise function and the molecules involved.

4. The molecular basis of mdDA axon guidance

The formation of neural circuits during development depends on a precise series of molecular and cellular events. Once neurons have migrated to their final destination, they elaborate axons and dendrites along predetermined routes in the

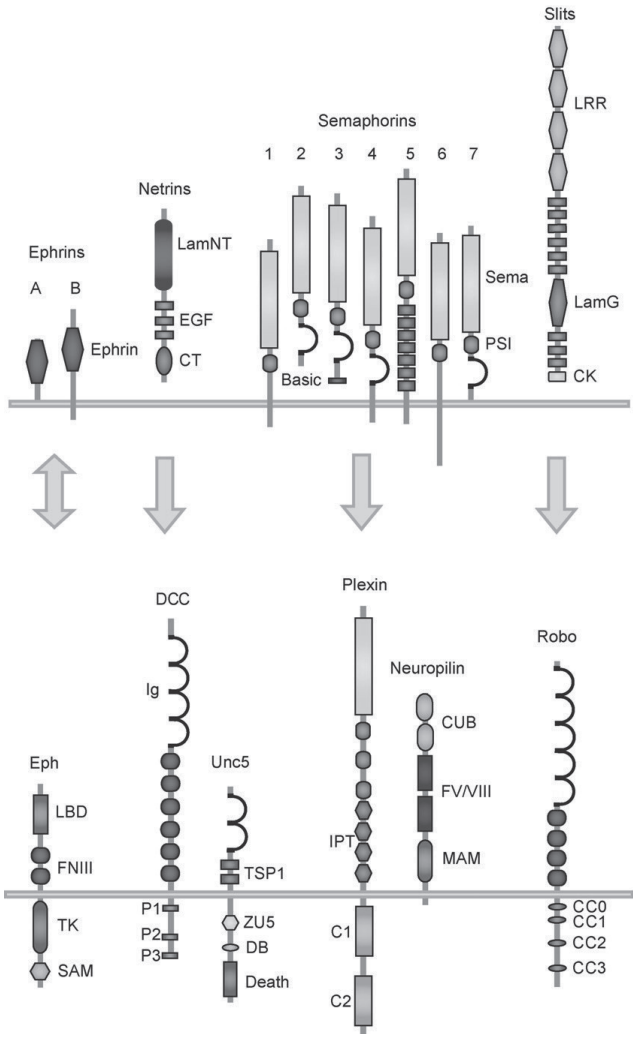

Fig. 5. Axon guidance molecules. Several conserved families of axon guidance molecules have been identified. Shown here are ephrins, netrins, semaphorins, Slits (upper part) and their cognate receptors (lower part). Ephrins exist as glycophosphatidylinositol (GPI)-linked (class A ephrins) or transmembrane (class B ephrins) proteins, both of which bind Eph receptors. Vice versa, Ephs can bind ephrins and function as axon guidance molecules. Netrins are secreted (or GPI-linked) proteins that bind deleted in corectal cancer (DCC) for attractive and axon growth promoting effects or Unc5, alone or in combination with DCC, for axon repulsion. Semaphorins exist as secreted and transmembrane proteins. Plexins, alone or in combination with neuropilins, function as neuronal semaphorin receptors. Semaphorin classes 1 and 2 contain semaphorins present in invertebrate species, classes 3–7 vertebrate semaphorins. Secreted Slit proteins bind Robo receptors. CC, conserved cytoplasmic motif; CK, cysteine-rich knot; CT, C-terminus; CUB, complement binding; DB, DCC-binding; EGF; epidermal growth factor; FNIII; fibronectin type III; FV/VIII, coagulation factor; Ig; immunoglobulin; IPT, immunoglobulin-like region; LamG, laminin G; LamNT, laminin N-terminal domain; LBD, ligand binding domain; LRR, leucine-rich repeat; MAM, meprin, A5, mu; P, conserved cytoplasmic motif; PSI, plexins, semaphorins, integrins; SAM, sterile alpha motif; Sema, semaphorin; TK, tyrosine kinase; TSP1, thrombospondin; ZU5, ZO-1 and Unc5-like.

developing embryo to establish highly specific connections with their targets. This not only requires the proper growth and guidance of extending axons and dendrites but also their subsequent branching and pruning, and the formation of functional synapses. Since our understanding of the molecular program that controls the branching and remodeling of mdDA projections or the formation of synapses by mdDA axons is rather rudimentary, this section will focus on early events during mdDA neuronal network formation, i.e. mdDA axon growth and guidance.

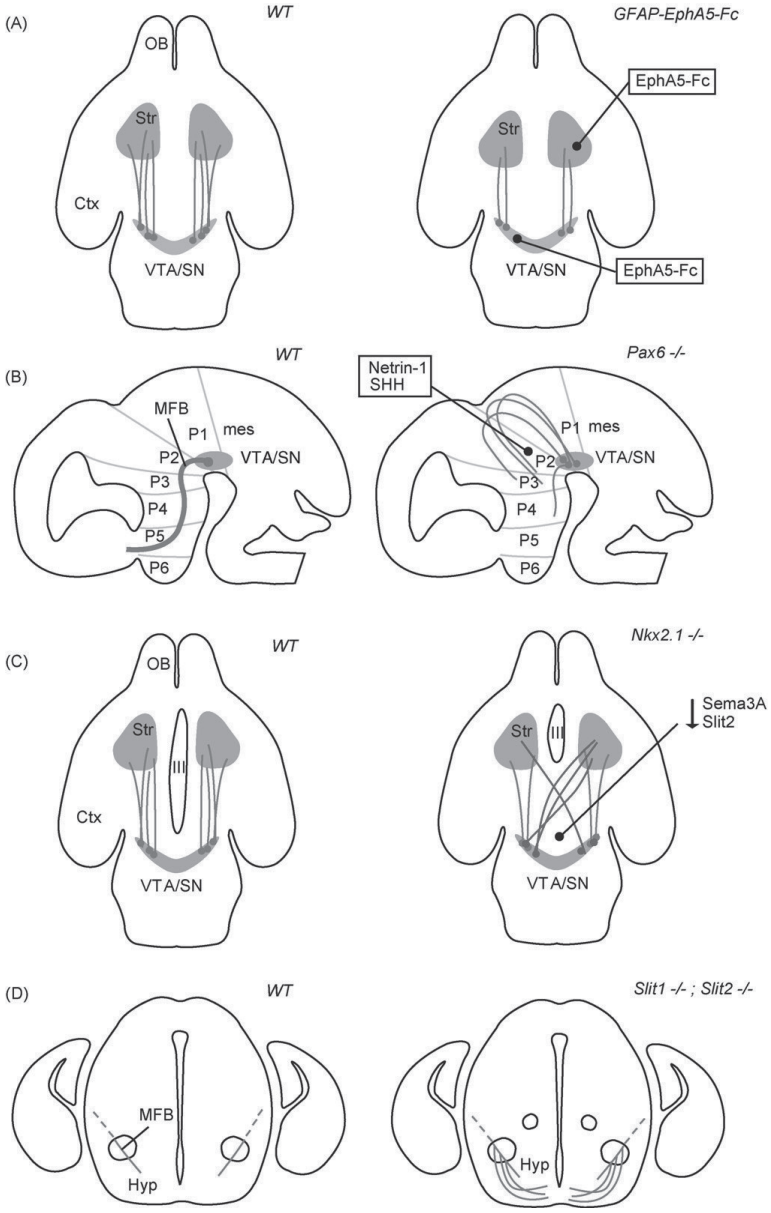

Fig. 6. Axon growth and guidance defects in the mesodiencephalic dopamine (mdDA) system. (A) Schematic representation of the mesostriatal pathway in a horizontal section of the adult CNS. Expression of EphA5-Fc, a soluble antagonist of ephrinA signaling, under the control of the glial fibrillary acidic protein (GFAP) promotor (*GFAP–EphA5-Fc*) results in a reduced innervation of the adult striatum by tyrosine hydroxylase (TH)-positive fibers. The substantia nigra (SN) is reduced in size in *GFAP–EphA5-Fc* as compared to wild type (WT) mice but contains normal numbers of mdDA neurons. The defect(s) that underlies this decreased mdDA innervation of the striatum remains to be determined but may include reduced outgrowth and/or mistargeting of mdDA axons during development. (B) Schematic representation of the mdDA pathway in a sagittal section of the E14.5 CNS. In mice lacking paired box 6 (Pax6), the majority of mdDA projections from the ventral tegmental area (VTA) and SN deflect dorsolaterally instead of following the route of the medial forebrain bundle (MFB) ventrorostrally. MdDA neurons do not express Pax6 and the wiring defects observed in mice deficient for Pax6 are therefore non-cell autonomous. *Pax6* mutant mice display an abnormal ventral-to-dorsal expansion of netrin-1 and sonic hedgehog (SHH) in the midbrain region which may be responsible for the aberrant trajectory of mdDA fibers in the absence of Pax6.

To help them find their way in the developing embryo, axons and dendrites are tipped with an exquisitely motile and sensitive structure, the growth cone. Growth cones are instructed by heterogeneously distributed guidance cues in the extracellular environment to follow highly specific trajectories. Receptor complexes at the growth cone cell surface detect these guidance molecules and consequently trigger intracellular signaling cascades that infringe upon the cytoskeleton and affect growth cone motility and steering. Guidance cues can act as axon attractants or repellents, that is, either directing them towards a specific structure or preventing them from entering inappropriate regions of the embryo. Furthermore, they exist as membrane-associated cues acting at short ranges or as secreted agents with long-distance effects. Several conserved families of guidance molecules have been identified. Prominent among these are the ephrins, netrins, semaphorins, and Slits and their cognate receptors (Fig. 5) (Huber et al., 2003). Here we summarize our current understanding of the role guidance molecules and their receptors play during the wiring of the mdDA system. We also briefly discuss other cues that are believed to contribute to the control of mdDA axon growth and pathfinding.

4.1. Ephrins and Ephs

Ephrins are cell-surface-tethered ligands for Eph receptors, the largest family of receptor tyrosine kinases. Vice versa, Ephs act as ligands for ephrin receptors (so-called 'reverse signaling') (Fig. 5). In mammalian species, EphAs (EphA1-A8) typically bind to most or all ephrinAs (ephrinA1–A5), which are tethered to the cell membrane by a glycophosphatidylinositol (GPI) anchor. EphBs (EphB1–B4, B6) bind to most or all ephrinBs (ephrinB1–B3), which exist as transmembrane proteins. In addition, some ephrinAs and ephrinBs can interact with EphBs and EphAs, respectively. During neural development, ephrins and Ephs have been shown to function as repulsive, attractive or growth promoting factors for neurites. During adulthood, the Eph/ephrin system continues to play a role during neuronal plasticity (Klein, 2004).

Neurons in the postnatal VTA and SN have been shown to express EphB1, EphA4, and EphA5 (Liebl et al., 2003; Maisonpierre et al., 1993; Yue et al., 1999). It seems likely, however, that additional Ephs are expressed in mdDA neurons during earlier or later stages of development. For example, microarray and in situ hybridization experiments reveal the differential localization of EphA7 and EphB3 transcripts in the adult SN and VTA (Chung et al., 2005; Grimm et al., 2004; Willson et al., 2006). Although several ephrinAs and ephrinBs have been detected in adult mdDA neurons (Chung et al., 2005; Yue et al., 1999), their spatiotemporal localization during development and in the adult remains largely unknown. Despite our limited understanding of the spatiotemporal distribution of Ephs and ephrins in the mdDA system, work by Yue et al. (1999) was the first to functionally implicate Ephs and ephrins in mdDA axonal pathfinding. This study showed that EphB1 is differentially expressed in the ventral midbrain; neurons in the SN were observed to display high EphB1 expression while VTA neurons only expressed low levels of EphB1. In addition, the EphB1 ligand ephrinB2 was differentially expressed in the striatum displaying strong expression in the NAc and olfactory tubercle and weak expression in the CPu. The idea that ephrinB2 serves to restrict EphB1-positive mesostriatal projections to the dorsal striatum was also supported by ephrinB2-mediated axon outgrowth inhibition of cultured mdDA neurons derived from the SN but not VTA (Yue et al., 1999). In addition, ephrinB2 induced the death of mdDA neurons *in vitro*. This may be another mechanism by which ephrinB2 confines mdDA projections to the dorsal striatum (Yue et al., 1999). Recent work by Richards et al. (2007) contrasts the idea that EphB1 contributes to the formation of mesostriatal projections. In this study, no EphB1 expression was found in mdDA neurons in the SNc from E18 and onward. In line with this observation, no anatomical defects were observed in the SNc, mesostriatal projections or striatum of *EphB1* mutant mice (Richards et al., 2007). These results argue against a role for EphB1 in the formation of mesostriatal connections. The in vivo role of ephrinB2 during mdDA neuron development remains to be established. Eph receptors other than EphB1 may be used by mdDA neurons to detect ephrinB2 in the striatum.

In contrast to EphB1, genetic manipulation of EphA5 signaling results in prominent defects in mdDA pathways. EphA5 expression has been detected in the SN and VTA and expression of ephrinA5 has been reported in the striatum (Maisonpierre et al., 1993; Sieber et al., 2004; Yue et al., 1999). Transgenic mice (ectopically) expressing an extracellular fragment of EphA5 in neurons or astrocytes display a marked reduction of the number of mesostriatal connections in the adult (Fig. 6A), as well as neurochemical and behavioral deficits characteristic of such a defect (Halladay et al., 2004; Sieber et al., 2004). EphA5 is able to interact with all ephrinAs (Gale et al., 1996) and the extracellular EphA5-Fc construct used in these studies is believed to antagonize ephrinA signaling in general. Interestingly, the number of TH-positive neurons is unchanged in EphA5-Fc transgenic mice suggesting that ephrinA signaling is not required for mdDA neuron survival but for the formation and/or maintenance of neuronal connections. Although it remains to be determined how ephrinA/EphA interactions affect mdDA projections, mice lacking ephrinA2 and ephrinA5 have also been reported to display a reduced

(C) Schematic representation of the mdDA pathway in a horizontal section of the E16.5 CNS. In mice lacking the transcription factor Nkx2.1, the majority of mdDA projections aberrantly cross the midline at the level of the caudal hypothalamus. *Nkx2.1* mice show various anatomical and molecular defects including a fusion of the third ventricle and reduced expression of Sema3A and Slit2 in the caudal hypothalamus. These changes may underlie the aberrant trajectory of mesotelencephalic projections in the absence of Nkx2.1. (D) Schematic representation of the mdDA pathway in a coronal section of the E16.5 CNS at the level of the hypothalamus. In *Slit1;Slit2* double mutant mice the MFB is split into two components and numerous fibers descend ventrally into the hypothalamus to approach the midline. At the level of the basal telencephalon many mdDA fibers aberrantly cross the midline (not shown). III, third ventricle; Ctx, cortex; Hyp, hypothalamus; mes, mesencephalon; OB, olfactory bulb; P, prosomere. Drawings in C and D are modified from Kawano et al. (2003) and Bagri et al. (2002), respectively.

mdDA innervation of the striatum providing further support for a role for ephrinAs and EphAs in the generation of mdDA connectivity in vivo (Cooper and Zhou, 2006).

4.2. Netrin and DCC

Netrins are multifunctional guidance cues that can trigger axon growth, attraction or repulsion. Two receptor families have been implicated in netrin-mediated axon growth and guidance: DCC and Unc5 proteins (Fig. 5). DCC receptors mediate attraction but also participate in repulsion and in the axon outgrowth promoting effects of netrins. Unc5 receptors act in repulsion, alone or in combination with DCC (Round and Stein, 2007). During development of the mdDA system, netrin-1 is expressed in mdDA, cortical and striatal neurons (Hamasaki et al., 2001; Livesey and Hunt, 1997; Vitalis et al., 2000). DCC is widely expressed in the embryonic midbrain and in cultured mdDA neurons derived from the SN and VTA (Lin et al., 2005; Livesey and Hunt, 1997). Furthermore, DCC is expressed in mdDA projection areas such as the PFC and striatum (Gad et al., 1997; Hamasaki et al., 2001; Livesey and Hunt, 1997). Complementary expression of DCC and netrin-1 in embryonic mdDA neurons and their targets, respectively, supports a role for netrin-1 as a target-derived guidance cue for mdDA fibers. In addition, expression of DCC in the embryonic striatum and PFC together with netrin-1 expression in the developing midbrain suggests that netrin-1/DCC signaling may also be involved in establishing afferent inputs to the SN or VTA. Finally, co-expression of netrin-1 and DCC in the midbrain or striatum hints at a function in the formation of local circuitry. The idea that netrin-1/DCC interactions function in wiring the mdDA system is supported by the observation that netrin-1 can promote axon outgrowth of dissociated mdDA neurons and attract mdDA axons in three-dimensional collagen gels. These effects are blocked by application of DCC function blocking antibodies confirming the presence of functional DCC receptors on mdDA axons (Lin et al., 2005). Axonal pathfinding errors observed in *Pax6* mutant mice may provide further (indirect) evidence for the responsiveness of mdDA axons to netrin-1. In *Pax6* mutant mice, most mdDA fibers fail to follow the route of the MFB and instead deflect dorsolaterally at the pretectal-dorsal thalamic transition zone and in the dorsal thalamic alar plate thereby seemingly avoiding areas of high ectopic netrin-1 expression (Fig. 6B) (Vitalis et al., 2000). Ectopic expression of sonic hedgehog (SHH) is believed to induce the ventral to dorsal expansion of netrin-1 in mice lacking Pax6 (Grindley et al., 1997; Vitalis et al., 2000). However, since SHH can act both as a morphogen and an axon guidance cue (see Section 4.5), it remains to be determined whether ectopic expression of netrin-1, SHH and/or other (guidance) molecules induces the misrouting of mdDA axons in *Pax6* mutant mice.

Interestingly, the region that displays the highest level of *netrin-1* in the adult CNS is the SN. *Netrin-1* is also present in the adult VTA, albeit at lower levels, while DCC is predominantly expressed in the ventral SN (Livesey and Hunt, 1997; Osborne et al., 2005; Volenec et al., 1997). In the adult striatum, *netrin-1* is present in large diameter cholinergic neurons, whereas DCC is expressed by large numbers of striatal neurons, but not by large cholinergic neurons (Livesey and Hunt, 1997). It has been postulated that the persistent expression of axon guidance molecules in the adult nervous system may serve a role in stabilizing neuronal connections and in regulating plasticity events. Adult heterozygous DCC mutant mice exhibit a functional reorganization of mdDA circuits and as a result abnormal behavioral responses following exposure to drugs-of-abuse (Flores et al., 2005). This suggests that mdDA pathway formation and/or maintenance by DCC is critical for the normal functioning of this system in the adult. DCC heterozygous mice display an increased release of dopamine in the medial PFC (Flores et al., 2005), which may indicate an increased innervation of this structure. However, determination of the precise role of netrin-1/DCC interactions during the formation, remodeling and plasticity of mesocortical and other mdDA pathways awaits a more detailed analysis of mdDA pathways in *netrin-1* and/or *DCC* mutant mice. In addition to DCC, Unc5 proteins, neogenin and integrins have been identified as netrin receptors or binding proteins. Interestingly, several of these molecules are expressed in mdDA neurons and/or their targets (Zhang et al., 2004). Future work will undoubtedly assess the role of these netrin receptors in mdDA development and plasticity.

4.3. Semaphorins, plexins and neuropilins

Semaphorins, a large family of secreted and membrane-associated proteins, are instrumental in establishing patterns of neuronal connectivity and influence many different aspects of neuronal network formation including axonal and dendritic growth, branching, guidance and pruning, target recognition, and synapse formation. Two receptor families have been implicated in neuronal semaphorin signaling: plexins and neuropilins. Mammalian semaphorins belonging to classes 4–7 bind directly to plexins, while class 3 semaphorins (with the exception of Sema3E) require a receptor complex of neuropilins and plexins, as ligand-binding and signal-transducing subunits, respectively. Thus far, nine plexins, two neuropilins and more than twenty semaphorins have been identified in vertebrate species (Pasterkamp and Kolodkin, 2003) (Fig. 5). One of the semaphorins that has been implicated in guiding embryonic mdDA axons is the secreted class 3 semaphorin Sema3A. In mice lacking the transcription factor Nkx2.1, MFB fibers aberrantly cross the ventral midline at the level of the caudal hypothalamus and predominantly project to the contralateral, instead of ipsilateral, striatum (Fig. 6C). This defect is specific for mdDA axons running in the MFB since mesohabenular projections are unaffected in the absence of Nkx2.1 (Kawano et al., 2003). Based on the reduced expression of Sema3A in the caudal hypothalamus of *Nkx2.1* mutant mice it has been postulated that Sema3A acts as a midline repellent maintaining the predominantly ipsilateral trajectory of the MFB (Kawano et al., 2003). It remains unclear, however, whether these MFB fibers express functional Sema3A receptors and are able to detect and respond to Sema3A. Several studies

have failed to detect significant levels of the Sema3A binding receptor NP-1 in mdDA neurons, but others show expression of both neuropilins and class A plexins in developing and adult mdDA neurons (Chung et al., 2005; Grimm et al., 2004; Gross et al., 2005; Gutekunst et al., 2005; Hermanson et al., 2006; Hernández-Montiel et al., 2008; Kawano et al., 2003). Also, Sema3A, like many other guidance cues, can act both as an axon repellent and attractant (Castellani et al., 2000). Thus, its presence in the caudal hypothalamus does not directly imply a role for Sema3A as an axon repellent. In contrast, several lines of evidence hint at a possible role for Sema3A as an mdDA axon attractant or growth-promoting factor rather than a repellent. First, MFB fibers express L1 (Kawano et al., 2003), a modulatory Sema3A receptor subunit involved in switching Sema3A repulsion to attraction (Castellani et al., 2000). Second, instead of repelling mdDA axons Sema3A promotes axon outgrowth from embryonic ventral midbrain explants (Hernández-Montiel et al., 2008). In all, further work is needed to define the role of Sema3A during mdDA neuron development and to study the molecular mechanisms that are affected in *Nkx2.1* mutant mice. Alternative explanations for the abnormal crossing of MFB fibers in the absence of Nkx2.1 include the loss of a physical instead of a molecular barrier for axon growth, and the decreased expression of other repulsive cues, such as Slit2 (see Section 4.4). However, the presence of several other class 3 semaphorins and their receptors in mdDA neurons and their target structures (see for example Bahi and Dreyer, 2005; Chung et al., 2005; Grunblatt et al., 2004; Miller et al., 2004) together with the ability of some of these cues to guide embryonic mdDA axons *in vitro* (Hernández-Montiel et al., 2008) supports a prominent role for class 3 semaphorins in establishing and maintaining patterns of mdDA connectivity. In addition to secreted semaphorins, membrane-associated semaphorins belonging to classes 4–7 have been identified in rodent and human mdDA neurons and their targets (see for example Bahi and Dreyer, 2005; Chung et al., 2005; Grunblatt et al., 2004; Miller et al., 2004). Thus far, expression of the GPI-linked semaphorin Sema7A and one of its binding proteins, plexinC1, has been best-characterized in the mdDA system. Sema7A has been shown to promote axon growth *in vitro* and is required for the proper growth of the mouse lateral olfactory tract in vivo (Pasterkamp et al., 2003). Sema7A labels a subpopulation of SNc neurons, whereas plexinC1 is expressed in a subset of mdDA neurons in the central VTA (Chung et al., 2005; Pasterkamp et al., 2007). Furthermore, prominent labeling of Sema7A and plexinC1 is observed in target structures of mdDA neurons, including the striatum and PFC. Based on the expression of Sema7A and plexinC1 in mdDA neurons and their targets it is tempting to speculate that these molecules contribute to the formation and maintenance of subsets of efferent and afferent mdDA connections (Pasterkamp et al., 2007).

4.4. Slits and Robos

Slit proteins can repel growing axons and inhibit sensory axon branching. In mammals, three Slits have been identified (Slit1, Slit2 and Slit3), all of which bind to roundabout (Robo) receptors (Robo1, Robo2, and Robo3/Rig1) (Fig. 5). Slits and Robos are crucial for the proper development of several major ascending and descending axon tracts (for a recent review see Dickson and Gilestro, 2006). Expression of Robo1 and Robo2 has been reported in developing and adult mdDA neurons. Robo1 is expressed in neurons throughout the SN and VTA, while Robo2 predominantly labels VTA neurons (Lin et al., 2005; Marillat et al., 2002). Robo1 and Robo2 are also expressed in the forebrain including, but not limited to, the developing striatum and surrounding areas (Marillat et al., 2002). The precise distribution of Robo3/Rig1 in the developing mdDA system at the time neuronal connections are being established remains to be determined. Similar to Robos, Slits display developmentally regulated patterns of expression in mdDA neurons and their synaptic targets. Surprisingly, none of the three Slits is expressed by mdDA neurons at embryonic and early postnatal stages. Slit1 is first detected in mdDA neurons in the SN and VTA around P10, while Slit2 is expressed in adult SN neurons only. In contrast, areas surrounding embryonic mdDA neurons in the midbrain exhibit prominent Slit expression (Marillat et al., 2002). The dorsal midbrain contains Slit1, which may explain the observation that the DM instructs mdDA axons to follow a rostral trajectory towards the forebrain (Fig. 4) (Nakamura et al., 2000). In addition, the caudal midbrain expresses high levels of Slit3, which may mediate the repulsive effect this brain region exerts on extending mdDA axons *in vitro* (Fig. 4) (Gates et al., 2004; Holmes et al., 1995). Based on these results, it is tempting to speculate that the combined actions of Slit1 and Slit3 prevent mdDA fibers from aberrantly extending in dorsal and caudal directions thereby contributing to the characteristic rostroventral trajectory of the MFB. Similar to the midbrain, Slits show highly dynamic distribution patterns in the forebrain including areas known as termination fields of mdDA projections. For example, Slit1 is strongly expressed in the embryonic striatum but its levels decrease as development progresses. In contrast, Slit3 expression can be detected in the striatum at P5 and increases towards adulthood suggesting a role in the stabilization and maintenance of mdDA projections. Slit2 is not detected in the striatum but labels adjacent regions such as the cerebral cortex and septum (Marillat et al., 2002). The tightly regulated expression of Slits and Robos suggests the involvement of Slit/Robo interactions in several early (in the midbrain) and late (in the forebrain) guidance events during mdDA development. This idea is also supported by the ability of Slit2 to repel mdDA axons and inhibit their outgrowth *in vitro* (Lin et al., 2005). These effects are blocked by addition of soluble Robo receptors suggesting the presence of a functional Robo receptor(s) on embryonic mdDA axons (Lin et al., 2005). Mice deficient for Slits or Robos display severe guidance errors in a variety of axon tracts including the MFB (e.g. Bagri et al., 2002; Lopez-Bendito et al., 2007). In *Slit2* mutants, mdDA axons are displaced ventrally as they course through the diencephalon. In *Slit1;Slit2* double mutants, the MFB is split into two components and numerous fibers descend ventrally into the hypothalamus, approaching the midline (Fig. 6D). In

addition, many fibers abnormally cross the midline in the basal telencephalon (Bagri et al., 2002). As mentioned above (see Section 4.3), mdDA axons in *Nkx2.1* mutant mice project abnormally into the ventral telencephalon and aberrantly across the midline (Kawano et al., 2003; Marin et al., 2002). The observation that *Nkx2.1* mutant mice display changes in *Slit1* and *Slit2* expression (Marin et al., 2002) and wiring defect resembling those observed in *Slit* mutants suggests that abnormal Slit function may underlie (some of) the pathfinding errors observed in mice lacking Nkx2.1 (Fig. 6C). It should be noted, however, that mdDA pathways are more severely and in part also differently affected in *Nkx2.1* as compared to *Slit* mutants. In addition, many mdDA axons project normally in the absence of Slit1 and Slit2. This suggests that multiple distinct guidance cues are needed for the proper formation of mdDA pathways. Interestingly, the expression of several other guidance molecules is regulated in *Nkx2.1* mutant mice including ephrins and semaphorins (Kawano et al., 2003; Marin et al., 2002).

4.5. Other factors

In addition to the 'classical' axon guidance molecules listed above, a wide variety of other molecular cues are believed to contribute to the formation and maintenance of mdDA tracts. These include but are not limited to: (1) *Neurotrophic factors*: neurotrophic factors such as glial cell line-derived neurotrophic factor (GDNF) have prominent effects on mdDA axon growth (for review see Krieglstein, 2004). (2) *Morphogens*: morphogens, including Wnts, bone morphogenetic proteins (BMPs) and SHH, are expressed in the midbrain region and are required for the proper development of mdDA neurons (for reviews see Castelo-Branco and Arenas, 2006; Smidt and Burbach, 2007). Morphogens also mediate axon growth and guidance functions (Ciani and Salinas, 2005; Zou and Lyuksyutova, 2007) and may contribute to the wiring of the mdDA system. (3) *Transcription factors*: similar to morphogens, transcription factors such as engrailed-2 contribute to the early development of mdDA neurons and may also act as extracellular axon growth and guidance factors for mdDA projections (Brunet et al., 2005). (4) *Proteoglycans*: proteoglycans are required for the formation and stabilization of a multitude of neural circuits. Both anatomical and functional studies support the involvement of proteoglycans in the formation and maintenance of mdDA pathways (Gates and Dunnett, 2001; Mace et al., 2002). (5) *Leucine-rich repeat proteins*: the leucine-rich repeat proteins leucine-rich repeat kinase-2 (LRRK2) and leucine-rich repeat Ig-containing (LINGO)-1 have been implicated in PD (Inoue et al., 2007; MacLeod et al., 2006; Paisan-Ruiz et al., 2004; Zimprich et al., 2004). Interestingly, both LRKK2 and LINGO-1 exert outgrowth inhibiting effects on mdDA axons and may contribute to the wiring of the mdDA system (Inoue et al., 2007; MacLeod et al., 2006). (6) *Neurotransmitters*: accumulating evidence suggests that neurotransmitters such as glutamate and dopamine may regulate axon outgrowth and guidance. For example, dopamine influences growth cone extension and steering (Spencer et al., 1998) and blockade of metabotropic glutamate receptors but not ionotropic glutamate receptors prevent the innervation of the striatum by SN axons (Plenz and Kitai, 1998). Neurotransmitters are believed to be especially critical for the final stages of axon growth and target innervation.

5. Implications for disease

5.1. Parkinson's disease and cell-replacement strategies

Studies of the cellular and molecular mechanisms that underlie neuronal network formation are not only essential for developing effective repair strategies for neurodegenerative disorders such as PD but may also provide insight into the onset and progression of these disorders. For example, microarray studies comparing gene expression profiles in the midbrain and striatal regions of control and PD patients or PD mouse models reveal marked differences in the expression of axon guidance cues and their receptors (Grunblatt et al., 2001, 2004; Hauser et al., 2005; Miller et al., 2004). Similarly, genomic pathway analyses reveal polymorphisms in axon guidance pathways of PD patients (Lesnick et al., 2007). Although it remains to be determined whether these genetic changes are functionally linked to the pathophysiology of PD, changes in the expression of axon guidance cues and their receptors could lead to altered patterns of neuronal connectivity in the mdDA system and as a consequence neuron dysfunction and loss. One should keep in mind, however, that although best known for their role as axonal repellents and attractants, axon guidance molecules also subserve diverse roles unrelated to axon growth and guidance, including the regulation of neuronal apoptosis, angiogenesis and cell migration (see for example Casazza et al., 2007; Neufeld et al., 2007; Pasterkamp and Kolodkin, 2003). Therefore, understanding the potential role of these molecules in PD will require a detailed evaluation of their different biological functions in the mdDA system. This notion is exemplified by the observation that Sema3A and ephrinB2 can affect both mdDA axon growth and induce mdDA neuron cell death *in vitro* (Hernández-Montiel et al., 2008; Yasuhara et al., 2005; Yue et al., 1999). Thus, if dysregulated these axon guidance molecules could induce neuronal loss not only through rearrangements of the neuronal network but also by directly activating cell death mechanisms.

Current pharmacological treatments for PD are focused on restoring cerebral dopamine levels and provide therapeutic benefit in the early stages of the disease. Unfortunately, they become increasingly less effective as neuronal degeneration proceeds. A promising approach to alleviating the more progressive symptoms of PD is the transplantation of healthy mdDA neurons into the brain of PD patients. Clinical studies underscore the feasibility of these cell replacement strategies but also highlight several problems (Lindvall and Bjorklund, 2004). One of these problems is the inability of many transplanted neurons to properly rewire the degenerated mdDA system. In addition to forming an insufficient number of functional connections, many transplanted neurons establish inappropriate axon projections that underlie the troublesome

side effects observed in transplantation patients. Our potential to replace or even sustain degenerating mdDA circuits seems therefore to be contingent with understanding the molecular program that controls the formation of mdDA connections. In other words, if we understand how mdDA connections normally form we can instruct transplanted mdDA neurons to correctly rewire the PD brain. Interestingly, transplantation studies suggest that some of the molecular mechanisms that regulate mdDA axon growth and guidance during development persist in the intact and denervated adult mdDA system of rodents (Isacson and Deacon, 1996; Thompson et al., 2005). Whether this is also true for the brains of patients suffering from PD remains to be determined. These and other studies also suggest that the site of transplantation and the subset of mdDA neurons transplanted are critical to the success of cell replacement strategies. Transplantation of fetal tissue in the SN instead of the striatum may allow for the reestablishment of appropriate afferent inputs on mdDA neurons and enable the regeneration of functional mdDA circuits. In addition, the grafting of specific subsets of mdDA neurons known to project to the striatum (i.e. subsets of SN but not VTA neurons) instead of the entire midbrain region may help to minimize the generation of inappropriate connections.

Another problem linked to cell replacement strategies is the lack of sufficient amounts of human embryonic tissue for transplantation and the variable quality of the tissue when available. Mounting evidence suggests that patient-derived embryonic stem (ES) cells may form an excellent substitute for the mesencephalic tissue used so far. ES cells allow for the generation of large numbers of mdDA neurons in standardized and quality-controlled preparations. Although initial attempts to generate mdDA neurons from ES cells were disappointing very recent insight into the molecular determinants of the DA phenotype have allowed the preparation of mdDA neurons with a correct midbrain identity from ES cells (Smidt and Burbach, 2007). Intriguingly, a recent study suggests that, similar to embryonic mdDA neurons, ES-derived mdDA neurons are responsive to netrin-1 and Slits (Lin and Isacson, 2006). This suggests that transplanted ES cell-derived mdDA neurons may be able to sense axon growth and guidance molecules in vivo.

5.2. Drug addiction and neurological disorders

Drug addiction is defined as the loss of control over drug use or the compulsive seeking and taking of drugs despite adverse consequences. Once formed, an addiction can be a life-long condition in which individuals show intense drug craving and increased risk for relapse after years of abstinence. This means that addiction involves extremely stable changes in brain and behavior. Recent studies indicate that structural adaptations in neuronal connectivity may serve as a neural substrate for the enduring behavioral abnormalities associated with drug use and addiction (Robinson and Kolb, 2004). The mdDA system is a key neural substrate for mediating persistent changes induced by repeated exposure to drugs of abuse. Although the molecular mechanisms that underlie these structural changes remain largely unknown, several recent studies hint at the involvement of axon guidance cues and their receptors. The expression of several different axon guidance cues is regulated in the mdDA system upon (prolonged) administration of drugs of abuse and genetic manipulation of some of these cues leads to changes in drug-induced behavior (Bahi and Dreyer, 2005; Flores et al., 2005; Halladay et al., 2000; Jassen et al., 2006; Lehrmann et al., 2006; Sieber et al., 2004; Yue et al., 1999; Zhang et al., 2004). Together these results suggest that drug-induced changes in the expression of axon guidance cues may cause structural adaptations of mdDA neural circuits leading to altered behavioral and physiological responses following exposure to drugs-of-abuse.

Dysregulation of the mdDA system has also been linked to various neurological disorders, for example depression and schizophrenia (Dailly et al., 2004; Dunlop and Nemeroff, 2007; Guillin et al., 2007; Sesack and Carr, 2002). Similar to drug addiction, structural changes in neural circuits are thought to underlie, at least in part, the pathogenesis of these disorders. Although genetic studies have implicated axon guidance cues in several of these disorders, it remains to be shown whether dysfunction of axon guidance cues in the mdDA system contributes to the onset and/or progression of these disorders.

6. Concluding remarks and future directions

Despite the fact that structural and biochemical changes in mdDA circuits have been associated with multiple psychiatric and neurodegenerative disorders, our understanding of the mechanisms that regulate the formation and maintenance of these circuits is rather rudimentary. Recent studies have begun to define the cellular and molecular signals that instruct mdDA axons to establish highly stereotypic connections to the forebrain. However, most of what we know today about mdDA axon growth and guidance derives from gene expression and *in vitro* experiments and many of these observations remain to be validated in in vivo mouse models.

Despite the distinct projection targets and functional properties of SNc and VTA neurons, the mdDA population as a whole is often considered to be physiologically and pharmacologically homogeneous. Recent work on the early development of mdDA neurons reveals that the mdDA system does not comprise a homogeneous population of neurons. Anatomically and functionally distinct subsets of mdDA neurons exist, even within the individual A8–A10 groups. These subsets are likely to require different molecular cues not only for their differentiation and migration but also for specific axon growth and guidance. In line with this idea, several axon guidance cues and receptors show highly unique and restricted patterns of expression in the mdDA system. It is therefore crucial to identify the different neuronal subsets that make up the mdDA system and develop molecular and genetic tools for studying their development and connectivity patterns.

The relatively simple model of the mdDA projection system that has been employed in the past, with largely separate forebrain projections arising from clearly distinct parts of the mdDA system, has evolved in a more complex model in which individual mdDA neurons intermingled in the mdDA system

contribute unique projections to one or more mdDA pathways. Evidence is emerging that processes such as axonal branching and pruning, target recognition and synapse formation are especially critical for the formation of these highly complex projections.

Studies of the cellular and molecular mechanisms that underlie neuronal network formation in the mdDA system are not only essential for developing effective repair strategies for neurodegenerative disorders such as PD but also provide insight into the onset and progression of these and other disorders. For example, our potential to replace or even sustain degenerating dopaminergic circuits in PD appears to be contingent with understanding the molecular and cellular events that underlie the establishment and maintenance of dopaminergic connectivity. Furthermore, structural changes in mdDA circuits caused by changes in axon guidance cue and receptor genes are thought to underlie, at least in part, the pathogenesis of specific neurological and psychiatric disorders. Therefore, these molecules seem to be excellent therapeutic targets for preventing and/or treating these disorders in the future.

Acknowledgements

We thank Marten Smidt, Peter Burbach, Sharon Kolk and Asheeta Prasad for reading the manuscript. Work in the laboratory of the authors is supported by grants from the Netherlands Organization of Scientific Research, Dutch Brain Foundation, the International Parkinson Foundation, the Human Frontier Science Program and ABC Genomics Center Utrecht. RJP is a NARSAD Henry and William Test Investigator.

References

Autillo-Touati, A., Chamak, B., Araud, D., Vuillet, J., Seite, R., Prochiantz, A., 1988. Region-specific neuro-astroglial interactions: ultrastructural study of the in vitro expression of neuronal polarity. J. Neurosci. Res. 19, 326–342.

Bagri, A., Marin, O., Plump, A.S., Mak, J., Pleasure, S.J., Rubenstein, J.L., Tessier-Lavigne, M., 2002. Slit proteins prevent midline crossing and determine the dorsoventral position of major axonal pathways in the mammalian forebrain. Neuron 33, 233–248.

Bahi, A., Dreyer, J.L., 2005. Cocaine-induced expression changes of axon guidance molecules in the adult rat brain. Mol. Cell. Neurosci. 28, 275–291.

Bentivoglio, M., Morelli, M., 2005. The organisation of circuits of mesencephalic dopaminergic neurons and the distribution of dopamine receptors in the brain. In: Dunnett, S.B., Bentivoglio, M., Bjorklund, A., Hokfelt, T. (Eds.), Handbook of Chemical Neuroanatomy (Dopamine), 21. Elsevier, Amsterdam, pp. 1–107.

Berger, B., Verney, C., Alvarez, C., Vigny, A., Helle, K.B., 1985. New dopaminergic terminal fields in the motor, visual (area 18b) and retrosplenial cortex in the young and adult rat. Immunocytochemical and catecholamine histochemical analyses. Neuroscience 15, 983–998.

Bjorklund, A., Dunnett, S.B., 2007. Dopamine neuron systems in the brain an update. Trends Neurosci. 30, 194–202.

Bjorklund, A., Lindvall, O., 1983. Dopamine- and norepinephrine-containing neuron systems: their anatomy in the rat brain. In: Emson, P.C. (Ed.), Chemical Neuroanatomy. Raven Press, New York, pp. 229–255.

Brunet, I., Weinl, C., Piper, M., Trembleau, A., Volovitch, M., Harris, W., Prochiantz, A., Holt, C., 2005. The transcription factor Engrailed-2 guides retinal axons. Nature 438, 94–98.

Carlsson, A., Falck, B., Hillarp, N.A., 1962. Cellular localization of brain monoamines. Acta Physiol. Scand. Suppl. 56, 1–28.

Casazza, A., Fazzari, P., Tamagnone, L., 2007. Semaphorin signals in cell adhesion and cell migration: functional role and molecular mechanisms. Adv. Exp. Med. Biol. 600, 90–108.

Castellani, V., Chedotal, A., Schachner, M., Faivre-Sarrailh, C., Rougon, G., 2000. Analysis of the L1-deficient mouse phenotype reveals cross-talk between Sema3A and L1 signaling pathways in axonal guidance. Neuron 27, 237–249.

Castelo-Branco, G., Arenas, E., 2006. Function of Wnts in dopaminergic neuron development. Neurodegen. Dis. 3, 5–11.

Chotard, C., Salecker, I., 2004. Neurons and glia: team players in axon guidance. Trends Neurosci. 27, 655–661.

Chung, C.Y., Seo, H., Sonntag, K.C., Brooks, A., Lin, L., Isacson, O., 2005. Cell type-specific gene expression of midbrain dopaminergic neurons reveals molecules involved in their vulnerability and protection. Hum. Mol. Genet. 14, 1709–1725.

Ciani, L., Salinas, P.C., 2005. WNTs in the vertebrate nervous system: from patterning to neuronal connectivity. Nat. Rev. Neurosci. 6, 351–362.

Cooper, M.A., Zhou, R., 2006. Ephrin-A/EphA interaction regulates the formation of the ascending midbrain dopaminergic pathways. Soc. Neurosci. Abstr. 36, 621–629.

Dahlström, A., Fuxe, K., 1964. Evidence for the existence of monoamine-containing neurons in the central nervous system. I. Demonstration of monoamines in the cell bodies of brainstem neurons. Acta Physiol. Scand. Suppl. 232, 1–55.

Dailly, E., Chenu, F., Renard, C.E., Bourin, M., 2004. Dopamine, depression and antidepressants. Fundam. Clin. Pharmacol. 18, 601–607.

Denis-Donini, S., Glowinski, J., Prochiantz, A., 1983. Specific influence of striatal target neurons on the in vitro outgrowth of mesencephalic dopaminergic neurites: a morphological quantitative study. J. Neurosci. 3, 2292–2299.

di Porzio, U., Daguet, M.C., Glowinski, J., Prochiantz, A., 1980. Effect of striatal cells on in vitro maturation of mesencephalic dopaminergic neurones grown in serum-free conditions. Nature 288, 370–373.

Dickson, B.J., 2002. Molecular mechanisms of axon guidance. Science 298, 1959–1964.

Dickson, B.J., Gilestro, G.F., 2006. Regulation of commissural axon pathfinding by slit and its Robo receptors. Annu. Rev. Cell Dev. Biol. 22, 651–675.

Dunlop, B.W., Nemeroff, C.B., 2007. The role of dopamine in the pathophysiology of depression. Arch. Gen. Psychiatr. 64, 327–337.

Engele, J., Bohn, M.C., 1991. The neurotrophic effects of fibroblast growth factors on dopaminergic neurons in vitro are mediated by mesencephalic glia. J. Neurosci. 11, 3070–3078.

Fallon, J.H., 1981. Collateralization of monoamine neurons: mesotelencephalic dopamine projections to caudate, septum, and frontal cortex. J. Neurosci. 1, 1361–1368.

Fallon, J.H., Loughlin, S.E., 1982. Monoamine innervation of the forebrain: collateralisation. Brain Res. Bull. 9, 295–307.

Fallon, J.H., Moore, R.Y., 1978. Catecholamine innervation of the basal forebrain. IV. Topography of the dopamine projection to the basal forebrain and neostriatum. J. Comp. Neurol. 180, 545–580.

Flores, C., Manitt, C., Rodaros, D., Thompson, K.M., Rajabi, H., Luk, K.C., Tritsch, N.X., Sadikot, A.F., Stewart, J., Kennedy, T.E., 2005. Netrin receptor deficient mice exhibit functional reorganization of dopaminergic systems and do not sensitize to amphetamine. Mol. Psychiatr. 10, 606–612.

Gad, J.M., Keeling, S.L., Wilks, A.F., Tan, S.S., Cooper, H.M., 1997. The expression patterns of guidance receptors, DCC and Neogenin, are spatially and temporally distinct throughout mouse embryogenesis. Dev. Biol. 192, 258–273.

Gale, N.W., Holland, S.J., Valenzuela, D.M., Flenniken, A., Pan, L., Ryan, T.E., Henkemeyer, M., Strebhardt, K., Hirai, H., Wilkinson, D.G., Pawson, T., Davis, S., Yancopoulos, G.D., 1996. Eph receptors and ligands comprise two major specificity subclasses and are reciprocally compartmentalized during embryogenesis. Neuron 17, 9–19.

Gates, M.A., Dunnett, S.B., 2001. The influence of astrocytes on the development, regeneration and reconstruction of the nigrostriatal dopamine system. Restor. Neurol. Neurosci. 19, 67–83.

Gates, M.A., O'Brien, T.F., Faissner, A., Steindler, D.A., 1993. Neuron–glial interactions during the in vivo and in vitro development of the nigrostriatal circuit. J. Chem. Neuroanat. 6, 179–189.

Gates, M.A., Coupe, V.M., Torres, E.M., Fricker-Gates, R.A., Dunnett, S.B., 2004. Spatially and temporally restricted chemoattractive and chemorepulsive cues direct the formation of the nigro-striatal circuit. Eur. J. Neurosci. 19, 831–844.

Grimm, J., Mueller, A., Hefti, F., Rosenthal, A., 2004. Molecular basis for catecholaminergic neuron diversity. Proc. Natl. Acad. Sci. U.S.A. 101, 13891–13896.

Grindley, J.C., Hargett, L.K., Hill, R.E., Ross, A., Hogan, B.L., 1997. Disruption of PAX6 function in mice homozygous for the Pax6Sey-1Neu mutation produces abnormalities in the early development and regionalization of the diencephalon. Mech. Dev. 64, 111–126.

Gross, R.E., Ren, Z., Gutekunst, C.A., Jackson, E.H., Wainer, B.H., 2005. The expression of neuropilins, plexins, and flk-1 in the adult nigrostriatal pathway. Soc. Neurosci. Abstr. 35, 833–836.

Grunblatt, E., Mandel, S., Maor, G., Youdim, M.B., 2001. Gene expression analysis in *N*-methyl-4-phenyl-1,2,3,6-tetrahydropyridine mice model of Parkinson's disease using cDNA microarray: effect of R-apomorphine. J. Neurochem. 78, 1–12.

Grunblatt, E., Mandel, S., Jacob-Hirsch, J., Zeligson, S., Amariglio, N., Rechavi, G., Li, J., Ravid, R., Roggendorf, W., Riederer, P., Youdim, M.B., 2004. Gene expression profiling of parkinsonian substantia nigra pars compacta; alterations in ubiquitin-proteasome, heat shock protein, iron and oxidative stress regulated proteins, cell adhesion/cellular matrix and vesicle trafficking genes. J. Neural Transm. 111, 1543–1573.

Guillin, O., Abi-Dargham, A., Laruelle, M., 2007. Neurobiology of dopamine in schizophrenia. Int. Rev. Neurobiol. 78, 1–39.

Gutekunst, C.A., Torre, E.R., Ren, Z., Lu, E., Jackson, E.H., Gross, R.E., 2005. Semaphorin 3A and 3F as guiding cues for the development of the nigrostriatal pathways. Soc. Neurosci. Abstr. 35, 833–835.

Halladay, A.K., Yue, Y., Michna, L., Widmer, D.A., Wagner, G.C., Zhou, R., 2000. Regulation of EphB1 expression by dopamine signalling. Brain Res. Mol. Brain Res. 85, 171–178.

Halladay, A.K., Tessarollo, L., Zhou, R., Wagner, G.C., 2004. Neurochemical and behavioral deficits consequent to expression of a dominant negative EphA5 receptor. Brain Res. Mol. Brain Res. 123, 104–111.

Hamasaki, T., Goto, S., Nishikawa, S., Ushio, Y., 2001. A role of netrin-1 in the formation of the subcortical structure striatum: repulsive action on the migration of late-born striatal neurons. J. Neurosci. 21, 4272–4280.

Hauser, M.A., Li, Y.J., Xu, H., Noureddine, M.A., Shao, Y.S., Gullans, S.R., Scherzer, C.R., Jensen, R.V., McLaurin, A.C., Gibson, J.R., Scott, B.L., Jewett, R.M., Stenger, J.E., Schmechel, D.E., Hulette, C.M., Vance, J.M., 2005. Expression profiling of substantia nigra in Parkinson disease, progressive supranuclear palsy, and frontotemporal dementia with parkinsonism. Arch. Neurol. 62, 917–921.

Hemmendinger, L.M., Garber, B.B., Hoffmann, P.C., Heller, A., 1981. Target neuron-specific process formation by embryonic mesencephalic dopamine neurons in vitro. Proc. Natl. Acad. Sci. U.S.A. 78, 1264–1268.

Hermanson, E., Borgius, L., Bergsland, M., Joodmardi, E., Perlmann, T., 2006. Neuropilin1 is a direct downstream target of Nurr1 in the developing brain stem. J. Neurochem. 97, 1403–1411.

Hernández-Montiel, H.L., Tamariz, E., Sandoval-Minero, M.T., Varela-Echavarría, A., 2008. Semaphorin 3A, 3C, and 3F in mesencephalic dopaminergic axon pathfinding. J. Comp. Neurol. 506, 387–397.

Hirata, T., Fujisawa, H., 1999. Environmental control of collateral branching and target invasion of mitral cell axons during development. J. Neurobiol. 38, 93–104.

Hökfelt, T., Martensson, R., Björklund, A., Goldstein, M., 1984. Distribution of tyrosine hydroxylase-immunoreactive neurons in the rat brain. In: Björklund, A., Hökfelt, T. (Eds.), Handbook of Chemical Neuroanatomy (Classical Transmitters in the CNS, Part I), 2. Elsevier, Amsterdam, pp. 409–440.

Holmes, C., Jones, S.A., Greenfield, S.A., 1995. The influence of target and non-target brain regions on the development of mid-brain dopaminergic neurons in organotypic slice culture. Brain Res. Dev. Brain Res. 88, 212–219.

Hu, Z., Cooper, M., Crockett, D.P., Zhou, R., 2004. Differentiation of the midbrain dopaminergic pathways during mouse development. J. Comp. Neurol. 476, 301–311.

Huber, A.B., Kolodkin, A.L., Ginty, D.D., Cloutier, J.F., 2003. Signaling at the growth cone: ligand-receptor complexes and the control of axon growth and guidance. Annu. Rev. Neurosci. 26, 509–563.

Inoue, H., Lin, L., Lee, X., Shao, Z., Mendes, S., Snodgrass-Belt, P., Sweigard, H., Engber, T., Pepinsky, B., Yang, L., Beal, M.F., Mi, S., Isacson, O., 2007. Inhibition of the leucine-rich repeat protein LINGO-1 enhances survival, structure, and function of dopaminergic neurons in Parkinson's disease models. Proc. Natl. Acad. Sci. U.S.A. 104, 14430–14435.

Isacson, O., Deacon, T.W., 1996. Specific axon guidance factors persist in the adult brain as demonstrated by pig neuroblasts transplanted to the rat. Neuroscience 75, 827–837.

Jassen, A.K., Yang, H., Miller, G.M., Calder, E., Madras, B.K., 2006. Receptor regulation of gene expression of axon guidance molecules: implications for adaptation. Mol. Pharmacol. 70, 71–77.

Jaumotte, J.D., Zigmond, M.J., 2005. Dopaminergic innervation of forebrain by ventral mesencephalon in organotypic slice co-cultures: effects of GDNF. Brain Res. Mol. Brain Res. 134, 139–146.

Johansson, S., Stromberg, I., 2002. Guidance of dopaminergic neuritic growth by immature astrocytes in organotypic cultures of rat fetal ventral mesencephalon. J. Comp. Neurol. 443, 237–249.

Johansson, S., Stromberg, I., 2003. Fetal lateral ganglionic eminence attracts one of two morphologically different types of tyrosine hydroxylase-positive nerve fibers formed by cultured ventral mesencephalon. Cell Transplant. 12, 243–255.

Kalsbeek, A., Voorn, P., Buijs, R.M., Pool, C.W., Uylings, H.B., 1988. Development of the dopaminergic innervation in the prefrontal cortex of the rat. J. Comp. Neurol. 269, 58–72.

Kawano, H., Horie, M., Honma, S., Kawamura, K., Takeuchi, K., Kimura, S., 2003. Aberrant trajectory of ascending dopaminergic pathway in mice lacking Nkx2.1. Exp. Neurol. 182, 103–112.

Klein, R., 2004. Eph/ephrin signaling in morphogenesis, neural development and plasticity. Curr. Opin. Cell Biol. 16, 580–589.

Krieglstein, K., 2004. Factors promoting survival of mesencephalic dopaminergic neurons. Cell Tissue Res. 318, 73–80.

Lehrmann, E., Colantuoni, C., Deep-Soboslay, A., Becker, K.G., Lowe, R., Huestis, M.A., Hyde, T.M., Kleinman, J.E., Freed, W.J., 2006. Transcriptional changes common to human cocaine, cannabis and phencyclidine abuse. PLoS ONE 1, e114.

Lesnick, T.G., Papapetropoulos, S., Mash, D.C., Ffrench-Mullen, J., Shehadeh, L., de Andrade, M., Henley, J.R., Rocca, W.A., Ahlskog, J.E., Maraganore, D.M., 2007. A genomic pathway approach to a complex disease: axon guidance and Parkinson disease. PLoS Genet. 3, e98.

Liebl, D.J., Morris, C.J., Henkemeyer, M., Parada, L.F., 2003. mRNA expression of ephrins and Eph receptor tyrosine kinases in the neonatal and adult mouse central nervous system. J. Neurosci. Res. 71, 7–22.

Lin, L., Isacson, O., 2006. Axonal growth regulation of fetal and embryonic stem cell-derived dopaminergic neurons by Netrin-1 and Slits. Stem Cells 24, 2504–2513.

Lin, L., Rao, Y., Isacson, O., 2005. Netrin-1 and slit-2 regulate and direct neurite growth of ventral midbrain dopaminergic neurons. Mol. Cell. Neurosci. 28, 547–555.

Lindvall, O., Bjorklund, A., 1974. The organization of the ascending catecholamine neuron systems in the rat brain as revealed by the glyoxylic acid fluorescence method. Acta Physiol. Scand. Suppl. 412, 1–48.

Lindvall, O., Bjorklund, A., 1979. Dopaminergic innervation of the globus pallidus by collaterals from the nigrostriatal pathway. Brain Res. 172, 169–173.

Lindvall, O., Bjorklund, A., 2004. Cell therapy in Parkinson's disease. NeuroRx 1, 382–393.

Livesey, F.J., Hunt, S.P., 1997. Netrin and netrin receptor expression in the embryonic mammalian nervous system suggests roles in retinal, striatal, nigral, and cerebellar development. Mol. Cell. Neurosci. 8, 417–429.

Loizou, L.A., 1972. The postnatal ontogeny of monoamine-containing neurones in the central nervous system of the albino rat. Brain Res. 40, 395–418.

Lopez-Bendito, G., Flames, N., Ma, L., Fouquet, C., Di Meglio, T., Chedotal, A., Tessier-Lavigne, M., Marin, O., 2007. Robo1 and Robo2 cooperate to control the guidance of major axonal tracts in the mammalian forebrain. J. Neurosci. 27, 3395–3407.

Luo, L., O'Leary, D.D., 2005. Axon retraction and degeneration in development and disease. Annu. Rev. Neurosci. 28, 127–156.

Mace, K., Saxod, R., Feuerstein, C., Sadoul, R., Hemming, F.J., 2002. Chondroitin and keratan sulfates have opposing effects on attachment and outgrowth of ventral mesencephalic explants in culture. J. Neurosci. Res. 70, 46–56.

MacLeod, D., Dowman, J., Hammond, R., Leete, T., Inoue, K., Abeliovich, A., 2006. The familial Parkinsonism gene LRRK2 regulates neurite process morphology. Neuron 52, 587–593.

Maisonpierre, P.C., Barrezueta, N.X., Yancopoulos, G.D., 1993. Ehk-1 and Ehk-2: two novel members of the Eph receptor-like tyrosine kinase family with distinctive structures and neuronal expression. Oncogene 8, 3277–3288.

Margolis, E.B., Lock, H., Chefer, V.I., Shippenberg, T.S., Hjelmstad, G.O., Fields, H.L., 2006. Kappa opioids selectively control dopaminergic neurons projecting to the prefrontal cortex. Proc. Natl. Acad. Sci. U.S.A. 103, 2938–2942.

Marillat, V., Cases, O., Nguyen-Ba-Charvet, K.T., Tessier-Lavigne, M., Sotelo, C., Chedotal, A., 2002. Spatiotemporal expression patterns of slit and robo genes in the rat brain. J. Comp. Neurol. 442, 130–155.

Marin, O., Baker, J., Puelles, L., Rubenstein, J.L., 2002. Patterning of the basal telencephalon and hypothalamus is essential for guidance of cortical projections. Development 129, 761–773.

Miller, R.M., Callahan, L.M., Casaceli, C., Chen, L., Kiser, G.L., Chui, B., Kaysser-Kranich, T.M., Sendera, T.J., Palaniappan, C., Federoff, H.J., 2004. Dysregulation of gene expression in the 1-methyl-4-phenyl-1,2,3,6-tetrahydropyridine-lesioned mouse substantia nigra. J. Neurosci. 24, 7445–7454.

Nakamura, S., Ito, Y., Shirasaki, R., Murakami, F., 2000. Local directional cues control growth polarity of dopaminergic axons along the rostrocaudal axis. J. Neurosci. 20, 4112–4119.

Nestler, E.J., 2000. Genes and addiction. Nat. Genet. 26, 277–281.

Neufeld, G., Lange, T., Varshavsky, A., Kessler, O., 2007. Semaphorin signaling in vascular and tumor biology. Adv. Exp. Med. Biol. 600, 118–131.

Osborne, P.B., Halliday, G.M., Cooper, H.M., Keast, J.R., 2005. Localization of immunoreactivity for deleted in colorectal cancer (DCC), the receptor for the guidance factor netrin-1, in ventral tier dopamine projection pathways in adult rodents. Neuroscience 131, 671–681.

Ostergaard, K., Schou, J.P., Zimmer, J., 1990. Rat ventral mesencephalon grown as organotypic slice cultures and co-cultured with striatum, hippocampus, and cerebellum. Exp. Brain Res. 82, 547–565.

Paisan-Ruiz, C., Jain, S., Evans, E.W., Gilks, W.P., Simon, J., van der Brug, M., Lopez de Munain, A., Aparicio, S., Gil, A.M., Khan, N., Johnson, J., Martinez, J.R., Nicholl, D., Carrera, I.M., Pena, A.S., de Silva, R., Lees, A., Marti-Masso, J.F., Perez-Tur, J., Wood, N.W., Singleton, A.B., 2004. Cloning of the gene containing mutations that cause PARK8-linked Parkinson's disease. Neuron 44, 595–600.

Pasterkamp, R.J., Kolodkin, A.L., 2003. Semaphorin junction: making tracks toward neural connectivity. Curr. Opin. Neurobiol. 13, 79–89.

Pasterkamp, R.J., Peschon, J.J., Spriggs, M.K., Kolodkin, A.L., 2003. Semaphorin 7A promotes axon outgrowth through integrins and MAPKs. Nature 424, 398–405.

Pasterkamp, R.J., Kolk, S.M., Hellemons, A.J.C.G.M., Kolodkin, A.L., 2007. Expression patterns of semaphorin7A and plexinC1 during rat neural development suggest roles in axon guidance and neuronal migration. BMC Dev. Biol. 7, 98.

Plenz, D., Kitai, S.T., 1996. Organotypic cortex–striatum–mesencephalon cultures: the nigrostriatal pathway. Neurosci. Lett. 209, 177–180.

Plenz, D., Kitai, S.T., 1998. Regulation of the nigrostriatal pathway by metabotropic glutamate receptors during development. J. Neurosci. 18, 4133–4144.

Richards, A.B., Scheel, T.A., Wang, K., Henkemeyer, M., Kromer, L.F., 2007. EphB1 null mice exhibit neuronal loss in substantia nigra pars reticulata and spontaneous locomotor hyperactivity. Eur. J. Neurosci. 25, 2619–2628.

Robinson, T.E., Berridge, K.C., 1993. The neural basis of drug craving: an incentive-sensitization theory of addiction. Brain Res. Brain Res. Rev. 18, 247–291.

Robinson, T.E., Kolb, B., 2004. Structural plasticity associated with exposure to drugs of abuse. Neuropharmacology 47 (Suppl. 1), 33–46.

Roffler-Tarlov, S., Graybiel, A.M., 1984. Weaver mutation has differential effects on the dopamine-containing innervation of the limbic and nonlimbic striatum. Nature 307, 62–66.

Round, J., Stein, E., 2007. Netrin signaling leading to directed growth cone steering. Curr. Opin. Neurobiol. 17, 15–21.

Savitt, J.M., Dawson, V.L., Dawson, T.M., 2006. Diagnosis and treatment of Parkinson disease: molecules to medicine. J. Clin. Invest. 116, 1744–1754.

Sesack, S.R., Carr, D.B., 2002. Selective prefrontal cortex inputs to dopamine cells: implications for schizophrenia. Physiol. Behav. 77, 513–517.

Sieber, B.A., Kuzmin, A., Canals, J.M., Danielsson, A., Paratcha, G., Arenas, E., Alberch, J., Ogren, S.O., Ibanez, C.F., 2004. Disruption of EphA/ephrin-a signaling in the nigrostriatal system reduces dopaminergic innervation and dissociates behavioral responses to amphetamine and cocaine. Mol. Cell. Neurosci. 26, 418–428.

Smidt, M.P., Burbach, J.P., 2007. How to make a mesodiencephalic dopaminergic neuron. Nat. Rev. Neurosci. 8, 21–32.

Smits, S.M., Burbach, J.P., Smidt, M.P., 2006. Developmental origin and fate of meso-diencephalic dopamine neurons. Prog. Neurobiol. 78, 1–16.

Specht, L.A., Pickel, V.M., Joh, T.H., Reis, D.J., 1981a. Light-microscopic immunocytochemical localization of tyrosine hydroxylase in prenatal rat brain. I. Early ontogeny. J. Comp. Neurol. 199, 233–253.

Specht, L.A., Pickel, V.M., Joh, T.H., Reis, D.J., 1981b. Light-microscopic immunocytochemical localization of tyrosine hydroxylase in prenatal rat brain. II. Late ontogeny. J. Comp. Neurol. 199, 255–276.

Spencer, G.E., Klumperman, J., Syed, N.I., 1998. Neurotransmitters and neurodevelopment. Role of dopamine in neurite outgrowth, target selection and specific synapse formation. Perspect. Dev. Neurobiol. 5, 451–467.

Sulzer, D., 2007. Multiple hit hypotheses for dopamine neuron loss in Parkinson's disease. Trends Neurosci. 30, 244–250.

Swanson, L.W., 1982. The projections of the ventral tegmental area and adjacent regions: a combined fluorescent retrograde tracer and immunofluorescence study in the rat. Brain Res. Bull. 9, 321–353.

Tessier-Lavigne, M., Goodman, C.S., 1996. The molecular biology of axon guidance. Science 274, 1123–1133.

Thompson, L., Barraud, P., Andersson, E., Kirik, D., Bjorklund, A., 2005. Identification of dopaminergic neurons of nigral and ventral tegmental area subtypes in grafts of fetal ventral mesencephalon based on cell morphology, protein expression, and efferent projections. J. Neurosci. 25, 6467–6477.

Tomozawa, Y., Appel, S.H., 1986. Soluble striatal extracts enhance development of mesencephalic dopaminergic neurons in vitro. Brain Res. 399, 111–124.

Ungerstedt, U., 1971. Stereotaxic mapping of the monoamine pathways in the rat brain. Acta Physiol. Scand. Suppl. 367, 1–48.

Van Eden, C.G., Hoorneman, E.M., Buijs, R.M., Matthijssen, M.A., Geffard, M., Uylings, H.B., 1987. Immunocytochemical localization of dopamine in the prefrontal cortex of the rat at the light and electron microscopical level. Neuroscience 22, 849–862.

Verney, C., 1999. Distribution of the catecholaminergic neurons in the central nervous system of human embryos and fetuses. Microsc. Res. Technol. 46, 24–47.

Verney, C., Berger, B., Adrien, J., Vigny, A., Gay, M., 1982. Development of the dopaminergic innervation of the rat cerebral cortex. A light microscopic immunocytochemical study using anti-tyrosine hydroxylase antibodies. Brain Res. 281, 41–52.

Vitalis, T., Cases, O., Engelkamp, D., Verney, C., Price, D.J., 2000. Defect of tyrosine hydroxylase-immunoreactive neurons in the brains of mice lacking the transcription factor Pax6. J. Neurosci. 20, 6501–6516.

Volenec, A., Bhogal, R.K., Moorman, J.M., Leslie, R.A., Flanigan, T.P., 1997. Differential expression of DCC mRNA in adult rat forebrain. Neuroreport 8, 2913–2917.

Voorn, P., Kalsbeek, A., Jorritsma-Byham, B., Groenewegen, H.J., 1988. The pre- and postnatal development of the dopaminergic cell groups in the

ventral mesencephalon and the dopaminergic innervation of the striatum of the rat. Neuroscience 25, 857–887.

Wang, G., Scott, S.A., 2000. The ''waiting period'' of sensory and motor axons in early chick hindlimb: its role in axon pathfinding and neuronal maturation. J. Neurosci. 20, 5358–5366.

Willson, C.A., Foster, R.D., Onifer, S.M., Whittemore, S.R., Miranda, J.D., 2006. EphB3 receptor and ligand expression in the adult rat brain. J. Mol. Histol. 37, 369–380.

Yasuhara, T., Shingo, T., Muraoka, K., Kameda, M., Agari, T., Wenji, Y., Hishikawa, T., Matsui, T., Miyoshi, Y., Kimura, T., Borlongan, C.V., Date, I., 2005. Toxicity of semaphorin3A for dopaminergic neurons. Neurosci. Lett. 382, 61–65.

Yue, Y., Widmer, D.A., Halladay, A.K., Cerretti, D.P., Wagner, G.C., Dreyer, J.L., Zhou, R., 1999. Specification of distinct dopaminergic neural pathways: roles of the Eph family receptor EphB1 and ligand ephrin-B2. J. Neurosci. 19, 2090–2101.

Zhang, L., Lou, D., Jiao, H., Zhang, D., Wang, X., Xia, Y., Zhang, J., Xu, M., 2004. Cocaine-induced intracellular signaling and gene expression are oppositely regulated by the dopamine D1 and D3 receptors. J. Neurosci. 24, 3344–3354.

Zhao, S., Maxwell, S., Jimenez-Beristain, A., Vives, J., Kuehner, E., Zhao, J., O'Brien, C., de Felipe, C., Semina, E., Li, M., 2004. Generation of embryonic stem cells and transgenic mice expressing green fluorescence protein in midbrain dopaminergic neurons. Eur. J. Neurosci. 19, 1133–1140.

Zimprich, A., Biskup, S., Leitner, P., Lichtner, P., Farrer, M., Lincoln, S., Kachergus, J., Hulihan, M., Uitti, R.J., Calne, D.B., Stoessl, A.J., Pfeiffer, R.F., Patenge, N., Carbajal, I.C., Vieregge, P., Asmus, F., Muller-Myhsok, B., Dickson, D.W., Meitinger, T., Strom, T.M., Wszolek, Z.K., Gasser, T., 2004. Mutations in LRRK2 cause autosomal-dominant parkinsonism with pleomorphic pathology. Neuron 44, 601–607.

Zou, Y., Lyuksyutova, A.I., 2007. Morphogens as conserved axon guidance cues. Curr. Opin. Neurobiol. 17, 22–28.

CHAPTER 3

Spatiotemporal expression of repulsive guidance molecules (RGMs) and their receptor Neogenin in the mouse brain

DIANNE M.A. VAN DEN HEUVEL,
ANITA J.C.G.M. HELLEMONS,
R. JEROEN PASTERKAMP

Department of Neuroscience and Pharmacology, Rudolf Magnus Institute of Neuroscience, University Medical Center Utrecht, Universiteitsweg 100, 3584 CG, Utrecht, The Netherlands

PLOS ONE (*in press*)

ABSTRACT

Neogenin has been implicated in a variety of developmental processes such as neurogenesis, neuronal differentiation, apoptosis, migration and axon guidance. Binding of repulsive guidance molecules (RGMs) to Neogenin inhibits axon outgrowth of different neuronal populations. This effect requires Neogenin to interact with co-receptors of the uncoordinated locomotion-5 (Unc5) family to activate downstream Rho signaling. Although previous studies have reported RGM, Neogenin, and/or Unc5 expression, a systematic comparison of RGM and Neogenin expression in the developing nervous system is lacking, especially at later developmental stages. Furthermore, information on RGM and Neogenin expression at the protein level is limited. To fill this void and to gain further insight into the role of RGM-Neogenin signaling during mouse neural development, we studied the expression of RGMa, RGMb, Neogenin and Unc5A-D using *in situ* hybridization, immunohistochemistry and RGMa section binding. Expression patterns in the primary olfactory system, cortex, hippocampus, habenula, and cerebellum were studied in more detail. Characteristic cell layer-specific expression patterns were detected for RGMa, RGMb, Neogenin and Unc5A-D. Furthermore, strong expression of RGMa, RGMb and Neogenin protein was found on several major axon tracts such as the primary olfactory projections, anterior commissure and fasciculus retroflexus. These data not only hint at a role for RGM-Neogenin signaling during the development of different neuronal systems, but also suggest that Neogenin partners with different Unc5 family members in different systems. Overall, the results presented here will serve as a framework for further dissection of the role of RGM-Neogenin signaling during neural development.

INTRODUCTION

The mammalian nervous system is composed of millions of neurons that are connected through dendritic and axonal processes. The formation of this exquisitely complex neuronal network is dependent on a precisely ordered series of developmental events including neurogenesis, neuronal differentiation and migration, neurite growth and guidance, and apoptosis. RGMs and their receptor Neogenin have been implicated in the molecular control of many of these cellular events [1–5]. The founding member of the RGM gene family, RGMa, was originally discovered through the biochemical characterization of a growth cone collapsing activity for chick retinal axons [6,7]. Within the chick retinotectal system, RGMa is expressed in the retina and in an anterior-low to posterior-high gradient in the tectum. In the tectum, RGMa repels temporal retinal axons away from the posterior part of the tectum [6,8,9]. In addition, RGMa is required for intraretinal pathfinding of retinal axons [10]. Following the initial discovery of chick RGMa, three different RGMs were identified in mammalian species; RGMa, RGMb (also known as Dragon), and RGMc (also known as hemojuvelin (HJV), HLA-like protein involved in

iron (Fe) homeostasis (HFE2), and Dragon-like muscle (DL-M)) (for review see [4]). RGMa and RGMb, but not RGMc, are expressed in the nervous system and can act as growth cone collapse factors and repulsive axon guidance cues for different populations of neurons [6,8,9,11–20–22].

Neogenin is the predominant RGM receptor in neurons. Neogenin is a member of the immunoglobulin (Ig) superfamily of cell surface proteins and a close homologue of deleted in colorectal cancer (DCC) [9,23]. Similar to DCC, Neogenin can bind Netrin-1 and mediate Netrin-1-dependent functions [20,24–27]. Interactions between RGMs and Neogenin are required for both the neuronal and non-neuronal functions of RGMa and RGMb, including their neurite growth inhibitory and axon repulsive effects [9,20,21,28–33]. In addition, RGMs and also Neogenin interact with bone morphogenetic proteins (BMPs) and their receptors, but thus far RGM-mediated modulation of BMP signaling has not been implicated in the neurodevelopmental functions of RGMs [12,34–47]. Binding of RGMa or RGMb to Neogenin on neuronal growth cones leads to activation of the Rho kinase pathway and inactivation of Ras signaling [13,14,48]. Interestingly, activation of RhoA by RGMs is dependent on another family of Netrin-1 receptors, Unc5s [15]. Unc5s interact with Neogenin through their extracellular domains and with leukemia-associated guanine nucleotide exchange factor (LARG), a RhoGEF, through their intracellular region. Binding of RGMa to Neogenin induces the focal adhesion kinase (FAK)-dependent tyrosine phosphorylation of LARG and as a result activation of RhoA. Neogenin can bind all four members of the Unc5 family (Unc5A-D), but only the role of Unc5B has been established at the functional level [15].

The best-characterized neuronal functions of RGMa and RGMb are in axon guidance and regeneration failure. During development, RGMs serve as repulsive axon guidance molecules in the chick retinotectal system, the mouse hippocampus and *Xenopus* forebrain [6,8,9,11,16,20]. In addition, RGMs contribute to the control of neuronal survival [31,49], neuron migration [28,29,50,51], neuronal differentiation [8,16], and dendritic branching and spine maturation [22]. *RGMa*$^{-/-}$ mice do not show overt defects in retinotectal mapping, as observed in chick, but display abnormalities in neural tube closure [8,52]. Depletion of RGMa in *Xenopus* embryos also results in aberrant development of the neural tube [30]. Following injury to the adult spinal cord, RGMa and RGMb are strongly expressed around the lesion site [14,48,53]. Local administration of a function-blocking anti-RGMa antibody in rats significantly improves anatomical and functional spinal cord regeneration [14]. This together with their potent neurite growth inhibitory effects suggests that RGMs inhibit axon regeneration in the spinal cord. Despite these advances, the precise contribution of RGMs and Neogenin to the development of most neuronal systems remains to be explored, especially in the mouse.

Although previous studies have reported RGMa, RGMb and/or Neogenin expression in different neuronal systems and species, a systematic comparison of RGM and Neogenin expression patterns in the developing nervous system is lacking, especially at later developmental stages. Furthermore, information on RGM and Neogenin expression at the protein level is limited. In this study, we therefore used *in situ* hybridization, immunohistochemistry and RGMa

section binding to perform a detailed expression analysis of RGMa, RGMb, Neogenin and Unc5A-D in a selection of neuronal systems in the mouse brain. The selected brain regions were complex multilayered structures (e.g. the olfactory system and cerebellum), connected to many other brain areas. Highly stereotypic patterns of expression were detected for RGMa, RGMb, Neogenin and Unc5A-D, including strong expression on several major axon tracts. These data support a widespread role for RGM-Neogenin signaling during neural development and suggest that Neogenin may partner with different Unc5 family members to subserve different functions in different systems. Our data, together with previous expression results, serve as a framework for further functional studies on the role of RGM-Neogenin signaling during neural development.

MATERIALS AND METHODS

ETHICS STATEMENT

The experiments performed in this study were approved by the Experimental Animal Committee (DEC) of Utrecht University (2008.I.05.037). All animal experiments were conducted in agreement with Dutch law (Wet op de Dierproeven, 1996) and European regulations (Guideline 86/609/EEC) related to the protection of vertebrate animals used for experimental and other scientific purposes.

ANIMALS AND TISSUE TREATMENT

C57BL/6 mice were obtained from Charles River. Pups and (timed-pregnant) adult mice were killed by means of decapitation or cervical dislocation, respectively. The morning on which a vaginal plug was detected was considered embryonic day 0.5 (E0.5) and the day of birth, postnatal day 0 (P0). For *in situ* hybridization and RGMa section binding experiments E16.5 and P5 heads, and adult brains were directly frozen in 2-methylbutane (Merck). For immunohistochemistry, E16.5 heads were collected in phosphate-buffered saline (PBS, pH 7.4) and fixed by immersion for 3 hours (hrs) in 4% paraformaldehyde (PFA) in PBS at 4°C. P5 and adult mice were transcardially perfused with saline followed by 4% PFA. Brains were dissected and postfixed overnight at 4°C, washed in PBS, cryoprotected in 30% sucrose at 4°C and frozen in 2-methylbutane. Sections (16 µm) were cut on a cryostat, mounted on Superfrost Plus slides (Fisher Scientific), air-dried and stored desiccated at -80°C for *in situ* hybridization and at -20°C for immunohistochemistry. All mRNA and protein expression patterns and AP binding patterns were examined in at least eight embryos, pups or adult mice. Embryos or pups were derived from at least three different litters. The reported expression and binding patterns were reproducible across individual mice.

CELL CULTURE AND TRANSFECTION

COS-7 cells (ATTC) were maintained in high glucose Dulbecco's modified Eagle's medium (DMEM; Gibco, Invitrogen) supplemented with 10% (v/v) heat-inactivated fetal bovine serum (FBS; Lonza, BioWhittaker), 2 mM L-glutamine (PAA) and 1x penicillin/streptomycin (pen/strep; PAA) in a humidified atmosphere with 5% CO_2 at 37°C. Cells were transfected with RGMa (pSectag2-RGMa-myc-his), RGMb (pSectag2-RGMb-myc-his; both were kind gifts of Silvia Arber), GFP-Neogenin (pcDNA3.1-GFP-Neogenin), GFP-DCC (a kind gift of Jean-François Cloutier), pcDNA3.1 (pcDNA3.1(-)/myc-his; Invitrogen) or pEGFP-N1 (Clontech), using polyethylenimine (PEI; Polysciences) (as described by [54]).

AP-PROTEIN PRODUCTION

For alkaline phosphatase (AP), RGMa-AP and Sema3F-AP protein production, HEK293 cells were transfected with AP-Fc (a kind gift of Roman Giger), RGMa-AP (APtag5-RGMa-AP; a kind gift of Thomas Skutella), or Sema3F-AP (a kind gift of Valerie Castellani). Transfected HEK293 cells were cultured in Opti-MEM reduced serum medium (Gibco, Invitrogen) supplemented with 3% (v/v) FBS (Lonza, BioWhittaker), 2 mM L-glutamine (PAA) and 1x pen/strep (PAA). Cell culture medium was collected after 5 days in culture, filter-sterilized and stored at 4°C. If required, culture medium containing AP-tagged proteins was concentrated using Centriprep YM-50 centrifugal filter units (Millipore).

IN SITU HYBRIDIZATION

Nonradioactive *in situ* hybridization was performed as described previously [55], with minor modification. In brief, probe sequences for *RGMa* [21], *RGMb* [21] and *Neogenin* (NM_008684.2: nt 2087-2587) were polymerase chain reaction (PCR)-amplified from cDNA, using primer sequences listed in Table S1. The probe sequences for *Unc5A* (genepaint.org: probe 1721), *Unc5B* (NM_029770.2: nt 665-1210), *Unc5C* (genepaint.org: probe 1568) and *Unc5D* [56] were generated by reverse transcription (RT)-PCR on adult mouse whole brain RNA (see Table S1). For the *tyrosine hydroxylase (TH)* probe a 1142 bp fragment of rat TH cDNA was used [57]. Digoxigenin (DIG)-labeled RNA probes were generated by a RNA polymerase reaction using 10x DIG RNA labeling mix (ENZO).

Tissue sections were postfixed with 4% PFA in PBS (pH 7.4) for 20 minutes (min) at room temperature (RT). To enhance tissue penetration and decrease aspecific background staining, sections were acetylated with 0.25% acetic anhydride in 0.1 M triethanolamine and 0.06% HCl for 10 min at RT. Sections were prehybridized for 2 hrs at RT in hybridization buffer (50% formamide, 5x Denhardt's solution, 5x SSC, 250 µg/ml baker's yeast tRNA and 500 µg/ml sonicated salmon sperm DNA). Hybridization was performed for 15 hrs at 68°C, using 400 ng/ml denatured DIG-labeled probe diluted in hybridization buffer. After hybridization, sections were first washed briefly in 2x SSC followed by incubation in 0.2x SCC for 2 hrs at 68°C. Sections were adjusted to RT in 0.2x SSC for 5 min. DIG-labeled RNA hybrids were detected

with anti-DIG Fab fragments conjugated to AP (Boehringer) diluted 1:2500 in Tris-buffered saline (TBS, pH 7.4) overnight at 4°C. Binding of AP-labeled antibody was visualized by incubating the sections in detection buffer (100 mM Tris-HCl, pH 9.5, 100 mM NaCl and 50 mM $MgCl_2$) containing 240 µg/ml levamisole and nitroblue tetrazolium chloride/5-bromo-4-chloro-3-indolyl-phosphatase (NBT/BCIP; Roche) for 14 hrs at RT. Sections subjected to the entire *in situ* hybridization procedure, but with no probe or sense probe added, did not exhibit specific hybridization signals. Sense probe data for RGMa are shown in Fig. S1. Sense probes for other genes examined in this study displayed a similar amount of background staining. The specificity of the *in situ* hybridization procedure was also inferred from the clearly distinct gene expression patterns observed. Staining was visualized using a Zeiss Axioskop 2 microscope.

IMMUNOCYTOCHEMISTRY

COS-7 cells were fixed with 4% PFA for 15 min at RT, washed in PBS (pH 7.4) and permeabilized and blocked in normal blocking buffer (PBS, 4% bovine serum albumin (BSA) and 0.1% Triton) for 1 hr at RT. COS-7 cells were incubated with goat anti-RGMa antibody (AF2458; R&D systems) 1:200, sheep anti-RGMb antibody (AF3597; R&D systems) 1:50 or goat anti-Neogenin antibody (AF1079; R&D systems) 1:50 in normal blocking buffer for 2 hrs at RT. Cells were washed in PBS and incubated with the appropriate Alexa Fluor-labeled secondary antibodies (Invitrogen) 1:500 at RT. After 1 hr, cells were washed in PBS and counterstained with with 4', 6'-diamidino-2-phenylindole (DAPI; Invitrogen).

IMMUNOHISTOCHEMISTRY

Immunohistochemistry was performed as described previously [58,59]. In brief, sections were washed in PBS (pH 7.4) and incubated in normal blocking buffer (PBS, 4% BSA and 0.1% Triton) for 1 hr at RT and incubated with goat anti-RGMa antibody (AF2458; R&D systems) 1:200, sheep anti-RGMb antibody (AF3597; R&D systems) 1:200 or goat anti-Neogenin antibody (AF1079; R&D systems) 1:200 overnight in normal blocking buffer at 4°C. The specificity of the RGMa and Neogenin antibodies has been confirmed previously using immunocytochemical, immunohistochemical and/or Western blot methods on transfected cells and endogenous tissues [38,60–63]. As a control, sections were incubated with immunoglobulin isotype controls matching the RGM or Neogenin antibodies (AB-108-C, 5-001-A; R&D systems) (representative examples are shown in Fig. 3J-L and 6G-I). For costainings with glial fibrillary protein (GFAP), rabbit anti-GFAP (Z0334; DAKO) 1:6000 was used. The next day, sections were washed in PBS and incubated with the appropriate Alexa Fluor-labeled secondary antibodies (Invitrogen) 1:500 for 1 hr at RT. Sections were washed in PBS, counterstained with fluorescent Nissl stain (NeuroTrace, Invitrogen) 1:500 for 15 min at RT, washed in PBS and embedded in Mowiol (Sigma-Aldrich). Staining was visualized using a Zeiss Axioskop 2 microscope.

SECTION BINDING

Sections were fixed by immersion in -20°C methanol for 6 min and rehydrated in TBS+ (TBS, pH 7.4, 4 mM $MgCl_2$ and 4 mM $CaCl_2$). Section were incubated in blocking buffer (TBS+ and 10% FBS (Lonza, BioWhittaker) for 1 hr at RT and incubated with 1.5 nM AP-Fc or AP-tagged protein-containing medium for 2 hrs at RT. After washing in TBS+, sections were incubated with fixation solution (20 mM HEPES, pH 7, 60% (v/v) acetone and 3.7% formaldehyde) for 2 min. After washing in TBS+, endogenous phosphatase activity was heat-inactivated by incubation at 65°C for 1 h. Section were equilibrated in detection buffer (100 mM Tris-HCl, pH 9.5, 100 mM NaCl and 5 mM $MgCl_2$) and bound AP-protein was visualized by incubation in detection buffer containing levamisole and NBT/BCIP (Roche). The specificity of RGMa-AP protein binding was determined by competition with excess RGMa protein. Furthermore, differential binding patterns were observed following RGMa-AP and Sema3F-AP section binding and no staining was observed for AP-Fc alone (see Fig. 8R).

RESULTS

To provide an overview of the expression of RGMa, RGMb and Neogenin during mouse neural development, we used a combination of *in situ* hybridization, immunohistochemistry and RGMa section binding. *In situ* hybridization not only revealed gene expression in specific structures and cell layers, but also aided in the identification of the cellular source of RGM or Neogenin protein expression as revealed by immunohistochemistry and allowed for comparison to previously reported gene expression patterns. Given the role of Unc5s as obligate RGM co-receptors [15], expression of *Unc5D* was also studied. Unfortunately, no suitable antibodies are available to perform immunohistochemistry for all Unc5s, therefore *in situ* hybridization was used [64].

Not much is known about the expression of RGM and Neogenin protein in the developing brain, therefore immunohistochemistry was used to reveal RGM and Neogenin protein expression in glial cells, neurons and their processes. Finally, given the ability of RGMs to bind cell surface receptors other than Neogenin [36], RGMa-AP (alkaline phosphatase) section binding was used to examine whether RGMa binding sites in the brain correspond to regions of Neogenin expression. Three different timepoints were selected for these studies: E16.5, as an early timepoint during which developmental processes such as neurogenesis, cell migration and axon guidance occur; postnatal day (P)5, characterized by late developmental processes such as synapse formation, pruning and apoptosis; and adulthood, to explore a possible role for RGM-Neogenin signaling in the plasticity of mature neuronal networks. The specificity of the observed expression patterns could be discerned from the various controls that were included (e.g. sense controls, use of isotype immunoglobulin controls, omission of primary antibody, section binding with AP only (see Fig. 3J-L, 6G-I, 8R, S1) and from the

clearly distinct expression patterns. The subsequent sections discuss expression profiles in a selection of neuronal systems displaying the most prominent RGM and Neogenin expression patterns in the mouse. The expression patterns reported here are largely in line with those reported in previous studies and apparent discrepancies are discussed if data from equivalent stages and species is available.

PRIMARY OLFACTORY SYSTEM

Olfactory sensory neurons (OSNs) in the olfactory epithelium (OE) express receptors for the detection of odorants and synapse their axons on mitral cell dendrites in select regions of the olfactory bulb, termed glomeruli [65]. Mitral cells then relay the olfactory information to higher brain structures [66]. *In situ* hybridization showed complementary expression patterns for *RGMa* and *RGMb* in the OE and olfactory bulb at E16.5 (Fig. 1A, A', B, B', Table S2). *RGMa* was most strongly expressed in the apical part of the OE and *RGMb* in its basal part. Weak expression of *Neogenin* was detected in the OE with strongest signals in the apical cell layer (Fig. 1C, C'). In the olfactory bulb, expression of *RGMa* was found in a dorsomedial subset of mitral cells, while *RGMb* was most strongly expressed in ventrolateral mitral cells (Fig. 1A, B). Weak *Neogenin* expression was present in the mitral cell layer (MCL) and the cribriform plate (Fig. 1C). In addition, *RGMa* and *Neogenin* were detected in the olfactory ventricular zone and the accessory olfactory bulb (Fig. 1A, C). *RGMb* was expressed at low levels in the accessory olfactory bulb but strongly in the granule cell and glomerular layers (GR and GL, respectively) (Fig. 1B). These expression patterns are largely unchanged at E18.5 [19,67].

To examine the expression of RGMs and Neogenin on the axonal projections of OSNs and mitral cells, immunohistochemistry was used. The specificity of the RGMa and Neogenin antibodies has been confirmed previously using immunocytochemical, immunohistochemical and/or Western blot methods on transfected cells and endogenous tissues [38,60–63]. Here, the specificity of the anti-RGM and anti-Neogenin antibodies was further tested by immunocytochemistry (Fig. S2) and by the inclusion of immunoglobulin isotype controls matching the RGM or Neogenin antibodies. Antibodies directed against RGMa detected RGMa but not RGMb, and vice versa. Anti-Neogenin antibodies specifically recognized Neogenin but not its close family member DCC (Fig. S2). The use of immunoglobulin isotype controls or the omission of primary antibodies resulted in the absence of specific signals (representative examples are shown in Fig. 3J-L and 6G-I). Immunohistochemistry at E16.5 revealed strong expression of RGMb and weak staining for RGMa and Neogenin on OSN axons in the OE and olfactory bulb glomeruli (Fig. 1D-F). In general, we found that the RGM and Neogenin antibodies more strongly labeled axonal projections as compared to cell bodies. Interestingly, previous work reports Neogenin protein expression in the basal part of the E14.5 OE, apparently contrasting the *in situ* data at E16.5 [68] (Fig. 1C'). It is possible that this difference is caused by a spatiotemporal change in Neogenin expression or by the use of different antibodies in the present study and that of Fitzgerald *et al.* [68]. The antibody used here recognizes the N-terminal

part of Neogenin, while in the other study antibodies are used against the Neogenin C-terminal region. In relation to this it is interesting to note that Neogenin can be cleaved resulting in the release of the extracellular domain [61]. This may also explain differences in expression patterns. In the olfactory bulb, RGMa, RGMb and Neogenin were observed in mitral cell axons in the internal and external plexiform layers (IPL and EPL) (Fig. 1D-F). Neogenin expression was also observed in the cribriform plate, in line with expression of *Neogenin* transcripts in this structure (Fig. 1C, F). RGMa-AP bound to the IPL, EPL and GL, resembling Neogenin expression (Fig. 1F, G). RGMb was also detected in the vomeronasal nerve (Fig. 1E). Mitral cells organize their axons in the lateral olfactory tract (LOT) en route to more caudal targets in the central nervous system. RGMa, RGMb and Neogenin were expressed by axons in the LOT (Fig. 1H-J). In addition, axons in the anterior commissure (pars anterior) (ACa), which connects olfactory structures to the anterior piriform cortex, strongly stained for RGMa and Neogenin (Fig. 1H, J). RGMb was weakly expressed in the ACa (Fig. 1I). RGMa-AP strongly bound to the LOT and the ACa (Fig. 1K).

At P5 and adult stages, *in situ* hybridization revealed strong expression of *RGMa*, *RGMb* and *Neogenin* in periglomerular cells in the GL and in the MCL (Fig. 1L-N, L'-N', Table S2). In the GR, *RGMb* and *Neogenin* were most strongly expressed in granule cells located adjacent to the IPL (Fig. 1M, M', N, N'). Expression patterns in the OE were as observed at E16.5 (Fig. 1A-C', L-N). Immunohistochemistry revealed expression of RGMa, RGMb and Neogenin on OSN axons in the GL. The GR expressed RGMa and Neogenin and the vomeronasal nerve was prominently stained for RGMb. Mitral cell axons in the olfactory bulb and LOT expressed RGMa, RGMb and Neogenin. The ACa expressed RGMa and Neogenin (data not shown).

The expression of *Unc5A-D* was studied using *in situ* hybridization (Fig. 2, Table S2). At E16.5, expression of all four *Unc5* family members was observed in the MCL of the olfactory bulb (Fig. 2A-D). Interestingly, *Unc5C* was only expressed by a small subset of dorsal mitral cells (Fig. 2C). *Unc5B* staining was observed in the OE and in blood vessels, in line with its proposed role in angiogenesis (Fig. 2B) [69]. *Unc5C* was detected in the GR and the cribriform plate (Fig. 2C). Unc5D was strongly expressed in the olfactory ventricular zone and weakly in the OE and GR (Fig. 2D). At P5 and adult stages, expression levels of *Unc5A-D* were reduced as compared to E16.5, but signals remained in the GL, MCL and GR (Fig. 2E-H, Table S2).

CORTEX

The adult mammalian cerebral cortex consists of six layers comprised of morphologically and functionally distinct neurons. These layers are formed between E11 and E18, as cortical neurons undergo radial migration from the ventricular progenitor zone to their final position in the cortex [70]. The cortex is the origin of several major axon tracts in the forebrain, including the corticothalamic and corticospinal tracts. Cortical expression of *RGMa*, *RGMb* and *Neogenin* has been reported and RGMa can inhibit the outgrowth of cortical axons *in vitro*

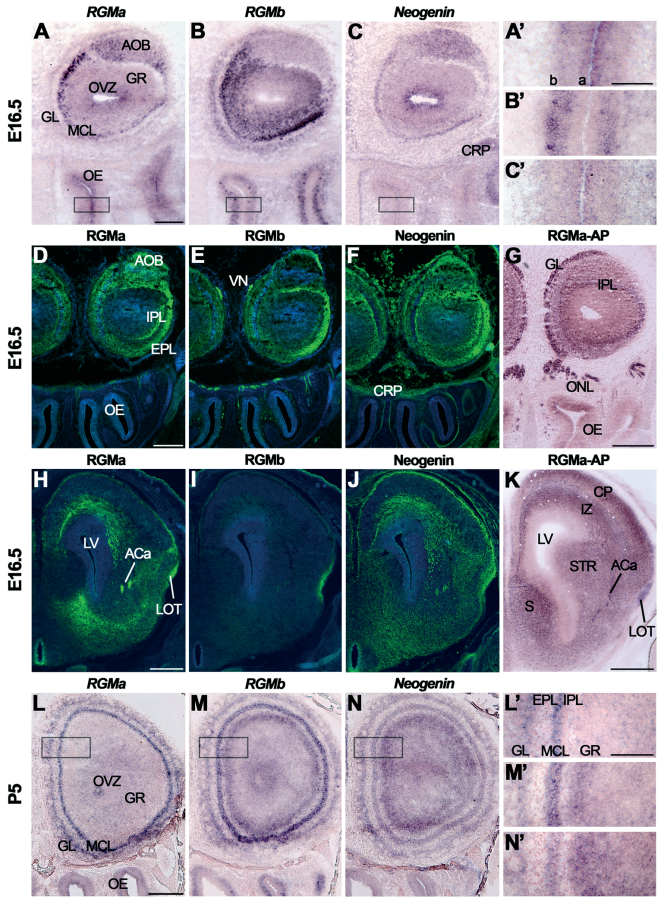

FIGURE 1. RGM and Neogenin expression in the mouse olfactory system.

In situ hybridization on coronal mouse brain sections at E16.5 (A-C') and P5 (L-N'). Panels A'-C' and L'-N' show higher magnifications of boxed areas in A-C and L-N, respectively. Immunohistochemistry (D-F, H-J) and RGMa-AP section binding (G, K) on E16.5 coronal mouse brain sections. Sections in D-F and H-J are counterstained in blue with fluorescent Nissl. (A-C') *In situ* hybridization shows differential expression patterns of *RGMa*, *RGMb* and *Neogenin* in the olfactory bulb and olfactory epithelium (OE). In line with this, immunohistochemistry reveals that axons of olfactory sensory neurons in the OE stain strongly for RGMb and weakly for RGMa and Neogenin. Furthermore, RGMa, RGMb and Neogenin are expressed on olfactory bulb axon projections such as the lateral olfactory tract (LOT). a, apical; ACa, anterior commissure pars anterior; AOB, accessory olfactory bulb; b, basal; CP, cortical plate; CRP, cribriform plate; EPL, external plexiform layer; GL, glomerular layer; GR, granule cell layer; IPL, internal plexiform layer; IZ, intermediate zone; LV, lateral ventricle; MCL, mitral cell layer; ONL, olfactory nerve layer; OVZ, olfactory ventricular zone; S, septum; STR, striatum; VN, vomeronasal nerve. Scale bar A-C 200 µm, A'-C' 100 µm, D-F 300 µm, G 500 µm, H-J 400 µm, K 500 µm, L-N 400 µm and L'-N' 200 µm.

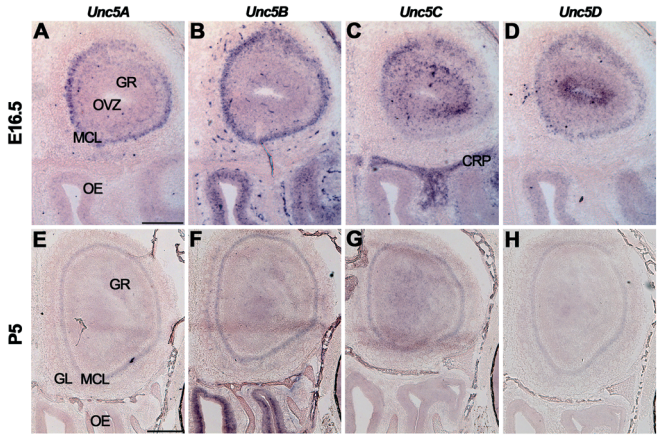

FIGURE 2. *Unc5* expression in the olfactory system.

In situ hybridization on coronal mouse brain sections at E16.5 (A-D) and P5 (E-H). All *Unc5s* are differentially expressed in the olfactory bulb but the olfactory epithelium (OE) only expresses *Unc5B* and *Unc5D*. CRP, cribriform plate; GL, glomerular layer; GR, granule cell layer; MCL, mitral cell layer; OVZ, olfactory ventricular zone. Scale bar A-D 300 µm and E-H 400 µm.

through Neogenin [13,15,18,19,22,67,71,72]. However, the precise role of RGMs and Neogenin during different stages of cortical development and maturation *in vivo* is still incompletely understood.

At E16.5, expression of *RGMa* was restricted to the cortical plate (CP) and the ventricular zone (VZ) (Fig. 3A, A', Table S3). *RGMb* expression was strongest in the pia, the upper part of the CP, and the subventricular zone (SVZ) (Fig. 3B, B') [19]. *Neogenin* was present throughout the developing cortex with prominent expression in the subplate (SP) and the upper CP (Fig. 3C, C'). This pattern is similar to that reported at E14.5 and E18.5 [18,19]. Immunohistochemistry at E16.5 revealed distinct and complementary expression patterns for RGMa and RGMb on cortical projections. Strong expression of RGMa was found on axons in the intermediate zone (IZ) and the internal capsule (IC). Weak RGMa labeling was present on axons traversing the striatum and on axons of the corpus callosum (CC) (Fig. 3D, D', G). Expression of RGMb was weak on axons in the IZ, IC and striatum, but strong at the level of the CC (Fig. 3E, E', H). Neogenin was found on axons in the IZ, CC, and on axons traversing the striatum (Fig. 3F, F', I). Interestingly, Neogenin-positive axons occupied the outer part of the IC, whereas RGMa-positive axons traversed its central part (Fig. 3G, I). Since RGMa, but not Neogenin, is strongly expressed in the dorsal thalamus, the IC labeling for RGMa is likely to represent thalamocortical axon projections (Fig. 6A, C, D, F). It should be noted that expression of RGMs and Neogenin on axon projections was more prominent as compared to the staining

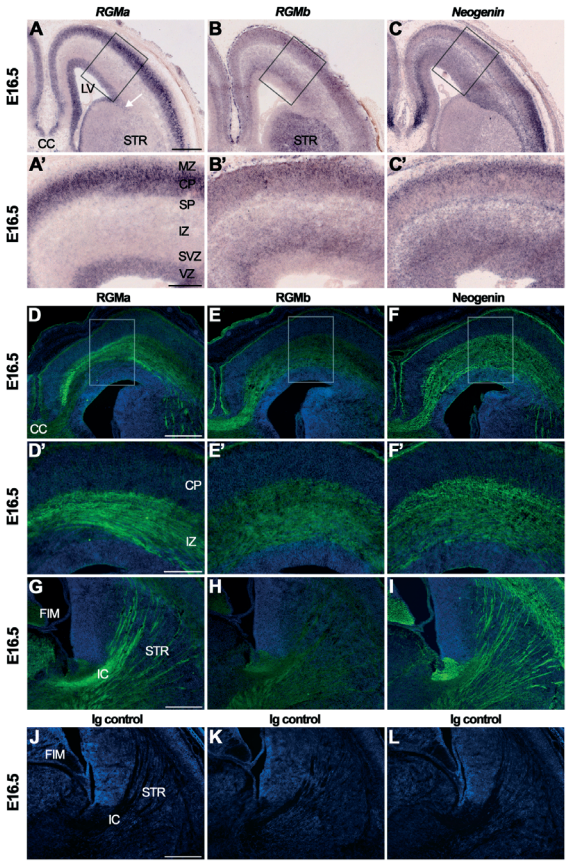

FIGURE 3. RGMa, RGMb and Neogenin display partially complementary patterns of expression in the developing cortex and on cortical projections.

In situ hybridization (A-C') and immunohistochemistry (D-L) on coronal mouse brain sections at E16.5. Panels A'-C' and D'-F' show higher magnifications of the boxed areas in A-C and D-F, respectively. Sections in D-L are counterstained in blue with fluorescent Nissl. (A-C') *In situ* hybridization reveals strong expression of *RGMa* and *Neogenin*, and moderate expression of *RGMb*, in the embryonic mouse cortex. Arrow in A indicates neurons of the lateral migratory stream. (D-I) RGMa and Neogenin protein are strongly expressed in the cortex and on various cortical axon projections. Strong staining for RGMb (E), and Neogenin (F), is detected in the corpus callosum (CC). The internal capsule (IC) stains strongly for RGMa (G). (J-L) Immunostaining with isotype-matched control antibodies did show significant staining. CP, cortical plate; FIM, fimbria; IZ, intermediate zone; LV, lateral ventricle; MZ, marginal zone; SP, subplate; STR, striatum; SVZ, subventricular zone; VZ, ventricular zone. Scale bar A-C 400 µm, A'-C' 200 µm, D-F 300 µm, D'-F' 150 µm, G-I 300 µm and J-M 300 µm.

of cell bodies in the CP that gave rise to these projections. Interestingly, assessment of the cortical expression of Neogenin at E14.5 using an antibody directed against the C-terminal part of Neogenin revealed a different, more widespread pattern of expression including strong labeling of the ventricular zone [68,71,72]. It will therefore be interesting to determine whether this difference arises from the cleavage of Neogenin [61]. In line with previous observations, RGMa and Neogenin were also expressed on cells with the appearance of radial glia cells in the CP and in cells in the VZ (Fig. 3D', F') [50,72]. Strong binding of RGMa-AP was detected in the upper CP, in the striatum, and on axon bundles in the IZ and the IC (Fig. 1K, S3A, B). These observations are in line with the expression of Neogenin detected by *in situ* hybridization

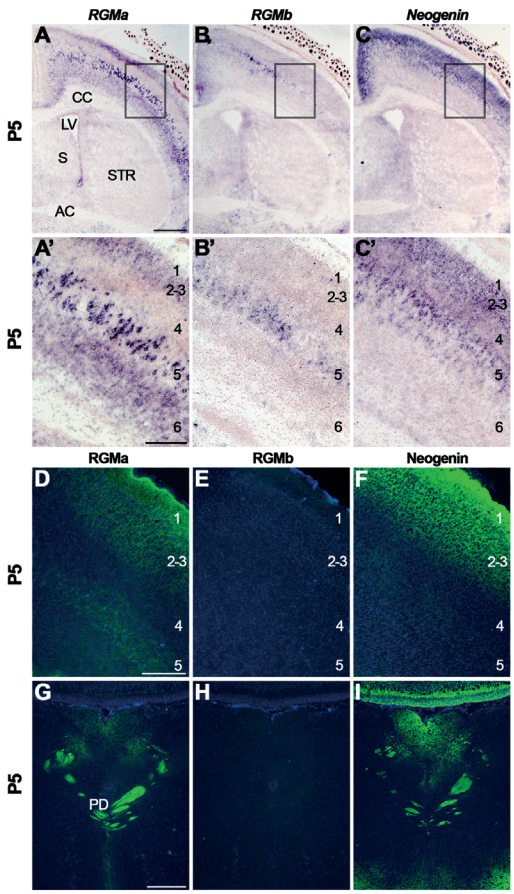

FIGURE 4. Postnatal expression of RGMa, RGMb and Neogenin in the cortex and corticospinal tract.

In situ hybridization (A-C') and immunohistochemistry (D-I) on coronal mouse brain sections at P5. Panels A'-C' show higher magnifications of boxed areas in A-C. Sections in D-I are counterstained in blue with fluorescent Nissl. (A-C') *In situ* hybridization detects strong expression of *RGMa* in cortical layers 1-3, 5 and 6. *RGMb* is mainly expressed in layer 5 in a medial to lateral gradient and *Neogenin* is expressed in layers 1-5. (D-F) RGMa protein is expressed in layers 1-3 and 5. Very weak staining is detected for RGMb and Neogenin is strongly expressed in cortical layers 1-3. (G-I) High levels of RGMa and Neogenin are detected in the corticospinal tract. AC, anterior commissure; CC, corpus callosum; LV, lateral ventricle; PD, pyramidal decussation; S, septum; STR, striatum. Scale bar A-C 600 µm, A'-C' 200 µm, D-F 200 µm and G-I 250 µm.

and immunohistochemistry in these brain areas (Fig. 3C, C', F, F', I). Sections incubated with isotype immunoglobulin controls did not show specific expression (Fig. 3J-L).

At P5, *RGMa* was expressed in layers 1-3, 5 and 6 of the cortex and expression of *RGMb* was confined to neurons of layer 5 displaying a medial high to lateral low gradient (Fig. 4A, A', B, B') [18]. *Neogenin* was expressed in layers 1-5 (Fig. 4C, C', Table S3). Immunohistochemistry detected staining for RGMa in layers 1-3 and 5 (Fig. 4D). RGMb was virtually absent from the P5 cortex and Neogenin staining was most prominent in layers 1-3 (Fig. 4E, F). RGMa, RGMb and Neogenin were expressed on axons in the CC and the IC (data not shown). Strong immunostaining for RGMa and Neogenin was also detected in the corticospinal tract (CST), which is formed by cortical efferents from layer 5 cortical neurons (Fig. 4G-I). In the adult, expression of *RGMa* was detected in layers 5-6 and the VZ while *RGMb* and *Neogenin* were expressed throughout the cortex (Table S3). However, no specific signals for RGMa, RGMb or Neogenin were detected in the adult cortex by immunohistochemistry (data not shown).

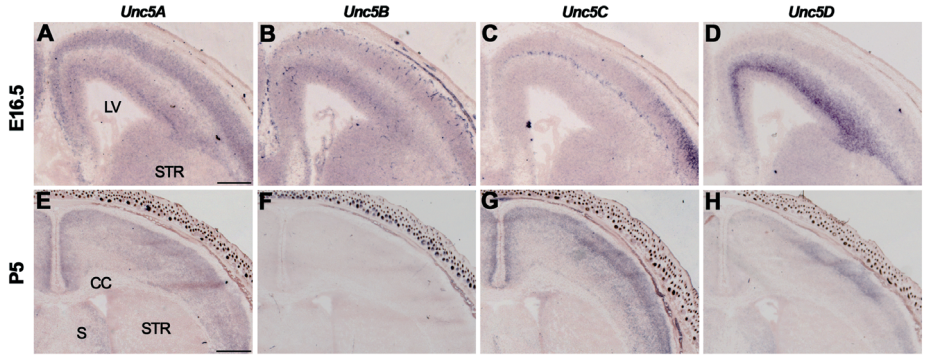

FIGURE 5. *Unc5* expression in the cortex.

In situ hybridization on coronal mouse brain sections at E16.5 (A-D) and P5 (E-H). (A-D) *Un5A-C* are expressed in the cortical plate (CP), and *Unc5A* and *Unc5C* in the subplate (SP). All *Unc5s* are expressed in the subventricular zone (SVZ) and ventricular zone (VZ). (E-H) At P5, *Unc5A*, *Unc5C* and *Unc5D* are expressed in the cortex. CC, corpus callosum; LV, lateral ventricle; S, septum; STR, striatum. Scale bar A-D 300 µm and E-H 600 µm.

At E16.5, *Unc*5A-C were expressed in the CP, *Unc*5A and *Unc*5C in the SP, and *Unc*5A-*D* in the SVZ and VZ (Fig. 5A-C, Table S3). Expression of Unc5D was especially strong in the SVZ (Fig. 5D). At P5 and in adulthood, *Unc*5A was expressed throughout the cortex, *Unc*5*D* in layers 1-4 and no signals for Unc5B were detected [73] (Fig. 5E, F, H, Table S3). *Unc*5C was expressed throughout the cortex at P5 but was restricted to layer 5 in the adult (Fig. 5G)

HIPPOCAMPUS

The hippocampus is a multilayered structure with an essential role in learning and memory. It receives afferent projections from different regions in the brain. Axons from entorhinal cortex (CEn) neurons project via the perforant pathway to the molecular layer (ML) of the dentate gyrus (DG) and via the alvear pathway to the stratum lacunosum moleculare (SLM). Axons from the septum project to the stratum oriens (SO) and stratum radiatum (SR). Within the hippocampus, mossy fibers from DG granule cells synapse on cornu ammonis (CA)3 pyramidal neurons, while Schaffer collaterals from CA3 neurons project to the CA1 region [74].

At E16.5, *RGMa* was strongly expressed in the hippocampal VZ and specifically labeled neurons in the DG and CA layers (Fig. 6A, Table S4). Although weak to moderate *RGMb* expression was detected throughout the hippocampal formation, *RGMb* was prominently expressed in the pial layer lining the hippocampal fissure (Fig.6B). Strong expression of *Neogenin* was observed in the DG, CA region and dentate migration stream. Lower signals were present in the SVZ and VZ (Fig. 6C) (for E18.5 patterns see [67]). Previous work has shown that pial RGMb expression

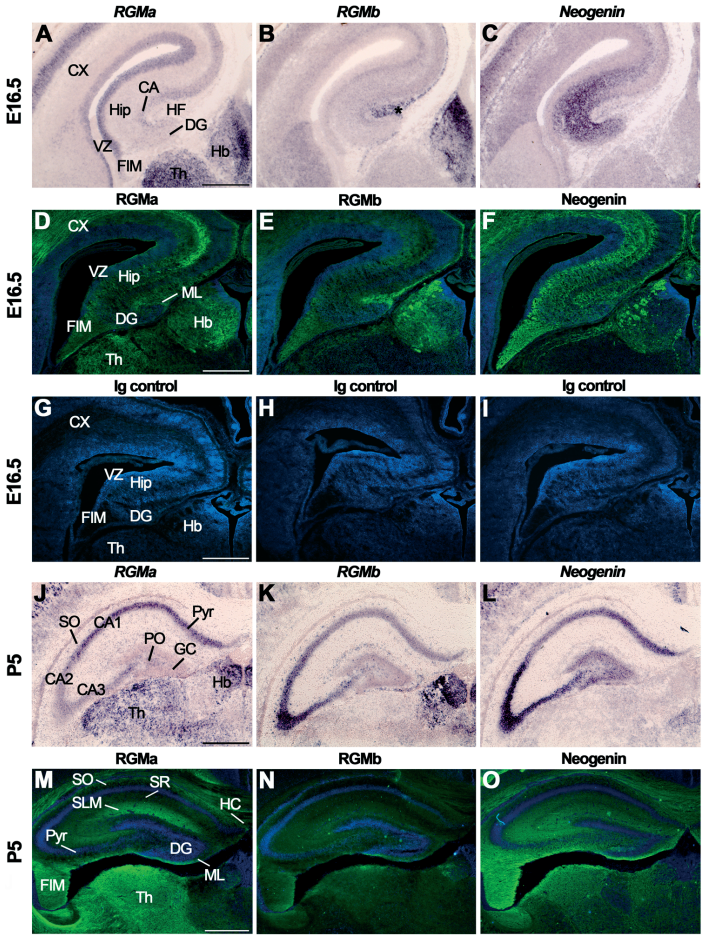

FIGURE 6. Subregion-specific expression of RGMs and Neogenin in the hippocampus.

In situ hybridization (A-C, J-L) and immunohistochemistry (D-I, M-O) on coronal mouse brain sections at E16.5 (A-I) and P5 (J-O). Sections in D-I and M-O are counterstained in blue with fluorescent Nissl. (A-F) RGMa mRNA and protein are expressed in the ventricular zone (VZ), dentate gyrus (DG) and cornu ammonis (CA) region. Strong expression of RGMb mRNA and protein is detected in the pial surface lining the hippocampal fissure (HF). Neogenin transcripts and protein are widely expressed in the developing hippocampus (Hip). (G-I) Immunostaining with isotype matched controls. (J-L) *In situ* hybridization at P5 shows strong but differential expression patterns of *RGMa, RGMb* and *Neogenin* in the CA pyramidal cell layers (Pyr). In addition, strong expression of *Neogenin* is detected in the granular layer (GC) of the DG. (M-O) Immunohistochemistry reveals expression of RGMa and weak expression of RGMb in the stratum lacunosum moleculare (SLM) and fimbria (FIM). Neogenin strongly labels different hippocampal layers. CX, cortex; Hb, habenula; HC, hippocampal commissure; PO, polymorph layer; SO, stratum oriens; SR, stratum radiatum; Th, thalamus. Scale bar A-C: 400 µm, D-F: 300 µm, G-I: 300 µm, J-L: 500 µm and M-O: 400 µm.

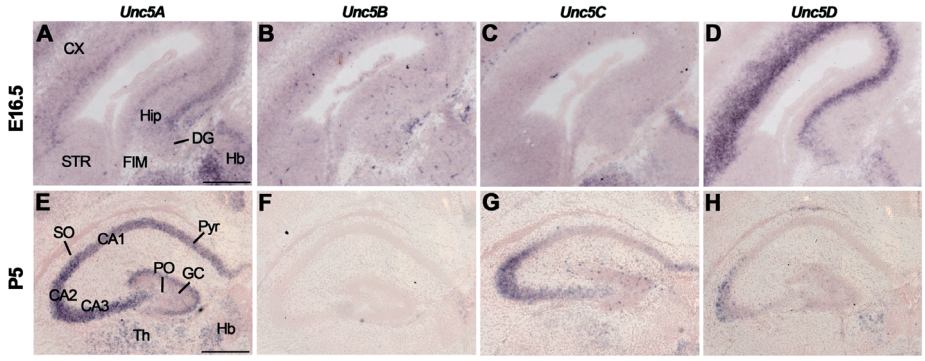

FIGURE 7. *Unc5* expression in the hippocampus.

In situ hybridization on coronal mouse brain sections at E16.5 (A-D) and P5 (E-H). (A-D) *Unc5A-D* are expressed in the E16.5 hippocampus (Hip) and dentate gyrus (DG). (E-H) At P5, *Unc5A* and *Unc5C* are expressed in cornu ammonis (CA) 1-3 and *Unc5D* expression is restricted to CA3. CX, cortex; FIM, fimbria; GC, granular layer; Hb, habenula; HC, hippocampal commissure; PO, polymorph layer; Pyr, pyramidal cell layers; SO, stratum oriens; SR, stratum radiatum; STR, striatum; Th, thalamus. Scale bar A-C: 400 µm and D-F: 300 µm.

directs the migration of Neogenin-positive granule cells in the dentate migratory stream [28,67]. Sections incubated with isotype immunoglobulin controls did not show specific expression (Fig. 6G-I). At E16.5, *RGMa*, *RGMb* and *Neogenin* were expressed in the CEn and the septum (Table S4, S5). Immunohistochemistry detected RGMa in the hippocampal VZ, CA region, fimbria (FIM) and in the inner ML of the DG at E16.5 (Fig. 6D). *In vitro* studies suggest that RGMa expression in the inner ML of the DG functions to restrict Neogenin-positive CEn axons to the outer ML [11]. Weak RGMb expression was detected in the CA region, DG and FIM. However, in line with the *in situ* hybridization data, strong staining was detected in the pia (Fig. 6B, E). Neogenin was present in the outer ML of the DG, CA region, VZ and FIM (Fig. 6F). In line with this pattern of expression, RGMa-AP bound to the DG, CA region and FIM (Fig. S3A, B).

Hippocampal expression of *RGMs* and *Neogenin* persisted at P5 (Fig. 6J-L, Table S4). In line with previous work, strongest expression of *RGMa* was detected in CA1 neurons, while *RGMb* expression was most prominent in the CA2 and CA3 region (Fig. 6J, K)[11,18]. *Neogenin* was detected in CA2 and CA3 neurons and in a medial high to lateral low expression gradient in the CA1 region (Fig. 6L). Granule cells in the DG displayed weak expression of *RGMa* and *RGMb*, and strong *Neogenin* expression (Fig. 6J-L). *RGMa*, *RGMb* and *Neogenin* were expressed in the polymorph layer (PO) of the DG (Fig. 6J-L). Immunohistochemistry at P5 revealed expression of RGMa in the SO, SLM, FIM, ML and hippocampal commissure (Fig. 6M). Weak expression of RGMb was detected in the SLM, FIM and the outer ML of the DG (Fig. 6N). Neogenin was detected throughout the hippocampus, including in the FIM, hippocampal commissure, SLM,

SO, SR and in the ML, granular layer and PO of the DG (Fig. 6O). Adult hippocampal expression of *RGMa*, *RGMb* and *Neogenin* resembled that observed at P5. However, *Neogenin* expression levels were decreased in the adult and *RGMa*, *RGMb* and *Neogenin* were absent from the SR and ML (Table S4). Furthermore, it should be noted that another study failed to detect RGMa expression in the adult hippocampus [19]. Immunohistochemistry in the adult hippocampus revealed weak expression of RGMa and RGMb in the SLM. Neogenin was prominently expressed in the PO and SR. Expression of RGMa, RGMb and Neogenin in the adult FIM was reduced as compared to P5 (data not shown).

Although Unc5A expression has been reported in hippocampal mossy fibers [75], the expression of Unc5 family members during hippocampal development is largely unknown. We detected *Unc5A-D* expression in different regions of the E16.5 hippocampus with highest *Unc5A-D* expression in the CA region and DG (Fig. 7A-D, Table S4). Of the four Unc5 family members, *Unc5A* displayed the most prominent expression in the developing hippocampus. At P5 and in the adult, *Unc5A-D* signals were detected in CA1-CA3 and the DG, though staining for Unc5B was not detected in the P5 hippocampus (Fig. 7E-H, Table S4).

HABENULA

The habenula is part of the epithalamus and is subdivided into a medial (MHb) and lateral part (LHb). The MHb receives major inputs from the septum and the LHb receives afferents from the basal ganglia. The fasciculus retroflexus (FR) is the main output bundle of the Hb and carries LHb and MHb axons to the midbrain [76]. The expression and role of RGMs and Neogenin during the development of the habenula and its projections are unknown.

At E16.5, *in situ* hybridization revealed strong *RGMa* expression in the MHb and lower signals in the LHb. Strong *RGMb* and weak *Neogenin* expression was detected in the MHb and in the medial part of the LHb (Fig. 8A-F). In addition, strong expression for *RGMa* was observed in the thalamus and for *RGMb* in the striatum (Fig. 8D, Table S5). Several of the synaptic targets of LHb and MHb axons in the FR expressed *RGMa*, *RGMb* and *Neogenin*, including the interpeduncular nucleus and the mesodiencephalic dopamine system (Table S5). Interestingly, the mesodiencephalic dopamine system not only receives habenular inputs but also projects axons to the LHb [77,78]. At E16.5, *RGMa* was expressed in the ventral tegmental area (VTA) and substantia nigra (SN), which were identified by *tyrosine hydroxylase (TH)* labeling (Fig. 8M, N). Strong expression of *RGMb* was detected in the VTA and *Neogenin* was present in a subset of neurons in the VTA and SN (Fig. 8O, P). Immunohistochemistry revealed that RGMa expression was confined to the MHb while RGMb and Neogenin were expressed in the MHb and LHb (Fig. 8G-I). Furthermore, strong staining of the FR for RGMa and RGMb and only weak expression of Neogenin was detected (Fig. 8J-L). RGMb and Neogenin were also expressed in the stria medularis (SM) (Fig. 8H, I). The SM contains afferent projections to the Hb from different brain areas several of which display high levels of *Neogenin* and *RGMb* (e.g. the septal nuclei and lateral hypothalamic region) (Table S5). RGMa-AP section binding detected moderate to weak binding to the FR and strong binding

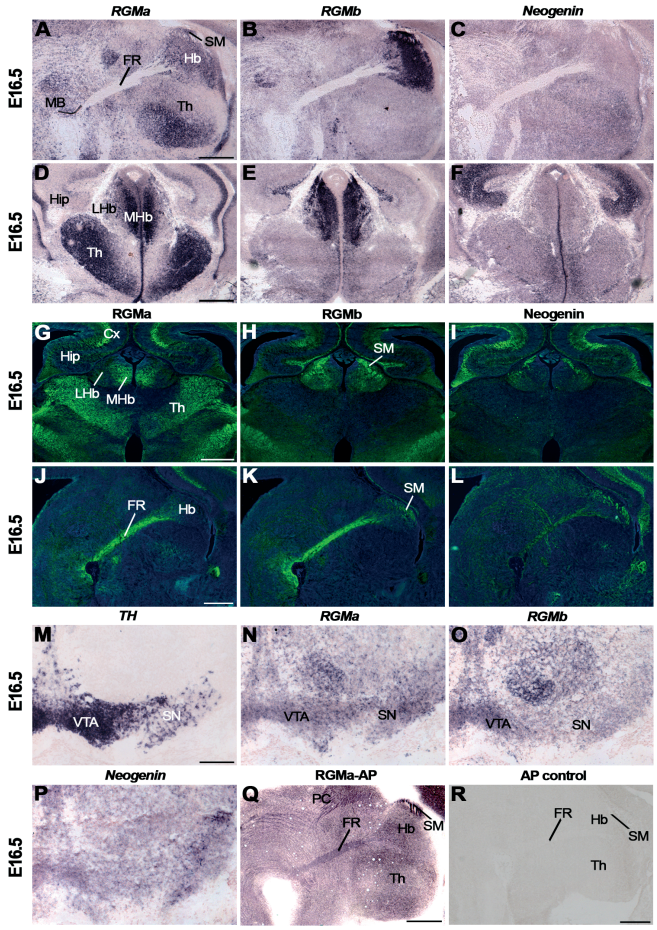

FIGURE 8. Differential expression of RGMs and Neogenin in the habenula and its efferent and afferent projections.

In situ hybridization (A-F, M-P), immunohistochemistry (G-L) and RGMa-AP (Q) and AP (R) section binding on coronal (A-I, M-P) and sagital (J-L, Q-R) mouse brain sections at E16.5. Sections G-L are counterstained in blue with fluorescent Nissl. (A-L) *In situ* hybridization and immunostaining reveal strong expression of RGMa in the medial habenula (MHb) and strong expression of RGMb in the MHb and lateral habenula (LHb). Weak Neogenin expression is detected in the LHb and MHb. In line with this, strong RGMa and RGMb immunostaining is detected on the fasciculus retroflexus (FR), the major output bundle of the Hb. (M-P) *In situ* hybridization for *tyrosine hydroxylase (TH)* stains dopaminergic neurons in the substantia nigra (SN) and ventral tegmental area (VTA). *RGMa* and *Neogenin* expression is detected in the SN and VTA, while *RGMb* is predominantly expressed in the VTA. (Q) RGMa-AP section binding shows strong staining of the stria medullaris (SM) and weak staining of the FR. (R) Section binding with AP control. CX, cortex; Hip, hippocampus; MB, midbrain; PC, posterior commissure; Th thalamus. Scale bars A-L: 400 µm, M-P: 200 µm and Q-R: 400 µm.

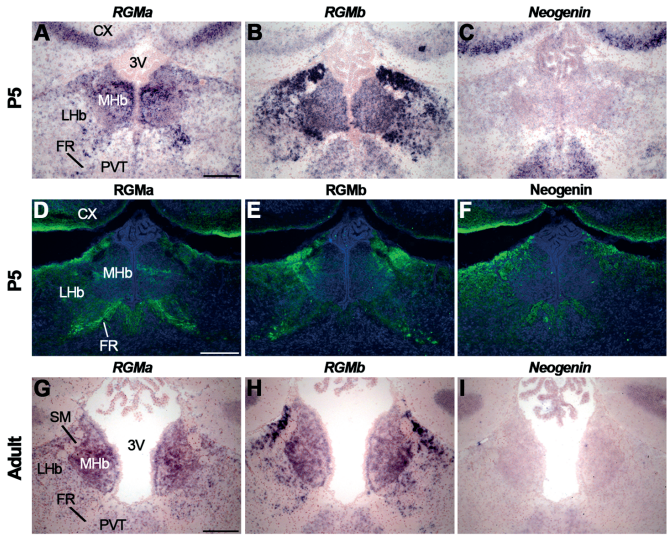

FIGURE 9. Postnatal RGM and Neogenin expression in the habenula and fasciculus retroflexus.

In situ hybridization (A-C, G-I) and immunohistochemistry (D-F) on coronal mouse brain sections at P5 (A-F) and in the adult (G-I). Sections D-F are counterstained in blue with fluorescent Nissl. (A-C, G-I) At P5 and in the adult, *in situ* hybridization reveals strong expression of *RGMa* and *RGMb* in the medial habenula (MHb). The lateral habenula (LHb) strongly expresses *RGMb*, while only weak expression of Neogenin is detected in Hb. (D-F) Immunohistochemistry detects strong expression of RGMa and RGMb and weak expression of Neogenin in the fasciculus retroflexus (FR). 3V, third ventricle; CX, cortex; SM, stria medullaris; PVT, paraventricular thalamic nucleus. Scale bars A-I: 200 µm.

to the SM. Sections incubated with AP control did not exhibit specific staining (Fig. 8Q, R). At P5 and in the adult, strong *RGMa* expression was observed in the MHb and *RGMb* expression was most prominent in the LHb and the lateral aspect of the MHb (Fig. 9A, B, G, H, Table S5) (see [18] for an equivalent pattern at P7). Only weak expression of *Neogenin* was detected (Fig. 9C, I). Expression of *RGMs* and *Neogenin* was also detected in the paraventricular thalamic nucleus, just ventral to the Hb (Fig. 9A-C, G-I). Immunohistochemistry revealed expression of RGMa and RGMb, and weak expression of Neogenin in the FR at P5 and in the adult (Fig. 9D-F, data not shown).

In situ hybridization at E16.5 revealed strong expression of *Unc5A* in the LHb and MHb (Fig. 10A, Table S5). Weak expression of *Unc5B* was detected in the Hb, particularly staining blood vessels, and expression of *Un5C* and *Unc5D* was confined to the LHb (Fig. 10B-D). At P5, *Unc5A* was weakly expressed in the MHb and LHb and expression of *Unc5D* was restricted to the LHb (Fig. 10E, H, Table S5). Expression of *Unc5B* and *Unc5C* was not detected in the Hb (Fig. 10F, G). In adult, almost no *Unc5* staining was observed in the Hb, except for very weak *Unc5B* labeling (Fig. 10I-L, Table S5)

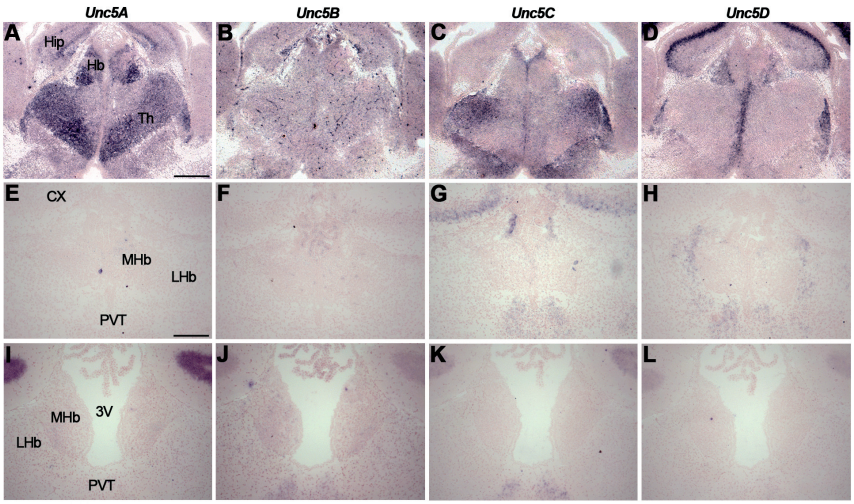

FIGURE 10. *Unc5* expression in the habenula.

In situ hybridization on coronal mouse brain sections at E16.5 (A-D), P5 (E-H) and adult (I-L). (A-D) At E16.5 *in situ* hybridization shows expression of *Unc5A-D* in the habenula (Hb). *Unc5B* expression labels blood vessels but not habenular neurons. (E-H) At P5, *Unc5A* is weakly expressed in the Hb and *Unc5D* expression is restricted to the lateral habenula (LHb). (I-L) In the adult Hb, weak *Unc5B* expression is detected. 3V, third ventricle; CX, cortex; MHb, medial habenula; PVT paraventricular thalamic nucleus. Scale bar A-D: 300 µm and E-L: 200 µm.

CEREBELLUM

The cerebellum is located in the hindbrain and is associated with motor coordination and controlled movement. The adult cerebellum consists of three different layers: the molecular layer (ML), the Purkinje cell layer (PCL) and the granular cell layer (GCL). Interestingly, the neurons that occupy these layers derive from two different progenitor zones. The cerebellar VZ gives rise to Purkinje cells (PCs), Bergmann glia (BG) and interneurons. Granule cells precursors (GCPs) are generated in the upper rhombic lip lining the fourth ventricle and migrate tangentially along the cerebellar surface to form the external granular layer (EGL). During the first two postnal weeks, cerebellar granule cells (CGCs) migrate from the EGL radially along BG in the ML to the internal granular cell layer (IGL) [79].

In situ hybridization at E16.5 revealed *RGMa* expression in the VZ of the cerebellum but not in the EGL (Fig. 11A, Table S6). *RGMb* was expressed in a subset of cells in the inner part of the EGL and *Neogenin* staining was detected in the VZ and throughout the EGL (Fig. 11B, C) [18,19,23]. This *RGM* expression profile is in line with previously reported expression patterns at E14.5 [18]. Interestingly, however, at E18.5 cerebellar *RGMb* signals are already much more restricted as compared to the expression observed at E16.5 (Fig. 11B) [19]. Furthermore,

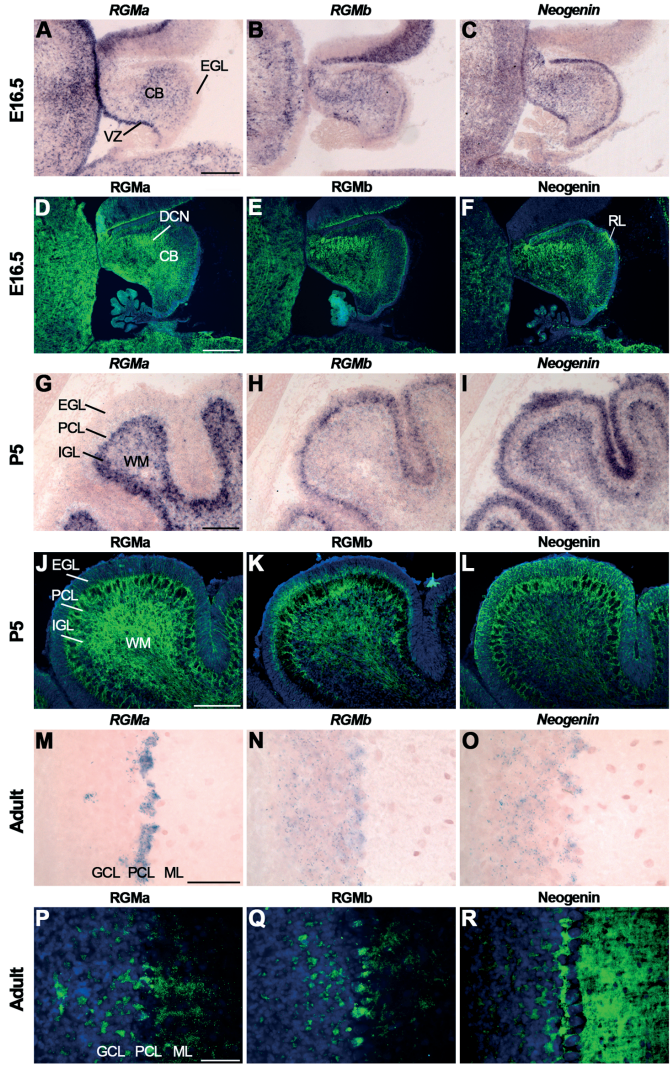

FIGURE 11. Differential expression of RGMs and Neogenin in the cerebellum.

In situ hybridization (A-C, G-I, M-O) and immunohistochemistry (D-F, J-L, P-R) on coronal mouse brain sections at E16.5 (A-F), P5 (G-L) and in the adult (M-R). (A-I, M-O) *In situ* hybridization and immunohistochemistry reveals strong and broad expression of RGMa, RGMb and Neogenin in the cerebellum (CB). (J-L) Immunostaining shows expression of RGMa and Neogenin in all cerebellar layers at P5. RGMb is expressed in the internal granular layer (IGL), Purkinje cell layer (PCL) and external granular layer (EGL). (P-R) In the adult, RGMa, RGMb and Neogenin protein are expressed in Purkinje cells (PCs) and axons in the granular cell layer (GCL), PCL and molecular layer (ML). Neogenin strongly labels PC dendrites in the ML. DCN, deep cerebellar nuclei; WM, white matter; VZ, ventricular zone. Scale bar A-C: 300 µm, D-F: 250 µm, G-I: 150 µm, J-L: 150 µm, M-O: 100 µm and P-R: 50 µm.

expression of *Neogenin* in the EGL has been reported previously at E13 and is in line with RGMa-AP binding patterns (Fig. S3C), but could not be detected at E18.5 [23,67]. *RGMa*, *RGMb* and *Neogenin* were expressed in the PCL and deep cerebellar nuclei (DCN) (Fig. 11A-C). In line with this expression, immunostaining revealed expression of RGMa, RGMb and Neogenin in the DCN (Fig. 11D-F). RGMa was also expressed in cellular processes traversing the EGL (Fig. 11D). In line with the *in situ* hybridization data, RGMb was confined to the inner part of the EGL (Fig. 11E). Neogenin expression was detected throughout the EGL and in a patch of GCPs in the EGL where the presumptive rhombic lip is located (Fig. 11F) [23].

At P5, *RGMa* was confined to the IGL (Fig. 11G, Table S6). *RGMb* was detected in the inner EGL, PCL and at lower levels in the IGL (Fig. 11H). *Neogenin* was strongly expressed in the outer part of the EGL, in the PCL and IGL (Fig. 11I). Immunohistochemistry showed staining for RGMa, RGMb and Neogenin in the EGL (Fig. 11J-L). Furthermore, RGMa, RGMb and Neogenin were expressed in the PCL and IGL including the white matter tracts in this structure. However, since no *RGMa* expression was detected in the PCL (Fig. 11G) this labeling may represent expression on migrating cerebellar granule neurons or BG. To determine whether RGMs and Neogenin are expressed on the radial processes of BG, co-immunostaining for glial fibrillary acidic protein (GFAP), a BG marker, and RGMa or Neogenin was performed. Both RGMa and Neogenin expression colocalized with the GFAP-positive BG fibers in the EGL (Fig. 12). In addition, cerebellar granule neurons along BG processes expressed Neogenin.

In the adult, *in situ* hybridization revealed expression of *RGMa*, *RGMb* and *Neogenin* in the PCL and GCL (Fig. 11M-O, Table S6). It should be noted that other work does not detect RGMb in the adult cerebellum [19]. Immunohistochemistry revealed staining for RGMa, RGMb and Neogenin in the GCL, PCs and the ML. Staining in the ML may represent the dendritic processes of PCs (Fig. 11P-R).

Expression of Unc5A-D in the cerebellum has been reported in embryonic and postnatal stages and in the adult [64,80–86]. *Unc5C* knockout mice display severe defects in cerebellar development, including disturbed GCP migration and ectopically located PCs [80,83,84,87]. In line with these observations, *Unc5A-C* but not *Unc5D* were expressed in the EGL at E16.5 (Fig. 13A-D, Table S6). At P5, *Unc5A* was restricted to the IGL, while *Unc5B* and *Unc5C* were detected in the EGL, PCL and IGL (Fig. 13E-G). Weak expression of *Unc5D* was only detected in the PCL (Fig. 13H). In adult *Un5A-C* were expressed in the PCL and IGL, while expression of *Unc5D* is only detected in the PCL (Table S6).

DISCUSSION

Since their original identification in 2002, RGMs have been implicated in several different aspects of neural development. A large part of this work has focused on the important roles

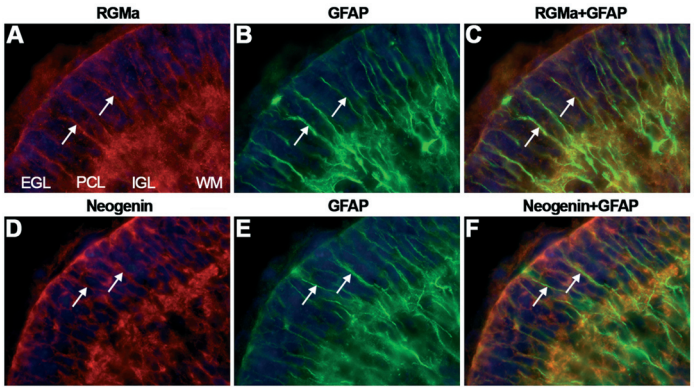

FIGURE 12. RGMa and Neogenin are expressed on Bergmann glia.

Immunohistochemistry for RGMa (A, C), glial fibrillary acidic protein (GFAP) (B-C, E-F) and Neogenin (D, F) on coronal mouse brain sections at P5 visualized by confocal microscopy. Sections are counterstained in blue with fluorescent Nissl. (A-F) RGMa and Neogenin immunostaining (in red) colocalizes with GFAP-positive staining (in green) on Bergmann glial fibers (arrows). Granule cells in the external granular layer (EGL) also express Neogenin. IGL, internal granular layer; PCL, Purkinje cell layer; WM, white matter.

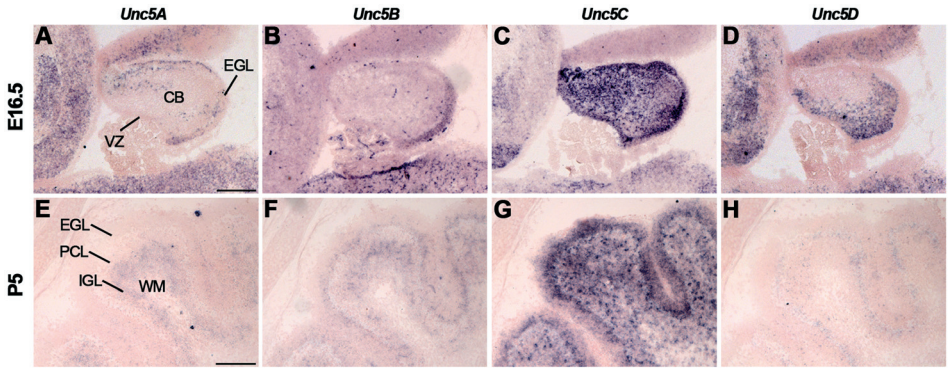

FIGURE 13. Dynamic expression of *Unc5* in the developing cerebellum.

In situ hybridization on coronal mouse brain sections at E16.5 (A-D) and P5 (E-H). (A-D) Expression of *Unc5A-D* is detected in the cerebellum (CB), although expression of *Unc5C* is most prominent. *Unc5A-C* are expressed in the external granular layer (EGL). (E-H) At P5, *Unc5B* and *Unc5C* are expressed in the EGL, Purkinje cell layer (PCL) and internal granular layer (IGL). Expression of *Unc5B* in the EGL is restricted to the inner cell layers. Expression of *Unc5A* is only detected in the IGL and expression of *Unc5D* is restricted to the PCL. VZ, ventricular zone; WM, white matter. Scale bar A-D: 300 µm and E-H: 150 µm.

of RGMa and its receptor Neogenin during axon pathfinding in the chick retinotectal system [6,8–10,52]. However, experiments in *Xenopus* embryos and on cultured rodent neuronal tissues have also highlighted more widespread roles for RGM-Neogenin signaling in axon guidance [11–17,20]. In addition, it has become clear that RGMs are pleiotropic and can regulate processes such as neurogenesis, differentiation, migration, and apoptosis [8,28,29,31,32,49–51,88]. Despite this progress, the precise role of RGMs and Neogenin in the development of many neuronal systems remains unknown, especially in the mouse. To begin to provide further insight into the possible roles of RGM-Neogenin signaling during mouse brain development, we performed a comparative analysis of the expression of RGMa, RGMb and Neogenin transcript and protein at different developmental stages. Unc5s were included in this analysis as they are obligate co-receptors for the axon repulsive effects of RGMs [15].

NEUROGENESIS, DIFFERENTIATION AND MIGRATION

Previous work has shown expression of RGMs and Neogenin in the proliferative zones of different brain structures [11,18,28,50,51,67,72,89]. Our data confirm and extend these findings and reveal expression of Neogenin, RGMs and Unc5s in the progenitor regions of the olfactory epithelium, olfactory bulb, cortex, hippocampus and cerebellum. For example, strong Neogenin expression was detected in the upper part of the cerebellar EGL, which contains progenitors for CGCs [90,91], and in the VZ of the olfactory bulb (Fig. 1C). Of the two RGMs expressed in the brain, RGMa was especially prominent in progenitor regions. On the other hand, expression of RGMb often appeared to mark regions containing differentiating cells immediately adjacent to the progenitor zones. For example, RGMb expression was detected in the SVZ of the cortex while RGMa was expressed in the adjacent VZ (Fig. 3A', B') [18,19]. Together these observations support widespread roles for RGMa and RGMb in neurogenesis and neuronal differentiation.

The moment that neuroblasts start to differentiate often coincides with their migration towards their target areas. The first indication that Neogenin regulates cell migration comes from the analysis of morpholino-induced Neogenin knockdown in zebrafish, which show defects in neural tube formation and somitogenesis [92]Ludwig Institute for Cancer Research, Royal Melbourne Hospital, Parkville, Victoria 3050, Australia. It is clear, however, that RGM-Neogenin signaling also plays a crucial role in cell migration at later developmental stages. This is nicely illustrated by the ability of RGMb, expressed along the hippocampal fissure, to guide Neogenin-positive DG granule cells though the DG migratory stream towards the hippocampus [28]. Such a role for RGMs and Neogenin is likely to be more general. For example, we, and others, report Neogenin expression on radially migrating neurons in the cortex and young interneurons tangentially migrating from the ganglionic eminence (GE) [51,93]. Furthermore, Neogenin is expressed in migrating olfactory interneuron precursors in the rostral migratory stream [50,94]. The role of RGM-Neogenin signaling in these populations of migrating neurons is largely unknown. Repulsive signaling induced by RGMs may guide cortical interneurons during their migration from the GE to the cortex. A recent study shows that overexpression

of Neogenin in the GE leads to a failure of interneurons to migrate out of the GE [93]. This migrational defect may be caused by an increased response of Neogenin-overexpressing cells to the attractive effects of Netrin-1, which is expressed in the GE [93]. Alternatively, however, increased Neogenin levels may enhance the responsiveness of interneurons to repulsive cues around the GE. An interesting candidate is RGMb, which is expressed in the striatum around the time of interneuron migration (Fig. 3B). Overexpression of Neogenin in interneurons may render these cells more sensitive to the repulsive effects of RGMb thereby confining them to the GE.

Another region where Neogenin and RGMs may regulate cell migration is the cerebellum. GCPs are generated in the rhombic lip and then migrate to the surface of the cerebellum to form the EGL. From this outer part of the EGL CGCs change their mode of migration from tangential to radial and migrate along radial glial projections towards the IGL. Strong *Neogenin* expression is detected in radially migrating CGCs in the outer EGL (Fig. 11I). In contrast, *Neogenin* is absent from CGCs in the inner EGL, where CGCs switch from tangential to radial migration. Interestingly, strong expression of RGMb is detected in the inner EGL complementary to Neogenin expression in the outer EGL (Fig. 11H). It is therefore tempting to speculate that RGMb-Neogenin signaling is involved in the switch from tangential to radial migration. Of the Unc5 family members, Unc5C has been shown to have an important role in cerebellar development. *Unc*5C is strongly expressed in the developing cerebellum [86] and mutations in the *Unc*5C gene result in severe defects in cerebellar development, including a reduction of cerebellar size, abnormal cerebellar foliation and ectopic localization of PCs and CGCs [80,83,84,87]. Analysis of the *Unc*5C mutant mice reveals that Unc5C regulates migration of GCPs along the caudo-rostral and dorso-ventral axes. GCPs expressing mutant Unc5C invade the superior colliculus and brain stem [80,83]. A possible explanation for these migrational defects is the inability of migrating GCPs to respond to repellent guidance cues in the environment. In line with this hypothesis, RGMs are expressed in the superior colliculus and in the VZ of the cerebellum [18,19,52] and are therefore in the appropriate location to repel Neogenin- and Unc5C-expressing migrating GCPs and restrict their migration to 'future cerebellar brain areas'. Further work is needed to examine whether or how interactions between RGMs, Neogenin and Unc5s regulate cerebellar development.

AXON GUIDANCE AND AXON TRACT DEVELOPMENT

RGMa- and RGMb-Neogenin signaling mediates neurite outgrowth inhibition of cultured chick retinal ganglion and mouse cortical, entorhinal cortical, cerebellar granule and dorsal root ganglia (DRG) neurons [6,9,11,12,14,15,17]. However, our understanding of the role of these neurite outgrowth inhibitory effects in regulating axon guidance events *in vivo* is far from complete. Our study together with previous work shows that RGMs and Neogenin are abundantly expressed throughout the developing mouse brain [18,19,67], indicating a potential role in regulating axon guidance events in different brain areas. Neogenin expression was

detected in many different axonal tracts in the brain, including the LOT, cortical efferents, the ACa and CST, and axonal tracts in the hippocampus (fimbria) and cerebellum. Interestingly, many axon tracts also showed staining for RGMa and RGMb. The LOT, ACa, IC, CST, FR and axonal tracts in the hippocampus and cerebellum were strongly stained for RGMa. The LOT and FR also expressed RGMb and strong expression of RGMb was detected in OSN axons and the CC.

Axonal expression of RGMs may aid in organizing axon bundles into sub-bundles or in creating exclusion zones for axons. For example, clear differential expression of RGMs and Neogenin was found on axon bundles in the IC. In the IC, expression of RGMa is predominant in the core, while Neogenin expression is detected in axonal tracts in the outer regions of the IC (Fig. 3G, I). This suggests that axonally expressed RGMa may instruct Neogenin-positive axons to grow in the outer parts of the IC. In addition, axonal RGM expression may mediate the adhesion of axons into tight bundles. Evidence for a possible role for RGMb as an adhesive cue for DRG axons comes from a coculture assay of Neogenin- and RGMb-positive DRG neurons and HEK-293 cells transiently expressing RGMb. In this assay, DRG neurites make contacts with RGMb-expressing HEK293 cells [95]. Furthermore, RGMb enhances the adhesion of dissociated cultured DRG neurons to HEK293 cells transiently expressing RGMb. RGMa can also exert adhesive effects through Neogenin, for example during neural tube closure [30,52,88,92]. Further experiments are needed to confirm the role of these potential homophilic and heterophilic RGM interactions in axon tract development *in vivo*.

NEURONAL RGM RECEPTOR COMPLEXES

The inhibitory effects of RGMs on neurite outgrowth depend on a multimeric receptor complex containing Neogenin and Unc5s. Although Unc5B has been shown to be required for these effects at the functional level, Neogenin can bind all Unc5 family members [15]. This suggests that Neogenin may interact with different Unc5s in different systems, cellular processes and/or at developmental stages. Our comparative analysis of *Unc5A-D* co-receptors during brain development revealed prominent and differential expression patterns at all developmental stages studied. At E16.5 multiple brain regions were identified that displayed expression of all *Unc5s*, including the olfactory bulb, hippocampus and hypothalamus (see Tables S2-6). However, even within these regions expression of *Unc5s* was often highly specific and confined to specific substructures. For example in the VZ of the E16.5 olfactory bulb, prominent expression of *Unc5D* and Neogenin was detected, while expression of *Unc5A-C* was absent (Fig. 1C, F, 2A-D, Table S2). This invites the speculation that a Neogenin/Unc5D receptor complex may play a role in neuronal cell proliferation and neurogenesis in the olfactory bulb. In the habenula, we detected very specific expression of *Unc5A* in the MHb, while the LHb expressed *Unc5A*, *Unc5C* and *Unc5D* at E16.5 (Fig. 10A-D, Table S5). This indicates differential roles for Unc5s in the development of MHb and LHb neurons. Although binding of all Unc5 molecules to Neogenin has been shown, it is currently not known whether binding of different Unc5s

results in different functional outcomes. Future work will focus on examining whether different Unc5 proteins serve as functional co-receptors for RGM receptors in different brain regions and during different developmental processes.

CONCLUSION

This study presents a comparative analysis of the expression of RGMa, RGMb, Neogenin and Unc5A-D in the mouse brain at three key developmental stages (E16.5, P5 and adult). The observed expression patterns support a widespread, and largely unexplored, role for RGMa/b and their Neogenin/Unc5 receptor complex in neuron proliferation, migration and axon guidance in the mouse brain. Interestingly, RGMs may function both as exogenous cues that are detected by cells or neurites or as axon-derived factors involved in axon tract development. Analysis of Unc5 expression patterns suggests that the composition of the RGM receptor complex, i.e. which Unc5 family member it contains, may differ between different brain regions and/or cellular processes. In all, these data serve as a valuable framework for the further dissection of the role of RGMs during mouse neural development.

ACKNOWLEDGEMENTS

We are grateful to Silvia Arber, Valerie Castellani, Jean-François Cloutier, Roman Giger and Thomas Skutella for sharing cDNA constructs. We thank Sharon Kolk, Roos Winter and Ewoud Schmidt and other members of the Pasterkamp lab for help and fruitful discussions.

REFERENCE LIST

De Vries M, Cooper HM (2008) Emerging roles for neogenin and its ligands in CNS development. J Neurochem 106: 1483-1492.

Key B, Lah GJ (2012) Repulsive guidance molecule A (RGMa): A molecule for all seasons. Cell Adh Migr 6: 85-90. 20167.

Matsunaga E, Chedotal A (2004) Repulsive guidance molecule/neogenin: a novel ligand-receptor system playing multiple roles in neural development. Dev Growth Differ 46: 481-486.

Severyn CJ, Shinde U, Rotwein P (2009) Molecular biology, genetics and biochemistry of the repulsive guidance molecule family. Biochem J 422: 393-403.

Yamashita T, Mueller BK, Hata K (2007) Neogenin and repulsive guidance molecule signaling in the central nervous system. Curr Opin Neurobiol 17: 29-34.

Monnier PP, Sierra A, Macchi P, Deitinghoff L, Andersen JS *et al*. (2002) RGM is a repulsive guidance molecule for retinal axons. Nature 419: 392-395.

Stahl B, Muller B, von Boxberg Y, Cox EC, Bonhoeffer F (1990) Biochemical characterization of a putative axonal guidance molecule of the chick visual system. Neuron 5: 735-743.

Matsunaga E, Nakamura H, Chedotal A (2006) Repulsive guidance molecule plays multiple roles in neuronal differentiation and axon guidance. J Neurosci 26: 6082-6088.

Rajagopalan S, Deitinghoff L, Davis D, Conrad S, Skutella T *et al*. (2004) Neogenin mediates the action of repulsive guidance molecule. Nat Cell Biol 6: 756-762.

Tassew NG, Chestopolava L, Beecroft R, Matsunaga E, Teng H *et al*. (2008) Intraretinal RGMa is involved in retino-tectal mapping. Mol Cell Neurosci 37: 761-769.

Brinks H, Conrad S, Vogt J, Oldekamp J, Sierra A *et al*. (2004) The repulsive guidance molecule RGMa is involved in the formation of afferent connections in the dentate gyrus. J Neurosci 24: 3862-3869.

Conrad S, Genth H, Hofmann F, Just I, Skutella T (2007) Neogenin-RGMa signaling at the growth cone is bone morphogenetic protein-independent and involves RhoA, ROCK, and PKC. J Biol Chem 282: 16423-16433.

Endo M, Yamashita T (2009) Inactivation of Ras by p120GAP via focal adhesion kinase dephosphorylation mediates RGMa-induced growth cone collapse. J Neurosci 29: 6649-6662.

Hata K, Fujitani M, Yasuda Y, Doya H, Saito T *et al*. (2006) RGMa inhibition promotes axonal growth and recovery after spinal cord injury. J Cell Biol 173: 47-58.

Hata K, Kaibuchi K, Inagaki S, Yamashita T (2009) Unc5B associates with LARG to mediate the action of repulsive guidance molecule. J Cell Biol 184: 737-750.

Lah, G. J. and B. Key. 2012. Dual roles of the chemorepellent axon guidance molecule RGMa in establishing pioneering axon tracts and neural fate decisions in embryonic vertebrate forebrain. Dev Neurobiol 72:1458-1470.

Liu X, Hashimoto M, Horii H, Yamaguchi A, Naito K *et al*. (2009) Repulsive guidance molecule b inhibits neurite growth and is increased after spinal cord injury. Biochem Biophys Res Commun 382: 795-800.

Oldekamp J, Kramer N, Alvarez-Bolado G, Skutella T (2004) Expression pattern of the repulsive guidance molecules RGM A, B and C during mouse development. Gene Expr Patterns 4: 283-288.

Schmidtmer J, Engelkamp D (2004) Isolation and expression pattern of three mouse homologues of chick Rgm. Gene Expr Patterns 4: 105-110.

Wilson NH, Key B (2006) Neogenin interacts with RGMa and netrin-1 to guide axons within the embryonic vertebrate forebrain. Dev Biol 296: 485-498.

Metzger M, Conrad S, Skutella T, Just L (2007) RGMa inhibits neurite outgrowth of neuronal progenitors from murine enteric nervous system via the neogenin receptor *in vitro*. J Neurochem 103: 2665-2678.

Yoshida J, Kubo T, Yamashita T (2008) Inhibition of branching and spine maturation by repulsive guidance molecule in cultured cortical neurons. Biochem Biophys Res Commun 372: 725-729.

Vielmetter J, Kayyem JF, Roman JM, Dreyer WJ (1994) Neogenin, an avian cell surface protein expressed during terminal neuronal differentiation, is closely related to the human tumor suppressor molecule deleted in colorectal cancer. J Cell Biol 127: 2009-2020.

Kang JS, Yi MJ, Zhang W, Feinleib JL, Cole F *et al*. (2004) Netrins and neogenin promote myotube formation. J Cell Biol 167: 493-504.

Lejmi E, Leconte L, Pedron-Mazoyer S, Ropert S, Raoul W *et al*. (2008) Netrin-4 inhibits angiogenesis via binding to neogenin and recruitment of Unc5B. Proc Natl Acad Sci U S A 105: 12491-12496.

Park KW, Crouse D, Lee M, Karnik SK, Sorensen LK *et al*. (2004) The axonal attractant Netrin-1 is an angiogenic factor. Proc Natl Acad Sci U S A 101: 16210-16215.

Srinivasan K, Strickland P, Valdes A, Shin GC, Hinck L (2003) Netrin-1/neogenin interaction stabilizes multipotent progenitor cap cells during mammary gland morphogenesis. Dev Cell 4: 371-382.

Conrad S, Stimpfle F, Montazeri S, Oldekamp J, Seid K *et al*. (2010) RGMb controls aggregation and migration of Neogenin-positive cells *in vitro* and *in vivo*. Mol Cell Neurosci 43: 222-231.

Gessert S, Maurus D, Kuhl M (2008) Repulsive guidance molecule A (RGM A) and its receptor neogenin during neural and neural crest cell development of *Xenopus* laevis. Biol Cell 100: 659-673.

Kee N, Wilson N, De Vries M, Bradford D, Key B *et al*. (2008) Neogenin and RGMa control neural tube closure and neuroepithelial morphology by regulating cell polarity. J Neurosci 28: 12643-12653.

Matsunaga E, Tauszig-Delamasure S, Monnier PP, Mueller BK, Strittmatter SM *et al*. (2004) RGM and its receptor neogenin regulate neuronal survival. Nat Cell Biol 6: 749-755.

Shin GJ, Wilson NH (2008) Overexpression of repulsive guidance molecule (RGM) a induces cell death through Neogenin in early vertebrate development. J Mol Histol 39: 105-113.

Zhang AS, West AP, Jr., Wyman AE, Bjorkman PJ, Enns CA (2005) Interaction of hemojuvelin with neogenin results in iron accumulation in human embryonic kidney 293 cells. J Biol Chem 280: 33885-33894.

Babitt JL, Zhang Y, Samad TA, Xia Y, Tang J *et al*. (2005) Repulsive guidance molecule (RGMa), a DRAGON homologue, is a bone morphogenetic protein co-receptor. J Biol Chem 280: 29820-29827.

Babitt JL, Huang FW, Wrighting DM, Xia Y, Sidis Y *et al*. (2006) Bone morphogenetic protein signaling by hemojuvelin regulates hepcidin expression. Nat Genet 38: 531-539.

Corradini E, Babitt JL, Lin HY (2009) The RGM/DRAGON family of BMP co-receptors. Cytokine Growth Factor Rev 20: 389-398.

Hagihara M, Endo M, Hata K, Higuchi C, Takaoka K *et al*. (2011) Neogenin, a receptor for bone morphogenetic proteins. J Biol Chem 286: 5157-5165.

Kuns-Hashimoto R, Kuninger D, Nili M, Rotwein P (2008) Selective binding of RGMc/hemojuvelin, a key protein in systemic iron metabolism, to BMP-2 and neogenin. Am J Physiol Cell Physiol 294: C994-C1003.

Samad TA, Rebbapragada A, Bell E, Zhang Y, Sidis Y *et al*. (2005) DRAGON, a bone morphogenetic protein co-receptor. J Biol Chem 280: 14122-14129.

Xia Y, Yu PB, Sidis Y, Beppu H, Bloch KD *et al*. (2007) Repulsive guidance molecule RGMa alters utilization of bone morphogenetic protein (BMP) type II receptors by BMP2 and BMP4. J Biol Chem 282: 18129-18140.

Xia Y, Babitt JL, Bouley R, Zhang Y, Da Silva N *et al*. (2010) Dragon enhances BMP signaling and increases transepithelial resistance in kidney epithelial cells. J Am Soc Nephrol 21: 666-677.

Zhang AS, Yang F, Wang J, Tsukamoto H, Enns CA (2009) Hemojuvelin-neogenin interaction is required for bone morphogenic protein-4-induced hepcidin expression. J Biol Chem 284: 22580-22589.

Zhou Z, Xie J, Lee D, Liu Y, Jung J *et al.* (2010) Neogenin regulation of BMP-induced canonical Smad signaling and endochondral bone formation. Dev Cell 19: 90-102.

Halbrooks PJ, Ding R, Wozney JM, Bain G (2007) Role of RGM coreceptors in bone morphogenetic protein signaling. J Mol Signal 2: 4.

Kanomata K, Kokabu S, Nojima J, Fukuda T, Katagiri T (2009) DRAGON, a GPI-anchored membrane protein, inhibits BMP signaling in C2C12 myoblasts. Genes Cells 14: 695-702.

Lee DH, Zhou LJ, Zhou Z, Xie JX, Jung JU *et al.* (2010) Neogenin inhibits HJV secretion and regulates BMP-induced hepcidin expression and iron homeostasis. Blood 115: 3136-3145.

Li J, Ye L, Sanders AJ, Jiang WG (2012) Repulsive guidance molecule B (RGMB) plays negative roles in breast cancer by coordinating BMP signaling. J Cell Biochem 113: 2523-2531.

Liu X, Hashimoto M, Horii H, Yamaguchi A, Naito K *et al.* (2009) Repulsive guidance molecule b inhibits neurite growth and is increased after spinal cord injury. Biochem Biophys Res Commun 382: 795-800.

Koeberle PD, Tura A, Tassew NG, Schlichter LC, Monnier PP (2010) The repulsive guidance molecule, RGMa, promotes retinal ganglion cell survival *in vitro* and *in vivo*. Neuroscience 169: 495-504.

Bradford D, Faull RL, Curtis MA, Cooper HM (2010) Characterization of the netrin/RGMa receptor neogenin in neurogenic regions of the mouse and human adult forebrain. J Comp Neurol 518: 3237-3253.

Fitzgerald DP, Cole SJ, Hammond A, Seaman C, Cooper HM (2006) Characterization of neogenin-expressing neural progenitor populations and migrating neuroblasts in the Niederkofler V, Salie R, Sigrist M, Arber S (2004) Repulsive guidance molecule (RGM) gene function is required for neural tube closure but not retinal topography in the mouse visual system. J Neurosci 24: 808-818.

Schwab JM, Conrad S, Monnier PP, Julien S, Mueller BK *et al.* (2005) Spinal cord injury-induced lesional expression of the repulsive guidance molecule (RGM). Eur J Neurosci 21: 1569-1576.

Reed SE, Staley EM, Mayginnes JP, Pintel DJ, Tullis GE (2006) Transfection of mammalian cells using linear polyethylenimine is a simple and effective means of producing recombinant adeno-associated virus vectors. J Virol Methods 138: 85-98.

Pasterkamp RJ, De Winter F, Holtmaat AJ, Verhaagen J (1998) Evidence for a role of the chemorepellent semaphorin III and its receptor neuropilin-1 in the regeneration of primary olfactory axons. J Neurosci 18: 9962-9976.

Engelkamp D (2002) Cloning of three mouse Unc5 genes and their expression patterns at mid-gestation. Mech Dev 118: 191-197.

Grima B, Lamouroux A, Blanot F, Biguet NF, Mallet J (1985) Complete coding sequence of rat tyrosine hydroxylase mRNA. Proc Natl Acad Sci U S A 82: 617-621.

Fenstermaker AG, Prasad AA, Bechara A, Adolfs Y, Tissir F *et al.* (2010) Wnt/planar cell polarity signaling controls the anterior-posterior organization of monoaminergic axons in the brainstem. J Neurosci 30: 16053-16064.

Kolk SM, Gunput RA, Tran TS, van den Heuvel DM, Prasad AA (2009) Semaphorin 3F is a bifunctional guidance cue for dopaminergic axons and controls their fasciculation, channeling, rostral growth, and intracortical targeting. J Neurosci 29: 12542-12557.

Mirakaj V, Brown S, Laucher S, Steinl C, Klein G *et al.* (2011) Repulsive guidance molecule-A (RGM-A) inhibits leukocyte migration and mitigates inflammation. Proc Natl Acad Sci U S A 108: 6555-6560.

Okamura Y, Kohmura E, Yamashita T (2011) TACE cleaves neogenin to desensitize cortical neurons to the repulsive guidance molecule. Neurosci Res 71: 63-70.

Schnichels S, Heiduschka P, Julien S (2011) Different spatial and temporal protein expressions of repulsive guidance molecule a and neogenin in the rat optic nerve after optic nerve crush with and without lens injury. J Neurosci Res 89: 490-505.

Schnichels S, Heiduschka P, Julien S (2012) RGMA and neogenin protein expression are influenced by lens injury following optic nerve crush in the rat retina. Graefes Arch Clin Exp Ophthalmol 250: 39-50.

Manitt C, Labelle-Dumais C, Eng C, Grant A, Mimee A et al. (2010) Peri-pubertal emergence of UNC-5 homologue expression by dopamine neurons in rodents. PLoS One 5: e11463.

Mori K, Sakano H (2011) How is the olfactory map formed and interpreted in the mammalian brain? Annu Rev Neurosci 34: 467-499.

Cho JH, Prince JE, Cloutier JF (2009) Axon guidance events in the wiring of the mammalian olfactory system. Mol Neurobiol 39: 1-9.

Gad JM, Keeling SL, Wilks AF, Tan SS, Cooper HM (1997) The expression patterns of guidance receptors, DCC and Neogenin, are spatially and temporally distinct throughout mouse embryogenesis. Dev Biol 192: 258-273.

Fitzgerald DP, Seaman C, Cooper HM (2006) Localization of Neogenin protein during morphogenesis in the mouse embryo. Dev Dyn 235: 1720-1725.

Lu X, Le NF, Yuan L, Jiang Q, De Lafarge B *et al.* (2004) The netrin receptor UNC5B mediates guidance events controlling morphogenesis of the vascular system. Nature 432: 179-186.

Gupta A, Tsai LH, Wynshaw-Boris A (2002) Life is a journey: a genetic look at neocortical development. Nat Rev Genet 3: 342-355.

Fitzgerald DP, Cole SJ, Hammond A, Seaman C, Cooper HM (2006) Characterization of neogenin-expressing neural progenitor populations and migrating neuroblasts in the embryonic mouse forebrain. Neuroscience 142: 703-716.

Fitzgerald DP, Bradford D, Cooper HM (2007) Neogenin is expressed on neurogenic and gliogenic progenitors in the embryonic and adult central nervous system. Gene Expr Patterns 7: 784-792.

Takemoto M, Hattori Y, Zhao H, Sato H, Tamada A *et al.* (2011) Laminar and areal expression of unc5d and its role in cortical cell survival. Cereb Cortex 21: 1925-1934.

Amaral DG, Witter MP (1995) The hippocampal formation. In The Rat Nervous System. (ed. G. Paxinos). 443-493.

Muramatsu R, Nakahara S, Ichikawa J, Watanabe K, Matsuki N *et al.* (2010) The ratio of 'deleted in colorectal cancer' to 'uncoordinated-5A' netrin-1 receptors on the growth cone regulates mossy fibre directionality. Brain 133: 60-75.

Bianco IH, Wilson SW (2009) The habenular nuclei: a conserved asymmetric relay station in the vertebrate brain. Philos Trans R Soc Lond B Biol Sci 364: 1005-1020.

Gruber C, Kahl A, Lebenheim L, Kowski A, Dittgen A *et al.* (2007) Dopaminergic projections from the VTA substantially contribute to the mesohabenular pathway in the rat. Neurosci Lett 427: 165-170.

Phillipson OT, Pycock CJ (1982) Dopamine neurones of the ventral tegmentum project to both medial and lateral habenula. Some implications for habenular function. Exp Brain Res 45: 89-94.

Chedotal A (2010) Should I stay or should I go? Becoming a granule cell. Trends Neurosci 33: 163-172.

Ackerman SL, Kozak LP, Przyborski SA, Rund LA, Boyer BB *et al.* (1997) The mouse rostral cerebellar malformation gene encodes an UNC-5-like protein. Nature 386: 838-842.

Leonardo ED, Hinck L, Masu M, Keino-Masu K, Ackerman SL *et al.* (1997) Vertebrate homologues of C. elegans UNC-5 are candidate netrin receptors. Nature 386: 833-838.

Zhong Y, Takemoto M, Fukuda T, Hattori Y, Murakami F *et al.* (2004) Identification of the genes that are expressed in the upper layers of the neocortex. Cereb Cortex 14: 1144-1152.

Przyborski SA, Knowles BB, Ackerman SL (1998) Embryonic phenotype of Unc5h3 mutant mice suggests chemorepulsion during the formation of the rostral cerebellar boundary. Development 125: 41-50.

Kim D, Ackerman SL (2011) The UNC5C netrin receptor regulates dorsal guidance of mouse hindbrain axons. J Neurosci 31: 2167-2179.

Guijarro P, Simo S, Pascual M, Abasolo I, Del Rio JA *et al.* (2006) Netrin1 exerts a chemorepulsive effect on migrating cerebellar interneurons in a Dcc-independent way. Mol Cell Neurosci 33: 389-400.

Alcantara S, Ruiz M, De Castro F, Soriano E, Sotelo C (2000) Netrin 1 acts as an attractive or as a repulsive cue for distinct migrating neurons during the development of the cerebellar system. Development 127: 1359-1372.

Kuramoto T, Kuwamura M, Serikawa T (2004) Rat neurological mutations cerebellar vermis defect and hobble are caused by mutations in the netrin-1 receptor gene Unc5h3. Brain Res Mol Brain Res 122: 103-108.

Lah GJ, Key B (2012) Novel Roles of the Chemorepellent Axon Guidance Molecule RGMa in Cell Migration and Adhesion. Mol Cell Biol 32: 968-980.

Jorge EC, Ahmed MU, Bothe I, Coutinho LL, Dietrich S (2012) RGMa and RGMb expression pattern during chicken development suggest unexpected roles for these repulsive guidance molecules in notochord formation, somitogenesis, and myogenesis. Dev Dyn 241: 1886-1900.

Martinez S, Alvarado-Mallart RM (1989) Rostral Cerebellum Originates from the Caudal Portion of the So-Called 'Mesencephalic' Vesicle: A Study Using Chick/Quail Chimeras. Eur J Neurosci 1: 549-560.

Wingate RJ, Hatten ME (1999) The role of the rhombic lip in avian cerebellum development. Development 126: 4395-4404.

Mawdsley DJ, Cooper HM, Hogan BM, Cody SH, Lieschke GJ *et al.* (2004) The Netrin receptor Neogenin is required for neural tube formation and somitogenesis in zebrafish. Dev Biol 269: 302-315.

Andrusiak MG, McClellan KA, Dugal-Tessier D, Julian LM, Rodrigues SP *et al.* (2011) Rb/E2F regulates expression of neogenin during neuronal migration. Mol Cell Biol 31: 238-247.

Murase S, Horwitz AF (2002) Deleted in colorectal carcinoma and differentially expressed integrins mediate the directional migration of neural precursors in the rostral migratory stream. J Neurosci 22: 3568-3579.

Samad TA, Srinivasan A, Karchewski LA, Jeong SJ, Campagna JA et al. (2004) DRAGON: a member of the repulsive guidance molecule-related family of neuronal- and muscle-expressed membrane proteins is regulated by DRG11 and has neuronal adhesive properties. J Neurosci 24: 2027-2036.

SUPPLEMENTARY INFORMATION

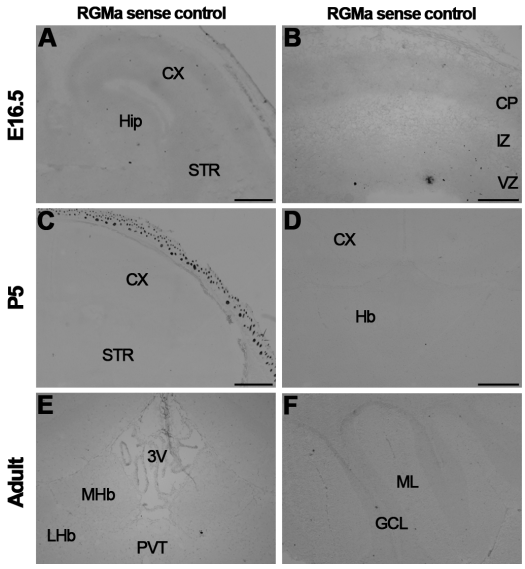

FIGURE S1. No specific staining for sense probes.

In situ hybridization on coronal mouse brain sections at E16.5 (A-B), P5 (C-D) and in adulthood (E- F) using RGMa sense probes. No specific *in situ* hybridization signals were detected at any of the timepoints or in any of the brain regions examined. Sections hybridized with sense probes for RGMb, Neogenin, and Unc5A-D displayed similar levels of background labeling (not shown). 3V, third ventricle; CP, cortical plate; CX, cortex; GCL, granular cell layer; Hb, habenula; Hip, hippocampus; IZ, intermediate zone; LHb, lateral habenula; MHb, medial habenula; ML, molecular layer; PVT, paraventricular thalamic nucleus STR, striatium; VZ, ventricular zone. Scale bar A: 400 µm, B: 200 µm, C: 700, D: 400 µm, E: 200 µm and F: 400 µm.

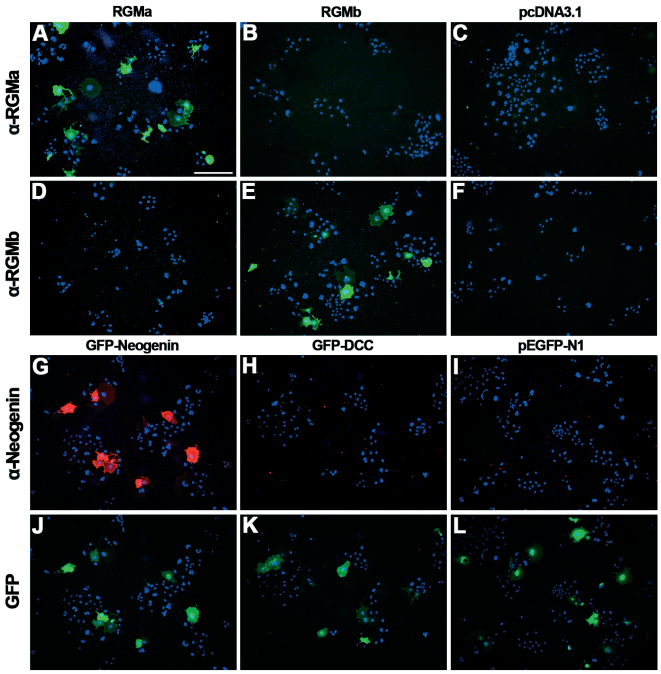

FIGURE S2. Specific immunostaining for anti-RGMa, anti-RGMb and anti-Neogenin antibodies.

COS-7 cells overexpressing RGMa (A, D), RGMb (B, E), GFP-Neogenin (G, J), GFP-DCC (H, K), pcDNA3.1 empty vector (C, F) or pEGFP-N1 (I, L). Cells are counterstained with DAPI in blue. Anti-RGMa and anti-RGMb antibodies specifically stain COS-7 cells overexpressing RGMa (A-C) or RGMb (D-F), respectively. Anti-Neogenin antibody specifically stains COS-7 cells overexpressing GFP-Neogenin and does not stain COS-7 cells overexpressing GFP-DCC or pEGFP-N1 (G-L). Scale bar A-L: 200 µm.

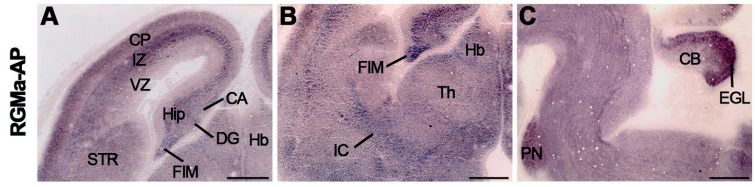

FIGURE S3. RGMa-AP binding to E16.5 mouse brain slices.

(A) RGMa-AP binding is detected in cells and neuronal projections in the cortical plate (CP) and intermediate zone (IZ) of the cortex. (B) The fimbria (FIM) of the hippocampus (Hip) and axonal projections in the internal capsule (IC) also bind RGMa-AP. In the hindbrain, the pontine nucleus (PN) and cerebellum (CB), in particular the external granular layer (EGL), are strongly stained for RGMa-AP. Scale bars A-C: 400 µm. CA, cornus ammonis; DG, dentate gyrus; Hb, habenula; STR, striatum; Th, thalamus; VZ ventricular zone.

TABLE S1. Sense and antisense primer sequences for *RGMa, RGMb, Neo* and *Unc5A-D in situ* hybridization probes.

Gene	Sense primer	Antisense primer	Size
RGMa	5′-TCAGCTGCCCCCAACTACACT-3′	5′-TCCTCCACGGCGTTGACTACC-3′	455 bp
RGMb	5′-CAGCCACGGGGGAGTCAGAG-3′	5′-CATCCGGATAGCGAGGGTTAG-3′	460 bp
Neo	5′-ACACCGTTATCTGGCAATGG-3′	5′-TTCAGCAGACAGCCAATCAG-3′	501 bp
Unc5A	5′-TGAGGTTGCCCCTAGCTG-3′	5′-GCTAGAGTTCGCCAGTCG-3′	880 bp
Unc5B	5′-CGAGTGGGTCAGCCAGAATG-3′	5′-CCTCGGCCACAGCGATT-3′	546 bp
Unc5C	5′-ATTGTGGCTGGGGTATCCTC-3′	5′-CAACTGGCTCCTCTTTCTTTCC-3′	714 bp
Unc5D	5′-AGCGGAGTACCATGGCAAGAATC-3′	5′-CTGCCTCCGGAGAAGAAACAGAC-3′	1391 bp

TABLE S2. Expression of *RGMa, RGMb, Neogenin* and *Unc5A-D* in the primary olfactory system.

Age		*RGMa*	*RGMb*	*Neo*	*Unc5A*	*Unc5B*	*Unc5C*	*Unc5D*
E16.5	Glomerular layer (GL)	+	++	+/-	+/-	+/-	+/-	+/-
	External plexiform layer (EPL)	+/-	+/-	+/-	+/-	+/-	+/-	+/-
	Mitral cell layer (MCL)	+++	+++	++	++	+++	++	++
	Internal plexiform layer (IPL)	+	+++	+	+	+	+	+
	Granule cell layer (GR)	+	+++	+	+	+	++	+
	Olfactory ventricular zone (OVZ)	++	-	+++	-	-	-	+++
	Olfactory epithelium (OE)	++[a]	++[b]	+[a]	-	+++	-	+
	Acessory olfactory bulb (AOB)	++	+	++	+	++	+	+
	Cribriform plate (CRP)	-	-	+	-	-	+++	-
P5	Glomerular layer	+	+	+	-	+/-	+/-	+/-
	External plexiform layer	+/-	+/-	+/-	-	-	-	-
	Mitral cell layer	+++	+++	+	+/-	+	+	+
	Internal plexiform layer	+/-	+/-	+/-	-	-	-	-
	Granule cell layer	+/-	++	++	+/-	+/-	+/-	+/-
	Olfactory ventricular zone	+	++	+	-	-	+	+
	Olfactory epithelium	+[a]	++[b]	+[a]	-	++	-	-
	Anterior olfactory nucleus	++	++	++	++	-	+	++
	Cribriform plate (CRP)	-	-	+	-	-	+	-
Adult	Glomerular layer	++	++	++	-	+	+/-	+/-
	External plexiform layer	+/-	+/-	+/-	-	-	-	-
	Mitral cell layer	++	++	+	+	+	+	+
	Internal plexiform layer	+/-	+/-	+/-	-	-	-	-
	Granule cell layer	+	+	+	+/-	+/-	+/-	-
	Olfactory ventricular zone	+	-	+	-	+	+	+/-
	Anterior olfactory nucleus	+	++	++	++	-	++	+/-

[a] apical expression, [b] basal expression.

Legend: - , no expression; +/-, weak expression; + moderate expression; ++, strong expression; +++, very strong expression.

TABLE S3. Expression of *RGMa, RGMb, Neogenin* and *Unc5A-D* in the cortex.

Age		*RGMa*	*RGMb*	*Neo*	*Unc5A*	*Unc5B*	*Unc5C*	*Unc5D*
E16.5	Pia	-	++	+	-	+	-	-
	Marginal zone (MZ)	-	+	+	-	-	-	-
	Cortical plate (CP)	+++	++[a]	+++[a]	++	+/-	+	-
	Subplate (SP)	-	+	++	+	-	++	-
	Intermediate zone (IZ)	-	+	+	+/-	-	-	-
	Subventricular zone (SVZ)	-	++	++	+	+	+/-	++
	Ventricular zone (VZ)	++	-	+	+	+	+/-	+/-
P5	Cortical layer 1	++	-	++	+/-	-	+	+
	Cortical layer 2	++	-	++	+/-	-	+	+
	Cortical layer 3	++	-	++	+/-	-	++	+
	Cortical layer 4	-	-	+	+/-	-	+	+
	Cortical layer 5	+++	++	+++	+/-	-	+	-
	Cortical layer 6	++	-	-	+/-	-	-	-
	Ventricular zone	+	-	+	-	-	+/-	-
Adult	Cortical layer 1	-	+	+/-	+/-	-	-	+
	Cortical layer 2	-	+	+/-	+/-	-	-	+
	Cortical layer 3	-	+	+/-	+/-	-	-	+
	Cortical layer 4	-	+	+/-	+/-	-	-	+
	Cortical layer 5	++	++	+/-	+	-	+/-	-
	Cortical layer 6	+/-	+	+/-	+/-	-	-	-
	Ventricular zone	+	+	+	-	-	-	-

[a] strongest expression in upper part

Legend: - , no expression; +/-, weak expression; + moderate expression; ++, strong expression; +++, very strong expression.

TABLE S4. Expression of *RGMa, RGMb, Neogenin* and *Unc5A-D* in the hippocampus and entorhinal cortex.

Age		*RGMa*	*RGMb*	*Neo*	*Unc5A*	*Unc5B*	*Unc5C*	*Unc5D*
E16.5	Hippocampus (Hip)	++	+	+++	++	+/-	+/-	+
	Dentate gyrus (DG)	++	+	+++	++	+	+	+
	Entorhinal cortex (CEn)	++	++	+++	++	+/-	-	+
	CA	++	++	+++	+	++	+/-	-
	Subventricular zone (SVZ)	-	++	+/-	+	+	+/-	++
	Ventricular zone (VZ)	++	-	+	+	+	+/-	+/-
P5	CA1	++	+	++	+	-	+/-	-
	CA2	+	++	++	+	-	+/-	-
	CA3	+	+++	++++	++	-	++	++
	Dentate gyrus	+	+	++	+	-	+/-	+/-
	Molecular layer (ML)	+	+/-	+	-	-	+/-	-
	Granular layer (GC)	+	+/-	++	+	-	+/-	+/-
	Polymorph layer (PO)	+	+	+	-	-	+/-	+
	Stratum oriens (SO)	+/-	+/-	+/-	-	-	-	+/-
	Stratum radiatum (SR)	+/-	+/-	-	-	-	-	-
	Stratum lacunosum moleculare (SLM)	+/-	+	+/-	-	-	-	-
	Entorhinal cortex (CEn)	++	++	++	+/-	-	-	+
Adult	CA1	+++	++	+	++	+/-	+/-	+/-
	CA2	++	++	+	+	+/-	+	+/-
	CA3	+	+++	+	+	+/-	++	+
	Dentate gyrus	++	++	+	++	+/-	+	+/-
	Molecular layer	-	-	-	-	-	-	-
	Granular layer	++	++	+	++	+/-	+	+/-
	Polymorph layer	+/-	++	+	-	-	+/-	+/-
	Stratum oriens	-	+	-	-	-	-	-
	Stratum radiatum	-	-	-	-	-	-	-
	Stratum lacunosum moleculare	+/-	+/-	-	-	-	-	-
	Entorhinal cortex	+/-	+/-	++	++	-	-	-

Legend: - , no expression; +/-, weak expression; + moderate expression; ++, strong expression; +++, very strong expression.

TABLE S5. Expression of *RGMa, RGMb, Neogenin* and *Unc5A-D* in the habenula, septum and thalamic area.

Age		*RGMa*	*RGMb*	*Neo*	*Unc5A*	*Unc5B*	*Unc5C*	*Unc5D*
E16.5	Lateral habenula (LHb)	+	+++	+	+++	+/-	+	+
	Medial habenula (MHb)	+++	+++	+	++	+/-	-	-
	Interpeduncular nucleus (IPN)	++	++	++	++	+/-	++	++
	Substantia nigra (SN)	++	+	+	-	-	+	+
	Ventral tegmental area (VTA)	++	++	+	+	-	+	+
	Septum (S)	+	+	++	++	+	+	++
	Striatum (STR)	+	+++	+	+/-	+	+	+
	Thalamus (Th)	+++	++	++	+++	-	++	-
	Lateral hypothalamus (LH)	+	++	++	++	+/-	++	++
P5	Lateral habenula	++	+++	+	+/-	-	-	+
	Medial habenula	+++	+++	+	+/-	-	-	-
	Interpeduncular nucleus	+	+	+/-	-	-	-	-
	Substantia nigra	+	+/-	+	-	-	+	+
	Ventral tegmental area	+	+/-	+	-	-	+	+
	Septum	+	+/-	++	+/-	+/-	-	+
	Striatum	+/-	+/-	+/-	-	-	-	-
	Thalamus	+++	+	++	+/-	-	+	+/-
	Lateral hypothalamus	+	+	+	-	-	-	+/-
	Paraventricular thalamic nucleus (PVT)	+	++	+++	-	-	+	+/-
Adult	Lateral habenula	+	+++	+/-	-	+/-	-	-
	Medial habenula	++	++	+/-	-	+/-	-	-
	Interpeduncular nucleus	++	++	+	-	-	-	-
	Substantia nigra	+	+	+	-	-	-	-
	Ventral tegmental area	+	+	+	-	-	-	-
	Septum	+	+	+	+	+/-	-	+/-
	Striatum	-	+/-	-	-	-	-	-
	Thalamus	+	+	+	-	+/-	+	-
	Lateral hypothalamus	+/-	+	+/-	-	-	-	-
	Paraventricular thalamic nucleus	+	+	+	-	+	+	-

Legend: - , no expression; +/-, weak expression; + moderate expression; ++, strong expression; +++, very strong expression.

TABLE S6. Expression of *RGMa, RGMb, Neogenin* and *Unc5A-D* in the cerebellum.

Age		*RGMa*	*RGMb*	*Neo*	*Unc5A*	*Unc5B*	*Unc5C*	*Unc5D*
E16.5	External granular layer (EGL)	-	+ [a]	++	+	++	++	-
	Purkinje cell layer (PCL)	+	+	++	+	+	++	++
	Ventricular zone (VZ)	++	-	++	-	+/-	+++	-
	Deep cerebellar nuclei (DCN)	++	++	++	++	+	+++	++
P5	External granular layer	-	++ [a]	++ [b]	-	+ [a]	++	-
	Purkinje cell layer	-	+	++	-	+	++	+
	Internal granular layer (IGL)	+++	+	+++	+	+	++	-
Adult	Molecular layer (ML)	-	-	-	-	-	-	-
	Purkinje cell layer	++	++	+	+	+	++	+
	Granular cell layer (GCL)	+	++	++	+	+	++	-

[a] inner EGL layers, [b] outer EGL layers

Legend: - , no expression; +/-, weak expression; + moderate expression; ++, strong expression; +++, very strong expression.

CHAPTER 4

The leucine-rich repeat protein Lrig2 binds Neogenin and is required for neurite growth inhibition by RGMa

DIANNE M.A. VAN DEN HEUVEL[1],
SUSAN VAN ERP[1],
ANITA J.C.G.M. HELLEMONS[1],
JEROEN DEMMERS[2] AND
R. JEROEN PASTERKAMP[1]

[1] Department of Neuroscience and Pharmacology, Rudolf Magnus Institute of Neuroscience, University Medical Center Utrecht, Universiteitsweg 100, 3584 CG, Utrecht, The Netherlands

[2] Proteomics Center, Erasmus University Medical Center, Dr. Molewaterplein 50, 3015 GE, Rotterdam, The Netherlands

Being prepared for submission

ABSTRACT

Neogenin is a transmembrane receptor that regulates several key cellular processes in the developing brain. Binding of repulsive guidance molecule A (RGMa) to Neogenin induces growth cone collapse and neurite growth inhibition. How Neogenin executes this effect is still poorly understood. Binding of RGMa to Neogenin activates RhoA signaling, which requires the association of Neogenin with its coreceptor Unc5B, and inactivates Ras signaling. In addition, Neogenin activation by RGMa can induce γ-secretase cleavage of the Neogenin intracellular domain (NeoICD), which can translocate to the nucleus and induce transcription. To further our understanding of the molecular basis of Neogenin signaling, we performed biotin-streptavidin-based pull down experiments using either full-length Neogenin or the NeoICD. Mass spectrometry analysis of Neogenin protein complexes identified a multitude of potential Neogenin-interacting proteins with known functions in cytoskeletal remodeling, signal transduction, apoptosis and gene transcription. One of the newly identified Neogenin-interacting proteins, leucine-rich repeats and immunoglobulin-like domains protein 2 (Lrig2), was studied in more detail. We show binding of Lrig2 to Neogenin *in vivo* and colocalization with Neogenin in mouse brain tissue. Functional experiments reveal a requirement of Lrig2 in RGMa-induced neurite outgrowth inhibition in dissociated cortical neurons. Furthermore, overexpression of Lrig2 in a mammalian cell line reveals a potential role for Lrig2 in controlling RGMa ligand binding to Neogenin. Altogether, this study identifies novel Neogenin-interacting proteins and shows a role for Lrig2, one of the newly identified Neogenin-interacting proteins, in repulsive RGMa-Neogenin signaling in neurons.

INTRODUCTION

Neogenin is a multifunctional receptor that regulates diverse developmental processes in the nervous system, including axon guidance, neurogenesis, neuronal migration, differentiation, apoptosis and neural tube closure (Conrad *et al.* 2010, Fitzgerald *et al.* 2006, Fujita *et al.* 2008, Matsunaga *et al.* 2004, Matsunaga *et al.* 2006, Mawdsley *et al.* 2004, Wilson and Key 2006). Outside the nervous system, Neogenin function is important for chondrogenesis, mammary gland formation, myogenesis and angiogenesis (Kang *et al.* 2004, Park *et al.* 2004, Srinivasan *et al.* 2003, Zhou *et al.* 2010).

Neogenin belongs, together with its close homolog deleted in colorectal cancer (DCC), to a subgroup of the immunoglobulin (Ig) superfamily of cell surface molecules characterized by the presence of four immunoglobulin-like (Ig-like) domains and six fibronectin type III (FNIII) repeats in the extracellular part of the protein (Fearon *et al.* 1990, Hedrick *et al.* 1994, Vielmetter *et al.* 1994). Neogenin can bind members of two different ligand families: Netrins, which are secreted molecules, and RGMs, which are glycosylphosphatidylinositol

(GPI)-linked (Keino-Masu *et al.* 1996, Rajagopalan *et al.* 2004). Both RGMs and Netrins bind to the FNIII domains of Neogenin. However, RGM molecules bind with a ten times higher affinity (Geisbrecht *et al.* 2003, Rajagopalan *et al.* 2004, Yamashita *et al.* 2007, Yang *et al.* 2008). The role and mechanism of RGMa-mediated Neogenin signaling in neurite growth inhibition and axon repulsion is best characterized. In chicken, RGMa induces growth cone collapse and neurite outgrowth inhibition of temporal retinal axons that express Neogenin. Within the chick tectum RGM is expressed in an anterior-low to posterior-high gradient guiding Neogenin-expressing temporal retinal axons to the anterior tectum (Matsunaga *et al.* 2006, Monnier *et al.* 2002, Rajagopalan *et al.* 2004). In the *Xenopus* forebrain, repulsive RGMa-Neogenin signaling mediates the proper formation of the supraoptic tract (SOT), by directing axon growth into a tight bundle (Lah and Key 2012, Wilson and Key 2006). In mice, RGMa-Neogenin signaling induces growth cone collapse and neurite retraction in cortical, cerebellar granule and dorsal root ganglia (DRG) neurons (Conrad *et al.* 2007, Endo and Yamashita 2009, Hata *et al.* 2006, Hata *et al.* 2009). Perinatal expression of RGMa in the inner molecular layer of the dentate gyrus directs entorhinal cortical axons specifically to the outer molecular layer of the dentate gyrus. Blockage of RGMa function in organotypic slice cultures induces severe targeting defects of entorhinal cortical axons (Brinks *et al.* 2004). Thus, RGMa and Neogenin play a crucial role in axon guidance events in different neuronal systems.

The inhibitory effect of RGMa-Neogenin interactions on axons and growth cones is mediated by activation of RhoA GTPase and downstream effectors Rho kinase and myosin II (Conrad *et al.* 2007, Hata *et al.* 2006, Kubo *et al.* 2008). Unc5B coreceptors are constitutively associated with Neogenin and bind leukemia-associated Rho guanine-nucleotide exchange factor (LARG) to their intracellular domain. Binding of RGMa to Neogenin activates RhoA signaling through focal adhesion kinase (FAK)-mediated phosphorylation of LARG (Hata *et al.* 2009). FAK is associated with the P3 domain of Neogenin and becomes dephosphorylated upon binding of RGMa (Hata *et al.* 2009, Ren *et al.* 2004). Dephosphorylation of FAK induces the release of the Ras-specific GTPase-activating protein p120GAP from FAK, thereby mediating inactivation of Ras and downstream effectors PI3-kinase and Akt (Endo and Yamashita 2009). In addition to its role in regulating axon growth, Neogenin can function as a dependence receptor and in the absence of RGMa activate a signaling pathway which involves death-associated protein (DAP) kinase to induce apoptosis (Fujita *et al.* 2008, Matsunaga *et al.* 2004). Another interesting aspect of Neogenin signaling is the cleavage and release of the NeoICD by γ-secretase. NeoICD can translocate to the nucleus and induce gene transcription (Goldschneider *et al.* 2008).

Despite the identification of several Neogenin signaling proteins over the past few years, our understanding of the mechanisms that regulate Neogenin signaling and of the components that comprise the Neogenin signaling cascade is rather rudimentary. To further our understanding of Neogenin signaling, we used an *in vitro* biotin-streptavidin-based pull down approach to purify Neogenin signaling complexes. Mass spectrometry analysis of the

retrieved complexes identified many putative Neogenin-interacting proteins involved in various biological processes including the organization of the cell cytoskeleton, migration, apoptosis and gene transcription. In this study we confirm the colocalization and interaction of one of the identified Neogenin-interacting proteins, Lrig2, with Neogenin in mouse brain tissue. So far no specific functions for Lrig2 signaling in the brain have been described. In this study, we used a functional neurite outgrowth assay to show the requirement for Lrig2 in RGMa-Neogenin-mediated neurite outgrowth inhibition in cortical neurons. In addition, a series of COS-7 cell binding assays revealed reduced binding of RGMa and Netrin-1 to Neogenin in the presence of Lrig2. Together, these experiments reveal a role for Lrig2 in neuronal RGMa-Neogenin signaling and show a potential role for Lrig2 in modulating Neogenin signaling by regulating Neogenin ligand binding.

MATERIALS AND METHODS

PLASMID CONSTRUCTION

A biotin- and GFP-tagged full-length mouse Neogenin cDNA (pcDNA3.1-NeoFL-GFP-Bio) was generated by subcloning a GFP and biotin tag (Lansbergen *et al.* 2006) C-terminal to the full-length Neogenin coding sequence amplified from wild-type Neogenin cDNA (pCMVXL-6-Neogenin; a kind gift of Denise Davis), separated by a five glycine linker, in a pcDNA3.1(-)/myc-his (Invitrogen) vector backbone. The Neogenin intracellular domain (NeoICD; 1158-1492) was subcloned C-terminal to the GFP sequence of a modified pEGFP-C1 vector expressing a biotin-GFP fusion protein (Lansbergen *et al.* 2006) to generate a biotin-GFP-NeoICD-expression vector (pEGFP-Bio-GFP-NeoICD). Full-length mouse Lrig2 and Lrig2 truncation mutants were amplified from pCDH-Lrig2 (a kind gift of Mathew Hemming) and subcloned into the GW1-myc vector (a kind gift of Casper Hoogenraad) using HindIII/BglII restriction sites. The myc tag was replaced by cloning a V5 tag into the GW1-myc backbone, using SalI/EcoRI restriction sites, to generate a GW1-Lrig2-V5 vector. For RNA interference knockdown experiments, DNA fragments encoding short hairpin (sh) RNAs directed against mouse Lrig2 (shLrig2-A; 5'-GCTAGAAGATGCTGGAAAA-3', shLrig2-B; 5'-AGTTAATCTTGCAAGGAAA-3' and shLrig2-C; 5'-CATTGTAGATGCTGGGCTA-3) were cloned into pSuper, using BglII/HindIII restriction sites (Brummelkamp *et al.* 2002). A pSuper vector expressing a scrambled, non-targeting shRNA (5'-GACAACCAATCGTAATACA-3') was used as a control.

ANIMALS AND TISSUE TREATMENT

All animal use and care were in accordance with institutional guidelines. C57BL/6 mice were obtained from Charles River. Timed-pregnant mice were killed by means of cervical dislocation. The morning on which a vaginal plug was detected was considered embryonic day 0.5 (E0.5). For *in situ* hybridization experiments, E16.5 heads were directly frozen in 2-methylbutane (Merck).

For immunohistochemistry, E16.5 heads were collected in phosphate-buffered saline (PBS, pH 7.4) and fixed by immersion for 3 hours (hrs) in 4% paraformaldehyde (PFA) in PBS at 4°C. Brains were washed in PBS, cryoprotected in 30% sucrose at 4°C and frozen in 2-methylbutane (Merck). Sections (16 µm) were cut on a cryostat, mounted on Superfrost Plus slides (Fisher Scientific), air-dried and stored desiccated at -80°C for *in situ* hybridization and at -20°C for immunohistochemistry.

CELL CULTURE AND TRANSFECTION

COS-7, HEK293 and N1E-115 neuroblastoma cells were maintained in high glucose Dulbecco's modified Eagle's medium (DMEM; Gibco, Invitrogen). CHO and stable RGMa-expressing CHO (CHO-RGMa) cell lines (Hata *et al.* 2006) were a kind gift of Toshihide Yamashita. CHO cells were cultured in Ham's F12 Nutrient Mixture (Gibco, Invitrogen). Cell culture media were supplemented with 10% (v/v) heat-inactivated fetal bovine serum (FBS; Lonza, BioWhittaker), 2 mM L-glutamine (PAA) and 1x penicillin/streptomycin (pen/strep; PAA) and cultured in a humidified atmosphere with 5% CO_2 at 37°C. Cell culture medium for CHO-RGMa cells was supplemented with 300 µg/ml hygromycin B (Roche). COS-7 cells and HEK293 cells were transfected using polyethylenimine (PEI; Polysciences) (Reed *et al.* 2006). N1E-115 cells were transfected using Lipofectamine 2000 (Invitrogen).

AP- AND FC-PROTEIN PRODUCTION

For alkaline phosphatase (AP)- and Fc-tagged protein production, HEK293 cells were transfected with AP-Fc (a kind gift of Roman Giger), RGMa-AP (APtag5-RGMa-AP; a kind gift of Thomas Skutella), Netrin-1-AP (pcDNA3.1-Netrin-1-AP; a kind gift of Kun-Liang Guan), Sema3F-AP (a kind gift of Valerie Castellani) or RGMa-Fc (pIgplus-RGMa-Fc; a kind gift of Herbert Lin) and cultured in Opti-MEM reduced serum medium (Gibco, Invitrogen) supplemented with 3% FBS (Lonza, BioWhittaker), 2 mM L-glutamine (PAA) and 1x pen/strep (PAA) to produce AP- or Fc-tagged proteins. Cell culture medium containing AP- or Fc-tagged proteins was collected after 5 days in culture, filter-sterilized and stored at 4°C. If required, culture medium containing AP-tagged proteins was concentrated using Centriprep YM-50 centrifugal filter units (Millipore). Cell culture medium containing RGMa-Fc was collected after 5 days in culture and filter-sterilized. RGMa-Fc-containing culture medium was incubated with protein A-agarose (Roche) on a roller overnight at 4°C. The next day, beads with bound RGMa-Fc were washed in ice-cold PBS. Beads were incubated with 100 mM glycine (pH 2.5) to elute RGMa-Fc from the beads. Eluted RGMa-Fc protein was neutralized by adding a small volume of 10mM Tris-HCl (pH 9.5). RGMa-Fc was dialyzed against PBS using centrifugal filter units Amicon Ultra 0.5 ml 10K Ultracel-10K membrane (Millipore). For Fc control protein, human IgG Fc fragment (Calbiochem) was used.

IN SITU HYBRIDIZATION

Nonradioactive *in situ* hybridization was performed according to (Pasterkamp *et al.* 1998). In brief, probe sequences for *RGMa* (Metzger *et al.* 2007), *Neogenin* (NM_008684.2: nt 2087-2587), *Lrig2* (NM_001025067: nt 1149-1761) and *Lrig3* (Genepaint.org: probe 43) were polymerase chain reaction (PCR)-amplified from cDNA, using primer sequences listed in Table 1. The probe sequence for *Lrig1* (Genepaint.org: probe 90) was generated by reverse transcription (RT)-PCR on adult mouse whole brain RNA (see Table 1). Digoxigenin (DIG)-labeled RNA probes were generated by a RNA polymerase reaction using 10x DIG RNA labeling mix (ENZO). Tissue sections were post-fixed in 4% PFA in PBS (pH 7.4) for 20 minutes (min) at room temperature (RT). To enhance tissue penetration and decrease aspecific background staining, sections were acetylated with 0.25% acetic anhydride in 0.1 M triethanolamine and 0.06% HCl for 10 min at RT. Sections were prehybridized for 2 hrs at RT in hybridization buffer (50% formamide, 5x Denhardt's solution, 5x SSC, 250 µg/ml baker's yeast tRNA and 500 µg/ml sonicated salmon sperm DNA). Hybridization was performed for 15 hrs at 68°C, using 400 ng/ml denatured DIG-labeled probe diluted in hybridization buffer. After hybridization, sections were first washed briefly in 2x SSC followed by incubation in 0.2x SCC for 2 hrs at 68°C. Sections were adjusted to RT in 0.2x SSC for 5 min. DIG-labeled RNA hybrids were detected with anti-DIG Fab fragments conjugated to AP (Boehringer) diluted in 1:2500 in TBS (pH 7.4) overnight at 4°C. Binding of AP-labeled antibody was visualized by incubating the sections in detection buffer (100 mM Tris-HCl, pH 9.5, 100 mM NaCl and 50 mM $MgCl_2$) containing 240 µg/ml levamisole and nitroblue tetrazolium chloride/5-bromo-4-chloro-3-indolyl-phosphatase (NBT/BCIP, Roche) for 14 hrs at RT. Sections subjected to the entire *in situ* hybridization procedure, but with no probe or sense probe added, did not exhibit specific hybridization signals. The specificity of the *in situ* hybridization procedure was also inferred from the clearly distinct gene expression patterns observed. Staining was visualized using a Zeiss Axioskop 2 microscope.

TABLE 1. Sense and antisense primer sequences for *RGMa, RGMb, Neogenin* and *Lrig1, -2* and *-3 in situ* hybridization probes.

Gene	Sense primer	Antisense primer	Size
RGMa	5'-TCAGCTGCCCCCAACTACACT-3'	5'-TCCTCCACGGCGTTGACTACC-3'	454 bp
Neogenin	5'-ACACCGTTATCTGGCAATGG-3'	5'-TTCAGCAGACAGCCAATCAG-3'	501 bp
Lrig1	5'-GACAGCTGCCCCACATACAA-3'	5'-TAGCTTCTCGGTGCCAATAGC-3'	528 bp
Lrig2	5'-TGCCTTTGTGGGTCTGAGCTTAC-3'	5'-CCATATGGTGGACATGGGTG-3'	613 bp
Lrig3	5'-ATGTGGAAGCCGCTTC-3'	5'-GATTCAGAGTCCAGCTCTG-3'	508 bp

IMMUNOCYTOCHEMISTRY

Cells were fixed with 4% PFA for 15 min at RT and washed in PBS (pH 7.4). CHO cells were permeabilized and blocked in normal blocking buffer (PBS, 4% bovine serum albumin (BSA) and 0.1% Triton) for 1 hr at RT. CHO cells were incubated with rabbit anti-Lrig2 (gift of Håkan Hedman) 1:2000 in normal blocking buffer for 2hrs at RT. Cells were washed in PBS and incubated with the Alexa Fluor-labeled goat anti-rabbit secondary antibody (Invitrogen) 1:500 for 1 hr at RT. Dissociated E14.5 cortical neurons were fixed after 2 days *in vitro* (DIV2) and incubated in normal blocking solution for 1 hr at RT and incubated with rabbit anti-Lrig2 antibody 1:1000 and goat anti-Neogenin antibody (AF1079; R&D systems) 1:400, in normal blocking solution overnight at 4°C. The next day, sections were washed in PBS and incubated with the appropriate Alexa Fluor-labeled secondary antibodies (Invitrogen) 1:500 for 1 hr at RT.

IMMUNOHISTOCHEMISTRY

Sections were washed in PBS (pH 7.4) and incubated in horse blocking buffer (PBS, 5% horse serum (Sigma-Aldrich), 1% BSA, 1% glycine, 0.1% lysine and 0.4% Triton) for 1 hr at RT and incubated with rabbit anti-Lrig2 antibody at 1:1000 and goat anti-Neogenin antibody (AF1079; R&D systems) 1:200 in horse blocking buffer overnight at 4°C. The next day, sections were washed in PBS and incubated with the appropriate Alexa Fluor-labeled secondary antibodies (Invitrogen) 1:500 for 1 hr at RT. Sections were washed in PBS, counterstained with fluorescent Nissl stain (NeuroTrace, Invitrogen) 1:500 for 15 min at RT, washed in PBS and embedded in Mowiol (Sigma-Aldrich). Staining was visualized using a Zeiss Axioskop 2 microscope and an Olympus FluoView FV1000 confocal microscope.

AP CELL BINDING

COS-7 cells were transfected with wild type mouse Neogenin (pCMVXL-6-Neogenin) or Neuropilin-2 (pBK-HA-Nrp2) together with GW1-myc (Casper Hoogenraad), GW1-Lrig2-V5 or GW1-Lrig2ΔICD-V5 (1:1). At DIV2, the culture medium was replaced by HBHA buffer (20 mM HEPES, pH 7.0, 1x Hank's balanced salt solution (HBSS; GIBCO, Invitrogen) and 0.5 mg/ml BSA) for 15 min at RT. Subsequently, cells were incubated with AP-proteins for 75 min, while gently rotating at RT, followed by 4 washes in HBHA buffer. Then, cells were incubated in fixation solution (20 mM HEPES, pH 7, 60% (v/v) acetone and 3.7% formaldehyde) for 30 seconds, followed by 2 washes in HBHA. HBHA was replaced by HBS (20 mM HEPES, pH 7.0, 150 mM NaCl) and endogenous phosphatase activity was heat-inactivated by incubation at 65°C for 90 min. Cells were equilibrated in detection buffer (100 mM Tris-HCl, pH 9.5, 100 mM NaCl and 5 mM $MgCl_2$) and bound AP-protein was visualized by incubation in detection buffer containing levamisole and NBT/BCIP (Roche). The specificity of RGMa-AP protein binding was determined by competition with excess RGMa protein. Furthermore, no staining was observed for AP alone.

WESTERN BLOTTING

Cells were collected in ice-cold PBS (pH 7.4) with a cell scraper and centrifuged at 1000 rpm for 5 min in a precooled centrifuge at 4°C. The cell pellet was resuspended in ice-cold lysis buffer (20 mM Tris-HCl, pH 8, 150 mM KCl, 1% Triton X-100 and Complete protease inhibitor cocktail (Roche)), incubated on ice for 10 min, followed by centrifugation at 14,000 rpm for 15 min at 4°C. The supernatant was collected, NuPAGE LDS sample buffer (Invitrogen) containing 2.5% β-mercaptoethanol was added and samples were boiled for 5 min at 90°C. Proteins were separated in 8% SDS-PAGE gels and transferred onto nitrocellulose membrane (Hybond-C Extra; Amersham). Membranes were incubated in blocking buffer (PBS, 0.05% (v/v) Tween 20 and 5% milk powder) for 30 min at RT. Membranes were incubated with corresponding primary antibodies in blocking buffer overnight at 4°C. Antibodies used: goat anti-Neogenin antibody (AF1079; R&D systems, 1:2000); mouse anti-V5 antibody (R960-25; Novex, Invitrogen, 1:5000); mouse anti-α-Tubulin antibody (T5168; Sigma-Aldrich, 1:8000); anti-Filamin A antibody (Thomas Stossel, 1:2000); rabbit anti-Cyfip1 antibody (Theresia Stradal, 1:500); rabbit anti-Lrig3-207 antibody (Håkan Hedman, 1:300); rabbit anti-Lrig2-C antibody (Håkan Hedman, 1:8000); mouse anti-annexin A6 antibody (610300; Transduction Laboratories, 1:1000); mouse anti-Kaiso antibody (6F; 05-659; Upstate; 1:500) and rabbit anti-casein kinase 2A antibody (06-873; Upstate; 1:1000). Blots were incubated with SuperSignal West Dura Extended Duration Substrate (Pierce) and exposed to ECL films (Pierce).

IMMUNOPRECIPITATION

Immunoprecipitation of biotin-tagged proteins was performed as described previously (Teuling *et al.* 2007). HEK-293 cells cotransfected with a cDNA for the biotin ligase BirA and the indicated biotin-tagged cDNA constructs (1:1.5), were collected in ice-cold PBS and centrifuged at 1000 rpm for 5 min in a precooled centrifuge at 4°C. Cell pellets were lysed in lysis buffer (20 mM Tris-HCl, pH 8.0, 150 mM KCl, 1% Triton X-100, 0.2 µg/µl, phosphatase inhibitor cocktail (Sigma-Aldrich) and Complete protease inhibitor cocktail (Roche)), incubated on ice for 15 min and centrifuged at 14,000 rpm for 15 min at 4°C. Cleared supernatant was mixed with 25 µl (volume of original suspension) paramagnetic streptavidin beads (Dynabeads M-280, Invitrogen), which had been blocked in 125 µl blocking buffer (20 mM Tris-HCl, pH 8.0, 150 mM KCl, 20% glycerol and 200 ng/µl albumin from chick egg white (Sigma-Aldrich) at 4°C. After an 1 hour incubation at 4°C, beads were washed 4 times in washing buffer (20 mM Tris-HCl, pH 8.0, 150 mM KCl, 0.1% Triton X-100 and Complete protease inhibitor cocktail). Precipitated proteins were eluted by boiling the pull down samples in NuPAGE LDS sample buffer (Invitrogen) containing 2.5% β-mercaptoethanol for 10 min at 70°C.

For endogenous pull down and co-immunoprecipitation experiments, P0 mouse brains or cells (10-cm plates) were lysed in lysis buffer (20 mM Tris-HCl, pH 8.0, 150 mM NaCl, 1% NP-40, 10% glycerol and Complete protease inhibitor cocktail), incubated for 30 min rotating at 4°C and centrifuged at 14,000 rpm for 15 min at 4°C. Cleared supernatants were incubated with

1 µg of the indicated antibodies at 4° C. After 2 hrs, 10 µl protein A/G Dynabeads (Invitrogen), which had been blocked in blocking buffer, were added and samples were incubated for 1 hour rotating at 4°C. Pull down samples were washed 3 times in washing buffer (20 mM Tris-HCl, pH 8.0, 150 mM NaCl, 1% NP-40 and 10% glycerol) and precipitated proteins were eluted by boiling in NuPAGE LDS sample buffer containing 2.5% β-mercaptoethanol for 10 min at 70°C.

IN-GEL ANALYSIS

Pull down samples were separated in a NuPAGE Novex 4-12% Bis-Tris gradient gel following the manufacturer´s description (Invitrogen). For mass spectrometry analysis, proteins were visualized using GelCode Blue Stain Reagent (Pierce). Silver staining was used to detect differential protein bands. The gel was soaked twice in 50% methanol, followed by a 10 min incubation in 5% methanol. After 3 rinses in water, the gel was incubated in 10 µM dithiothreitol (DTT) for 20 min, followed by 0.1% (w/v) $AgNO_3$ for 20 min. The gel was washed once in water and twice in developer solution (3% (w/v) Na_2CO_3 and 0.02% (w/v) formaldehyde). The gel was incubated in the developer solution until protein bands appeared. The staining reaction was stopped by adding 5% (w/v) citric acid.

GEL DIGESTION AND NANOFLOW LC-MS/MS ANALYSIS

1D SDS-PAGE gel lanes were cut into 2-mm slices using an automatic gel slicer and subjected to in-gel reduction with DTT, alkylation with iodoacetamide and digestion with trypsin (Promega, sequencing grade), essentially as described previously (Wilm and Mann 1996). Nanoflow LC-MS/MS was performed on a CapLC system (Waters, Manchester, UK) coupled to a Q-TOF Ultima mass spectrometer (Waters, Manchester, UK) operating in positive mode and equipped with a Z-spray source. Peptide mixtures were trapped on a JupiterTM C18 reversed phase column (Phenomenex; column dimensions 1.5 cm × 50 µm, packed in-house) using a linear gradient from 0 to 80% B (A = 0.1 M acetic acid; B = 80% (v/v) acetonitrile, 0.1 M acetic acid) in 70 min and at a constant flow rate of 200nl/min using a splitter. The column eluent was directly sprayed into the ESI source of the mass spectrometer. Mass spectra were acquired in continuum mode; fragmentation of the peptides was performed in data-dependent mode. Peak lists were automatically created from raw data files using the Protein Lynx Global Server software (version 2.0). The background subtraction threshold for noise reduction was set to 35% (background polynomial 5). Smoothing (Savitzky-Golay) was performed (number of interactions: 1, smoothing window: 2 channels). Deisotoping and centroiding settings were: minimum peak width: 4 channels, centroid top: 80%, TOF resolution: 5000, NP multiplier: 1. Mascot search algorithm (version 2.0, MatrixScience) was used for searching against the NCBInr database that was available on the MatrixScience server. The peptide tolerance was typically set to 150 ppm and the fragment ion tolerance was set to 0.2 Da. A maximum number of 1 missed cleavage by trypsin was allowed and carbamidomethylated cysteine and oxidized methionine were set as fixed and variable modifications, respectively.

NEURONAL CULTURE

E14.5 cerebral cortices were dissected and dissociated in 0.25% trypsin (PAA) in DMEM/F12 (Gibco, Invitrogen) for 15 min at 37°C. Trypsin was inactivated by adding an equal volume of DMEM/F12 containing 20% FBS (Lonza, BioWhittaker). Cerebral cortices were dissociated by trituration in DMEM/F12 containing 10% FBS and 20 µg/ml DNase I (Roche) using a fire-polished Pasteur pipette. Dissociated cortical neurons were cultured in Neurobasal medium (Gibco, Invitrogen) containing 2 mM L-glutamine (PAA), 1x pen/strep (PAA) and B-27 Supplement (Gibco, Invitrogen) on 100 µg/ml poly-L-lysine-coated (Sigma-Aldrich) acid-washed coverslips in a humidified atmosphere with 5% CO_2 at 37°C.

NEURITE OUTGROWTH ASSAY

Dissociated cortical neurons (400.000/50 µl sample) were electroporated with 4 µg DNA in 50 µl electroporation buffer (135 mM KCl, 2 mM $MgCl_2$, 0.2 mM $CaCl_2$ and 5 mM EGTA, pH 7.3) using a BTX Electro Square Porator ECM 830 (BTX Harvard Apparatus; settings: 100 V, 3 pulses, 900 µs pulse length, 2 s pulse interval). 170 µl 37°C RPMI 1640 medium (Gibco, Invitrogen) was added to the electroporation sample and electroporated neurons were transferred to 4 wells of a 24-well plate. Electroporated neurons were cultured on a confluent layer of CHO or CHO-RGMa cells in DMEM/F12 (Gibco, Invitrogen) containing 2% FBS (Lonza, BioWhittaker), 2 mM L-glutamine (PAA), 1x pen/strep (PAA) and B-27 Supplement (Gibco, Invitrogen) in a humidified atmosphere with 5% CO_2 at 37°C. After 4 days cells were fixed with 4% PFA for 15 min at RT and washed in PBS (pH 7.4). Cells were permeabilized and blocked in blocking solution (PBS, 4% BSA and 0.1% Triton) for 1 hr at RT and incubated with rabbit anti-GFP (A11122; Invitrogen) at 1:3000 and mouse anti-β-III-Tubulin (MMS-435P; Covance) at 1:2000 in blocking solution overnight at 4°C. The next day, sections were washed in PBS and incubated with Alexa Fluor 594 goat anti-mouse and Alexa Fluor 488 goat anti-rabbit (Invitrogen) at 1:500 for 1 hr at RT. Images were taken using a Cellomics ArrayScan VTI HCS Reader (Thermo Scientific) and the length of the longest neurite was measured using NeuronJ (Meijering *et al.* 2004). Data were statistically analyzed by two-tailed Student's t-test and represented as means ±SEM.

RESULTS

NEOGENIN-INTERACTING PROTEINS IDENTIFIED BY BIOTIN-STREPTAVIDIN-BASED PULL DOWN EXPERIMENTS AND MASS SPECTROMETRY

Our understanding of Neogenin signaling is incomplete and only very few Neogenin signaling proteins have been identified. Here we used biotin-streptavidin-based pull down assays combined with mass spectrometry analysis to identify novel Neogenin-interacting proteins. To identify Neogenin-interacting proteins in the signaling complexes of full-length Neogenin and the NeoICD, we generated biotin- and GFP-tagged full-length Neogenin (NeoFL-GFP-Bio) and

NeoICD (Bio-GFP-NeoICD) constructs (Fig. 1A). NeoFL-GFP-Bio, Bio-GFP-NeoICD or a control cDNA, Bio-GFP, were transiently expressed in HEK293 cells together with a cDNA encoding the BirA biotin ligase. HEK293 cells express endogenous Neogenin protein suggesting that endogenous Neogenin signaling complexes exist in these cells (Zhang *et al.* 2005). Although in our experiments a murine Neogenin fusion protein was expressed in a human cell line, mouse and human Neogenin are highly homologous (92.8 %) (Meyerhardt *et al.* 1997). Therefore, it is assumed that endogenously expressed human Neogenin-interacting proteins in HEK293 cells will interact with transiently expressed mouse Neogenin.

Streptavidin-coated beads were used to precipitate biotinylated proteins from cell lysates of HEK293 cells expressing NeoFL-GFP-Bio, Bio-GFP-NeoICD or Bio-GFP (Fig. 1B). The interaction between biotin and streptavidin has a high affinity (dissociation constant, $K_d \approx 10^{-14}$–10^{-16} M), allowing for specific binding and stringent washing conditions (De Boer *et al.* 2003, Laitinen *et al.* 2006). Isolated Neogenin protein complexes were analyzed by Western blotting (Fig. 1C), on silver- and Coomassie-stained gels (Fig. 1D, data not shown) and by mass spectrometry. Western blots probed with an anti-GFP antibody revealed a high yield of NeoFL-GFP-Bio, Bio-GFP-NeoICD and Bio-GFP protein in the biotin pull down samples (Fig. 1C). Anti-GFP antibody staining of the NeoFL-GFP-Bio pull down sample showed the full-length 190 kDa protein and a smaller 85 kDa-sized fragment. The 85 kDa protein might represent the Neogenin fragment that results from α-secretase cleavage of Neogenin, which cuts Neogenin just N-terminal of the transmembrane region (Goldschneider *et al.* 2008). Anti-GFP antibody staining of the Bio-GFP-NeoICD pull down sample also revealed two bands: the 67 kDa-sized band representing the NeoICD domain and a smaller protein fragment, which might represent the caspase-3 cleaved NeoICD fragment (Matsunaga *et al.* 2004).

Silver staining of the NeoFL-GFP-Bio, Bio-GFP-NeoICD and Bio-GFP biotin pull down samples separated on gel revealed many co-immunoprecipitated proteins in each sample (Fig. 1D). The strongly stained bands of the bait proteins: NeoFL-GFP-Bio, Bio-GFP-NeoICD and Bio-GFP are easily detected in the silver-stained gel (Fig. 1D, green dots). Besides non-specific bands of co-immunoprecipitated proteins identified in all pull down samples, several protein bands were specific for Neogenin pull down samples, indicating the presence of putative Neogenin-interacting proteins (Fig. 1D, orange dots).

Mass spectrometry analysis was used to identify the proteins precipitated in the different biotin pull down samples. For mass spectrometry analysis, an additional NeoFL-GFP-Bio pull down sample was included from HEK293 cells stimulated with RGMa. This sample would allow for the comparison of the binding of interactors to Neogenin in the presence and absence of ligand. Lanes from Coomassie-stained gels were analyzed by mass spectrometry and peptide sequences were mapped to known protein sequences using Mascot software. For the identification of putative Neogenin-interacting proteins the Mascot score cut-off value for a positive hit was set at 65 and the Neogenin pull down results were corrected for non-specific

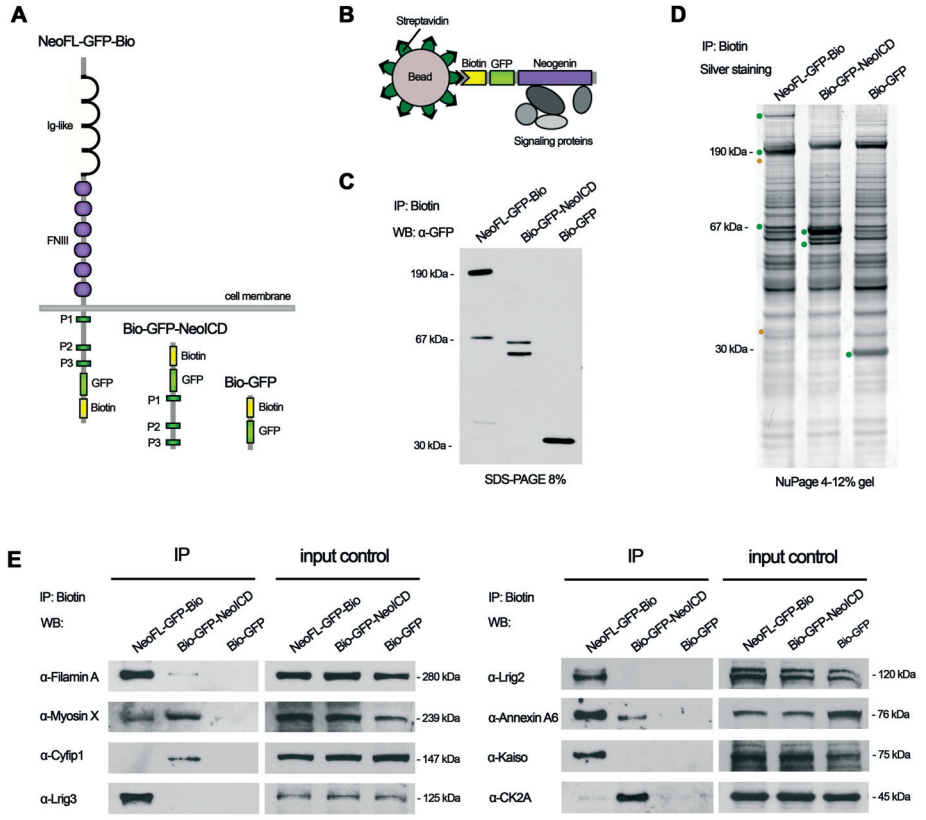

FIGURE 1. Biotin-streptavidin-based pull down experiments identify novel Neogenin-interacting proteins.(A) Biotin- and GFP-tagged Neogenin fusion cDNAs were generated to purify signaling complexes of full-length Neogenin (NeoFL-GFP-Bio) and the Neogenin intracellular domain (Bio-GFP-NeoICD). (B) Schematic representation of the biotin-streptavidin pull down assay. The biotin tag of the Neogenin fusion protein is biotinylated by BirA biotin ligase and specifically precipitated by streptavidin-coated beads. (C) Immunoblotting using an anti-GFP antibody detected NeoFL-GFP-Bio, Bio-GFP-NeoICD and Bio-GFP in the biotin pull down samples. (D) Silver staining of the biotin pull down samples revealed NeoFL-GFP-Bio, Bio-GFP-NeoICD and Bio-GFP (green dots) and putative Neogenin-interacting proteins (orange dots). (E) Western blot analysis confirmed the interaction of novel Neogenin-interacting proteins to NeoFL-GFP-Bio and Bio-GFP-NeoICD, using the antibodies indicated. CK2A, casein kinase 2A; Cyfip-1, cytoplasmic FMR1 interacting protein 1; FNIII, fibronectin type III; GFP, green fluorescent protein; Ig-like, immunoglobulin-like; IP, immunoprecipitation; Lrig, leucine-rich repeats and immunoglobulin-like domains; P1-3, conserved domains 1-3; WB, Western blot.

interacting proteins identified in the control Bio-GFP pull down and common contaminants (e.g. heat shock proteins, keratins, ribosomal proteins and proteins related to cell metabolism).

Mass spectrometry analysis of the biotin-streptavidin pull down samples revealed 53 putative Neogenin-interacting proteins which are listed in Table 2. Many of the putative Neogenin-interacting proteins identified have reported functions in cytoskeleton organization, cell adhesion, apoptosis and transcription. Interestingly, Neogenin plays an important role in all of these biological processes (De Vries and Cooper 2008). One of the Neogenin-interacting proteins identified, myosin X, is a known interactor of Neogenin (Zhu *et al.* 2007). Mass spectrometry analysis detected myosin X in the Bio-GFP-NeoICD pull down sample (Table 2). In line with our findings, myosin X was originally identified in a yeast two-hybrid screen using the NeoICD as a bait. Myosin X is an unconventional actin-based motor protein involved in filopodia formation (Berg *et al.* 2000, Liu *et al.* 2012). We confirmed the interaction of myosin X and Neogenin by Western blotting using an anti-myosin X antibody (Fig. 1E).

The validity of the mass spectrometry results was further confirmed by Western blot analysis of new biotin pull down samples with specific antibodies for a selection of newly identified Neogenin-interacting proteins. Based on Mascot scores and potential relevance for Neogenin signaling in neural development, filamin A, annexin A6, casein kinase 2A, Kaiso, Cyfip-1, Lrig2 and Lrig3 were selected for Western blot analysis and their interaction with Neogenin was confirmed (Fig. 1E). Filamin A (Hartwig and Stossel 1975), annexin A6 (Monastyrskaya *et al.* 2009) and Cyfip-1 (Kobayashi *et al.* 1998) are known regulators of actin cytoskeleton dynamics. Casein kinase 2A phosphorylates substrates that have been implicated in neuritogenesis, synaptic transmission and plasticity, and neuronal survival (Blanquet 2000, Meggio and Pinna 2003). Kaiso is a transcription factor that associates with the signaling molecule p120-catenin and is a known modulator of Wnt signaling (Daniel and Reynolds 1999, Kim *et al.* 2004, Prokhortchouk *et al.* 2001).

Lrig2 and Lrig3 are among the very few transmembrane proteins identified in the biotin Neogenin pull down screen. At the moment there is little knowledge about Lrig2 and 3 function. Lrig proteins are modulators of growth factor tyrosine kinase receptor signaling and Lrig expression has been associated with tumor growth and patient survival (Hedman and Henriksson 2007). Lrig1, the third member of the Lrig protein family, is a potent inhibitor of ErbB, Met and Ret receptor signaling (Laederich *et al.* 2004, Ledda *et al.* 2008, Shattuck *et al.* 2007). Accordingly, Lrig1 has been suggested to be a tumor suppressor that inhibits tumor growth by antagonizing growth factor signaling (Shattuck *et al.* 2007). Lrig3 has been described as an essential factor in neural crest formation in *Xenopus*, by modulating Wnt and fibroblast growth factor (FGF) signaling pathways (Zhao *et al.* 2008). So far, no specific function has been described for Lrig2. Although Lrig molecules are expressed in the brain, their function in neural development and plasticity is poorly understood (Holmlund *et al.* 2004, Homma *et al.* 2009).

TABLE 2. Neogenin-interacting proteins identified in the biotin-streptavidin-based pull down assay in HEK293 cells.

				NeoFL		NeoFL+RGMa		NeoICD		
#	Protein name		MW (kDa)	Mascot score	Unique peptides	Mascot score	Unique peptides	Mascot score	Unique peptides	Biological function
1	Filamin A	FLNA	280	1904	29	2851	43	439	6	Rac/Rho GTPase binding; actin filament binding; actin cytoskeleton organization; receptor clustering
2	Myosin X	MYO10	239	x	x	x	x	2763	57	actin binding; axon guidance; signal transduction
3	**Neogenin***	**NEO1**	**160**	**2501**	**178**	**2612**	**202**	**835**	**144**	**axon guidance; cell adhesion; migration; apoptosis; transcription regulation**
4	Annexin A6	ANXA6	76	107	2	871	15	202	4	actin cytoskeleton reorganization; calcium-dependent phospholipid binding; exocytotic and endocytotic pathways
5	Leucine-rich PPR motif-containing protein	LRPPRC	159	591	10	550	10	677	12	DNA binding; RNA binding; microtubule binding; regulation of transcription; mRNA transport
6	Leucine-rich repeats and immunoglobulin-like domains 2*	LRIG2	120	506	9	633	13	x	x	growth factor signaling
7	Leucine-rich repeats and immunoglobulin-like domains 3*	LRIG3	125	563	12	463	11	x	x	growth factor signaling; Wnt signaling; neural crest formation
8	Mitochondrial trifunctional protein	HADHA	84	460	7	266	3	x	x	cellular lipid metabolic process
9	Desmoglein-1*	DSG1	115	433	6	x	x	x	x	apoptotic process; calcium-dependent cell-cell adhesion
10	Damage-specific DNA binding protein 1	DDB1	123	296	5	416	7	x	x	DNA binding; DNA repair; Wnt receptor signaling pathway
11	Copine 3	CPNE3	61	x	x	360	5	x	x	calcium-dependent phospholipid binding; protein serine/threonine kinase activity; vesicle-mediated transport
12	Filaggrin family member 2	FLG2	249	298	5	x	x	x	x	calcium ion binding
13	Casein kinase 2A	CSNK2A1	45	36	1	x	x	288	5	ATP binding, beta-catenin binding, axon guidance, protein serine/threonine kinase activity, cell cycle, signal transduction
14	MYB-binding protein 1A	MYBBP1A	15	172	2	284	4	104	1	nucleocytoplasmic transport; regulation of transcription;
15	Kaiso	ZBTB33	75	274	4	278	4	x	x	regulation of transcription; Wnt receptor signaling pathway
16	Caspase 14 precursor	CASP14	28	272	3	x	x	x	x	cell differentiation
17	Cytoplasmic FMR1 interacting protein 1	CYFIP1	147	x	x	146	3	240	4	Rac GTPase binding, actin filament binding, axon extension, cell differentiation
18	AHNAK nucleoprotein	AHNAK	629	44	2	224	5	x	x	nervous system development
19	Exosome component 10	EXOSC10	103	214	3	48	1	x	x	RNA binding; RNA processing
20	Filamin B	FLNB	283	79	2	206	3	x	x	actin binding protein; actin cytoskeleton organization; cell differentiation; signal transduction
21	Transportin 1	TNPO1	104	206	3	154	2	x	x	protein import to the nucleus
22	Programmed cell death 6 interacting protein	PDCD6IP	97	107	2	129	2	x	x	apoptotic process
23	Cytoplasmic FMR1 interacting protein 2	CYFIP2	115	128	3	x	x	x	x	cell-cell adhesion; apoptotic process
24	SAR1a gene homolog 1	SAR1A	23	125	2	x	x	x	x	GTP binding; GTPase activity; intracellular protein transport; vesicle-mediated transport
25	LZTS2 leucine zipper	LZTS2	73	x	x	x	x	122	1	Wnt receptor signaling pathway; cell cycle; positive regulation of cell death
26	Desmocollin 1*	DSC1	101	120	3	x	x	x	x	cell adhesion; cell junction; desmosome

				NeoFL		NeoFL+RGMa		NeoICD		
#	Protein name		MW (kDa)	Mascot score	Unique peptides	Mascot score	Unique peptides	Mascot score	Unique peptides	Biological function
28	RAB13	RAB13	23	x	x	114	2	x	x	GTP binding; small GTPase mediated signal transduction; cell adhesion; vesicle-mediated transport
29	Plectin 1	PLEC1	516	113	3	47	2	x	x	actin binding; apoptotic process
30	U2-associated SR140 protein	SR140	119	x	x	111	2	93	1	RNA binding; RNA processing
31	Desmoplakin	DSP	202	110	1	x	x	x	x	cell-cell adhesion; desmosome; adherens junction organization; apoptotic process
32	Protein tyrosine phosphatase-like A domain containing 1	PTPLAD1	43	107	1	98	1	103	1	GTPase activator activity
33	General transcription factor II	GTF2I	111	x	x	x	x	96	3	DNA binding; regulation of transcription
34	Exosome component 4	EXOSC4	27	88	1	x	x	x	x	RNA processing
35	GRB10 interacting GYF protein 2	GIGYF2	153	x	x	x	x	87	1	cell death
36	WDR77	WDR77	36	81	1	72	1	x	x	RNA transcription; RNA metabolism
37	Calpain 1	CAPN1	82	79	1	x	x	x	x	calcium ion binding; positive regulation of cell proliferation; apoptotic process
38	Moloney leukemia virus 10	MOV10	102	78	1	87	1	x	x	ATP binding; RNA binding
39	Metadherin*	MTDH	64	x	x	76	1	x	x	transcription co-activator activity; negative regulation of apoptotic process; tight junction assembly; positive regulation angiogenesis
40	Adapter-related protein complex 3	AP3D1	145	75	1	x	x	x	x	synaptic vesicle membrane organization; vesicle-mediated transport
41	Brain abundant, membrane attached signal protein 1	BASP1	23	x	x	74	2	x	x	transcription corepressor activity
42	Emerin	EMD	29	74	1	x	x	x	x	actin binding; regulation of canonical Wnt receptor signaling; apoptotic process
43	Tripartite motif-containing 27	TRIM27	60	x	x	x	x	73	1	DNA binding; regulation of transcription
44	Survival of motor neuron 1/2	SMN1/2	32	72	1	73	1	x	x	RNA transport; RNA metabolism
45	Beta-arrestin 1	ARRB1	47	72	2	x	x	x	x	GTPase activator activity, protein ubiquitination, transcription regulation
46	Low-density lipoprotein receptor-related protein 4*	LRP4	221	x	x	72	2	x	x	calcium ion binding; cell differentiation; endocytosis; negative regulation of canonical Wnt receptor signaling pathway
47	CDC42 binding protein kinase A (DMPK-like)	CDC42BPA	188	71	3	x	x	x	x	protein serine/threonine kinase activity; actin cytoskeleton organization; cell migration; signal transduction; microtubule cytoskeleton organization
48	Cortactin	CTTN	72	x	x	71	2	x	x	actin cytoskeleton organization; dendritic spine morphogenesis; cell migration; cell adhesion junctions
49	Calponin 2	CNN2	34	x	x	x	x	70	2	actin binding; cytoskeleton organization; negative regulation of cell migration
50	PCTAIRE protein kinase 3	PCTK3	58	x	x	69	2	x	x	ATP binding; protein phosphorylation; protein serine/threonine kinase activity
51	GrpE-like 1, mitochondrial	GRPEL1	24	x	x	x	x	68	1	protein homodimerization activity; protein import into mitochondrial matrix
52	Utrophin	UTRN	396	68	3	x	x	x	x	actin binding; positive regulation of cell-matrix adhesion
53	Defender against cell death 1	DAD1	13	67	1	x	x	x	x	apoptotic process
54	Kinectin 1	KTN1	156	67	2	x	x	x	x	kinesin binding; microtubule-based movement

* Transmembrane protein

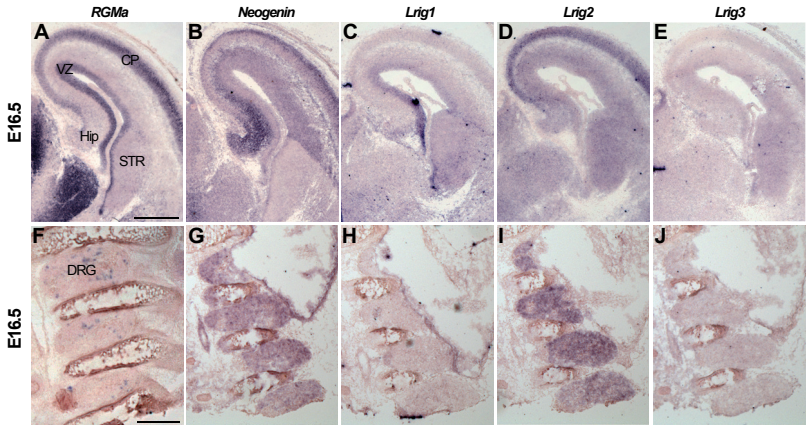

FIGURE 2. *Lrig2* and *Neogenin* are strongly expressed in mouse embryonic cortex and dorsal root ganglia (DRG) neurons.

In situ hybridization on coronal (A-E) and sagital (F-J) E16.5 mouse tissue sections. (A, B) *In situ* hybridization revealed abundant expression of *RGMa* and *Neogenin* in the cortex, with strong expression levels in the cortical plate (CP). (C) *Lrig1* expression is detected in the ventricular zone (VZ). (D) Abundant expression of *Lrig2* is detected in the cortex and strong expression levels are detected in the CP. (E) *Lrig3* expression was most prominent in the striatum (STR). Only weak *Lrig3* expression is detected in the CP and VZ. (F-J) *In situ* hybridization revealed prominent expression of *Neogenin* and *Lrig2* in DRGs. Hip, hippocampus. Scale bar A-E: 500 µm, F-J: 300 µm.

To study a possible role of Lrig proteins in RGMa-Neogenin signaling during neural development, we first investigated the expression of Lrig1, -2 and -3 in the developing brain in comparison to RGMa and Neogenin.

LRIG2 AND *NEOGENIN* ARE EXPRESSED IN THE CORTEX AND IN DRG NEURONS

Several studies report RGMa-Neogenin-mediated neurite outgrowth inhibition of embryonic cortical and DRG neurons (Brinks *et al.* 2004, Conrad *et al.* 2007, Endo and Yamashita 2009, Hata *et al.* 2006, Hata *et al.* 2009, Rajagopalan *et al.* 2004). To begin to study a potential functional role for Lrigs in RGMa-Neogenin signaling, we investigated the expression of *RGMa*, *Neogenin* and *Lrig*1, -2, and -3 in mouse embryonic cortex and DRG neurons by *in situ* hybridization. *In situ* hybridization at E16.5 revealed strong expression of *RGMa* and *Neogenin* in the cortex (Fig. 2A, B). High levels of *RGMa* were detected in the cortical plate (CP) and in the ventricular zone (VZ). *Neogenin* was expressed in all layers of the developing cortex with high expression levels in the outer region of the CP. Expression of *Lrig*1, -2 and -3 was also detected in the cortex (Fig. 2C-E). Expression of *Lrig*1 was restricted to the VZ. *Lrig*2 was detected in all layers of the developing cortex with strong expression in the CP. Weak expression of *Lrig*3 was detected

in the VZ and CP. E16.5 DRGs also expressed *Lrig*1, -2 and -3, *RGMa*, and *Neogenin* (Fig. 2F-J). However, whereas strong expression of *Lrig*2 and *Neogenin* was detected in DRG neurons, these neurons only expressed low levels of *Lrig*1, *Lrig*3 and *RGMa*. Altogether, *in situ* hybridization revealed strong co-expression of *Lrig*2 and *Neogenin* in the CP and DRGs.

LRIG2 AND NEOGENIN COLOCALIZE IN CORTICAL NEURONS

To confirm that Lrig2 and Neogenin are co-expressed in neurons at the protein level, we performed immunostainings on E16.5 mouse brain sections and dissociated mouse cortical neurons. The anti-Lrig2 antibody specifically detected Lrig2 and not Lrig1 and Lrig3 as determined by immunostaining on COS-7 cells transiently expressing Lrig1, -2 or -3 (Suppl. Fig. 1). Immunostaining for Neogenin revealed strong Neogenin expression in the marginal zone (MZ) and in cortical efferents in the external capsule (EC). Weak-to-moderate Neogenin expression was observed in the CP (Fig. 3A, A'). Immunostaining for Lrig2 detected Lrig2 expression in the MZ, the CP and in a subset of cortical axons in the EC (Fig. 3B, B'). Confocal imaging of E16.5 cortex revealed strong Neogenin expression at the neuronal cell membrane. Cytoplasmic Neogenin immunostaining was generally weak, with the exception of neurons in the MZ. Lrig2 immunostaining was detected at the cell membrane and in the cytoplasm of cortical neurons. A subset of CP neurons revealed very strong cytoplasmic Lrig2 expression (Fig. 3B'). Co-immunostaining for Neogenin and Lrig2 revealed clear colocalization of Neogenin and Lrig2 in CP neurons and in neurons of the MZ (Fig. 3C, C').

Immunostaining of E14.5 mouse dissociated cortical neurons (DIV2) revealed strong Neogenin and Lrig2 expression in the cell body, the axon and the growth cone (Fig. 3D, D', E, E'). However, whereas Neogenin was equally distributed throughout the neuron, Lrig2 expression was more punctate and less pronounced at the outer parts of the neuron. Co-immunostaining for Neogenin and Lrig2 revealed clear colocalization, but no complete overlap of Neogenin and Lrig2 expression (Fig. 3F, F'). Neogenin expression was detected throughout the growth cone, while Lrig2 expression was most abundant in the central area of the growth cone. Nevertheless, expression of both Neogenin and Lrig2 was detected in the filopodia of the growth cone. In all, immunohistochemistry revealed colocalization of Lrig2 and Neogenin in E16.5 cortex and dissociated cortical neurons.

LRIG2 AND NEOGENIN INTERACT *IN VIVO*

The interaction between Neogenin and Lrig2, identified by Neogenin biotin pull down assays, was verified by antibody-based co-immunoprecipitation experiments. In an endogenous pull down experiment on N1E-115 neuroblastoma cell lysate, anti-Lrig2 antibodies were used to pull down Lrig2. A non-specific anti-IgG goat antibody was used as a control. Immunoblotting with an anti-Neogenin antibody revealed the presence of Neogenin in the Lrig2 pull down sample (Fig. 4A). Reversely, Neogenin was immunoprecipitated from N1E-115 cell or P0 mouse brain lysates using a specific anti-Neogenin antibody. Immunoblotting with an anti-Lrig2 antibody confirmed that Lrig2 coprecipitated with Neogenin (Fig. 4B, C).

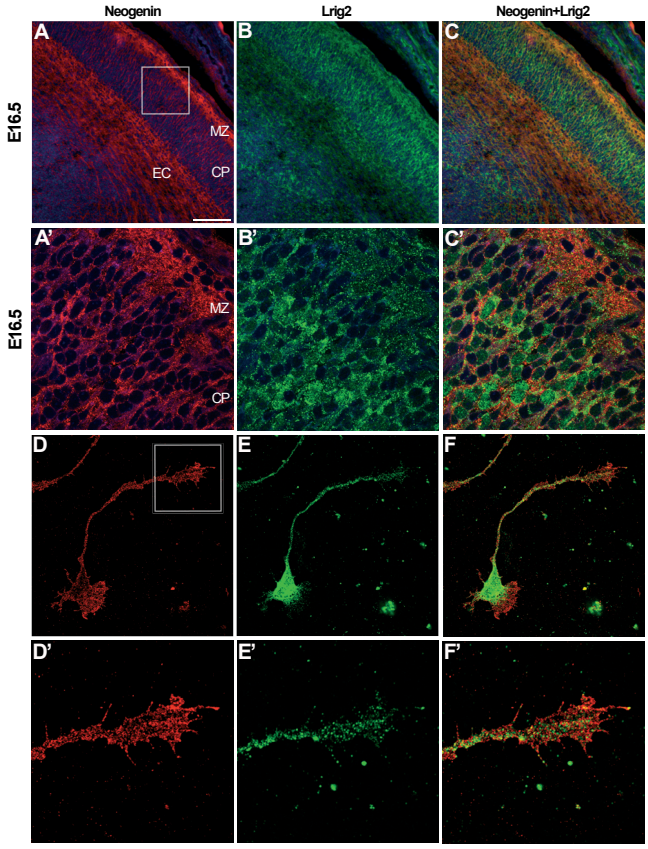

FIGURE 3. Colocalization of Lrig2 and Neogenin in E16.5 mouse cortex neurons.

Immunohistochemistry on E16.5 coronal mouse brain sections (A-C') and cultured mouse dissociated cortical neurons (D-F'). Confocal microscopy images in panels A'-F'. Panels A'-C' show higher magnifications of the cortical plate (CP) and marginal zone (MZ) in A-C (boxed area in A). Panels D'-F' show higher magnifications of the growth cone in D-F (boxed area in D). Sections A-C' are counterstained in blue with fluorescent Nissl. (A-C') Immunohistochemistry revealed strong expression and colocalization of Neogenin and Lrig2 in the CP, MZ and external capsule (EC) of the E16.5 mouse cortex. (D-F') Neogenin and Lrig2 immunostaining on dissociated cortical neurons detected strong expression and colocalization of Neogenin and Lrig2 in the cell body, axon and growth cone. Scale bar A-C: 100 µm.

Neogenin and Lrig2 are multi-domain proteins with large extracellular domains (ECDs). The ECD of Neogenin is composed of four Ig-like domains and six FNIII domains. In the NeoICD three conserved domains (P1-P3) are recognized, which have a high degree of homology to the P1-P3 domains of DCC (De Vries and Cooper 2008, Vielmetter *et al.* 1994). The ECD of Lrig2 contains 15 leucine-rich repeats (LRR) and three Ig-like domains. In the ICD of Lrig2 no

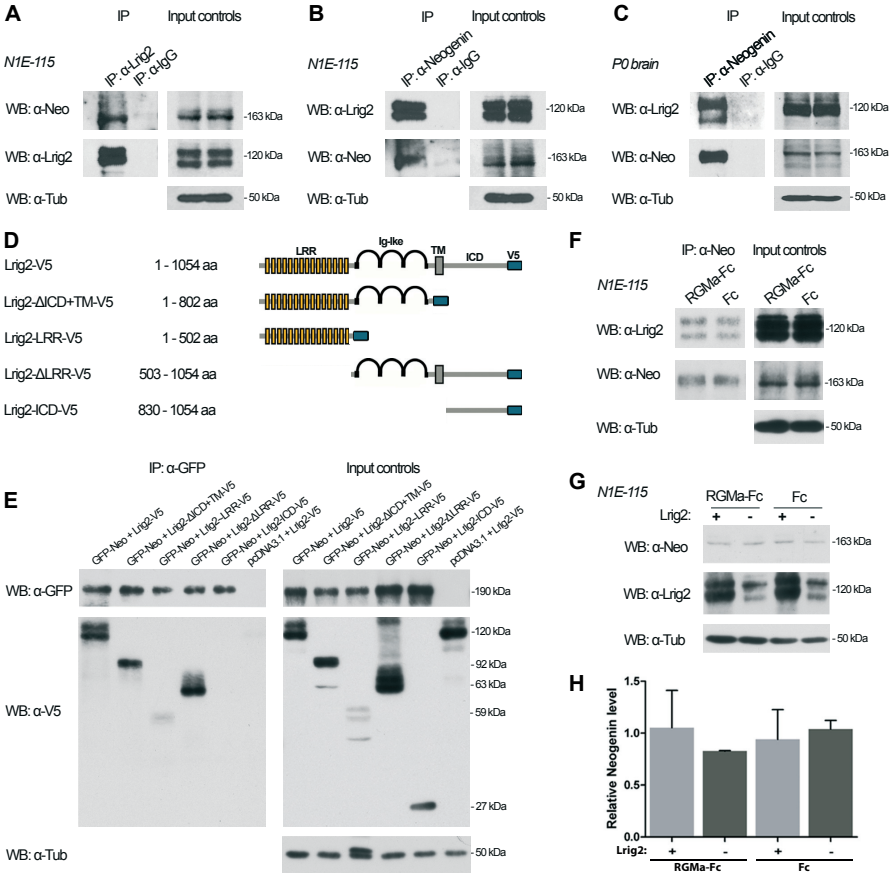

FIGURE 4. Lrig2 interacts with Neogenin *in vivo*.

(A) Immunoblotting revealed endogenous Neogenin protein in an anti-Lrig2 pull down experiment on N1E-115 neuroblastoma cell lysate. (B, C) Lrig2 is detected in Neogenin pull down samples from N1E-115 cell (B) and P0 brain lysates (C). No Lrig2 or Neogenin is detected in pull down experiments using a control anti-IgG antibody. (D) Schematic representation of the V5-tagged Lrig2 truncation mutants used in this study. (E) Anti-GFP pull down on HEK293 cell lysates cotransfected with pcDNA3.1-GFP-Neogenin and GW1-Lrig2-V5 truncation mutants, revealed that the extracellular domain of Lrig2 interacts with Neogenin. (F) Presence of RGMa ligand (30 min incubation) did not affect Lrig2 levels in Neogenin pull down samples from N1E-115 cells. (G) Lrig2 overexpression did not affect endogenous Neogenin levels in N1E-115 cells stimulated with RGMa-Fc or control Fc protein. Anti-Tubulin immunoblotting is used as loading control. Quantification in H. Fc, immunoglobulin Fc tag; FNIII, fibronectin type III; GFP, green fluorescent protein; Ig-like, immunoglobulin-like; IP, immunoprecipitation; Lrig2, leucine-rich repeats and immunoglobulin-like domains 2; LRR, leucine-rich repeats; Neo, Neogenin; P1-3, conserved domains 1-3; TM, transmembrane; Tub, tubulin; WB, Western blot.

specific domains or motifs have been reported (Holmlund *et al*. 2004). To identify the Lrig2 and Neogenin protein domains that are required for the Neogenin-Lrig2 interaction, a series of V5-tagged Lrig2 truncation mutants was generated (Fig. 4D). The Lrig2 truncation mutant cDNAs were cotransfected with a GFP-tagged full-length Neogenin cDNA in HEK293 cells. Anti-GFP pull down of GFP-Neogenin revealed co-immunoprecipitation of all Lrig2 truncation mutants that contain the full or parts of the Lrig2 ECD (Fig. 4E). The Lrig2 truncation mutant that only expressed the Lrig2 ICD did not interact with Neogenin. These results show that Lrig2 interacts with Neogenin through its ECD and that the ICD of Lrig2 is not involved in the Lrig2-Neogenin interaction.

Activation of Neogenin by RGMa changes the interaction between Neogenin and several intracellular signaling partners, like LIM domain only 4 (LMO4) and DAP kinase (Fujita *et al*. 2008, Schaffar *et al*. 2008). To investigate whether activation of Neogenin by RGMa stimulation increases binding of Lrig2 to Neogenin, N1E-115 cells were stimulated with RGMa-Fc or control Fc protein for 30 min. Endogenous Neogenin protein was precipitated followed by immunoblotting with anti-Lrig2 and anti-Neogenin antibodies. These experiments did not reveal an effect of RGMa on the Neogenin-Lrig2 interaction (Fig. 4F).

Lrig1 interacts with ErBb and Met receptors, via their ectodomains, and inhibits signaling of these receptors by enhancing their degradation (Gur *et al*. 2004, Inoue *et al*. 2007, Laederich *et al*. 2004, Shattuck *et al*. 2007). Similarly, Lrig3 interacts with FGF-1 receptors, decreases FGF-1 expression and attenuates FGF-1 signaling (Zhao *et al*. 2008). To investigate whether Lrig2 affects Neogenin expression levels by inducing Neogenin degradation, endogenous Neogenin levels were studied in N1E-115 cells cotransfected with Lrig2 or an empty vector and stimulated with RGMa. Triplicate experiments did not show a reduction of Neogenin expression in N1E-115 cells that co-express Lrig2 (Fig. 4G, quantification shown in H).

KNOCKDOWN OF LRIG2 BLOCKS RGMA-NEOGENIN-MEDIATED OUTGROWTH INHIBITION

Biochemical experiments revealed an *in vivo* interaction of Lrig2 and Neogenin and hint at a possible function for Lrig2 in Neogenin signaling. To study the requirement of Lrig2 in RGMa-Neogenin signaling, we designed three different shRNAs (shLrig2-A, -B and -C) targeting mouse Lrig2, which were cloned in pSuper (a vector for expression of short interfering RNA). First, the specificity and knockdown efficiency of the Lrig2 shRNAs was verified by cotransfection of pSuper-shLrig2-A, -B or -C together with mouse Lrig2 (pcDH-FLAG-Lrig2) or mouse Lrig3 (pcDH-FLAG-Lrig3) cDNA in HEK293 cells. shLrig2-A and -B, but not -C, induced a strong and specific knockdown of FLAG-Lrig2, compared to HEK293 cells cotransfected with the pSuper empty vector (Fig. 5A). The Lrig2 shRNAs did not reduce FLAG-Lrig3 expression levels (Fig. 5B). Secondly, we verified the potential of shLrig2-A to reduce endogenous Lrig2 expression in N1E-115 neuroblastoma cells. After four days in culture, knockdown efficiency was determined by immunoblotting with a specific anti-Lrig2 antibody. Endogenous Lrig2 levels were clearly

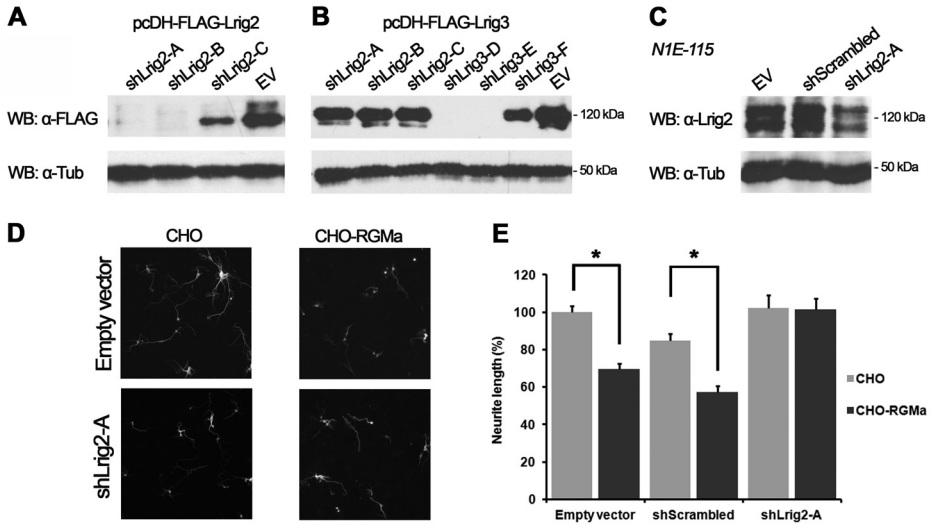

FIGURE 5. Lrig2 knockdown blocks RGMa-Neogenin-induced neurite outgrowth inhibition.

(A) Immunoblotting of HEK293 cell lysates cotransfected with pcDH-FLAG-Lrig2 and shLrig2-A, -B and -C expressed in pSuper or pSuper empty vector (EV) revealed shLrig2-mediated knockdown of FLAG-Lrig2. Anti-α-Tubulin immunoblotting is used as loading control. (B) shLrig2-A-C did not induce knockdown of FLAG-Lrig3, while shLrig3-D and -E did induce strong knockdown of Flag-Lrig3. (C) Anti-Lrig2 immunoblotting revealed knockdown of endogenous Lrig2 in cell lysate of N1E-115 neuroblastoma cells transfected with pSuper-shLrig2-A, compared to pSuper-shScrambled or pSuper empty vector. (D) Dissociated cortical neurons are electroporated with pSuper empty vector, pSuper-shScrambled or pSuper-shLrig2-A and cultured on a confluent layer of CHO control or CHO-RGMa cells. After 4 days, neurons are stained with anti-Tubulin and neurite length is measured. Knockdown of Lrig2 in dissociated cortical neurons blocked RGMa-Neogenin-induced neurite outgrowth inhibition. (E) Graph shows average length of the longest neurite per neuron ±SEM, *p<0.001, Student T-test. The average neurite length of the empty vector-transfected cells on control CHO cells was set to 100%. EV, empty vector; sh, short hairpin; Tub, tubulin; WB, Western blot.

reduced in N1E-115 cells transfected with shLrig2-A compared to N1E-115 cells transfected with pSuper empty vector or pSuper expressing a scrambled shRNA (Fig. 5C).

To investigate a potential role for Lrig2 in RGMa-mediated Neogenin signaling we tested knockdown of Lrig2 in a neurite outgrowth assay of dissociated cortical neurons plated on a confluent layer of either RGMa-expressing CHO cells (CHO-RGMa) or control CHO cells as described previously (Hata *et al.* 2006). Dissociated mouse E14.5 cortical neurons were electroporated with shLrig2-A, scrambled shRNA or pSuper empty vector (together with GFP) and plated on CHO-RGMa or control CHO cells. After four days in culture, cells were fixed and

neurites were visualized by anti-β-III-Tubulin antibody staining. Cellomics ArrayScan (Thermo Scientific) was used to take random images of the cultured neurons. Neurite outgrowth of electroporated neurons was analyzed by measuring the length of the longest neurite per neuron using ImageJ. Cortical neurons electroporated with pSuper empty vector or scrambled shRNA revealed a significant reduction in neurite length when cultured on CHO-RGMa cells compared to control CHO cells. In cortical neurons electroporated with shLrig2-A no significant difference in neurite length between neurons cultured on CHO-RGMa or control CHO cells was observed (Fig. 5D, E). Taken together, the results of the neurite outgrowth assay revealed a requirement for Lrig2 in RGMa-induced neurite outgrowth inhibition.

LRIG2 REDUCES NEOGENIN LIGAND BINDING

To get a better understanding of the role of Lrig2 in inhibitory RGMa-Neogenin signaling, we investigated the effect of Lrig2 on Neogenin ligand binding. Binding of Lrig1 to Ret receptors has been shown to attenuate Ret receptor tyrosine kinase activation by reducing binding of glial cell line-derived neurotrophic factor (GDNF) and GFRα coreceptor to Ret (Ledda *et al.* 2008). Neogenin ligand binding was evaluated in COS-7 cell binding assays using AP-tagged RGMa and Netrin-1. Strong binding of RGMa-AP or Netrin-1-AP was observed to COS-7 cells transfected with wild-type Neogenin and GW1 empty vector (1:1) (Fig. 6A, D). Surprisingly, in COS-7 cells co-expressing full-length Lrig2 (Lrig2-V5) the number of cells displaying RGMa-AP or Netrin-1-AP binding was greatly reduced (Fig. 6B, E). In addition, co-expression of ICD-deleted Lrig2 (Lrig2ΔICD-V5), had a similar effect (Fig. 6C, F).

To study whether the reduction of ligand binding induced by Lrig2 expression is specific for Neogenin ligand binding, the effect of Lrig2 expression on Semaphorin3F (Sema3F) binding to Neuropilin-2 was evaluated in another series of COS-7 cell binding experiments. COS-7 cells were transfected with Neuropilin-2 receptor together with either GW1 empty vector, Lrig2-V5 or Lrig2ΔICD-V5 (1:1). No difference in binding of AP-tagged Sema3F ligand to Neuropilin-2 was observed in the different experimental settings, indicating that the effect of Lrig2 on ligand binding is specific for RGMa-AP and Netrin-1-AP binding to Neogenin (Fig. 6G-I). AP protein alone did not bind Neogenin or Neuropilin-2 (Fig. 6J and data not shown). In addition, RGMa-AP and Netrin-1-AP did not bind Lrig2-V5 or Lrig2ΔICD-V5 (Fig. 6K and data not shown). Western blot analysis of transfected COS-7 cell lysates revealed expression of Neogenin, Neuropilin-2, Lrig2-V5 and Lrig2ΔICD-V5 (Fig. 6L). No reduction of Neogenin expression was observed in COS-7 cells co-expressing Lrig2-V5 or Lrig2ΔICD-V5, which is in line with unaltered levels of GDNF receptors, Ret and GFRα, after overexpression of Lrig1 (Ledda *et al.* 2008).

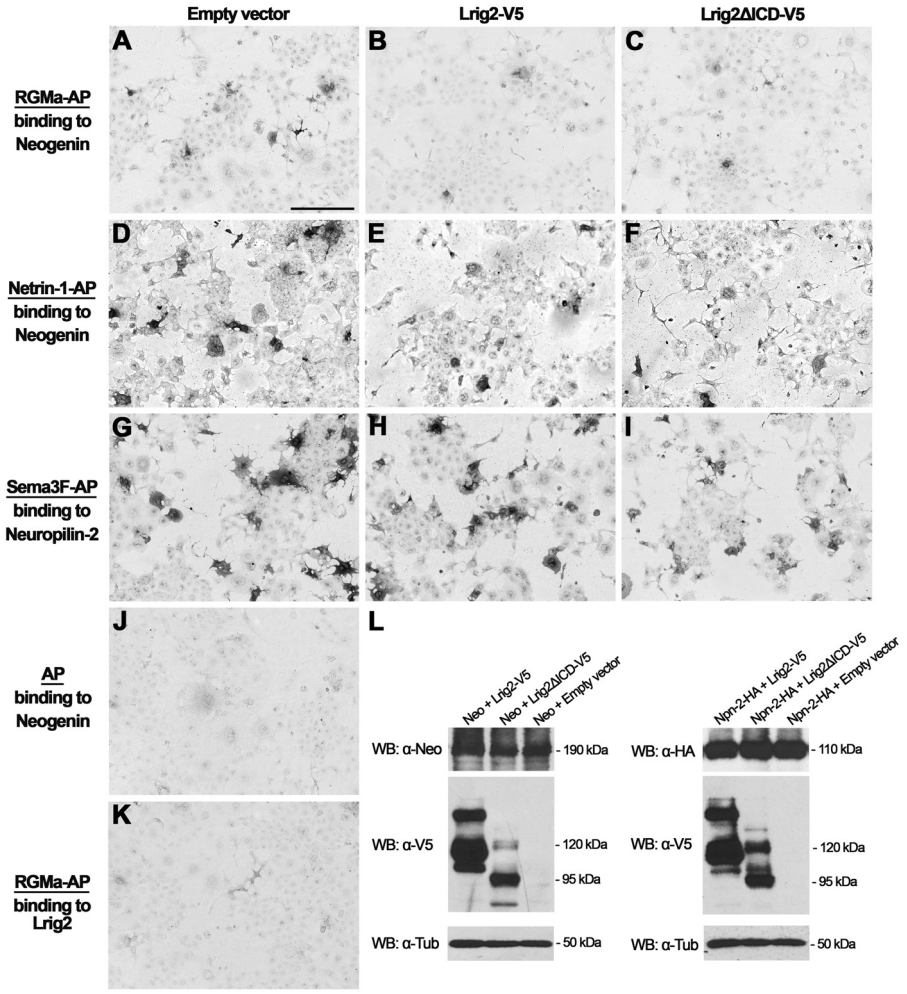

FIGURE 6. Lrig2 overexpression in COS-7 cells reduces RGMa-AP and Netrin-1-AP binding to Neogenin.

(A-F) Binding of RGMa-AP (A) and Netrin-1-AP (D) to Neogenin-expressing COS-7 cells is blocked in COS-7 cells co-expressing Lrig2-V5 (B, E) or ICD-deleted Lrig2 (Lrig2ΔICD-V5) (C, F). (G-I) Binding of Sema3F-AP to Neuropilin-2 is not affected by Lrig2 overexpression (G-I). (J) AP protein alone did not bind Neogenin. (K) RGMa-AP does not bind Lrig2. (L) Western blot analysis shows the expression of Neogenin (Neo), Neuropilin-2 (Npn2), Lrig2-V5 and Lrig2ΔICD-V5 in COS-7 cells used for the AP binding assay. Tub, tubulin; WB, Western blot.

DISCUSSION

BIOTIN-STREPTAVIDIN PULL DOWN IDENTIFIES NOVEL NEOGENIN SIGNALING PROTEINS

The mechanisms that mediate or regulate Neogenin signaling are poorly understood. In this study we applied biotin-streptavidin-based pull down experiments in HEK293 cells, transiently expressing NeoFL-GFP-Bio or Bio-GFP-NeoICD, to precipitate Neogenin signaling complexes. Mass spectrometry analysis of the Neogenin signaling complexes isolated by biotin pull down revealed 53 putative Neogenin-interacting proteins (Table 2). Among the novel Neogenin-interacting proteins identified are seven transmembrane proteins. The majority of transmembrane proteins identified are desmosomal junction proteins, for example desmoglein 1 and desmocollin 1. The desmosomal junction proteins identified could very well be true Neogenin-interacting proteins considering the role of Neogenin signaling in adhesion of multipotent cap cells (epithelial cells) of the developing mammary gland (Srinivasan *et al.* 2003). Five of the identified Neogenin-interacting proteins were detected in all Neogenin biotin pull down samples, which greatly enlarges the probability of these proteins being true Neogenin-interacting proteins (Table 2).

Neogenin-interacting proteins that are identified in the NeoFL-GFP-Bio pull down sample of RGMa-stimulated HEK293 cells could represent Neogenin-interacting proteins that are involved in RGMa-activated Neogenin signaling cascades (Table 2). These include copine 3, a serine/threonine kinase (Caudell *et al.* 2000, Creutz *et al.* 1998), and Cyfip-1, which binds Rac GTPases and functions in actin cytoskeleton dynamics (Caudell *et al.* 2000, Creutz *et al.* 1998, Kobayashi *et al.* 1998, Schenck *et al.* 2001, Schenck *et al.* 2003). In addition, Neogenin-interacting proteins that are only identified in the NeoFL-GFP-Bio pull down sample of non-stimulated HEK293 cells could potentially be linked to dependence receptor function of Neogenin to induce apoptosis in the absence of RGMa ligand (Matsunaga *et al.* 2004). Neogenin-interacting proteins identified in the NeoFL-GFP-Bio pull down sample of unstimulated HEK293 cells with known functions in apoptosis signaling are desmoglein 1 (Dusek *et al.* 2006), Cyfip-2 (Jackson *et al.* 2007, Mongroo *et al.* 2011), calpain 1 (Altznauer *et al.* 2004, Raynaud and Marcilhac 2006, Squier *et al.* 1994), emerin (Columbaro *et al.* 2001, Gotzmann *et al.* 2000) and defender against cell death 1 (Columbaro . 2001, Nakashima *et al.* 1993, Sugimoto *et al.* 1995) (Table 2). Finally, the Bio-GFP-NeoICD pull down could potentially identify putative Neogenin-interacting proteins that are located in the nucleus. General transcription factor 2 (Sumimoto *et al.* 1990) and tripartite motif-containing 27 (Krutzfeldt *et al.* 2005), two transcription factors that can bind DNA and induce transcription, are only identified in the Bio-GFP-NeoICD pull down sample (Table 2). Together, known biological functions of putative novel Neogenin-interacting proteins unique for one of the Neogenin pull down samples can be related to specific Neogenin signaling mechanisms.

One of the proteins identified in the screen, myosin X, is a known interactor of Neogenin (Liu *et al.* 2012, Zhu *et al.* 2007). Myosin X is an unconventional actin-based motor protein involved in filopodia formation (Berg *et al.* 2000). A recent study shows that Neogenin directs myosin X movement towards the apical and dorsal side of a cell, promoting dorsal filopodia formation and growth. Furthermore, Neogenin inhibits, integrin-dependent FAK tyrosine phosphorylation and basal F-actin reorganization (Liu *et al.* 2012). Immunoblotting confirmed the interaction of myosin X and Neogenin (Fig. 1E). In addition, the interaction of Neogenin and a selection of Neogenin-interacting proteins: filamin A, annexin A6, casein kinase 2A, Kaiso, Cyfip-1 and Lrig2 and 3, was confirmed by Western blot analysis of the biotin pull down samples with specific antibodies. These novel Neogenin-interacting proteins are interesting candidates for future studies on Neogenin signaling mechanisms. Filamin A could link Neogenin signaling to the regulation of the actin cytoskeleton. Former studies revealed the ability of filamin A to interact with transmembrane receptors, small GTPases and F-actin (Hartwig and Stossel 1975, Nakamura *et al.* 2011, Ohta *et al.* 1999). Annexin A6 and Cyfip-1 are also known regulators of cytoskeletal dynamics (Kobayashi *et al.* 1998, Monastyrskaya *et al.* 2009). Annexin A6 mediates the targeting of p120GAP an important inactivator of Ras signaling to the plasma membrane (Grewal *et al.* 2005, Davis *et al.* 1996, Grewal *et al.* 2005). Inactivation of Ras by p120GAP is essential for RGMa-Neogenin-induced neurite outgrowth inhibition (Endo and Yamashita 2009). Furthermore, annexin A6 was identified in the RGMa-stimulated NeoFL-GFP-Bio pull down sample and was not present in the unstimulated NeoFL-GFP-Bio pull down sample (Table 2). Therefore it would be interesting to investigate the involvement of annexin A6 in RGMa-activated Neogenin signaling. Casein kinase 2A was identified as a strong interactor of Bio-GFP-NeoICD (Table 2, Fig. 1E). Casein kinase 2A is a serine/threonine kinase for which over 300 substrates have been identified (Meggio and Pinna 2003). Kaiso is a transcription factor that associates with p120-catenin and is a known modulator of Wnt signaling (Daniel and Reynolds 1999, Kim *et al.* 2004, Prokhortchouk *et al.* 2001). Localization of Kaiso could either be nuclear or cytoplasmic indicating a role for Kaiso in translating signals from the cell surface to regulation of gene transcription (Soubry *et al.* 2005). This could be an interesting signaling mechanism for RGMa-Neogenin signaling as Kaiso was only indentified in the NeoFL-GFP-Bio pull down samples (Table 2, Fig. 1E).

Lrig2 and 3 are among the few transmembrane proteins identified in the Neogenin pull down screen. Lrig proteins are known modulators of growth factor receptor tyrosine kinase signaling (Gur *et al.* 2004, Laederich *et al.* 2004, Shattuck *et al.* 2007). We analyzed the expression of Lrig1, -2 and -3 in embryonic mouse brain by *in situ* hybridization and detected strong expression of Lrig2, while Lrig1 and Lrig3 were only expressed at very low levels (Fig. 2). Immunohistochemistry revealed colocalization of Neogenin and Lrig2 in mouse embryonic cortical neurons and endogenous pull down experiments revealed an *in vivo* interaction for Lrig2 and Neogenin in mouse P0 brain lysates (Fig. 3, 4C). Together, these results show

that endogenous Neogenin and Lrig2 interact *in vivo* suggesting a role for Lrig2 in Neogenin signaling.

LRIG2 IS A NOVEL NEOGENIN-INTERACTING PROTEIN

Different Neogenin-expressing neuron types show a reduction in neurite outgrowth *in vitro* following exposure to RGMa (Brinks *et al*. 2004, Conrad *et al*. 2007, Endo and Yamashita 2009, Hata *et al*. 2006, Hata *et al*. 2009). In this study, we show a neurite outgrowth inhibiting effect of RGMa on mouse E16.5 cortical neurons cultured on a confluent layer of CHO-RGMa cells compared to control CHO cells. shRNA-mediated knockdown of Lrig2 expression in these neurons completely abolished the RGMa-induced outgrowth inhibitory effect (Fig. 5E). This shows that Lrig2 is required for RGMa-Neogenin-mediated outgrowth inhibition.

Despite the strong expression of Lrig2 protein in the developing brain, no specific function or signaling mechanism of Lrig2 in neurodevelopment has been described (Guo *et al*. 2004, Homma *et al*. 2009). Recent work on the Lrig family members Lrig1 and Lrig3 have started to elucidate Lrig functions and signaling mechanisms. Lrig1 is best characterized and several studies stress its potential as a tumor suppressor for being a strong negative regulator of growth factor signaling (Laederich *et al*. 2004, Lindstrom *et al*. 2011, Miller *et al*. 2008, Sheu *et al*. 2009, Thomasson *et al*. 2003). Lrig1 inhibits ErbB and Met tyrosine kinase receptor signaling by inducing receptor degradation (Gur *et al*. 2004, Laederich *et al*. 2004, Shattuck *et al*. 2007). In addition, Lrig1 inhibits Ret receptor signaling by blocking GDNF ligand binding to Ret and recruitment of Ret to lipid rafts, which is essential for activation of the Ret signaling cascade (Ledda *et al*. 2008). Lrig3 can interact with FGF-1 receptors, decrease FGF-1 expression and attenuates FGF-1 activity (Zhao *et al*. 2008). Expression of Lrig3 regulates neural crest formation in *Xenopus* by modulating FGF and Wnt signaling pathways.

Our observation for the requirement for Lrig2 in RGMa-Neogenin signaling is not in line with the described roles for Lrig1 and Lrig3 in blocking receptor signaling by reducing receptor expression levels. If Lrig2 would block Neogenin signaling, knockdown of Lrig2 expression is expected to increase RGMa-Neogenin-mediated neurite outgrowth inhibition. Instead, a complete loss of RGMa sensitivity was observed in the CHO-RGMa neurite outgrowth assay following Lrig2 knockdown (Fig. 5E). Furthermore, no reduction in Neogenin expression was observed in N1E-115 neuroblastoma cells overexpressing Lrig2 (Fig. 4G, H). These results indicate that Lrig2 is essential in mediating Neogenin signaling in cortical neurons and does not affect Neogenin expression levels.

A CORECEPTOR FUNCTION FOR LRIG2 IN NEOGENIN SIGNALING?

Biochemical experiments in this study reveal that the association of Neogenin and Lrig2 is not changed upon RGMa stimulation (Fig. 4F). This observation resembles the interaction of Neogenin with coreceptor Unc5B, of which the association with Neogenin is not affected by RGMa (Hata *et al*. 2009). The interaction of Unc5B with RhoGEF LARG mediates RhoA

GTPase activation, which is required for RGMa-Neogenin signaling. The mechanism by which Lrig2 mediates RGMa-Neogenin signaling is not known. Similar to Unc5B, Lrig2 could recruit cytoplasmic signaling proteins to the Neogenin signaling complex that function in RGMa-Neogenin signaling. So far no cytoplasmic proteins have been identified that bind the Lrig2 intracellular domain. C-Cbl, an ubiquitin ligase that binds to the ICD of Lrig1 is the only cytoplasmic signaling molecule known that interacts with Lrig molecules (Gur *et al.* 2004).

Besides a possible role for Lrig2 in recruiting cytoplasmic signal transduction proteins, Lrig2 could also function in transporting Neogenin to lipid raft compartments in the cell membrane. For Ret receptor signaling, GDNF ligand binding to lipid-anchored GFRα1 coreceptors induces the recruitment of Ret receptor to lipid raft compartments, a dynamic event required for effective GDNF signaling (Ledda *et al.* 2008). Lrig1 is localized outside lipid rafts and binds Ret receptors. Expression of Lrig1 inhibits the interaction between Ret and the GDNF/GFRα1 complexes, retaining Ret molecules outside the raft compartment and in this way Ret signaling is blocked. Besides inducing repulsive signaling by activation of the Neogenin receptor, RGMs function as coreceptors in bone morphogenetic protein (BMP) signaling (Babitt *et al.* 2005, Samad *et al.* 2005, Zhang *et al.* 2005). RGMs bind BMP ligands and associate with BMP receptors to activate Smad signaling. BMPs are important regulators of chondrogenesis and osteoblastogenesis (Pathi *et al.* 1999, Yoon and Lyons 2004). Neogenin-deficient mice revealed impaired digit development and defective endochondral ossification (Zhou *et al.* 2010). In developing chondrocytes, Neogenin interacts with RGMs and BMP receptors and is essential for the localization of this signaling complex to lipid rafts and activation of Smad signaling. Lipid raft localization of DCC and Unc5s has been shown to be required for activation of Netrin-1-induced axon guidance and induction of apoptotic signaling (Guirland *et al.* 2004, Herincs *et al.* 2005, Maisse *et al.* 2008). In line with these findings, localization of Neogenin to lipid rafts might be essential for activation of the Neogenin signaling cascade after binding RGMa.

LRIG2 BLOCKS NEOGENIN LIGAND BINDING

AP ligand binding assays revealed reduced binding of RGMa and Netrin-1 to Neogenin-expressing COS-7 cells co-expressing full-length Lrig2 (Lrig2-V5) or ICD-deleted Lrig2 (Lrig2ΔICD) (Fig. 6A-F). Western blot analysis did not show a reduction of Neogenin expression in COS-7 cells transfected with Lrig2 or Lrig2ΔICD (Fig. 6L). Together, these results hint at a ligand-blocking function of Lrig2. In Ret receptor signaling, interaction of Lrig1 and Ret was shown to reduce GDNF ligand binding to Ret, which resulted in reduced activation of Ret signaling (Ledda *et al.* 2008). So far a putative Lrig2 blocking effect on Neogenin ligand binding was only shown in a Neogenin- and Lrig2-overexpressing COS-7 cells. Further experiments are needed to reveal whether Lrig2 expression also reduces Neogenin ligand binding in Neogenin-expressing neurons in the brain.

At first sight our observation that Lrig2 blocks Neogenin ligand binding in COS-7 cells seems contradictory to the results of the neurite outgrowth assay revealing a requirement for Lrig2 in RGMa-Neogenin-mediated neurite outgrowth inhibition. However, Lrig2 could be involved in terminating Neogenin signaling by blocking RGMa-binding to Neogenin receptors that have already been activated by RGMa molecules and have triggered Neogenin signaling. It is believed that ligand-activated receptors have to return to their inactivated state in order to keep the intracellular signaling machinery sensitive to novel signaling cues in the environment. Ligand-induced endocytosis of receptors is a general mechanism to inactivate receptor signaling (O'Donnell *et al*. 2009). Non-functional Neogenin signaling by overactivation of the Neogenin receptor could be a possible explanation for the insensitivity to RGMa of cortical neurons electroporated with Lrig2 shRNA constructs.

Neogenin has been classified as a dependence receptor, which induces apoptosis in the absence of RGMa (Matsunaga *et al*. 2004). With respect to this Neogenin signaling mechanism, blockage of RGMa binding by Lrig2 could activate Neogenin-mediated apoptotic pathways. Another possibility is that binding of Lrig2 to Neogenin induces a conformational change of the Neogenin protein which mimics its activated state. In this way activation of apoptotic pathways could be blocked.

Overall the experiments in this study identified Lrig2 as a Neogenin-interacting protein essential in mediating RGMa-Neogenin-induced outgrowth inhibition in dissociated cortical neurons. Furthermore, COS-7 cell binding assays revealed a Neogenin ligand-blocking effect of Lrig2 overexpression. This is the first study that reveals a role for Lrig2 during brain development. Further studies are needed to unravel the complete signaling mechanisms of the Neogenin-Lrig2 interaction in the developing brain.

ACKNOWLEDGEMENT

We would like to thank Phebe Wulf and Casper Hoogenraad for their expertise on biotin-streptavidin-based pull down assays. We are grateful to Toshihide Yamashita for sharing CHO and CHO-RGMa cell lines, and to Håkan Hedman, Thomas Stossel and Theresia Stradal for providing us with antibodies. We thank Valerie Castellani, Denise Davis, Roman Giger, Kun-Liang Guan, Håkan Hedman, Mathew Hemming, Casper Hoogenraad, Herbert Lin, and Thomas Skutella for their gift of cDNA vectors. This work was supported by HFSP (CDA), NWO (VIDI), Parkinson foundation and Hersenstichting Nederland grants to R.J.P.

REFERENCE LIST

Altznauer, F., S. Conus, A. Cavalli, G. Folkers, and H. U. Simon. 2004. Calpain-1 regulates Bax and subsequent Smac-dependent caspase-3 activation in neutrophil apoptosis. J. Biol. Chem. 279:5947-5957.

Babitt, J. L., Y. Zhang, T. A. Samad, Y. Xia, J. Tang, J. A. Campagna, A. L. Schneyer, C. J. Woolf, and H. Y. Lin. 2005. Repulsive guidance molecule (RGMa), a DRAGON homologue, is a bone morphogenetic protein co-receptor. J. Biol. Chem. 280:29820-29827.

Berg, J. S., B. H. Derfler, C. M. Pennisi, D. P. Corey, and R. E. Cheney. 2000. Myosin-X, a novel myosin with pleckstrin homology domains, associates with regions of dynamic actin. J. Cell Sci. 113 Pt 19:3439-3451.

Blanquet, P. R. 2000. Casein kinase 2 as a potentially important enzyme in the nervous system. Prog. Neurobiol. 60:211-246.

Brinks, H., S. Conrad, J. Vogt, J. Oldekamp, A. Sierra, L. Deitinghoff, I. Bechmann, G. Alvarez-Bolado, B. Heimrich, P. P. Monnier, B. K. Mueller, and T. Skutella. 2004. The repulsive guidance molecule RGMa is involved in the formation of afferent connections in the dentate gyrus. J. Neurosci. 24:3862-3869.

Brummelkamp, T. R., R. Bernards, and R. Agami. 2002. A system for stable expression of short interfering RNAs in mammalian cells. Science 296:550-553.

Caudell, E. G., J. J. Caudell, C. H. Tang, T. K. Yu, M. J. Frederick, and E. A. Grimm. 2000. Characterization of human copine III as a phosphoprotein with associated kinase activity. Biochemistry 39:13034-13043.

Columbaro, M., E. Mattioli, G. Lattanzi, C. Rutigliano, A. Ognibene, N. M. Maraldi, and S. Squarzoni. 2001. Staurosporine treatment and serum starvation promote the cleavage of emerin in cultured mouse myoblasts: involvement of a caspase-dependent mechanism. FEBS Lett. 509:423-429.

Conrad, S., H. Genth, F. Hofmann, I. Just, and T. Skutella. 2007. Neogenin-RGMa signaling at the growth cone is bone morphogenetic protein-independent and involves RhoA, ROCK, and PKC. J. Biol. Chem. 282:16423-16433.

Conrad, S., F. Stimpfle, S. Montazeri, J. Oldekamp, K. Seid, G. Alvarez-Bolado, and T. Skutella. 2010. RGMb controls aggregation and migration of Neogenin-positive cells *in vitro* and *in vivo*. Mol. Cell Neurosci. 43:222-231.

Creutz, C. E., J. L. Tomsig, S. L. Snyder, M. C. Gautier, F. Skouri, J. Beisson, and J. Cohen. 1998. The copines, a novel class of C2 domain-containing, calcium-dependent, phospholipid-binding proteins conserved from Paramecium to humans. J. Biol. Chem. 273:1393-1402.

Daniel, J. M. and A. B. Reynolds. 1999. The catenin p120(ctn) interacts with Kaiso, a novel BTB/POZ domain zinc finger transcription factor. Mol. Cell Biol. 19:3614-3623.

Davis, A. J., J. T. Butt, J. H. Walker, S. E. Moss, and D. J. Gawler. 1996. The Ca2+-dependent lipid binding domain of P120GAP mediates protein-protein interactions with Ca2+-dependent membrane-binding proteins. Evidence for a direct interaction between annexin VI and P120GAP. J. Biol. Chem. 271:24333-24336.

De Boer, E., P. Rodriguez, E. Bonte, J. Krijgsveld, E. Katsantoni, A. Heck, F. Grosveld, and J. Strouboulis. 2003. Efficient biotinylation and single-step purification of tagged transcription factors in mammalian cells and transgenic mice. Proc. Natl. Acad. Sci. U. S. A 100:7480-7485.

De Vries, M. and H. M. Cooper. 2008. Emerging roles for neogenin and its ligands in CNS development. J. Neurochem. 106:1483-1492.

Dusek, R. L., S. Getsios, F. Chen, J. K. Park, E. V. Amargo, V. L. Cryns, and K. J. Green. 2006. The differentiation-dependent desmosomal cadherin desmoglein 1 is a novel caspase-3 target that regulates apoptosis in keratinocytes. J. Biol. Chem. 281:3614-3624.

Endo, M. and T. Yamashita. 2009. Inactivation of Ras by p120GAP via focal adhesion kinase dephosphorylation mediates RGMa-induced growth cone collapse. J. Neurosci. 29:6649-6662.

Fearon, E. R., K. R. Cho, J. M. Nigro, S. E. Kern, J. W. Simons, J. M. Ruppert, S. R. Hamilton, A. C. Preisinger, G. Thomas, K. W. Kinzler, *et al.* 1990. Identification of a chromosome 18q gene that is altered in colorectal cancers. Science 247:49-56.

Fitzgerald, D. P., S. J. Cole, A. Hammond, C. Seaman, and H. M. Cooper. 2006. Characterization of neogenin-expressing neural progenitor populations and migrating neuroblasts in the embryonic mouse forebrain. Neuroscience 142:703-716.

Fujita, Y., J. Taniguchi, M. Uchikawa, M. Endo, K. Hata, T. Kubo, B. K. Mueller, and T. Yamashita. 2008. Neogenin regulates neuronal survival through DAP kinase. Cell Death. Differ. 15:1593-1608.

Geisbrecht, B. V., K. A. Dowd, R. W. Barfield, P. A. Longo, and D. J. Leahy. 2003. Netrin binds discrete subdomains of DCC and UNC5 and mediates interactions between DCC and heparin. J. Biol. Chem. 278:32561-32568.

Goldschneider, D., N. Rama, C. Guix, and P. Mehlen. 2008. The neogenin intracellular domain regulates gene transcription via nuclear translocation. Mol. Cell Biol. 28:4068-4079.

Gotzmann, J., S. Vlcek, and R. Foisner. 2000. Caspase-mediated cleavage of the chromosome-binding domain of lamina-associated polypeptide 2 alpha. J. Cell Sci. 113 Pt 21:3769-3780.

Grewal, T., R. Evans, C. Rentero, F. Tebar, L. Cubells, D. de, I, M. F. Kirchhoff, W. E. Hughes, J. Heeren, K. A. Rye, F. Rinninger, R. J. Daly, A. Pol, and C. Enrich. 2005. Annexin A6 stimulates the membrane recruitment of p120GAP to modulate Ras and Raf-1 activity. Oncogene 24:5809-5820.

Guirland, C., S. Suzuki, M. Kojima, B. Lu, and J. Q. Zheng. 2004. Lipid rafts mediate chemotropic guidance of nerve growth cones. Neuron 42:51-62.

Guo, D., C. Holmlund, R. Henriksson, and H. Hedman. 2004. The LRIG gene family has three vertebrate paralogs widely expressed in human and mouse tissues and a homolog in Ascidiacea. Genomics 84:157-165.

Gur, G., C. Rubin, M. Katz, I. Amit, A. Citri, J. Nilsson, N. Amariglio, R. Henriksson, G. Rechavi, H. Hedman, R. Wides, and Y. Yarden. 2004. LRIG1 restricts growth factor signaling by enhancing receptor ubiquitylation and degradation. EMBO J. 23:3270-3281.

Hartwig, J. H. and T. P. Stossel. 1975. Isolation and properties of actin, myosin, and a new actinbinding protein in rabbit alveolar macrophages. J. Biol. Chem. 250:5696-5705.

Hata, K., M. Fujitani, Y. Yasuda, H. Doya, T. Saito, S. Yamagishi, B. K. Mueller, and T. Yamashita. 2006. RGMa inhibition promotes axonal growth and recovery after spinal cord injury. J. Cell Biol. 173:47-58.

Hata, K., K. Kaibuchi, S. Inagaki, and T. Yamashita. 2009. Unc5B associates with LARG to mediate the action of repulsive guidance molecule. J. Cell Biol. 184:737-750.

Hedman, H. and R. Henriksson. 2007. LRIG inhibitors of growth factor signalling - double-edged swords in human cancer? Eur. J. Cancer 43:676-682.

Hedrick, L., K. R. Cho, E. R. Fearon, T. C. Wu, K. W. Kinzler, and B. Vogelstein. 1994. The DCC gene product in cellular differentiation and colorectal tumorigenesis. Genes Dev. 8:1174-1183.

Herincs, Z., V. Corset, N. Cahuzac, C. Furne, V. Castellani, A. O. Hueber, and P. Mehlen. 2005. DCC association with lipid rafts is required for netrin-1-mediated axon guidance. J. Cell Sci. 118:1687-1692.

Holmlund, C., J. Nilsson, D. Guo, A. Starefeldt, I. Golovleva, R. Henriksson, and H. Hedman. 2004. Characterization and tissue-specific expression of human LRIG2. Gene 332:35-43.

Homma, S., T. Shimada, T. Hikake, and H. Yaginuma. 2009. Expression pattern of LRR and Ig domain-containing protein (LRRIG protein) in the early mouse embryo. Gene Expr. Patterns. 9:1-26.

Inoue, H., L. Lin, X. Lee, Z. Shao, S. Mendes, P. Snodgrass-Belt, H. Sweigard, T. Engber, B. Pepinsky, L. Yang, M. F. Beal, S. Mi, and O. Isacson. 2007. Inhibition of the leucine-rich repeat protein LINGO-1 enhances survival, structure, and function of dopaminergic neurons in Parkinson's disease models. Proc. Natl. Acad. Sci. U. S. A 104:14430-14435.

Jackson, R. S., Y. J. Cho, S. Stein, and P. Liang. 2007. CYFIP2, a direct p53 target, is leptomycin-B sensitive. Cell Cycle 6:95-103.

Kang, J. S., M. J. Yi, W. Zhang, J. L. Feinleib, F. Cole, and R. S. Krauss. 2004. Netrins and neogenin promote myotube formation. J. Cell Biol. 167:493-504.

Keino-Masu, K., M. Masu, L. Hinck, E. D. Leonardo, S. S. Chan, J. G. Culotti, and M. Tessier-Lavigne. 1996. Deleted in Colorectal Cancer (DCC) encodes a netrin receptor. Cell 87:175-185.

Kim, S. W., J. I. Park, C. M. Spring, A. K. Sater, H. Ji, A. A. Otchere, J. M. Daniel, and P. D. McCrea. 2004. Non-canonical Wnt signals are modulated by the Kaiso transcriptional repressor and p120-catenin. Nat. Cell Biol. 6:1212-1220.

Kobayashi, K., S. Kuroda, M. Fukata, T. Nakamura, T. Nagase, N. Nomura, Y. Matsuura, N. Yoshida-Kubomura, A. Iwamatsu, and K. Kaibuchi. 1998. p140Sra-1 (specifically Rac1-associated protein) is a novel specific target for Rac1 small GTPase. J. Biol. Chem. 273:291-295.

Krutzfeldt, M., M. Ellis, D. B. Weekes, J. J. Bull, M. Eilers, M. D. Vivanco, W. R. Sellers, and S. Mittnacht. 2005. Selective ablation of retinoblastoma protein function by the RET finger protein. Mol. Cell 18:213-224.

Kubo, T., M. Endo, K. Hata, J. Taniguchi, K. Kitajo, S. Tomura, A. Yamaguchi, B. K. Mueller, and T. Yamashita. 2008. Myosin IIA is required for neurite outgrowth inhibition produced by repulsive guidance molecule. J. Neurochem. 105:113-126.

Laederich, M. B., M. Funes-Duran, L. Yen, E. Ingalla, X. Wu, K. L. Carraway, III, and C. Sweeney. 2004. The leucine-rich repeat protein LRIG1 is a negative regulator of ErbB family receptor tyrosine kinases. J. Biol. Chem. 279:47050-47056.

Lah, G. J. and B. Key. 2012. Dual roles of the chemorepellent axon guidance molecule RGMa in establishing pioneering axon tracts and neural fate decisions in embryonic vertebrate forebrain. Dev Neurobiol 72:1458-1470.

Laitinen, O. H., V. P. Hytonen, H. R. Nordlund, and M. S. Kulomaa. 2006. Genetically engineered avidins and streptavidins. Cell Mol. Life Sci. 63:2992-3017.

Lansbergen, G., I. Grigoriev, Y. Mimori-Kiyosue, T. Ohtsuka, S. Higa, I. Kitajima, J. Demmers, N. Galjart, A. B. Houtsmuller, F. Grosveld, and A. Akhmanova. 2006. CLASPs attach microtubule plus ends to the cell cortex through a complex with LL5beta. Dev. Cell 11:21-32.

Ledda, F., O. Bieraugel, S. S. Fard, M. Vilar, and G. Paratcha. 2008. Lrig1 is an endogenous inhibitor of Ret receptor tyrosine kinase activation, downstream signaling, and biological responses to GDNF. J. Neurosci. 28:39-49.

Lindstrom, A. K., A. Asplund, and D. Hellberg. 2011. Correlation between LRIG1 and LRIG2 expressions and expression of 11 tumor markers, with special reference to tumor suppressors, in CIN and normal cervical epithelium. Gynecol. Oncol. 122:372-376.

Liu, Y., Y. Peng, P. G. Dai, Q. S. Du, L. Mei, and W. C. Xiong. 2012. Differential regulation of myosin X movements by its cargos, DCC and neogenin. J. Cell Sci. 125:751-762.

Maisse, C., A. Rossin, N. Cahuzac, A. Paradisi, C. Klein, M. L. Haillot, Z. Herincs, P. Mehlen, and A. O. Hueber. 2008. Lipid raft localization and palmitoylation: identification of two requirements for cell death induction by the tumor suppressors UNC5H. Exp. Cell Res. 314:2544-2552.

Matsunaga, E., H. Nakamura, and A. Chedotal. 2006. Repulsive guidance molecule plays multiple roles in neuronal differentiation and axon guidance. J. Neurosci. 26:6082-6088.

Matsunaga, E., S. Tauszig-Delamasure, P. P. Monnier, B. K. Mueller, S. M. Strittmatter, P. Mehlen, and A. Chedotal. 2004. RGM and its receptor neogenin regulate neuronal survival. Nat. Cell Biol. 6:749-755.

Mawdsley, D. J., H. M. Cooper, B. M. Hogan, S. H. Cody, G. J. Lieschke, and J. K. Heath. 2004. The Netrin receptor Neogenin is required for neural tube formation and somitogenesis in zebrafish. Dev. Biol. 269:302-315.

Meggio, F. and L. A. Pinna. 2003. One-thousand-and-one substrates of protein kinase CK2? FASEB J. 17:349-368.

Meijering, E., M. Jacob, J. C. Sarria, P. Steiner, H. Hirling, and M. Unser. 2004. Design and validation of a tool for neurite tracing and analysis in fluorescence microscopy images. Cytometry A 58:167-176.

Metzger, M., S. Conrad, T. Skutella, and L. Just. 2007. RGMa inhibits neurite outgrowth of neuronal progenitors from murine enteric nervous system via the neogenin receptor *in vitro*. J. Neurochem. 103:2665-2678.

Meyerhardt, J. A., A. T. Look, S. H. Bigner, and E. R. Fearon. 1997. Identification and characterization of neogenin, a DCC-related gene. Oncogene 14:1129-1136.

Miller, J. K., D. L. Shattuck, E. Q. Ingalla, L. Yen, A. D. Borowsky, L. J. Young, R. D. Cardiff, K. L. Carraway, III, and C. Sweeney. 2008. Suppression of the negative regulator LRIG1 contributes to ErbB2 overexpression in breast cancer. Cancer Res. 68:8286-8294.

Monastyrskaya, K., E. B. Babiychuk, A. Hostettler, P. Wood, T. Grewal, and A. Draeger. 2009. Plasma membrane-associated annexin A6 reduces $Ca2^{+}$ entry by stabilizing the cortical actin cytoskeleton. J. Biol. Chem. 284:17227-17242.

Mongroo, P. S., F. K. Noubissi, M. Cuatrecasas, J. Kalabis, C. E. King, C. N. Johnstone, M. J. Bowser, A. Castells, V. S. Spiegelman, and A. K. Rustgi. 2011. IMP-1 displays cross-talk with K-Ras and modulates colon cancer cell survival through the novel proapoptotic protein CYFIP2. Cancer Res. 71:2172-2182.

Monnier, P. P., A. Sierra, P. Macchi, L. Deitinghoff, J. S. Andersen, M. Mann, M. Flad, M. R. Hornberger, B. Stahl, F. Bonhoeffer, and B. K. Mueller. 2002. RGM is a repulsive guidance molecule for retinal axons. Nature 419:392-395.

Nakamura, F., T. P. Stossel, and J. H. Hartwig. 2011. The filamins: organizers of cell structure and function. Cell Adh. Migr. 5:160-169.

Nakashima, T., T. Sekiguchi, A. Kuraoka, K. Fukushima, Y. Shibata, S. Komiyama, and T. Nishimoto. 1993. Molecular cloning of a human cDNA encoding a novel protein, DAD1, whose defect causes apoptotic cell death in hamster BHK21 cells. Mol. Cell Biol. 13:6367-6374.

O'Donnell, M., R. K. Chance, and G. J. Bashaw. 2009. Axon growth and guidance: receptor regulation and signal transduction. Annu. Rev. Neurosci. 32:383-412.

Ohta, Y., N. Suzuki, S. Nakamura, J. H. Hartwig, and T. P. Stossel. 1999. The small GTPase RalA targets filamin to induce filopodia. Proc. Natl. Acad. Sci. U. S. A 96:2122-2128.

Park, K. W., D. Crouse, M. Lee, S. K. Karnik, L. K. Sorensen, K. J. Murphy, C. J. Kuo, and D. Y. Li. 2004. The axonal attractant Netrin-1 is an angiogenic factor. Proc. Natl. Acad. Sci. U. S. A 101:16210-16215.

Pasterkamp RJ, De Winter F, Holtmaat AJ, Verhaagen J (1998) Evidence for a role of the chemorepellent semaphorin III and its receptor neuropilin-1 in the regeneration of primary olfactory axons. J Neurosci 18: 9962-9976.

Pathi, S., J. B. Rutenberg, R. L. Johnson, and A. Vortkamp. 1999. Interaction of Ihh and BMP/Noggin signaling during cartilage differentiation. Dev. Biol. 209:239-253.

Prokhortchouk, A., B. Hendrich, H. Jorgensen, A. Ruzov, M. Wilm, G. Georgiev, A. Bird, and E. Prokhortchouk. 2001. The p120 catenin partner Kaiso is a DNA methylation-dependent transcriptional repressor. Genes Dev. 15:1613-1618.

Rajagopalan, S., L. Deitinghoff, D. Davis, S. Conrad, T. Skutella, A. Chedotal, B. K. Mueller, and S. M. Strittmatter. 2004. Neogenin mediates the action of repulsive guidance molecule. Nat. Cell Biol. 6:756-762.

Raynaud, F. and A. Marcilhac. 2006. Implication of calpain in neuronal apoptosis. A possible regulation of Alzheimer's disease. FEBS J. 273:3437-3443.

Reed, S. E., E. M. Staley, J. P. Mayginnes, D. J. Pintel, and G. E. Tullis. 2006. Transfection of mammalian cells using linear polyethylenimine is a simple and effective means of producing recombinant adeno-associated virus vectors. J. Virol. Methods 138:85-98.

Ren, X. R., G. L. Ming, Y. Xie, Y. Hong, D. M. Sun, Z. Q. Zhao, Z. Feng, Q. Wang, S. Shim, Z. F. Chen, H. J. Song, L. Mei, and W. C. Xiong. 2004. Focal adhesion kinase in netrin-1 signaling. Nat. Neurosci. 7:1204-1212.

Samad, T. A., A. Rebbapragada, E. Bell, Y. Zhang, Y. Sidis, S. J. Jeong, J. A. Campagna, S. Perusini, D. A. Fabrizio, A. L. Schneyer, H. Y. Lin, A. H. Brivanlou, L. Attisano, and C. J. Woolf. 2005. DRAGON, a bone morphogenetic protein co-receptor. J. Biol. Chem. 280:14122-14129.

Schaffar, G., J. Taniguchi, T. Brodbeck, A. H. Meyer, M. Schmidt, T. Yamashita, and B. K. Mueller. 2008. LIM-only protein 4 interacts directly with the repulsive guidance molecule A receptor Neogenin. J. Neurochem. 107:418-431.

Schenck, A., B. Bardoni, C. Langmann, N. Harden, J. L. Mandel, and A. Giangrande. 2003. CYFIP/Sra-1 controls neuronal connectivity in *Drosophila* and links the Rac1 GTPase pathway to the fragile X protein. Neuron 38:887-898.

Schenck, A., B. Bardoni, A. Moro, C. Bagni, and J. L. Mandel. 2001. A highly conserved protein family interacting with the fragile X mental retardation protein (FMRP) and displaying selective interactions with FMRP-related proteins FXR1P and FXR2P. Proc. Natl. Acad. Sci. U. S. A 98:8844-8849.

Shattuck, D. L., J. K. Miller, M. Laederich, M. Funes, H. Petersen, K. L. Carraway, III, and C. Sweeney. 2007. LRIG1 is a novel negative regulator of the Met receptor and opposes Met and Her2 synergy. Mol. Cell Biol. 27:1934-1946.

Sheu, J. J., C. H. Lee, J. Y. Ko, G. S. Tsao, C. C. Wu, C. Y. Fang, F. J. Tsai, C. H. Hua, C. L. Chen, and J. Y. Chen. 2009. Chromosome 3p12.3-p14.2 and 3q26.2-q26.32 are genomic markers for prognosis of advanced nasopharyngeal carcinoma. Cancer Epidemiol. Biomarkers Prev. 18:2709-2716.

Soubry, A., H. J. van, E. Parthoens, C. Colpaert, M. E. Van, D. Waltregny, A. B. Reynolds, and R. F. van. 2005. Expression and nuclear location of the transcriptional repressor Kaiso is regulated by the tumor microenvironment. Cancer Res. 65:2224-2233.

Squier, M. K., A. C. Miller, A. M. Malkinson, and J. J. Cohen. 1994. Calpain activation in apoptosis. J. Cell Physiol 159:229-237.

Srinivasan, K., P. Strickland, A. Valdes, G. C. Shin, and L. Hinck. 2003. Netrin-1/neogenin interaction stabilizes multipotent progenitor cap cells during mammary gland morphogenesis. Dev. Cell 4:371-382.

Sugimoto, A., R. R. Hozak, T. Nakashima, T. Nishimoto, and J. H. Rothman. 1995. dad-1, an endogenous programmed cell death suppressor in Caenorhabditis elegans and vertebrates. EMBO J. 14:4434-4441.

Sumimoto, H., Y. Ohkuma, T. Yamamoto, M. Horikoshi, and R. G. Roeder. 1990. Factors involved in specific transcription by mammalian RNA polymerase II: identification of general transcription factor TFIIG. Proc. Natl. Acad. Sci. U. S. A 87:9158-9162.

Teuling, E., S. Ahmed, E. Haasdijk, J. Demmers, M. O. Steinmetz, A. Akhmanova, D. Jaarsma, and C. C. Hoogenraad. 2007. Motor neuron disease-associated mutant vesicle-associated membrane protein-associated protein (VAP) B recruits wild-type VAPs into endoplasmic reticulum-derived tubular aggregates. J. Neurosci. 27:9801-9815.

Thomasson, M., H. Hedman, D. Guo, B. Ljungberg, and R. Henriksson. 2003. LRIG1 and epidermal growth factor receptor in renal cell carcinoma: a quantitative RT--PCR and immunohistochemical analysis. Br. J. Cancer 89:1285-1289.

Vielmetter, J., J. F. Kayyem, J. M. Roman, and W. J. Dreyer. 1994. Neogenin, an avian cell surface protein expressed during terminal neuronal differentiation, is closely related to the human tumor suppressor molecule deleted in colorectal cancer. J. Cell Biol. 127:2009-2020.

Wilson, N. H. and B. Key. 2006. Neogenin interacts with RGMa and netrin-1 to guide axons within the embryonic vertebrate forebrain. Dev. Biol. 296:485-498.

Yamashita, T., B. K. Mueller, and K. Hata. 2007. Neogenin and repulsive guidance molecule signaling in the central nervous system. Curr. Opin. Neurobiol. 17:29-34.

Yang, F., A. P. West, Jr., G. P. Allendorph, S. Choe, and P. J. Bjorkman. 2008. Neogenin interacts with hemojuvelin through its two membrane-proximal fibronectin type III domains. Biochemistry 47:4237-4245.

Yoon, B. S. and K. M. Lyons. 2004. Multiple functions of BMPs in chondrogenesis. J. Cell Biochem. 93:93-103.

Zhang, A. S., A. P. West, Jr., A. E. Wyman, P. J. Bjorkman, and C. A. Enns. 2005. Interaction of hemojuvelin with neogenin results in iron accumulation in human embryonic kidney 293 cells. J. Biol. Chem. 280:33885-33894.

Zhao, H., K. Tanegashima, H. Ro, and I. B. Dawid. 2008. Lrig3 regulates neural crest formation in *Xenopus* by modulating Fgf and Wnt signaling pathways. Development 135:1283-1293.

Zhou, Z., J. Xie, D. Lee, Y. Liu, J. Jung, L. Zhou, S. Xiong, L. Mei, and W. C. Xiong. 2010. Neogenin regulation of BMP-induced canonical Smad signaling and endochondral bone formation. Dev. Cell 19:90-102.

Zhu, X. J., C. Z. Wang, P. G. Dai, Y. Xie, N. N. Song, Y. Liu, Q. S. Du, L. Mei, Y. Q. Ding, and W. C. Xiong. 2007. Myosin X regulates netrin receptors and functions in axonal path-finding. Nat. Cell Biol. 9:184-192.

SUPPLEMENTARY INFORMATION

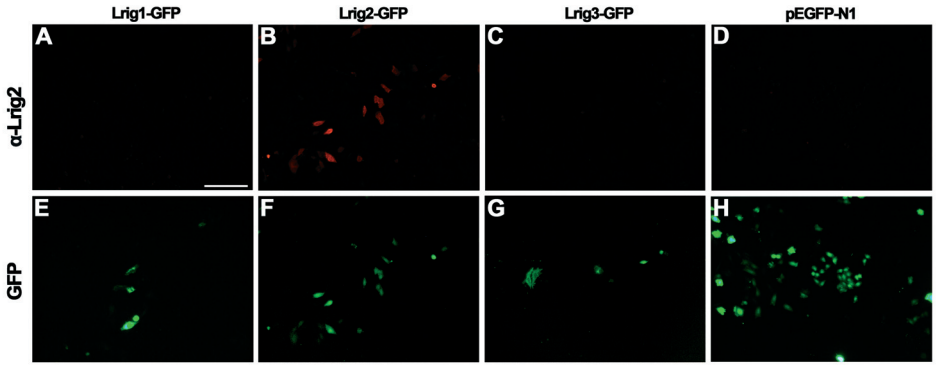

FIGURE S1. Anti-Lrig2 antibody specifically stains COS-7 cells overexpressing Lrig2.

(A-D) Anti-Lrig2 immunostaining of COS-7 cells overexpressing Lrig1-GFP (A), Lrig2-GFP (B), Lrig3-GFP (C) or pEGFP-N1 (D). (E-H) GFP fluorescence revealed expression of Lrig1-GFP (E), Lrig2-GFP (F), Lrig3-GFP (G) and pEGFP-N1 (H). Scale bar A-H: 300 µm.

CHAPTER 5

In vivo proteomics screen using a synapsin I-driven *GFP-Neogenin* transgenic mouse identifies novel Neogenin-interacting proteins

DIANNE M.A. VAN DEN HEUVEL[1],
ANITA J.C.G.M. HELLEMONS[1],
JEROEN DEMMERS[2] AND
R. JEROEN PASTERKAMP[1]

[1] Department of Neuroscience and Pharmacology, Rudolf Magnus Institute of Neuroscience, University Medical Center Utrecht, Universiteitsweg 100, 3584 CG, Utrecht, The Netherlands

[2] Proteomics Center, Erasmus University Medical Center, Dr. Molewaterplein 50, 3015 GE, Rotterdam, The Netherlands

ABSTRACT

Neogenin signaling has been implicated in key neurodevelopmental processes, including neurogenesis, neuronal differentiation, migration, axon guidance and apoptosis. During neuronal network formation activation of the Neogenin receptor by repulsive guidance molecule A (RGMa) induces growth cone collapse and axon repulsion. RGMa signaling through Neogenin and the coreceptor Unc5B activates RhoA signaling and inhibits Ras signaling. However, our understanding of additional components of the Neogenin signaling cascade in neurons is rather incomplete. To further our understanding of Neogenin signaling, we generated *Syn-GFP-Neogenin* transgenic mice that express a GFP-Neogenin fusion protein under the control of the neuron-specific synapsin I (Syn) promoter. In the transgenic line, a broad but specific GFP-Neogenin expression pattern was detected in neurons and axon projections during brain development. GFP-Neogenin expression was particularly strong at late embryonic and early postnatal stages. An anti-GFP *in vivo* Neogenin pull down on brain lysates of perinatal *Syn-GFP-Neogenin* mice, followed by mass spectrometry analysis, identified several putative Neogenin-interacting proteins with known functions in the regulation of cytoskeletal dynamics, neuronal process formation, migration, apoptosis and transcription regulation. These novel interactors are a valuable starting point for future studies on the role and mechanisms of Neogenin signaling during neural development.

INTRODUCTION

Neogenin is a close homolog of deleted in colorectal cancer (DCC) and belongs to the immunoglobulin (Ig) superfamily of cell surface receptors, containing four Ig-like domains and six fibronectin type III (FNIII) repeats in its extracellular domain (Fearon *et al.* 1990, Hedrick *et al.* 1994, Vielmetter *et al.* 1994). Both RGM and Netrin ligands interact with Neogenin by binding to the FNIII repeat-containing domain (Geisbrecht *et al.* 2003, Rajagopalan *et al.* 2004, Yang *et al.* 2008). The role and mechanism of RGMa-Neogenin signaling is best characterized and both RGMa and Neogenin are broadly expressed in the developing mouse brain (Bradford *et al.* 2010, Gad *et al.* 1997, Oldekamp *et al.* 2004, Schmidtmer and Engelkamp 2004).

During neuronal network formation, binding of RGMa to Neogenin induces growth cone collapse and neurite growth inhibition of cortical, cerebellar granule and dorsal root ganglia neurons (Brinks *et al.* 2004, Conrad *et al.* 2007, Endo and Yamashita 2009, Hata *et al.* 2006, Hata *et al.* 2009). Axons from neurons in the entorhinal cortex express Neogenin and are targeted to the outer molecular layer of the dentate gyrus by RGMa expressed in the inner molecular layer. Blocking of RGMa results in severe mistargeting of these entorhinal cortical projections in hippocampal slice cultures (Brinks *et al.* 2004). In the rat spinal cord, lesion-induced expression

of RGMa severely blocks regeneration of spinal cord connectivity, which is greatly improved upon local administration of function-blocking RGMa antibodies (Hata *et al.* 2006).

The inhibitory effect of RGMa-Neogenin interactions on neurite growth is mediated by activation of RhoA and inactivation of Ras signaling pathways (Conrad *et al.* 2007, Endo and Yamashita 2009, Hata *et al.* 2006). Unc5B is an essential coreceptor for repulsive RGMa-Neogenin signaling and mediates activation of RhoA GTPase through its association with leukemia-associated Rho guanine-nucleotide exchange factor (LARG) (Hata *et al.* 2009). In addition, activation of Neogenin by RGMa induces the release of the Ras-specific GTPase-activating protein p120GAP from the Neogenin receptor complex, thereby mediating the inactivation of Ras (Endo and Yamashita 2009).

In addition to their role in axon guidance, RGMa and Neogenin affect apoptosis signaling in different systems (Koeberle *et al.* 2010, Lah and Key 2012, Matsunaga *et al.* 2004, Shin and Wilson 2008). Neogenin belongs, together with DCC and Unc5 molecules, to the family of dependence receptors that induce apoptosis signaling in the absence of ligand (Bredesen *et al.* 2005, Goldschneider and Mehlen 2010, Llambi *et al.* 2001, Matsunaga *et al.* 2004, Mehlen and Fearon 2004). Activation of apoptosis signaling in the absence of RGMa involves death-associated protein (DAP) kinase and Neogenin cleavage by caspase-3 (Fujita *et al.* 2008, Matsunaga *et al.* 2004). In addition, the Neogenin receptor can be processed by secretase enzymes. γ-Secretase cleavage of Neogenin releases the Neogenin intracellular domain (NeoICD), which is able to translocate to the nucleus and induce gene transcription (Goldschneider *et al.* 2008).

Despite the identification of several Neogenin signaling proteins over the past few years, our understanding of the proteins that comprise the Neogenin signaling cascade is far from complete. To further our understanding of the role and mechanism of Neogenin signaling in the developing nervous system, we used an *in vivo* proteomics approach to purify Neogenin signaling complexes from brain tissue. We generated *Syn-GFP-Neogenin* mice in which neuron-specific expression of GFP-tagged Neogenin protein is induced by the synapsin I promoter. An anti-GFP *in vivo* Neogenin pull down on brain lysates of perinatal *Syn-GFP-Neogenin* transgenic mice, followed by mass spectrometry analysis, identified numerous putative Neogenin-interacting proteins. Many of these interacting proteins have known functions in cytoskeletal remodeling, apoptosis, neuronal migration, transcription regulation and axon guidance. The novel Neogenin-interacting proteins are interesting candidates for future studies on Neogenin signaling mechanisms.

MATERIALS AND METHODS

PLASMID CONSTRUCTION

For the construction of the pcDNA3.1-Syn-GFP-Neogenin vector the Neogenin coding sequence without signal peptide (aa 46-1492) was PCR-amplified from wild-type mouse Neogenin (pCMVXL-6-Neogenin; a kind gift of Denise Davis). This fragment was cloned into the blunt-made MluI/NotI sites of the PCI-Syn-GlyS267Q plasmid, containing the rat synapsin I promoter (a kind gift of Manfred Kiliman (Hoesche *et al.* 1993)). The Syn-Neogenin fragment was released from the PCI vector backbone by ClaI restriction and ligated into the EcoRV site of pcDNA3.1 (pcDNA3.1(-)/myc-his; Invitrogen). A signal peptide, GFP and 3xFLAG tag were PCR-amplified from the pRK5-DR/GABA(A)a1 vector (a kind gift of Guus Smit) and ligated N-terminal of the Neogenin coding sequence into the newly generated restriction sites AgeI and PshAI. For construction of the pcDNA3.1-CMV-GFP-Neogenin vector, the GFP-Neogenin fragment was isolated from the pcDNA3.1-Syn-GFP-Neogenin vector using ClaI and PshA restriction. The restriction sites were made blunt-ended and the GFP-Neogenin fragment was ligated into the EcoRV site of pcDNA3.1 (pcDNA3.1(-)/myc-his; Invitrogen).

GENERATION OF *SYN-GFP-NEOGENIN* MICE

Syn-GFP-Neogenin mice were generated by pronuclear injections executed in the Central Laboratory Animal Facility (GDL, Utrecht University). Before injection, a 10.1 Kb DNA fragment containing the Syn-GFP-Neogenin cassette was PmeI-cut from the pcDNA3.1-Syn-GFP-Neogenin vector and isolated by agarose gel electrophoresis and electro-elution, followed by phenol-chloroform extraction and ethanol precipitation. DNA was injected into male pronuclei of fertilized eggs isolated from superovulated B6CBAF1/Jico mice (Charles River). Superovulation was induced by intraperitoneal injection of 5IU pregnant mare's serum gonadotrophin (PMSG; Folligonan), followed by injection of 5IU human chorionic gonadotrophin (hCG; Chorulon) 42-48 hours later. Superovulated females were immediately mated with appropriate stud males. Microinjections were performed with a Narishige IM-300 microinjector. After injection of DNA into the pronucleus, embryos were cultured overnight in M2 medium (Sigma-Aldrich) in a humidified atmosphere with 5% CO_2 at 37°C. The next day, 2-cell stage embryos were implanted into Crl:CD-1(ICR) (Charles River) foster mothers. 15-20 Embryos were transferred into one oviduct of each recipient mouse. Transgenic founders were selected by PCR genotyping, using the following primers; FW, 5'-TTAGACCTTGGTCCCACCATGTTCAAGATCCTGCTG-3'; and RV, 5'-TCGACCGGTCTTGTCATCGTCATCCTTGTAATCGATATC-3', and backcrossed with C57BL/6 (Charles River) females to generate stable transgenic mouse lines.

ANIMAL AND TISSUE TREATMENT

All animal use and care were in accordance with institutional guidelines. C57BL/6 mice were obtained from Charles River. Pups and (timed-pregnant) adult mice were killed by means of

decapitation or cervical dislocation, respectively. The morning on which a vaginal plug was detected was considered embryonic day 0.5 (E0.5) and the day of birth, postnatal day 0 (P0). For immunohistochemistry, E14.5, E18.5 and P0 heads were collected in phosphate-buffered saline (PBS; pH 7.4) and fixed by immersion for 3-6 hours (hrs) in 4% paraformaldehyde (PFA) in PBS at 4°C. P10, P20 and adult mice were transcardially perfused with saline followed by 4% PFA. Brains were dissected and postfixed overnight at 4°C, washed in PBS, cryoprotected in 30% sucrose at 4°C and frozen in 2-methylbutane (Merck). Sections (16 µm) were cut on a cryostat, mounted on Superfrost Plus slides (Fisher Scientific), air-dried and stored desiccated at -20°C for immunohistochemistry.

CELL CULTURE AND TRANSFECTION

COS-7, HEK293 and SH-SY5Y neuroblastoma cells were maintained in high glucose Dulbecco's modified Eagle's medium (DMEM; Gibco, Invitrogen) supplemented with 10% (v/v) heat-inactivated fetal bovine serum (FBS; Lonza, BioWhittaker), 2 mM L-glutamine (PAA) and 1x penicillin/streptomycin (pen/strep; PAA), in a humidified atmosphere with 5% CO_2 at 37°C. COS-7 cells and HEK293 cells were transfected using polyethylenimine (PEI; Polysciences) (Reed *et al.* 2006). Lipofectamine 2000 (Invitrogen) was used for transfection of SH-SY5Y cells.

AP-PROTEIN PRODUCTION

For alkaline phosphatase (AP), RGMa-AP and Netrin-1-AP protein production, HEK293 cells were transfected with AP-Fc (a kind gift of Roman Giger), RGMa-AP (APtag5-RGMa-AP; a kind gift of Thomas Skutella), or Netrin-1-AP (pcDNA3.1-Netrin-1-AP; a kind gift of Kun-Liang Guan). Transfected HEK293 cells were cultured in Opti-MEM reduced serum medium (Gibco, Invitrogen) supplemented with 3% (v/v) FBS (Lonza, BioWhittaker), 2 mM L-glutamine (PAA) and 1x pen/strep (PAA). Cell culture medium was collected after 5 days in culture, filter-sterilized and stored at 4°C. If required, culture medium containing AP-tagged proteins was concentrated using Centriprep YM-50 centrifugal filter units (Millipore).

IN SITU HYBRIDIZATION

Nonradioactive *in situ* hybridization was performed according to (Pasterkamp *et al.* 1998), with minor modification. In brief, the probe sequence for Neogenin (NM_008684.2: 2087-2587) was polymerase chain reaction (PCR)-amplified from cDNA, using sense primer 5'-ACACCGTTATCTGGCAATGG-3' and antisense primer 5'-TTCAGCAGACAGCCAATCAG-3'. Digoxigenin (DIG)-labeled RNA probes were generated by a RNA polymerase reaction using 10x DIG RNA labeling mix (ENZO). Tissue sections were post-fixed with 4% PFA in PBS (pH 7.4) for 20 minutes (min) at room temperature (RT). To enhance tissue penetration and decrease aspecific background staining, sections were acetylated with 0.25% acetic anhydride in 0.1 M triethanolamine and 0.06% HCl for 10 min at RT. Sections were prehybridized for 2 hrs at RT in hybridization buffer (50% formamide, 5x Denhardt's solution, 5x SSC, 250 µg/ml baker's

yeast tRNA and 500 µg/ml sonicated salmon sperm DNA). Hybridization was performed for 15 hrs at 68°C, using 400 ng/ml denatured DIG-labeled probe diluted in hybridization buffer. After hybridization, sections were first washed briefly in 2x SSC followed by incubation in 0.2x SCC for 2 hrs at 68°C. Sections were adjusted to RT in 0.2x SSC for 5 min. DIG-labeled RNA hybrids were detected with anti-DIG Fab fragments conjugated to AP (Boehringer) diluted in 1:2500 in Tris-buffered saline (TBS; pH 7.4) overnight at 4°C. Binding of AP-labeled antibody was visualized by incubating the sections in detection buffer (100 mM Tris-HCl, pH 9.5, 100 mM NaCl and 50 mM $MgCl_2$) containing 240 µg/ml levamisole and nitroblue tetrazolium chloride/5-bromo-4-chloro-3-indolyl-phosphatase (NBT/BCIP, Roche) for 14 hrs at RT. Sections subjected to the entire *in situ* hybridization procedure, but with no probe or sense probe added, did not exhibit specific hybridization signals. Staining was visualized using a Zeiss Axioskop 2 microscope.

IMMUNOCYTOCHEMISTRY

Cells were fixed with 4% PFA for 15 min at RT and washed in PBS (pH 7.4). COS-7 cells were permeabilized and blocked in normal blocking buffer (PBS, 4% bovine serum albumin (BSA) and 0.1% Triton) for 1 hr at RT. COS-7 cells were incubated with rabbit anti-Neogenin (H-175; Santa Cruz) 1:100, rabbit anti-GFP (A11122; Invitrogen) 1:2000 and mouse anti-FLAG (Stratagene) 1:1000 for 2 hrs at RT. Cells were washed in PBS and incubated with the appropriate Alexa Fluor-labeled secondary antibodies (Invitrogen) 1:500 for 1 hr at RT.

IMMUNOHISTOCHEMISTRY

For anti-GFP DAB immunohistochemistry, sections were washed in TBS (pH 7.4), quenched in 3% H2O2 and 10% methanol in TBS for 15 min, and incubated in blocking buffer (TBS, pH 7.4, 0.1% Triton X-100 and 0.4% BSA) for 1 hr at RT. Sections were incubated with rabbit anti-GFP antibody (A11122; Invitrogen) 1:2000 in blocking buffer. The next day, sections were washed in TBS and incubated with biotin-labeled secondary antibody 1:500 in TBS containing 0.4% BSA for 1.5 hrs at RT. Sections were washed in TBS and incubated with avidin-biotin complex (ABC; Vectastain Elite ABC kit, Vector Laboratories) for 90 min. Then, sections were briefly washed in TBS and incubated with 3.3'-diaminobenzidine (DAB) solution to visualize primary antibody binding. Finally, sections were rinsed twice in 0.05 M phosphate buffer, dehydrated in ascending alcohol concentrations, cleared in xylene and embedded in Entellan (Merck). For fluorescent anti-Neogenin immunohistochemistry, sections were washed in PBS (pH 7.4) and incubated in blocking buffer (PBS, 4% BSA and 0.1% Triton) for 1 hr at RT and incubated with goat anti-Neogenin antibody (AF1079; R&D systems) 1:200 overnight in blocking buffer at 4°C. The next day, sections were washed in PBS and incubated with the appropriate Alexa Fluor-labeled secondary antibodies (Invitrogen) 1:500 for 1 hr at RT. Sections were washed in PBS, counterstained with fluorescent Nissl stain (NeuroTrace, Invitrogen) 1:500 for 15 min at

RT, washed in PBS and embedded in Mowiol (Sigma-Aldrich). Staining was visualized using a Zeiss Axioskop 2 microscope.

AP CELL BINDING

COS-7 cells were transfected with wild-type mouse Neogenin (pCMVXL-6-Neogenin), GFP-Neogenin (pcDNA3.1-CMV-GFP-Neogenin) or pcDNA3.1 (pcDNA3.1(-)/myc-his; Invitrogen). After 2 days in culture, the culture medium was replaced by HBHA buffer (20 mM HEPES, pH 7.0, 1x Hank's balanced salt solution (HBSS; GIBCO, Invitrogen) and 0.5 mg/ml BSA) for 15 min at RT. Subsequently, cells were incubated with AP-ligands for 75 min, while gently rotating at RT, followed by 2 washes in HBHA buffer. Then, cells were incubated in fixation solution (20 mM HEPES, pH 7, 60% (v/v) acetone and 3.7% formaldehyde) for 30 seconds, followed by 2 washes in HBHA. HBHA was replaced by HBS (20 mM HEPES, pH 7.0 and 150 mM NaCl) and endogenous phosphatase activity was heat-inactivated by incubation at 65°C for 90 min. Cells were equilibrated in detection buffer (100 mM Tris-HCl, pH 9.5, 100 mM NaCl and 5 mM $MgCl_2$) and bound AP-ligand was visualized by incubation in detection buffer containing levamisole and NBT/BCIP (Roche). The specificity of RGMa-AP ligand binding was determined by competition with excess RGMa protein. Furthermore, no staining was observed for AP alone.

SECTION BINDING

Sections were fixed by immersion in -20°C methanol for 6 min and rehydrated in TBS+ (TBS, pH 7.4, 4 mM $MgCl_2$ and 4 mM $CaCl_2$). Section were incubated in blocking buffer (TBS+ and 10% FBS (Lonza, BioWhittaker)) for 1 hr at and incubated with 1.5 nM AP-tagged protein-containing medium for 2 hrs at RT. After washing in TBS+, sections were incubated with fixation solution (20 mM HEPES, pH 7, 60% (v/v) acetone and 3.7% formaldehyde) for 2 min. After washing in TBS+, endogenous phosphatase activity was heat-inactivated by incubation at 65°C for 1 h. Section were equilibrated in detection buffer (100 mM Tris-HCl, pH 9.5, 100 mM NaCl and 5 mM $MgCl_2$) and bound AP-protein was visualized by incubation in detection buffer containing levamisole and NBT/BCIP (Roche). The specificity of RGMa-AP protein binding was determined by competition with excess RGMa protein. Furthermore, no staining was observed for AP alone.

WESTERN BLOTTING

HEK293 cells were collected in ice-cold PBS (pH 7.4) with a cell scraper and centrifuged in a precooled centrifuge at 1000 rpm for 5 min at 4°C. E18.5 mouse brain tissue was dissected in ice-cold PBS. Cell pellets and dissected brain tissue were resuspended in ice-cold lysis buffer (20 mM Tris-HCl, pH 8, 150 mM KCl, 1% Triton X-100 and Complete protease inhibitor cocktail (Roche)) by pipetting and incubated on ice for 10 min, followed by centrifugation at 14,000 rpm for 15 min at 4°C. The supernatant was collected, NuPAGE LDS sample buffer (Invitrogen) with 2.5% β-mercaptoethanol was added and the samples were boiled for 5 min

at 90°C. Proteins were separated on 8% SDS-PAGE gels and transferred onto nitrocellulose membrane (Hybond-C Extra; Amersham). Membranes were incubated in blocking buffer (PBS, 0.05% (v/v) Tween 20 and 5% milk powder) for 30 min at RT. Membranes were incubated with corresponding primary antibodies in blocking buffer overnight at 4°C. Antibodies used: rabbit anti-GFP antibody (ab290, Abcam, 1:6000); mouse anti-FLAG (Stratagene, 1:2000); mouse anti-α-Tubulin (T5168, Sigma-Aldrich, 1:8000); rabbit anti-Neogenin antibody (H175, SantaCruz, 1:500). Blots were incubated with SuperSignal West Dura Extended Duration Substrate and exposed to ECL films (Pierce).

IN VIVO IMMUNOPRECIPITATION

E18.5 and P0 dissected brains were lysed in 1500 µl lysis buffer (20 mM Tris-HCl, pH 7.5, 150 mM NaCl, 10% glycerol, 1% NP-40 and 200 ng/µl albumin from chick egg white (CEA; Sigma-Aldrich) and Complete protease inhibitor cocktail (Roche)) and incubated for 30 min at 4°C while rotating and centrifuged at 14,000 rpm for 30 min at 4°C. Cleared supernatants were incubated with 1 µg of rabbit anti-GFP antibody (ab290; Abcam) and incubated rotating at 4°C. After 2 hrs, 10 µl protein A Dynabeads (Invitrogen), which had been blocked in blocking buffer (20 mM Tris-HCl, pH 7.5, 150 mM NaCl, 20% glycerol and 200 ng/µl CEA (Sigma-Aldrich)), was added to each sample and the samples were incubated for 40 min rotating at 4°C. Brain lysates of either 4 *Syn-GFP-Neogenin* or 4 wild-type littermates were pooled and beads were washed 4 times in washing buffer (20 mM Tris-HCl, pH 7.5, 150 mM NaCl, 10% glycerol and 1% NP-40). Precipitated proteins were eluted by boiling in NuPAGE LDS sample buffer (Invitrogen) with 2.5% β-mercaptoethanol for 10 min at 70°C.

IN-GEL ANALYSIS

Pull down samples were separated in a NuPAGE Novex 4-12% Bis-Tris gradient gel following the manufacturer´s description (Invitrogen). For mass spectrometry analysis, proteins were visualized using GelCode Blue Stain Reagent (Pierce). Silver staining was used to detect differential protein bands. The gel was soaked twice in 50% methanol, followed by a 10 min incubation in 5% methanol. After 3 rinses in water, the gel was incubated in 10 µM dithiothreitol (DTT) for 20 min, followed by 0.1% (w/v) $AgNO_3$ for 20 min. The gel was washed once in water and twice in developer solution (3% (w/v) Na_2CO_3 and 0.02% (w/v) formaldehyde). The gel was incubated in the developer solution until protein bands appeared. The staining reaction was stopped by adding 5% (w/v) citric acid.

GEL DIGESTION AND NANOFLOW LC-MS/MS ANALYSIS

1D SDS-PAGE gel lanes were cut into 2-mm slices using an automatic gel slicer and subjected to in-gel reduction with DTT, alkylation with iodoacetamide and digestion with trypsin (Promega, sequencing grade), essentially as described previously (Wilm and Mann 1996). Nanoflow LC-MS/MS was performed on a CapLC system (Waters, Manchester, UK) coupled to

a Q-TOF Ultima mass spectrometer (Waters, Manchester, UK) operating in positive mode and equipped with a Z-spray source. Peptide mixtures were trapped on a JupiterTM C18 reversed phase column (Phenomenex; column dimensions 1.5 cm × 50 µm, packed in-house) using a linear gradient from 0 to 80% B (A = 0.1 M acetic acid; B = 80% (v/v) acetonitrile, 0.1 M acetic acid) in 70 min and at a constant flow rate of 200nl/min using a splitter. The column eluent was directly sprayed into the ESI source of the mass spectrometer. Mass spectra were acquired in continuum mode; fragmentation of the peptides was performed in data-dependent mode. Peak lists were automatically created from raw data files using the Protein Lynx Global Server software (version 2.0). The background subtraction threshold for noise reduction was set to 35% (background polynomial 5). Smoothing (Savitzky-Golay) was performed (number of interactions: 1, smoothing window: 2 channels). Deisotoping and centroiding settings were: minimum peak width: 4 channels, centroid top: 80%, TOF resolution: 5000, NP multiplier: 1. Mascot search algorithm (version 2.0, MatrixScience) was used for searching against the NCBInr database that was available on the MatrixScience server. The peptide tolerance was typically set to 150 ppm and the fragment ion tolerance was set to 0.2 Da. A maximum number of 1 missed cleavage by trypsin was allowed and carbamidomethylated cysteine and oxidized methionine were set as fixed and variable modifications, respectively.

RESULTS

CONSTRUCTION OF A GFP-NEOGENIN FUSION CDNA

Over the past few years several Neogenin-interacting proteins have been identified, using *in vitro* pull down experiments (Fujita *et al.* 2008, Hata *et al.* 2009) and yeast two-hybrid assays (Schaffar *et al.* 2008, Zhu *et al.* 2007). However, despite these advances, our understanding of the Neogenin signaling pathway in neurons remains rather rudimentary. To further our understanding of neuronal Neogenin function and signaling, we generated a transgenic mouse overexpressing a GFP-Neogenin construct. We generated a wild-type mouse Neogenin cDNA with N-terminal GFP and 3xFLAG tags, under control of a 4.3 kb rat synapsin I promoter (Hoesche *et al.* 1993) (Fig. 1A). This promoter drives neuron-specific expression (Heumann *et al.* 2000, Schoch *et al.* 1996, Thiel *et al.* 1991).

In order to verify correct expression of the GFP-Neogenin fusion protein and the binding of the Neogenin ligands RGMa and Netrin-1, we cloned the protein coding region of the GFP-Neogenin construct under direct control of the CMV promoter. Expression regulation by the CMV promoter enables expression of GFP-Neogenin in non-neuronal cell lines. Anti-GFP immunoblotting on lysate of HEK293 cells transiently expressing CMV-GFP-Neogenin, confirmed expression of GFP-Neogenin at the predicted size of 190 kDa (Fig. 1B). Fluorescence of the GFP-Neogenin fusion protein was clearly detected in fibroblast cells transfected with CMV-GFP-Neogenin, as is shown for COS-7 cells in Fig. 1C (lower panel). In these cells,

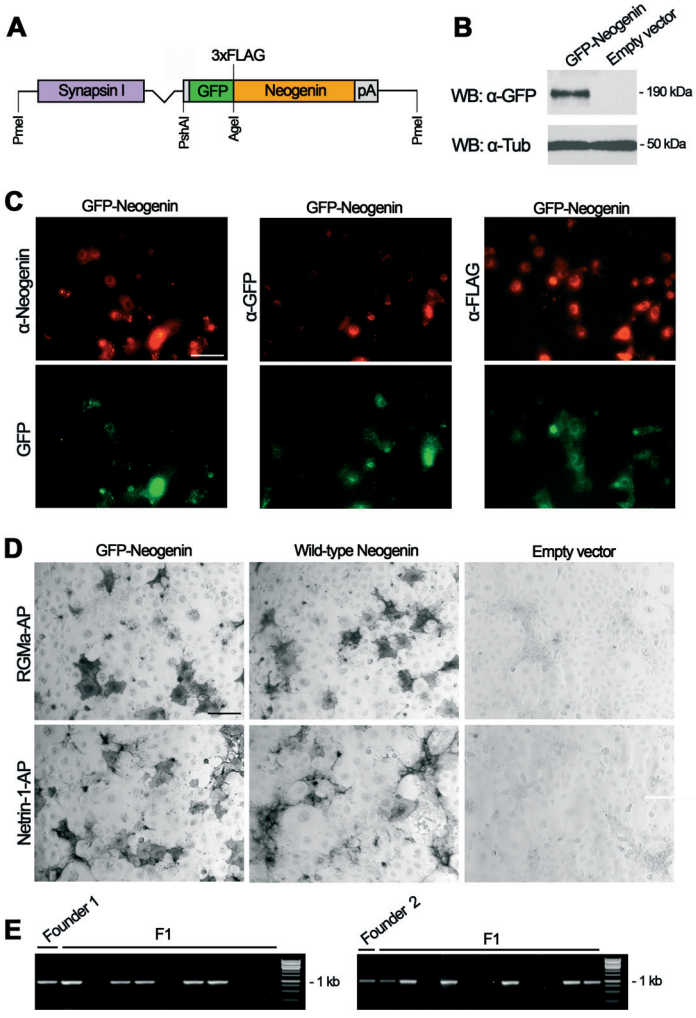

FIGURE 1. Characterization of the GFP-Neogenin fusion construct.

(A) Schematic representation of the Syn-GFP-Neogenin fusion DNA fragment containing N-terminally GFP- and 3xFLAG-tagged mouse Neogenin cDNA cloned downstream of the neuron-specific synapsin-I promoter. pA: SV40 late polyadenylation signal. (B) Anti-GFP immunoblotting shows expression of GFP-Neogenin in lysate of HEK293 cells transfected with pcDNA3.1-CMV-GFP-Neogenin. (C) GFP fluorescence (lower panel) and anti-Neogenin, anti-GFP and anti-FLAG immunostaining (upper panel) reveals GFP-Neogenin expression in COS-7 cells transfected with pcDNA3.1-CMV-GFP-Neogenin. (D) RGMa-AP and Netrin-1-AP binding to COS-7 cells transfected with pcDNA3.1-CMV-GFP-Neogenin or wild-type Neogenin (pCMVXL6-Neogenin). Empty vector (pcDNA3.1)-transfected COS-7 cells do not bind RGMa-AP or Netrin-1-AP. (E) *Syn-GFP-Neogenin* founders 1 and 2, and transgenic offspring (F1) identified by PCR. Scale bar C and D: 50 µm.

TABLE 1. GFP-Neogenin expression in different brain areas of *Syn-GFP-Neogenin* mouse line 1.

	E14.5	E18.5	P0	P10	P20
Olfactory epithelium (OE)	+++	+++	+++	+++	+/-
Olfactory bulb (OB)	+	+	+	+/-	+/-
Anterior commissure (AC)	+	+	+	+/-	-
Cortex (CX)	+	+	+	+/-	-
Septum (S)	-	+/-	+/-	++	-
Striatum (STR)	+	++	++	+	-
Corticothalamic/ thalamocortical tract	+	++	++	+	-
Thalamus (Th)	+/-	+/-	+/-	++	-
Hippocampus (Hip)	+/-	+	+	++	-
Habenula (Hb)	++	++	++	++	-
Fasciculus retroflexus (FR)	++	++	++	++	-
Midbrain (MB)	++	++	++	++	-
Cerebellum (CB)	++	++	++	-	-

Legend: - , no expression; +/-, weak expression; + moderate expression; ++, strong expression; +++, very strong expression.

GFP-Neogenin expression was also detected by anti-Neogenin, anti-GFP and anti-FLAG immunostaining (Fig. 1C, upper panel). Anti-GFP immunostaining on SH-SY5Y neuroblastoma cells transfected with Syn-GFP-Neogenin, revealed weak GFP-Neogenin expression induced by the synapsin I promoter (data not shown).

Ligand binding of the GFP-Neogenin protein was evaluated in COS-7 cell binding assays using AP-tagged RGMa and Netrin-1. Strong binding of RGMa-AP and Netrin-1-AP to GFP-Neogenin was observed and no obvious difference in binding as compared to wild-type Neogenin was detected. COS-7 cells transfected with pcDNA3.1 empty vector did not bind RGMa-AP or Netrin-1-AP (Fig. 1D). Taken together, immunoblotting, immunohistochemistry and COS-7 cell binding assays, showed correct expression of the GFP-Neogenin fusion protein and intact binding of RGMa and Netrin-1.

NEURONAL GFP-NEOGENIN EXPRESSION IN *SYN-GFP-NEOGENIN* TRANSGENIC MICE

Transgenic *Syn-GFP-Neogenin* mice were generated by pronuclear injection (Gordon and Ruddle 1983). Of the 36 mice born out of one-cell stage zygotes injected with Syn-GFP-Neogenin DNA,

two transgenic founders were identified by PCR genotyping. Two stable transgenic mouse lines were generated by crossing the two founders with C57BL/6 mice. Approximately 50% of the offspring of these crosses contained the transgene (Fig. 1E), indicating a stable insertion of the Syn-GFP-Neogenin DNA into the mouse genome as was also verified by Southern blot analysis (data not shown).

To select an appropriate developmental stage for *in vivo* GFP-Neogenin pull down on brain tissue, we analyzed the expression of GFP-Neogenin on brain sections of transgenic mice and littermate controls at E14.5, E18.5, P0, P10 and P20. For *Syn-GFP-Neogenin* transgenic mouse line 1, abundant expression of GFP-Neogenin was detected from E14.5 till P10, using anti-GFP immunohistochemistry (Fig. 2, Table 1). In contrast, analysis of *Syn-GFP-Neogenin* transgenic mouse line 2 did not reveal any expression of GFP-Neogenin at any of the developmental stages investigated.

In *Syn-GFP-Neogenin* mouse line 1, prominent GFP-Neogenin expression was detected in axonal projections of the olfactory sensory neurons (OSNs) in the olfactory epithelium (OE) from E14.5 till P10 (Fig. 2A, B, J, R, Table 1). The olfactory bulb (OB) also stained for GFP-Neogenin. At E18.5 and P0, GFP-Neogenin expression was detected in axon projections in the external plexiform layer and internal plexiform layer of the OB (Fig. 2J). Furthermore, the anterior commissure pars anterior, which connects olfactory structures to the anterior piriform cortex, stained strongly for GFP-Neogenin (Fig. 1O). At E14.5, E18.5 and P0 labeling of GFP-Neogenin was detected in the cortical plate (CP) and on cortical axon projections in the intermediate zone (IZ) and internal capsule (Fig. 2C, F, G, K, L, Table 1). Other axon bundles that stained for GFP-Neogenin at E14.5 were the posterior commissure and axon tracts along the midbrain flexure (Fig. 2A). In addition, strong GFP-Neogenin expression was detected in the major output bundle of the habenula, the fasciculus retroflexus, and also in the habenula itself (Fig. 2P, Table 1). At E18.5 and P0, GFP-Neogenin staining was particularly strong in the lateral habenula (Fig. 2H, N). In the hippocampus and dentate gyrus, GFP-Neogenin expression was most obvious at E18.5, P0 and P10 (Fig. 2M, S, Table 1). In the cerebellum (CB) the deep cerebellar nuclei stained strongly for GFP-Neogenin at E14.5 (Fig. 2D). At E18.5 and P0 an overall GFP-Neogenin staining was detected in the CB (Fig. 2Q, Table 1). At P20, no GFP-Neogenin expression was detected in the brain areas described above, except for the olfactory bulb and olfactory epithelium that displayed weak GFP-Neogenin expression (Table 1).

COMPARISON OF TRANSGENIC GFP-NEOGENIN AND ENDOGENOUS NEOGENIN EXPRESSION DURING MOUSE BRAIN DEVELOPMENT

Immunohistochemistry of *Syn-GFP-Neogenin* transgenic mouse line 1 revealed strong and broad expression of GFP-Neogenin at late embryonic and early postnatal stages. Importantly, GFP-Neogenin expression was detected in neuronal cell layers and axon bundles that normally express endogenous Neogenin (Fig. 3 and see also Chapter 3). This is critical information as a

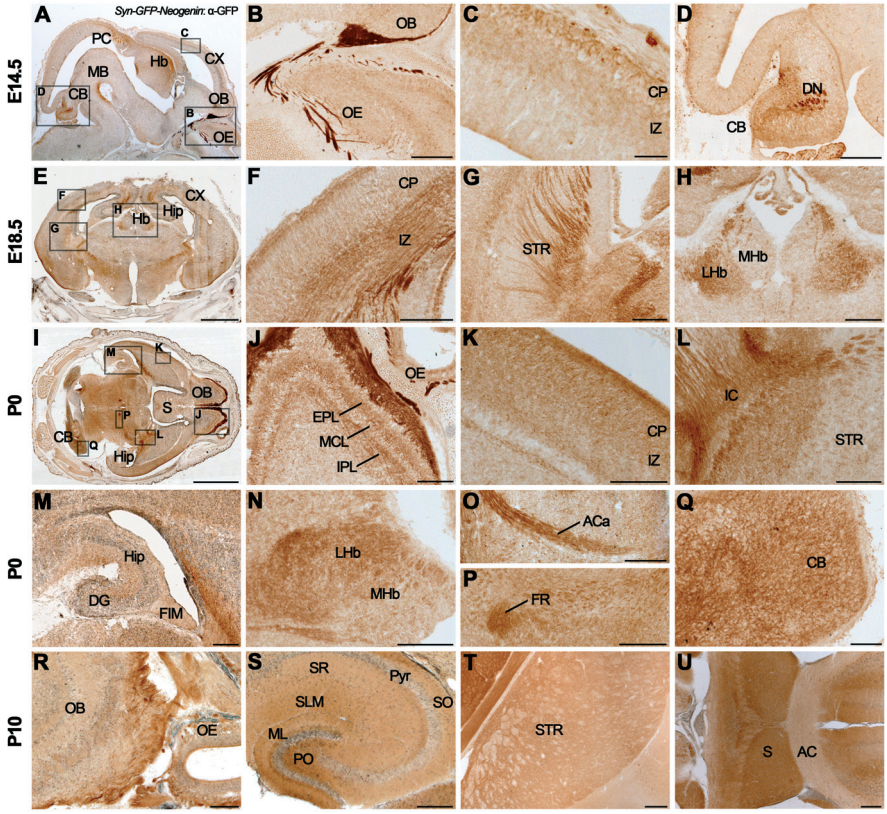

FIGURE 2. Neuronal GFP-Neogenin expression in *Syn-GFP-Neogenin* transgenic mice.

Anti-GFP DAB immunohistochemistry on sagital E14.5 (A-D), coronal E18.5 (E-H), horizontal P0 (I-Q), and horizontal P10 (R-U) mouse brain sections. (A-D) Immunostaining reveals GFP-Neogenin expression in the E14.5 olfactory epithelium (OE), olfactory bulb (OB), cortex (CX), and cerebellum (CB). (E-H) At E18.5 expression of GFP-Neogenin is detected in the CX, striatum (STR) and habenula (Hb). (I-Q) At P0 GFP-Neogenin is expressed in the OE, OB, CX, internal capsule (IC), hippocampus (Hip), Hb , anterior commissure pars anterior (ACa), fasciculus retroflexus (FR) and CB. (R-U) At P10, expression of GFP-Neogenin is detected in the OE, OB, Hip, STR and septum (S). CP, cortical plate; EPL, external plexiform layer; LHb lateral habenula; IPL, internal plexiform layer; IZ intermediate zone; MB, midbrain; MCL, mitral cell layer; MHb medial habenula; ML, molecular layer; PC, posterior commissure; PO, polymorph layer; Pyr, pyramidal cell layer; SLM, stratum lacunosum molecular; SO, stratum oriens; SR, stratum radiatum. Scale bar A: 800 µm, B: 200 µm, C: 50 µm, D: 200 µm, E: 1000 µm, F-H: 200 µm, I: 2000 µm, J-Q: 200 µm and R-U: 200 µm.

GFP-Neogenin pull down experiment on brain tissue with endogenous Neogenin expression would increase the chance of precipitating relevant Neogenin signaling proteins that function in the endogenous situation.

Immunostaining on *Syn-GFP-Neogenin* mouse brains revealed expression of GFP-Neogenin in OSNs in the OE and in OSN axon bundles projecting to the OB at E14.5 (Fig. 3A). RGMa-AP section binding and Neogenin immunohistochemistry on E14.5 wild-type mouse brain tissue showed similar expression patterns (Fig. 3B, C). Furthermore, immunohistochemistry detected expression of GFP-Neogenin in neurons and axonal projections in the CP and IZ of the *Syn-GFP-Neogenin* mouse cortex at E16.5 (Fig. 3D). At the endogenous level, strong *Neogenin* expression was detected throughout all cortical layers in E16.5 wild-type brains (Fig. 3E). Immunostaining revealed strong expression of endogenous Neogenin in cortical neurons and axonal projections in the CP and IZ at E16.5 (Fig. 3F). Finally, immunostaining revealed expression of GFP-Neogenin in the embryonic *Syn-GFP-Neogenin* CB (Fig. 3G). Similarly, *in situ* hybridization and immunostaining revealed strong Neogenin expression in the embryonic wild-type CB (Fig. 3H, I). Thus, in many brain areas and axon tracts co-expression of transgenic GFP-Neogenin and endogenous Neogenin was detected.

Next, we determined the level of Neogenin expression in transgenic *Syn-GFP-Neogenin* mouse brains. Anti-Neogenin immunoblotting on lysates of different brain regions of late embryonic *Syn-GFP-Neogenin* mice and wild-type littermate controls revealed that the total amount of Neogenin, that is endogenous Neogenin and transgenic GFP-Neogenin protein, was increased in transgenic mice as compared to wild-type mice (Fig. 4A). In wild-type mice, Neogenin expression was most prominent in the cortex. Low Neogenin expression levels were detected in the striatum, hippocampus and CB. In brain lysates of *Syn-GFP-Neogenin* mice, total Neogenin expression levels were moderately increased in the CB compared to wild-type. A very strong increase of Neogenin expression was observed in the cortex, striatum and hippocampus of Syn-GFP-Neogenin mice compared to wild-type (Fig. 4A).

IDENTIFICATION OF NOVEL NEOGENIN-INTERACTING PROTEINS BY *IN VIVO* NEOGENIN PULL DOWN EXPERIMENTS ON *SYN-GFP-NEOGENIN* BRAIN LYSATES

Our understanding of the role and mechanism of Neogenin signaling during brain development is very limited and only a few Neogenin signaling proteins have been identified so far. To identify Neogenin-interacting proteins that function in Neogenin signaling during brain development we performed an *in vivo* Neogenin pull down on brain lysates of perinatal *Syn-GFP-Neogenin* and wild-type mice. At perinatal stages, many neurodevelopmental processes take place in which Neogenin function has been shown to be involved, for example neuronal cell differentiation, migration, apoptosis and axon guidance (Andrusiak *et al.* 2011, Conrad *et al.* 2010, Matsunaga *et al.* 2004, Matsunaga *et al.* 2006, Monnier *et al.* 2002, Rajagopalan *et al.* 2004). Furthermore, both GFP-Neogenin and endogenous Neogenin are prominently expressed at these developmental stages (Fig. 3, Fig. 4A).

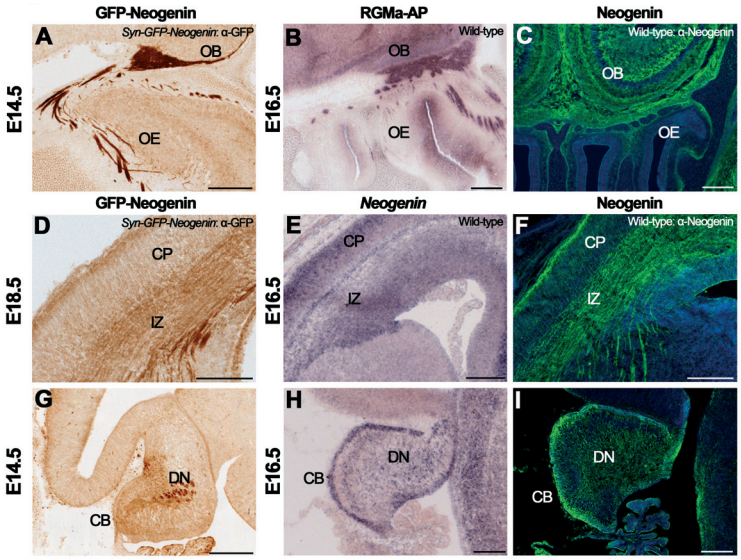

FIGURE 3. Overlapping expression of GFP-Neogenin and endogenous Neogenin.

GFP-Neogenin expression was compared to endogenous Neogenin expression, using anti-GFP (A, D, G) and anti-Neogenin (C, F, I) immunostaining, Neogenin *in situ* hybridization (E, H) and RGMa-AP section binding (B) on E14.5 sagital (A, B, G-I) and E18.5 coronal (C-F) brain sections of *Syn-GFP-Neogenin* (A, D, G) and wild-type mice (B, C, E, F, H, I). Anti-GFP immunostaining is visualized with DAB. Sections C, F and I are counterstained in blue with fluorescent Nissl. (A) GFP-Neogenin expression in the olfactory epithelium (OE) and olfactory sensory neuron (OSN) projections to the olfactory bulb (OB) in *Syn-GFP-Neogenin* mice. (B, C) Endogenous Neogenin expression in the OE and OSN projections to the OB revealed by RGMa-AP section binding (B) and anti-Neogenin immunostaining (C). (D-F) Expression of GFP-Neogenin (D) and endogenous Neogenin (E, F) in the cortical plate (CP) and cortical projections in the intermediate zone (IZ). (G-I) Expression of GFP-Neogenin (G) and endogenous Neogenin (H, I) in the deep nuclei (DN) and axonal projections of the cerebellum (CB). Scale bars A-I: 200 µm.

Anti-GFP immunoprecipitation on *Syn-GFP-Neogenin* total brain lysates revealed a high and specific yield of GFP-Neogenin protein (Fig. 4B). We detected a double band for GFP-Neogenin in the pull down and input control samples that were run on a gradient gel. The smaller protein fragment detected might represent a cleaved fragment of the GFP-Neogenin protein, since Neogenin has recognition sites for α-secretase in the extracellular domain and γ-secretase and caspase-3 in the intracellular domain (Goldschneider *et al.* 2008, Matsunaga *et al.* 2004).

Silver staining of the *Syn-GFP-Neogenin* and wild-type *in vivo* pull down samples separated on a gradient gel revealed a strong band of 190 kDa for GFP-Neogenin in the pull down sample of *Syn-GFP-Neogenin* transgenic brain lysates (Fig. 4C, green dot). Although several non-specific co-immunoprecipitated proteins were identified in both pull down samples, several protein

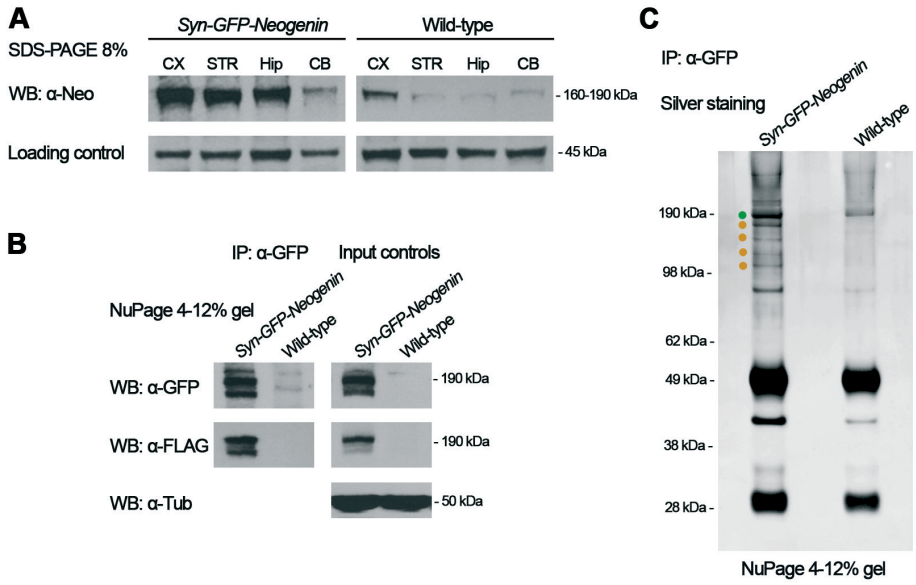

FIGURE 4. ***In vivo*** **pull down of neuronal Neogenin signaling complexes from** ***Syn-GFP-Neogenin*** **transgenic mice.**

(A) Anti-Neogenin immunoblotting to detect Neogenin expression in lysates of dissected cortex (CX), striatum (STR), hippocampus (Hip) and cerebellum (CB) of E18.5 *Syn-GFP-Neogenin* mice compared to wild-type littermate controls. Anti-Neogenin immunoblotting on brain lysates of *Syn-GFP-Neogenin* mice shows GFP-Neogenin and endogenous Neogenin protein. (B) Immunoblotting using anti-GFP and anti-FLAG antibodies shows GFP-Neogenin protein in an anti-GFP *in vivo* pull down experiment on brain lysates of perinatal *Syn-GFP-Neogenin* mice. (C) Silver staining of an anti-GFP *in vivo* pull down on brain lysates of perinatal *Syn-GFP-Neogenin* mice shows GFP-Neogenin protein (green dot) and putative Neogenin-interacting proteins (orange dots).

bands were specific for the *in vivo* pull down sample of *Syn*-GFP-N*eogenin* brain lysates. These proteins are likely to be putative Neogenin-interacting proteins (Fig. 4C, orange dots).

Mass spectrometry analysis was used to identify the proteins in the *in vivo* pull down samples. Lanes from Coomassie-stained gels were analyzed by mass spectrometry and peptide sequences were mapped to known protein sequences using Mascot software. Based on results from former studies, by us and others, the Mascot score cut-off value for a positive hit was set at 65. The results of the *in vivo* anti-GFP pull down on brain lysates of *Syn-GFP-Neogenin* mice were corrected for unspecific interacting proteins identified in the *in vivo* pull down on wild-type mouse brain lysates and for common contaminants identified in previous unrelated pull downs (e.g. heat shock proteins, keratins, ribosomal proteins and proteins related to cell metabolism).

TABLE 2. Neogenin-interacting proteins identified in the anti-GFP *in vivo* Neogenin proteomics screen.

				GFP-Neogenin		
#	Protein name		MW (kDa)	Mascot score	Unique peptides	Biological function
1	Neogenin	NEO1	160	661	16	axon guidance; cell adhesion; migration
2	Desmin	DES	53	227	5	actin cytoskeleton organization; type III intermediate filament; neuromuscular junction
3	RNA binding motif protein 14	RBM14	69	276	6	RNA transcription
4	Doublecortin-like kinase 2	DCLK1	47	248	6	protein serine/threonine kinase activity; cell differentiation; axon outgrowth; dendrite morphogenesis; neuron migration
5	Actin binding LIM protein family, member 3	ABLIM3	78	236	5	actin cytoskeleton organization; axon guidance; regulation of transcription
6	Topoisomerase (DNA) II beta	TOP2B	182	220	5	DNA binding; neuromuscular junction; neuron migration; neuronal differentiation; neurite outgrowth; corticogenesis
7	Actin binding LIM protein 1	ABLIM1	97	201	6	actin cytoskeleton organization; axon guidance; transcription regulation
8	Cortactin	CTTN	61	188	6	actin cytoskeleton organization; dendritic spine morphogenesis; cell migration; cell adhesion junctions
9	Calcium/calmodulin-dependent protein kinase II beta	CAMK2B	61	178	4	protein serine/threonine kinase activity; regulation of long-term neuronal plasticity; regulation of neuron projection development; apoptosis; Wnt signaling
10	Interleukin enhancer binding factor 2	ILF2	43	170	4	DNA binding; RNA binding; regulation of transcription
11	Interleukin enhancer binding factor 3	ILF3	96	126	4	DNA binding; RNA binding; regulation of transcription; immune response
12	Casein kinase 2A	CSNK2A1	45	125	4	ATP binding, beta-catenin binding, axon guidance, protein serine/threonine kinase activity, cell cycle, signal transduction
13	Metastasis associated 1	MTA1	79	104	3	DNA binding; regulation of transcription; Wnt signaling
14	Metastasis associated 1 family, member 2	MTA2	75	104	3	DNA binding; regulation of transcription; Wnt signaling
15	RAN binding protein 10	RANBP10	70	104	3	Ran GTPase binding; beta-tubulin binding; microtubule cytoskeleton organization
16	Dedicator of cytokinesis 7	DOCK7	238	102	4	Rac GTPase binding; microtubule cytoskeleton organization; axonogenesis; cell polarity; Schwann cell differentiation and myelination
17	Nitric oxide synthase 1 (neuronal) adaptor protein	NOS1AP	56	100	2	Nitric-oxide synthase binding; link Abl family kinases and the actin cytoskeleton
18	Nucleolin	NCL	77	99	2	DNA binding; RNA binding
19	Actin filament associated protein 1	AFAP1	81	93	2	actin binding
20	Cytoplasmic linker associated protein 1	CLASP1	169	88	3	actin and microtubule cytoskeleton organization; axon guidance
21	Regulating synaptic membrane exocytosis 1	RIMS1	163	88	4	Rab GTPase binding; exocytosis; neurotransmitter transport; regulation of long-term synaptic neuronal plasticity
22	Contactin 1	CTN1	113	80	2	cell adhesion; axon guidance
23	Neuron navigator 1	NAV1	202	80	2	cell differentiation; microtubule cytoskeleton organization
24	Metastasis associated 1 family, member 3	MTA3	66	78	2	DNA binding; regulation of transcription; Wnt signaling
25	Lysosomal trafficking regulator	LYST	425	76	3	endosome to lysosome transport
26	Molecule interacting with CasL 1	MICAL1	109	75	2	actin cytoskeleton organization; microtubule cytoskeleton organization; regulation of protein phosphorylation; apoptosis
27	CDC42 binding protein kinase alpha (DMPK-like)	CDC42BPA	197	72	3	protein serine/threonine kinase activity; actin cytoskeleton organization; cell migration; signal transduction; microtubule cytoskeleton organization
28	Dynactin 1	DCTN1	140	70	2	microtubule cytoskeleton organization; axonogenesis
29	Nuclear mitotic apparatus protein 1	NUMA1	236	70	3	microtubule binding; mitotic spindle orientation
30	Valosin-containing protein	VCP	89	68	2	ATPase activity; ER to Golgi vesicle-mediated transport; regulation of protein complex assembly; apoptosis
31	CDC5 cell division cycle 5-like (S. pombe)	CDC5L	92	68	3	DNA binding; RNA binding; regulation of transcription
32	Leucine rich repeat (in FLII) interacting protein 2	LRRFIP2	47	67	2	Wnt receptor signaling

Mass spectrometry analysis of the *in vivo* pull down samples revealed 31 putative novel Neogenin-interacting proteins that were specifically detected in the *in vivo* pull down sample of *Syn-GFP-Neogenin* brain lysates and not in the *in vivo* pull down sample of wild-type brain lysates (Table 2). Many of these proteins have reported functions in cytoskeleton organization, axon guidance, neuronal migration, regulation of transcription and apoptosis, all cellular processes in which Neogenin has been implicated (De Boer and Cooper 2008). It is remarkable that the biological function of roughly half of the Neogenin-interacting proteins identified was related to regulation of cytoskeleton organization. Putative Neogenin-interacting proteins identified with a function related to the actin cytoskeleton were desmin (Hubbard and Lazarides 1979), actin binding LIM protein family member 3 (Roof *et al.* 1997), and cortactin (Uruno *et al.* 2001). Doublecortin-like kinase 2 (Dclk2) (Burgess and Reiner 2000), dedicator of cytokinesis 7 (Dock7) (Watabe-Uchida *et al.* 2006), neuron navigator 1 (NAV1) (Van Haren *et al.* 2009) and dynactin 1 (DCTN1) (Culver-Hanlon *et al.* 2006) have been implicated in the control of microtubule dynamics. Calcium/calmodulin-dependent protein kinase II beta (Lin *et al.* 2004), molecule interacting with CasL (MICAL-1) (Zhou *et al.* 2011) and valosin-containing protein (Klein *et al.* 2005, Watts *et al.* 2004) have been implicated in apoptosis. A role in transcription regulation has been reported for RNA binding motif protein 14 (Iwasaki *et al.* 2001, O'Malley and Kumar 2009), interleukin enhancer binding factor 3 (ILF3) (Buaas *et al.* 1999) and metastasis associated 1 (Molli *et al.* 2008).

All together, an anti-GFP Neogenin *in vivo* pull down on brain lysates of transgenic *Syn-GFP-Neogenin* mice specifically immunoprecipitated GFP-Neogenin and 31 putative novel Neogenin-interacting proteins with known functions in biological processes that are regulated by Neogenin.

DISCUSSION

Neogenin function and signaling in the brain have been related to neurodevelopmental processes such as neurogenesis, neuronal differentiation, migration, axon guidance and apoptosis (Fitzgerald *et al.* 2006, Fujita *et al.* 2008, Hata *et al.* 2006, Matsunaga *et al.* 2004, Matsunaga *et al.* 2006, Mawdsley *et al.* 2004, Rajagopalan *et al.* 2004, Vielmetter *et al.* 1994). In recent years, several Neogenin-interacting proteins have been identified that function in neuronal Neogenin signaling. However, our knowledge of neuronal Neogenin signaling is far from complete. To increase our understanding of Neogenin signaling mechanisms, we performed an anti-GFP *in vivo* Neogenin pull down on brain lysates of perinatal *Syn-GFP-Neogenin* transgenic mice. Mass spectrometry analysis identified putative Neogenin-interacting proteins with known functions in cytoskeletal dynamics, axon guidance, neuronal migration, transcription regulation and apoptosis. The results of the *in vivo* Neogenin pull down are a valuable starting point for

the further elucidation of Neogenin signaling mechanisms in different neurodevelopmental processes.

SYN-GFP-NEOGENIN TRANSGENIC MICE EXPRESS HIGH LEVELS OF GFP-NEOGENIN AT PERINATAL STAGES

In this study, two stable *Syn-GFP-Neogenin* transgenic mouse lines were generated that contained a GFP-Neogenin fusion cDNA under the control of the neuron-specific synapsin I promoter (Fig. 1A) (Heumann *et al.* 2000, Hoesche *et al.* 1993, Schoch *et al.* 1996, Thiel *et al.* 1991). However, *Syn-GFP-Neogenin* transgenic mouse line 2 did not express GFP-Neogenin in the brain at the developmental stages investigated. Transgenesis by pronuclear injection is characterized by the random integration of a the DNA fragment into the genome (Gordon and Ruddle 1983). Enhancer and repressor elements in the vicinity of the integration site may affect transcription of the transgene and a transcription repressive environment could reduce or block transcription. In contrast, transgenic mouse line 1 abundantly expressed the GFP-Neogenin protein from embryonic stage E14.5, the earliest time point studied, until postnatal stage P10 (Fig. 2, Table 1). At P20 no significant GFP-Neogenin expression was detected in this mouse line, except for some weak GFP-Neogenin expression in the OB and OE. The spatiotemporal expression pattern induced by the synapsin I promoter for endogenous synapsin I mRNA or synapsin I-driven transgenes has been reported to show a sharp increase in expression level from P10 onwards, with a characteristic maximum around P20 (Hoesche *et al.* 1993). The seemingly aberrant spatiotemporal pattern observed in this study for GFP-Neogenin could be caused by the presence of transcription regulatory elements around the Syn-GFP-Neogenin integration site.

During late embryonic and early postnatal stages *Syn-GFP-Neogenin* transgenic mouse line 1 showed broad GFP-Neogenin expression in many areas of the brain (Fig. 2E-Q). At these stages, many neurodevelopmental processes take place, making this mouse line highly suitable for the isolation of Neogenin signaling complexes involved in neurodevelopmental processes like neuronal migration and axon guidance. In different brain areas of *Syn-GFP-Neogenin* transgenic mice, Neogenin levels were more than doubled as compared to endogenous Neogenin expression in wild-type mice (Fig. 4A). This increase could affect neurodevelopmental processes in which Neogenin signaling is involved. Neogenin is a dependence receptor and both absence of RGMa and overexpression of Neogenin induces apoptosis signaling in neurons, while Neogenin knockdown attenuates this apoptotic effect (Fujita *et al.* 2008, Matsunaga *et al.* 2004). Neogenin overexpression in the embryonic chick mesencephalon has been shown to stimulate neuronal differentiation (Matsunaga *et al.* 2006). In addition, Neogenin overexpression has been shown to perturb neuroblast migration in mouse and knockdown of Neogenin expression caused severe axon guidance defects in the formation of the *Xenopus* supraoptic tract (Andrusiak *et al.* 2011, Wilson and Key 2006). We performed

anti-β-III-tubulin stainings on brain sections of *Syn-GFP-Neogenin* mice to study axon bundle formation. For the different developmental time points investigated no abnormalities were observed (data not shown). We also investigated the occurrence of apoptosis in late embryonic *Syn-GFP-Neogenin* and wild-type brains by TUNEL staining. No difference was detected in the number of apoptotic neurons in *Syn-GFP-Neogenin* transgenic brains as compared to controls (data not shown).

Together, these results indicate that GFP-Neogenin is expressed at sites of endogenous Neogenin expression and that overexpression of Neogenin has no overt defects in the *Syn-GFP-Neogenin* mouse line.

NOVEL NEOGENIN-INTERACTING PROTEINS IDENTIFIED BY *IN VIVO* NEOGENIN PULL DOWN

A Neogenin *in vivo* pull down on brain lysates of *Syn-GFP-Neogenin* transgenic mouse line 1 identified 31 putative Neogenin-interacting proteins with reported functions in cellular processes in which Neogenin signaling is involved, i.e. cytoskeleton regulation, axon guidance, neuronal migration, regulation of transcription and apoptosis (De Boer and Cooper 2008). Except for contactin 1, which is a GPI-linked protein, all proteins identified were cytoplasmic proteins. Contactin-1 has a role in regulating neurite outgrowth, which is interesting given the effect of RGMa on neurite outgrowth (Berglund *et al.* 1999, Shimoda and Watanabe 2009).

Interestingly, the function of half of the putative Neogenin-interacting proteins identified was related to the regulation of the cytoskeleton (Table 2). It is of particular interest that at least 8 Neogenin-interacting proteins identified in the proteomics screen are known modulators of the microtubule cytoskeleton: Dclk2 (Burgess and Reiner 2000), RAN binding protein 10 (Kunert *et al.* 2009), Dock7 (Watabe-Uchida *et al.* 2006), cytoplasmic linker associated protein 1 (Clasp1) (Mimori-Kiyosue *et al.* 2005), NAV1 (van Haren 2009), MICAL-1 (Fischer *et al.* 2005), CDC42 binding protein kinase alpha (DMPK-like) (CDC42BPA) (Harwood and Braga 2003), DCTN1 (Culver-Hanlon *et al.* 2006) and nuclear mitotic apparatus protein 1 (VanThuan 2006). Although the effects of axon guidance signaling on the actin cytoskeleton have become more clear over the past few years, their effect on microtubule cytoskeleton dynamics is still poorly understood (O'Donnell *et al.* 2009). Some of the Neogenin-interacting proteins, like CDC42BPA, Clasp1 and MICAL-1, affect both actin and microtubule cytoskeleton dynamics and could therefore provide a link between the different regulatory mechanisms acting on the actin and microtubule cytoskeleton (Fischer *et al.* 2005, Panapakkam Giridharan *et al.* 2012, Tsvetkov *et al.* 2007, Zhou *et al.* 2011). Future research will focus on investigating the role of these factors in Neogenin signaling.

TABLE 3. Neogenin-interacting proteins identified in both the biotin-streptavidin-based *in vitro* and anti-GFP *in vivo* Neogenin proteomics screens.

				Anti-GFP *in vivo* pull down		Biotin-streptavidin-based *in vitro* pull down							
				GFP-Neogenin		NeoFL-GFP-Bio		NeoFL-GFP-Bio + RGMa stimulation		NeoICD-GFP-Bio		Control GFP-Bio	
#	Protein name		MW (kDa)	Mascot score	Unique peptides	Mascot score	Unique peptides	Mascot score	Unique peptides	Mascot score	Unique peptides	Mascot score	Unique peptides
1	Neogenin	NEO1	160	661	16	2501	178	2612	202	835	144	x	x
2	Cortactin	CTTN	61	188	6	x	x	71	2	x	x	x	x
3	Interleukin enhancer binding factor 2	ILF2	43	170	4	537	7	533	8	545	8	449	5
4	Interleukin enhancer binding factor 3	ILF3	96	126	4	523	10	626	11	265	6	160	3
5	Casein kinase 2A	CSNK2A1	45	125	4	36	1	x	x	288	5	x	x
6	Nucleolin	NCL	77	99	2	828	11	656	10	516	7	463	12
7	CDC42 binding protein kinase alpha (DMPK-like)	CDC42BPA	197	72	3	71	3	x	x	x	x	x	x
8	Dynactin 1	DCTN1	140	70	2	39	1	x	x	x	x	x	x
9	Valosin-containing protein	VCP	89	68	2	165	3	247	4	187	3	62	1
10	Cytoplasmic FMR1 interacting protein 1	CYFIP1	147	52	2	x	x	146	3	240	4	x	x
11	Cytoplasmic FMR1 interacting protein 2	CYFIP2	115	52	2	128	3	x	x	x	x	x	x
12	U2-associated SR140 protein	SR140	119	64	2	x	x	111	2	93	1	x	x
13	Kinectin 1	KTN1	156	45	2	67	2	x	x	x	x	x	x

UNIQUE AND OVERLAPPING NEOGENIN-INTERACTING PROTEINS IN THE *IN VIVO* NEOGENIN PULL DOWN ON *SYN-GFP-NEOGENIN* BRAIN LYSATES AND *IN VITRO* NEOGENIN BIOTIN PULL DOWN

In Chapter 3, we describe the results of an *in vitro* biotin-streptavidin-based pull down experiment in HEK293 cells to purify Neogenin signaling complexes. Mass spectrometry analysis of the biotin pull down samples identified 52 putative novel Neogenin-interacting proteins and 1 known interactor of Neogenin, myosin X (Berg *et al.* 2000, Liu *et al.* 2012, Zhu *et al.* 2007). One possible explanation for the higher number of Neogenin-interacting proteins identified in the Neogenin biotin pull down screen compared to the Neogenin *in vivo* pull down is the higher yield of Neogenin protein in the first experiment. In the Neogenin biotin pull down experiments the number of Neogenin peptides detected by mass spectrometry analysis was 144 for the NeoICD and on average 190 for full-length Neogenin (Table 3). Mass spectrometry analysis of the Neogenin *in vivo* pull down samples only identified 16 Neogenin peptides.

Most of the Neogenin-interacting proteins identified by the two proteomics screens were unique for one of the two experiments. The difference in pull down methods and the use of a mammalian fibroblast cells versus mouse brain tissue as starting material, are important factors that could contribute to this difference. 12 Interacting proteins were identified in both screens (Table 3). Cortactin, CDC42BPA, cytoplasmic FMR1 interacting protein 1 and 2, and kinectin are involved in the regulation of cytoskeletal dynamics. Cortactin is a known regulator of actin cytoskeleton dynamics and dendritic spine morphology (Hering and Sheng 2003, Uruno et al. 2001). ILF2, ILF3 (Buaas et al. 1999), nucleolin (Yang et al. 1994) and U2-associated SR140 protein (Long and Caceres 2009) are involved in transcription regulation. Two serine/threonine kinases: casein kinase 2A and CDC42BPA were detected in both pull down screens. CDC42BPA regulates the dynamics of both the actin and microtubule cytoskeleton and regulates cell migration (Harwood and Braga 2003, Wilkinson et al. 2005). There are over 300 known substrates that can be phosphorylated by casein kinase 2A (Meggio and Pinna 2003). In the nervous system some of these substrates have been implicated in neuritogenesis, synaptic transmission and plasticity, and neuronal survival (Blanquet 2000). Four of the Neogenin-interacting proteins detected in both pull down experiments: interleukin enhancer binding factor 2 and 3, nucleolin and vasolin-containing protein were also identified in the control GFP-Biotin pull down sample, which makes their identification as putative Neogenin-interacting proteins doubtful (Table 3). Further investigation of these putative Neogenin-interacting proteins is required to verify their interaction with Neogenin in vivo and to unravel their role in Neogenin signaling.

Overall, the in vivo proteomics screen described in this chapter led to the identification of 31 putative Neogenin-interacting proteins. These proteins have reported functions in the regulation of cytoskeleton dynamics, neuron migration, transcriptional regulation and axon guidance. The results of the screen are a valuable starting point for the design of future studies on the role and mechanisms of Neogenin signaling during brain development (see Chapter 6).

ACKNOWLEDGEMENT

We would like to thank Marco Hoekman of the Central Laboratory Animal Research Facility Utrecht (GDL, Utrecht University) for his help with pronuclear injections. We are grateful to Denise Davis, Manfred Kiliman and Guus Smit for sharing DNA constructs. This work was supported by HFSP (CDA), ZonMW (VIDI), Hersenstichting Nederland and International Parkinson Foundation grants to R.J.P.

REFERENCE LIST

Andrusiak, M. G., K. A. McClellan, D. Dugal-Tessier, L. M. Julian, S. P. Rodrigues, D. S. Park, T. E. Kennedy, and R. S. Slack. 2011. Rb/E2F regulates expression of neogenin during neuronal migration. Mol. Cell Biol. 31:238-247.

Berg, J. S., B. H. Derfler, C. M. Pennisi, D. P. Corey, and R. E. Cheney. 2000. Myosin-X, a novel myosin with pleckstrin homology domains, associates with regions of dynamic actin. J. Cell Sci. 113 Pt 19:3439-3451.

Berglund, E. O., K. K. Murai, B. Fredette, G. Sekerkova, B. Marturano, L. Weber, E. Mugnaini, and B. Ranscht. 1999. Ataxia and abnormal cerebellar microorganization in mice with ablated contactin gene expression. Neuron 24:739-750.

Blanquet, P. R. 2000. Casein kinase 2 as a potentially important enzyme in the nervous system. Prog. Neurobiol. 60:211-246.

Bradford, D., R. L. Faull, M. A. Curtis, and H. M. Cooper. 2010. Characterization of the netrin/RGMa receptor neogenin in neurogenic regions of the mouse and human adult forebrain. J. Comp Neurol. 518:3237-3253.

Bredesen, D. E., P. Mehlen, and S. Rabizadeh. 2005. Receptors that mediate cellular dependence. Cell Death. Differ. 12:1031-1043.

Brinks, H., S. Conrad, J. Vogt, J. Oldekamp, A. Sierra, L. Deitinghoff, I. Bechmann, G. Alvarez-Bolado, B. Heimrich, P. P. Monnier, B. K. Mueller, and T. Skutella. 2004. The repulsive guidance molecule RGMa is involved in the formation of afferent connections in the dentate gyrus. J. Neurosci. 24:3862-3869.

Buaas, F. W., K. Lee, S. Edelhoff, C. Disteche, and R. E. Braun. 1999. Cloning and characterization of the mouse interleukin enhancer binding factor 3 (Ilf3) homolog in a screen for RNA binding proteins. Mamm. Genome 10:451-456.

Burgess, H. A. and O. Reiner. 2000. Doublecortin-like kinase is associated with microtubules in neuronal growth cones. Mol. Cell Neurosci. 16:529-541.

Conrad, S., H. Genth, F. Hofmann, I. Just, and T. Skutella. 2007. Neogenin-RGMa signaling at the growth cone is bone morphogenetic protein-independent and involves RhoA, ROCK, and PKC. J. Biol. Chem. 282:16423-16433.

Conrad, S., F. Stimpfle, S. Montazeri, J. Oldekamp, K. Seid, G. Alvarez-Bolado, and T. Skutella. 2010. RGMb controls aggregation and migration of Neogenin-positive cells *in vitro* and *in vivo*. Mol. Cell Neurosci. 43:222-231.

Culver-Hanlon, T. L., S. A. Lex, A. D. Stephens, N. J. Quintyne, and S. J. King. 2006. A microtubule-binding domain in dynactin increases dynein processivity by skating along microtubules. Nat. Cell Biol. 8:264-270.

Endo, M. and T. Yamashita. 2009. Inactivation of Ras by p120GAP via focal adhesion kinase dephosphorylation mediates RGMa-induced growth cone collapse. J. Neurosci. 29:6649-6662.

Fearon, E. R., K. R. Cho, J. M. Nigro, S. E. Kern, J. W. Simons, J. M. Ruppert, S. R. Hamilton, A. C. Preisinger, G. Thomas, K. W. Kinzler, and . 1990. Identification of a chromosome 18q gene that is altered in colorectal cancers. Science 247:49-56.

Fischer, J., T. Weide, and A. Barnekow. 2005. The MICAL proteins and rab1: a possible link to the cytoskeleton? Biochem. Biophys. Res. Commun. 328:415-423.

Fitzgerald, D. P., S. J. Cole, A. Hammond, C. Seaman, and H. M. Cooper. 2006. Characterization of neogenin-expressing neural progenitor populations and migrating neuroblasts in the embryonic mouse forebrain. Neuroscience 142:703-716.

Fujita, Y., J. Taniguchi, M. Uchikawa, M. Endo, K. Hata, T. Kubo, B. K. Mueller, and T. Yamashita. 2008. Neogenin regulates neuronal survival through DAP kinase. Cell Death. Differ. 15:1593-1608.

Gad, J. M., S. L. Keeling, A. F. Wilks, S. S. Tan, and H. M. Cooper. 1997. The expression patterns of guidance receptors, DCC and Neogenin, are spatially and temporally distinct throughout mouse embryogenesis. Dev. Biol. 192:258-273.

Geisbrecht, B. V., K. A. Dowd, R. W. Barfield, P. A. Longo, and D. J. Leahy. 2003. Netrin binds discrete subdomains of DCC and UNC5 and mediates interactions between DCC and heparin. J. Biol. Chem. 278:32561-32568.

Goldschneider, D. and P. Mehlen. 2010. Dependence receptors: a new paradigm in cell signaling and cancer therapy. Oncogene 29:1865-1882.

Goldschneider, D., N. Rama, C. Guix, and P. Mehlen. 2008. The neogenin intracellular domain regulates gene transcription via nuclear translocation. Mol. Cell Biol. 28:4068-4079.

Gordon, J. W. and F. H. Ruddle. 1983. Gene transfer into mouse embryos: production of transgenic mice by pronuclear injection. Methods Enzymol. 101:411-433.

Harwood, A. and V. M. Braga. 2003. Cdc42 & GSK-3: signals at the crossroads. Nat. Cell Biol. 5:275-277.

Hata, K., M. Fujitani, Y. Yasuda, H. Doya, T. Saito, S. Yamagishi, B. K. Mueller, and T. Yamashita. 2006. RGMa inhibition promotes axonal growth and recovery after spinal cord injury. J. Cell Biol. 173:47-58.

Hata, K., K. Kaibuchi, S. Inagaki, and T. Yamashita. 2009. Unc5B associates with LARG to mediate the action of repulsive guidance molecule. J. Cell Biol. 184:737-750.

Hedrick, L., K. R. Cho, E. R. Fearon, T. C. Wu, K. W. Kinzler, and B. Vogelstein. 1994. The DCC gene product in cellular differentiation and colorectal tumorigenesis. Genes Dev. 8:1174-1183.

Hering, H. and M. Sheng. 2003. Activity-dependent redistribution and essential role of cortactin in dendritic spine morphogenesis. J. Neurosci. 23:11759-11769.

Heumann, R., C. Goemans, D. Bartsch, K. Lingenhohl, P. C. Waldmeier, B. Hengerer, P. R. Allegrini, K. Schellander, E. F. Wagner, T. Arendt, R. H. Kamdem, K. Obst-Pernberg, F. Narz, P. Wahle, and H. Berns. 2000. Transgenic activation of Ras in neurons promotes hypertrophy and protects from lesion-induced degeneration. J. Cell Biol. 151:1537-1548.

Hoesche, C., A. Sauerwald, R. W. Veh, B. Krippl, and M. W. Kilimann. 1993. The 5'-flanking region of the rat synapsin I gene directs neuron-specific and developmentally regulated reporter gene expression in transgenic mice. J. Biol. Chem. 268:26494-26502.

Hubbard, B. D. and E. Lazarides. 1979. Copurification of actin and desmin from chicken smooth muscle and their copolymerization *in vitro* to intermediate filaments. J. Cell Biol. 80:166-182.

Iwasaki, T., W. W. Chin, and L. Ko. 2001. Identification and characterization of RRM-containing coactivator activator (CoAA) as TRBP-interacting protein, and its splice variant as a coactivator modulator (CoAM). J. Biol. Chem. 276:33375-33383.

Klein, J. B., M. T. Barati, R. Wu, D. Gozal, L. R. Sachleben, Jr., H. Kausar, J. O. Trent, E. Gozal, and M. J. Rane. 2005. Akt-mediated valosin-containing protein 97 phosphorylation regulates its association with ubiquitinated proteins. J. Biol. Chem. 280:31870-31881.

Koeberle, P. D., A. Tura, N. G. Tassew, L. C. Schlichter, and P. P. Monnier. 2010. The repulsive guidance molecule, RGMa, promotes retinal ganglion cell survival *in vitro* and *in vivo*. Neuroscience 169:495-504.

Kunert, S., I. Meyer, S. Fleischhauer, M. Wannack, J. Fiedler, R. A. Shivdasani, and H. Schulze. 2009. The microtubule modulator RanBP10 plays a critical role in regulation of platelet discoid shape and degranulation. Blood 114:5532-5540.

Lah, G. J. and B. Key. 2012. Dual roles of the chemorepellent axon guidance molecule RGMa in establishing pioneering axon tracts and neural fate decisions in embryonic vertebrate forebrain. Dev Neurobiol 72:1458-1470.

Lin, K. F., R. C. Chang, K. C. Suen, K. F. So, and J. Hugon. 2004. Modulation of calcium/calmodulin kinase-II provides partial neuroprotection against beta-amyloid peptide toxicity. Eur. J. Neurosci. 19:2047-2055.

Liu, Y., Y. Peng, P. G. Dai, Q. S. Du, L. Mei, and W. C. Xiong. 2012. Differential regulation of myosin X movements by its cargos, DCC and neogenin. J. Cell Sci. 125:751-762.

Llambi, F., F. Causeret, E. Bloch-Gallego, and P. Mehlen. 2001. Netrin-1 acts as a survival factor via its receptors UNC5H and DCC. EMBO J. 20:2715-2722.

Long, J. C. and J. F. Caceres. 2009. The SR protein family of splicing factors: master regulators of gene expression. Biochem. J. 417:15-27.

Matsunaga, E., H. Nakamura, and A. Chedotal. 2006. Repulsive guidance molecule plays multiple roles in neuronal differentiation and axon guidance. J. Neurosci. 26:6082-6088.

Matsunaga, E., S. Tauszig-Delamasure, P. P. Monnier, B. K. Mueller, S. M. Strittmatter, P. Mehlen, and A. Chedotal. 2004. RGM and its receptor neogenin regulate neuronal survival. Nat. Cell Biol. 6:749-755.

Mawdsley, D. J., H. M. Cooper, B. M. Hogan, S. H. Cody, G. J. Lieschke, and J. K. Heath. 2004. The Netrin receptor Neogenin is required for neural tube formation and somitogenesis in zebrafish. Dev. Biol. 269:302-315.

Meggio, F. and L. A. Pinna. 2003. One-thousand-and-one substrates of protein kinase CK2? FASEB J. 17:349-368.

Mehlen, P. and E. R. Fearon. 2004. Role of the dependence receptor DCC in colorectal cancer pathogenesis. J. Clin. Oncol. 22:3420-3428.

Mimori-Kiyosue, Y., I. Grigoriev, G. Lansbergen, H. Sasaki, C. Matsui, F. Severin, N. Galjart, F. Grosveld, I. Vorobjev, S. Tsukita, and A. Akhmanova. 2005. CLASP1 and CLASP2 bind to EB1 and regulate microtubule plus-end dynamics at the cell cortex. J. Cell Biol. 168:141-153.

Molli, P. R., R. R. Singh, S. W. Lee, and R. Kumar. 2008. MTA1-mediated transcriptional repression of BRCA1 tumor suppressor gene. Oncogene 27:1971-1980.

Monnier, P. P., A. Sierra, P. Macchi, L. Deitinghoff, J. S. Andersen, M. Mann, M. Flad, M. R. Hornberger, B. Stahl, F. Bonhoeffer, and B. K. Mueller. 2002. RGM is a repulsive guidance molecule for retinal axons. Nature 419:392-395.

O'Donnell, M., R. K. Chance, and G. J. Bashaw. 2009. Axon growth and guidance: receptor regulation and signal transduction. Annu. Rev. Neurosci. 32:383-412.

O'Malley, B. W. and R. Kumar. 2009. Nuclear receptor coregulators in cancer biology. Cancer Res. 69:8217-8222.

Oldekamp, J., N. Kramer, G. Alvarez-Bolado, and T. Skutella. 2004. Expression pattern of the repulsive guidance molecules RGM A, B and C during mouse development. Gene Expr. Patterns. 4:283-288.

Panapakkam Giridharan, S. S., J. L. Rohn, N. Naslavsky, and S. Caplan. 2012. Differential regulation of actin microfilaments by human MICAL proteins. J. Cell Sci. 125:614-624.

Pasterkamp RJ, De Winter F, Holtmaat AJ, Verhaagen J (1998) Evidence for a role of the chemorepellent semaphorin III and its receptor neuropilin-1 in the regeneration of primary olfactory axons. J Neurosci 18: 9962-9976.

Rajagopalan, S., L. Deitinghoff, D. Davis, S. Conrad, T. Skutella, A. Chedotal, B. K. Mueller, and S. M. Strittmatter. 2004. Neogenin mediates the action of repulsive guidance molecule. Nat. Cell Biol. 6:756-762.

Reed, S. E., E. M. Staley, J. P. Mayginnes, D. J. Pintel, and G. E. Tullis. 2006. Transfection of mammalian cells using linear polyethylenimine is a simple and effective means of producing recombinant adeno-associated virus vectors. J. Virol. Methods 138:85-98.

Roof, D. J., A. Hayes, M. Adamian, A. H. Chishti, and T. Li. 1997. Molecular characterization of abLIM, a novel actin-binding and double zinc finger protein. J. Cell Biol. 138:575-588.

Schaffar, G., J. Taniguchi, T. Brodbeck, A. H. Meyer, M. Schmidt, T. Yamashita, and B. K. Mueller. 2008. LIM-only protein 4 interacts directly with the repulsive guidance molecule A receptor Neogenin. J. Neurochem. 107:418-431.

Schmidtmer, J. and D. Engelkamp. 2004. Isolation and expression pattern of three mouse homologues of chick Rgm. Gene Expr. Patterns. 4:105-110.

Schoch, S., G. Cibelli, and G. Thiel. 1996. Neuron-specific gene expression of synapsin I. Major role of a negative regulatory mechanism. J. Biol. Chem. 271:3317-3323.

Shimoda, Y. and K. Watanabe. 2009. Contactins: emerging key roles in the development and function of the nervous system. Cell Adh. Migr. 3:64-70.

Shin, G. J. and N. H. Wilson. 2008. Overexpression of repulsive guidance molecule (RGM) a induces cell death through Neogenin in early vertebrate development. J. Mol. Histol. 39:105-113.

Thiel, G., P. Greengard, and T. C. Sudhof. 1991. Characterization of tissue-specific transcription by the human synapsin I gene promoter. Proc. Natl. Acad. Sci. U. S. A 88:3431-3435.

Tsvetkov, A. S., A. Samsonov, A. Akhmanova, N. Galjart, and S. V. Popov. 2007. Microtubule-binding proteins CLASP1 and CLASP2 interact with actin filaments. Cell Motil. Cytoskeleton 64:519-530.

Uruno, T., J. Liu, P. Zhang, Y. Fan, C. Egile, R. Li, S. C. Mueller, and X. Zhan. 2001. Activation of Arp2/3 complex-mediated actin polymerization by cortactin. Nat. Cell Biol. 3:259-266.

Van Haren, J., K. Draegestein, N. Keijzer, J. P. Abrahams, F. Grosveld, P. J. Peeters, D. Moechars, and N. Galjart. 2009. Mammalian Navigators are microtubule plus-end tracking proteins that can reorganize the cytoskeleton to induce neurite-like extensions. Cell Motil. Cytoskeleton 66:824-838.

VanThuan, N. 2006. Donor centrosome regulation of initial spindle formation in mouse somatic cell nuclear transfer: roles of gamma-tubulin and nuclear mitotic apparatus protein 1.Biol Reprod. 74:777-787.

Vielmetter, J., J. F. Kayyem, J. M. Roman, and W. J. Dreyer. 1994. Neogenin, an avian cell surface protein expressed during terminal neuronal differentiation, is closely related to the human tumor suppressor molecule deleted in colorectal cancer. J. Cell Biol. 127:2009-2020.

Watabe-Uchida, M., K. A. John, J. A. Janas, S. E. Newey, and A. L. Van Aelst. 2006. The Rac activator DOCK7 regulates neuronal polarity through local phosphorylation of stathmin/Op18. Neuron 51:727-739.

Watts, G. D., J. Wymer, M. J. Kovach, S. G. Mehta, S. Mumm, D. Darvish, A. Pestronk, M. P. Whyte, and V. E. Kimonis. 2004. Inclusion body myopathy associated with Paget disease of bone and frontotemporal dementia is caused by mutant valosin-containing protein. Nat. Genet. 36:377-381.

Wilkinson, S., H. F. Paterson, and C. J. Marshall. 2005. Cdc42-MRCK and Rho-ROCK signalling cooperate in myosin phosphorylation and cell invasion. Nat. Cell Biol. 7:255-261.

Wilson, N. H. and B. Key. 2006. Neogenin interacts with RGMa and netrin-1 to guide axons within the embryonic vertebrate forebrain. Dev. Biol. 296:485-498.

Yang, F., A. P. West, Jr., G. P. Allendorph, S. Choe, and P. J. Bjorkman. 2008. Neogenin interacts with hemojuvelin through its two membrane-proximal fibronectin type III domains. Biochemistry 47:4237-4245.

Yang, T. H., W. H. Tsai, Y. M. Lee, H. Y. Lei, M. Y. Lai, D. S. Chen, N. H. Yeh, and S. C. Lee. 1994. Purification and characterization of nucleolin and its identification as a transcription repressor. Mol. Cell Biol. 14:6068-6074.

Zhou, Y., Y. Adolfs, W. W. Pijnappel, S. J. Fuller, R. C. Van der Schors, K. W. Li, P. H. Sugden, A. B. Smit, A. Hergovich, and R. J. Pasterkamp. 2011. MICAL-1 is a negative regulator of MST-NDR kinase signaling and apoptosis. Mol. Cell Biol. 31:3603-3615.

Zhou, Y., R. A. Gunput, Y. Adolfs, and R. J. Pasterkamp. 2011. MICALs in control of the cytoskeleton, exocytosis, and cell death. Cell Mol. Life Sci. 68:4033-4044.

Zhu, X. J., C. Z. Wang, P. G. Dai, Y. Xie, N. N. Song, Y. Liu, Q. S. Du, L. Mei, Y. Q. Ding, and W. C. Xiong. 2007. Myosin X regulates netrin receptors and functions in axonal path-finding. Nat. Cell Biol. 9:184-192.

CHAPTER 6

Dock7 binds Neogenin and is required for repulsive RGMa-Neogenin signaling in neurons

DIANNE M.A. VAN DEN HEUVEL,
ANITA J.C.G.M. HELLEMONS AND
R. JEROEN PASTERKAMP

Department of Neuroscience and Pharmacology, Rudolf Magnus Institute of Neuroscience, University Medical Center Utrecht, Universiteitsweg 100, 3584 CG, Utrecht, The Netherlands

ABSTRACT

Neogenin is a multifunctional receptor involved in neurodevelopmental processes like neurogenesis, neuronal cell differentiation, migration and axon guidance. Neogenin signaling activated by repulsive guidance molecule A (RGMa) induces growth cone collapse and axon repulsion. The Neogenin signaling cascade mediating this effect is poorly understood. An *in vivo* proteomics screen using *Syn-GFP-Neogenin* transgenic mice identified dedicator of cytokinesis 7 (Dock7) as a novel Neogenin-interacting protein. Dock7 is an activator of Rac and Cdc42 GTPases and functions in neurogenesis, cell polarity, axon formation, migration and myelination. Co-immunoprecipitation confirmed the interaction between Neogenin and Dock7 *in vivo*, while *in situ* hybridization and immunostaining experiments revealed co-expression and colocalization of Neogenin and Dock7 in neurons in different cortical layers during embryonic development. A functional neurite outgrowth assay using dissociated cortical neurons revealed a requirement for Dock7 in RGMa-Neogenin-induced axon outgrowth inhibition. Upon stimulation with RGMa, no effect on phosphorylation of Dock7 or Op18/stathmin, a microtubule-destabilizing protein and downstream effector of Dock7, was found. In all, these studies indentify Dock7 as an interactor of Neogenin and a downstream signaling cue in RGMa-Neogenin-mediated neurite outgrowth inhibition. Further experiments are needed to elucidate how Dock7 mediates the inhibitory effects of RGMa.

INTRODUCTION

Neogenin, a member of the immunoglobulin (Ig) superfamily of cell surface receptors, is a receptor for RGM molecules (Rajagopalan *et al.* 2004, Vielmetter *et al.* 1994). Among other neurodevelopmental processes, RGM-Neogenin signaling functions in axon guidance and induces axon repulsive effects. A role for RGM-Neogenin signaling in axon guidance was first revealed during retinotectal map formation in chicken. An anterior-low to posterior-high gradient of RGM expression in the tectum was found to direct Neogenin-expressing temporal retinal axons to the anterior tectum (Matsunaga *et al.* 2006, Monnier *et al.* 2002, Rajagopalan *et al.* 2004). Furthermore, RGMa-Neogenin signaling is pivotal for proper axon bundle formation in the *Xenopus* forebrain. In *in vivo* experiments in which RGMa and Neogenin expression were manipulated by either morpholino-induced knockdown, expression of dominant-negative Neogenin or overexpression of RGMa, the development of the *Xenopus* forebrain bundles was severely disturbed (Lah and Key 2012, Wilson and Key 2006). In mice, RGMa-Neogenin signaling inhibits neurite outgrowth of cerebellar granule, cortical and dorsal root ganglia neurons (Conrad *et al.* 2007, Endo and Yamashita 2009, Hata *et al.* 2006, Hata *et al.* 2009). In slice preparations, RGMa guides entorhinal cortical axons to the outer molecular layer of the dentate gyrus. RGMa expression in the adjacent inner molecular layer blocks their extension

in and beyond this area (Brinks *et al*. 2004). Together, these experiments reveal the importance of RGMa-mediated Neogenin signaling in proper axon targeting.

Repulsive RGMa-Neogenin signaling events during axon guidance depend on the activation of RhoA GTPase and inactivation of Ras GTPase signaling (Conrad *et al*. 2007, Endo and Yamashita 2009, Hata *et al*. 2006). Uncoordinated locomotion-5 (Unc5) molecules A-D interact with Neogenin through their extracellular domains. For Unc5B a role as coreceptor in Neogenin signaling has been revealed (Hata *et al*. 2009). The Rho-specific GEF leukemia-associated Rho guanine-nucleotide exchange factor (LARG) associates with the intracellular part of Unc5B. Activation of Neogenin by RGMa induces focal adhesion kinase (FAK)-mediated phosphorylation of LARG, resulting in activation of RhoA/Rho kinase signaling (Hata *et al*. 2009). Ras signaling is inactivated by the Ras-specific GTPase-activating protein p120GAP, which is in a complex with FAK. Upon RGMa activation of Neogenin, p120GAP dissociates from FAK leading to the inactivation of Ras GTPase and its downstream effectors PI3-kinase and Akt (Endo and Yamashita 2009). The identification of the involvement of these signaling components in the Neogenin signaling cascade has provided the first insight into RGMa-Neogenin signaling mechanisms. However, our understanding of RGMa-Neogenin signaling in axon guidance, leading to axon repulsion and neurite outgrowth inhibition, is still very limited.

A Neogenin *in vivo* pull down on brain lysates of *Syn-GFP-Neogenin* transgenic mice identified several putative Neogenin-interacting proteins with known functions in neurite formation and cytoskeletal organization (see Chapter 5). In this study we focused on one of these Neogenin-interacting proteins, Dock7. Dock7 is a member of the Dock180-related protein superfamily and Dock7 function has been related to axonogenesis and neuron migration (Watabe-Uchida *et al*. 2006, Yang *et al*. 2012). Dock7 contains two dock homology regions (DHRs), highly conserved domains throughout the Dock180 superfamily, of which DHR2 has GEF activity for Rac and Cdc42 GTPases (Cote and Vuori 2002, Watabe-Uchida *et al*. 2006, Yamauchi *et al*. 2008).

In this study we used immunohistochemistry and co-immunoprecipitation experiments to show the *in vivo* colocalization and interaction of Dock7 and Neogenin in the developing brain. Furthermore, short hairpin RNA (shRNA)-mediated knockdown of Dock7 in mouse cortical neuron cultures revealed a requirement for Dock7 in RGMa-Neogenin-mediated neurite outgrowth inhibition. In a first attempt to reveal the role of Dock7 in RGMa-Neogenin signaling, we studied the phosphorylation level of Dock7 and of its downstream effector Op18/stathmin upon RGMa stimulation. Together, we established a role for Dock7 in RGMa-Neogenin-mediated neurite outgrowth inhibition. Future experiments should be designed to unveil the precise signaling mechanisms by which Dock7 mediates RGMa-Neogenin functions.

MATERIALS AND METHODS

PLASMIDS

The construction of the pcDNA3.1-CMV-GFP-Neogenin vector is described in Chapter 5. A plasmid expressing a FLAG-tagged full-length Dock7; pcDNA3.1/CMV-Flag-Dock7, was a kind gift of Linda Van Aelst. GFP-tagged Op18/stathmin cDNA was a kind gift of Karin Boekhoorn. For RNA interference knockdown experiments, a pSuper vector containing a DNA fragment encoding a shRNA directed against mouse Dock7 5'-GCTAATCGGGATGCAAAGA-3' was used (pSuper-Dock7#1; a kind gift of Linda Van Aelst). A scrambled non-targeting shRNA was designed as a control: 5'-GACAACCAATCGTAATACA-3'.

ANIMALS AND TISSUE TREATMENT

All animal use and care were in accordance with institutional guidelines. C57BL/6 mice were obtained from Charles River. Timed-pregnant mice were killed by means of cervical dislocation. The morning on which a vaginal plug was detected was considered embryonic day 0.5 (E0.5). For *in situ* hybridization experiments, E16.5 heads were directly frozen in 2-methylbutane (Merck). For immunohistochemistry, E16.5 heads were collected in phosphate-buffered saline (PBS; pH 7.4) and fixed by immersion for 3 hours (hrs) in 4% paraformaldehyde (PFA) in PBS at 4°C. Brains were washed in PBS, cryoprotected in 30% sucrose at 4°C and frozen in 2-methylbutane (Merck). Sections (16 µm) were cut on a cryostat, mounted on Superfrost Plus slides (Fisher Scientific), air-dried and stored desiccated at -80°C for *in situ* hybridization and at -20°C for immunohistochemistry.

CELL CULTURE AND TRANSFECTION

HEK293 cells were maintained in high glucose Dulbecco's modified Eagle's medium (DMEM; Gibco, Invitrogen). CHO and stable RGMa-expressing CHO (CHO-RGMa) cell lines (Hata *et al.* 2006) were a kind gift of Toshihide Yamashita. CHO cells were cultured in Ham's F12 nutrient mixture (Gibco, Invitrogen). Cell culture media were supplemented with 10% (v/v)

heat-inactivated fetal bovine serum (FBS; Lonza, BioWhittaker), 2 mM L-glutamine (PAA) and 1x penicillin/streptomycin (pen/strep; PAA) in a humidified atmosphere with 5% CO_2 at 37°C. Cell culture medium for CHO-RGMa cells was supplemented with 300 µg/ml hygromycin B (Roche). HEK293 cells were transfected using polyethylenimine (PEI; Polysciences) (Reed *et al.* 2006). N1E-115 cells were maintained in high glucose DMEM supplemented with 2% (v/v) FBS, 1x L-glutamine and pen/strep in a humidified atmosphere with 5% CO_2 at 37°C. N1E-115 cells were transfected using Lipofectamine 2000 (Invitrogen).

FC-PROTEIN PRODUCTION

For RGMa-Fc protein production, HEK293 cells were transfected with RGMa-Fc (pIgplus-RGMa-Fc; a kind gift of Herbert Lin) and cultured in Opti-MEM reduced serum medium (Gibco, Invitrogen)

supplemented with 3% FBS (Lonza, BioWhittaker), 2 mM L-glutamine (PAA) and 1x pen/strep (PAA) to produce Fc-tagged proteins. Cell culture medium containing Fc-tagged ligands was collected after 5 days in culture, filter-sterilized and stored at 4°C. RGMa-Fc-containing culture medium was incubated with protein A-agarose (Roche) on a roller overnight at 4°C. The next day, beads with bound RGMa-Fc were washed in ice-cold PBS. Beads were incubated with 100 mM glycine (pH 2.5) to elute RGMa-Fc from the beads. Eluted RGMa-Fc protein was neutralized by adding a small volume of 10mM Tris-HCl (pH 9.5). RGMa-Fc was dialyzed against PBS using centrifugal filter units Amicon Ultra 0.5 ml 10K Ultracel-10K membrane (Millipore). For Fc control protein, human IgG Fc fragment (Calbiochem) was used.

IN SITU HYBRIDIZATION

Nonradioactive *in situ* hybridization was performed according to (Pasterkamp *et al.* 1998), with minor modification. In brief, probe sequences for *RGMa* (Metzger *et al.* 2007), Neogenin (NM_008684.2: nt 2087-2587) and *Dock*7 (NM_026082.4: nt 181-746 bp) were polymerase chain reaction (PCR)-amplified from cDNA, using primer sequences listed in Table 1. Digoxigenin (DIG)-labeled RNA probes were generated by a RNA polymerase reaction using 10x DIG RNA labeling mix (ENZO).

Tissue sections were post-fixed in 4% PFA in PBS (pH 7.4) for 20 minutes (min) at room temperature (RT). To enhance tissue penetration and decrease aspecific background staining, sections were acetylated with 0.25% acetic anhydride in 0.1 M triethanolamine and 0.06% HCl for 10 min at RT. Sections were prehybridized for 2 hrs at RT in hybridization buffer (50% formamide, 5x Denhardt's solution, 5x SSC, 250 µg/ml baker's yeast tRNA and 500 µg/ml sonicated salmon sperm DNA). Hybridization was performed for 15 hrs at 68°C, using 400 ng/ml denatured DIG-labeled probe diluted in hybridization buffer. After hybridization, sections were first washed briefly in 2x SSC followed by incubation in 0.2x SCC for 2 hrs at 68°C. Sections were adjusted to RT in 0.2x SSC for 5 min. DIG-labeled RNA hybrids were detected with anti-DIG Fab fragments conjugated to alkaline phosphatase (AP; Boehringer) diluted in 1:2500 in Tris-buffered saline (TBS; pH 7.4) overnight at 4°C. Binding of AP-labeled antibody was visualized by incubating the sections in detection buffer (100 mM Tris-HCl, pH 9.5, 100 mM NaCl and 50 mM $MgCl_2$) containing 240 µg/ml levamisole and nitroblue tetrazolium chloride/5-bromo-4-chloro-3-indolyl-phosphatase (NBT/BCIP, Roche) for 14 hrs at RT. Sections subjected to the entire *in situ* hybridization procedure, but with no probe or sense probe added, did not exhibit specific hybridization signals. The specificity of the *in situ* hybridization procedure was also inferred from the clearly distinct gene expression patterns observed. Staining was visualized using a Zeiss Axioskop 2 microscope.

TABLE 1. Sense and antisense primer sequences for *RGMa, Neogenin* and *Dock7 in situ* hybridization probes.

Gene	Sense primer	Antisense primer	Size
RGMa	5′-TCAGCTGCCCCCAACTACACT-3′	5′-TCCTCCACGGCGTTGACTACC-3′	455 bp
Neogenin	5′-ACACCGTTATCTGGCAATGG-3′	5′-TTCAGCAGACAGCCAATCAG-3′	501 bp
Dock7	5′-AAGATCAGCAGAACTGTTGC-3′	5′-AAGTCAAAGATACTGCAGGC-3′	566 bp

IMMUNOCYTOCHEMISTRY

Dissociated E14.5 cortical neurons were fixed after 2 days *in vitro* (DIV2) with 4% PFA for 15 min at RT and washed in PBS (pH 7.4). Neurons were permeabilized and blocked in normal blocking buffer (PBS, 4% bovine serum albumin (BSA) and 0.1% Triton) for 1 hr at RT and incubated with rabbit anti-Dock7 antibody (28057; IBL) 1:100 and goat anti-Neogenin antibody (AF1079; R&D systems) 1:400 in normal blocking buffer overnight at 4°C. The next day, sections were washed in PBS and incubated with the appropriate Alexa Fluor-labeled secondary antibodies (Invitrogen) at 1:500 for 1 hr at RT.

IMMUNOHISTOCHEMISTRY

Sections were washed in PBS (pH 7.4) and incubated in horse blocking buffer (PBS, 5% horse serum (Sigma-Aldrich), 1% BSA, 1% glycine, 0.1% lysine and 0.4% Triton) for 1 hr at RT and incubated with rabbit anti-Dock7 antibody (28057; IBL) 1:100 and goat anti-Neogenin antibody (AF1079; R&D systems) 1:200 in horse blocking buffer overnight at 4°C. The next day, sections were washed in PBS and incubated with the appropriate Alexa Fluor-labeled secondary antibodies (Invitrogen) at 1:500 for 1 hr at RT. Sections were washed in PBS, counterstained with fluorescent Nissl stain (NeuroTrace, Invitrogen) 1:500 for 15 min at RT, washed in PBS and embedded in Mowiol (Sigma-Aldrich). Staining was visualized using a Zeiss Axioskop 2 microscope and an Olympus FluoView FV1000 confocal microscope.

WESTERN BLOTTING

Cells were collected in ice-cold PBS (pH 7.4) with a cell scraper and centrifuged at 1000 rpm for 5 min in a precooled centrifuge at 4°C. The cell pellet was resuspended in ice-cold lysis buffer (20 mM Tris-HCl, pH 8, 150 mM KCl, 1% Triton X-100 and Complete protease inhibitor cocktail (Roche)), incubated on ice for 10 min, followed by centrifugation at 14,000 rpm for 15 min at 4°C. For immunoblotting with phosphoepitope-specific antibodies, cells were collected in ice-cold lysis buffer (20 mM Tris-HCl, pH 8, 150 mM NaCl, 10% glycerol, 1% NP-40, 5 mM EDTA, 20 mM β-glycerophosphate, 1mM Na_3VO_4 and Complete protease inhibitor cocktail (Roche))

with a cell scraper, incubated on ice for 10 min, followed by centrifugation at 14,000 rpm for 15 min at 4°C. Supernatant were collected in a new Eppendorf tube, NuPAGE LDS sample buffer (Invitrogen) with 2.5% β-mercaptoethanol was added and the samples were boiled for 5 min at 90°C. Proteins were separated in 8% SDS-PAGE gels and transferred onto nitrocellulose membrane (Hybond-C Extra; Amersham). Membranes were incubated in BSA blocking buffer (TBS, 0.05% (v/v) Tween 20 and 2% BSA) for immunoblotting with phosphoepitope-specific antibodies and in blocking buffer (PBS, 0.05% (v/v) Tween 20 and 5% milk powder) for all other antibodies for 30 min at RT. Membranes were incubated with corresponding primary antibodies in blocking buffer overnight at 4°C. Antibodies used: rabbit anti-Dock7 antibody (28057; IBL, 1:500); rabbit anti-(pTyr1118)Dock7 antibody (28079; IBL, 1:100); mouse anti-FLAG (Stratagene, 1:2000); goat anti-Neogenin antibody (AF1079; R&D systems, 1:2000); mouse anti-α-Tubulin antibody (T5168; Sigma-Aldrich, 1:8000); rabbit anti-Op18/stathmin antibody (a kind gift of André Sobel, 1:8000) and rabbit anti-(pS16)Op18/stathmin antibody (a kind gift of André Sobel, 1:2500). Blots were incubated with SuperSignal West Dura Extended Duration Substrate (Pierce) and exposed to ECL films (Pierce).

IMMUNOPRECIPITATION

For endogenous pull down and co-immunoprecipitation experiments, P0 mouse brains or cells (10-cm plates) were lysed in lysis buffer (20 mM Tris-HCl, pH 8.0, 150 mM NaCl, 1% NP-40, 10% glycerol and Complete protease inhibitor cocktail (Roche)) and incubated for 30 min in a rotor and centrifuged at 14,000 rpm for 15 min at 4°C. Cleared supernatants were incubated with 1 µg of the indicated antibodies at 4° C. After 2 hrs, 10 µl protein A/G Dynabeads (Invitrogen), which had been blocked in blocking buffer (20 mM Tris-HCl, pH 8.0, 150 mM KCl, 20% glycerol and 200 ng/µl albumin from chick egg white (Sigma-Aldrich)) were added and samples were incubated for 1 hour rotating at 4°C. Pull down samples were washed 3 times in washing buffer (20 mM Tris-HCl, pH 8.0, 150 mM NaCl, 1% NP-40 and 10% glycerol) and precipitated proteins were eluted by boiling the beads in NuPAGE LDS sample buffer (Invitrogen) with 2.5% β-mercaptoethanol for 10 min at 70°C.

For endogenous pull down followed by immunoblotting with phosphoepitope-specific antibodies, cells were lysed in ice-cold lysis buffer (20 mM Tris-HCl, pH 8, 150 mM NaCl, 10% glycerol, 1% NP-40, 5 mM EDTA, 20 mM β-glycerophosphate, 1mM Na_{3VO4} and Complete protease inhibitor cocktail), incubated for 30 min on ice and centrifuged at 14,000 rpm for 15 min at 4°C. Cleared supernatants were incubated with 1 µg of the indicated antibodies at 4° C. After 2 hrs, 10 µl protein A/G Dynabeads, which had been blocked in blocking buffer, were added and samples were incubated for 1 hour rotating at 4°C. Pull down samples were washed 3 times in washing buffer (20 mM Tris-HCl, pH 8, 150 mM NaCl, 10% glycerol, 1% NP-40, 5 mM EDTA, 20 mM β-glycerophosphate and 1mM Na3VO4) and precipitated proteins were eluted by boiling the beads in NuPAGE LDS sample buffer with 2.5% β-mercaptoethanol for 10 min at 70°C.

NEURONAL CULTURE

E14.5 cerebral cortices were dissected and dissociated in 0.25% trypsin (PAA) in DMEM/F12 (Gibco, Invitrogen) for 15 min at 37°C. Trypsin was inactivated by adding an equal volume of DMEM/F12 containing 20% FBS (Lonza, BioWhittaker). Cerebral cortices were dissociated by trituration in DMEM/F12 containing 10% FBS and 20 µg/ml DNase I (Roche) using a fire-polished Pasteur pipette. Dissociated cortical neurons were cultured in Neurobasal medium (Gibco, Invitrogen) containing 2 mM L-glutamine (PAA), 1x pen/strep (PAA) and B-27 Supplement (Gibco, Invitrogen) on 100 µg/ml poly-L-lysine-coated (Sigma-Aldrich) acid-washed coverslips in a humidified atmosphere with 5% CO_2 at 37°C.

NEURITE OUTGROWTH ASSAY

Dissociated cortical neurons (400.000/50 µl sample) were electroporated with 4 µg DNA in 50 µl electroporation buffer (135 mM KCl, 2 mM $MgCl_2$, 0.2 mM $CaCl_2$ and 5 mM EGTA, pH 7.3) using a BTX Electro Square Porator ECM 830 (BTX Harvard Apparatus; settings: 100 V, 3 pulses, 900 µs pulse length, 2 s pulse interval). 170 µl 37°C RPMI 1640 medium (Gibco, Invitrogen) was added to the electroporation sample and electroporated neurons were transferred to 4 wells of a 24-well plate. Electroporated neurons were cultured on a confluent layer of CHO or CHO-RGMa cells in DMEM/F12 (Gibco, Invitrogen) containing 2% FBS (Lonza, BioWhittaker), 2 mM L-glutamine (PAA), 1x pen/strep (PAA) and B-27 Supplement (Gibco, Invitrogen) in a humidified atmosphere with 5% CO_2 at 37°C. After 4 days cells were fixed with 4% PFA for 15 min at RT and washed in PBS (pH 7.4). Cells were permeabilized and blocked in blocking solution (PBS, 4% BSA and 0.1% Triton) for 1 hr at RT and incubated with rabbit anti-GFP (A11122; Invitrogen) at 1:3000 and mouse anti-β-III-Tubulin (MMS-435P; Covance) at 1:2000 in blocking solution overnight at 4°C. The next day, sections were washed in PBS and incubated with Alexa Fluor 594 goat anti-mouse and Alexa Fluor 488 goat anti-rabbit (Invitrogen) at 1:500 for 1 hr at RT. Images were taken using a Cellomics ArrayScan VTI HCS Reader (Thermo Scientific) and the length of the longest neurite was measured using NeuronJ (Meijering *et al*. 2004). Data were statistically analyzed by two-tailed Student´s t-test and represented as means ±SEM.

RESULTS

DOCK7 AND NEOGENIN INTERACT *IN VIVO*

In vivo GFP-Neogenin pull down on brain lysates of *Syn-GFP-Neogenin* transgenic mice (see Chapter 5) identified Dock7 as a putative Neogenin-interacting protein. Dock7 is a GTPase guanine nucleotide exchange factor (GEF) and controls axon formation and myelination through activation of Rac and/or Cdc42 GTPases (Torii *et al*. 2012, Watabe-Uchida *et al*. 2006, Yamauchi *et al*. 2008, Yamauchi *et al*. 2011). Recently, Dock7 has also been shown to be involved in neurogenesis and migration during cortex development (Yang *et al*. 2012). Neogenin has

been related to cortical neurogenesis and migration (Andrusiak *et al.* 2011, Bradford *et al.* 2010, Conrad *et al.* 2010, Fitzgerald *et al.* 2006). The functional resemblance of Dock7 and Neogenin hints at a cooperative role for these proteins in cell signaling.

To verify the interaction between Neogenin and Dock7, we performed several co-immunoprecipitation experiments. First, an anti-GFP pull down precipitated GFP-Neogenin from lysate of HEK293 cells transfected with GFP-Neogenin and FLAG-Dock7. Immunoblotting using anti-FLAG antibodies revealed coprecipitation of FLAG-Dock7 (Fig. 1A). Secondly, endogenous pull down experiments on N1E-115 neuroblastoma and mouse P0 whole brain lysates specifically detected Neogenin in Dock7 pull down samples (Fig. 1B, C). In control pull down experiments, using a non-specific anti-IgG rabbit antibody, Neogenin was not detected. Together, these pull down experiments confirm the interaction between Neogenin and Dock7 and reveal the presence of this protein complex in the embryonic mouse brain.

NEOGENIN AND DOCK7 COLOCALIZE IN CORTICAL NEURONS

To explore a potential role for Dock7 in RGMa-Neogenin signaling during neurodevelopment, we investigated the expression of *RGMa*, *Neogenin* and *Dock*7 in E16.5 mouse cortex by *in situ* hybridization. We detected strong *RGMa* expression in the cortical plate (CP) and in the ventricular zone (VZ) (Fig. 2A, A'). *Neogenin* expression was detected in all layers of the developing cortex, with very strong expression in the outer cell layers of the CP (Fig. 2B, B'). *Dock*7 expression was observed throughout the different cortical layers and was most prominent in the CP (Fig. 2C, C'). In all, *in situ* hybridization revealed overlapping expression of Dock7 and Neogenin in the mouse embryonic cortex, especially in the CP and VZ.

Next, we used immunohistochemistry to study colocalization of Dock7 and Neogenin. Immunostaining revealed colocalization of Neogenin and Dock7 in the marginal zone, the CP and in a subset of cortical axons in the external capsule (Fig. 3A-C'). Moderate to very strong Dock7 expression was observed in the cytoplasm of different cortical neurons. Neogenin expression was detected in the cytoplasm as well, as in the cell membranes of cortical neurons. Confocal imaging of E14.5 mouse dissociated cortical neurons cultured for two days *in vitro* (DIV2) revealed colocalization of Neogenin and Dock7 in the cytoplasm and at the cell membrane (Fig. 3D-F). Furthermore, despite different expression patterns, colocalization of Neogenin and Dock7 was also observed in the axon and growth cone (Fig. 3D-F´). Together, co-expression and colocalization of Dock7 and Neogenin in the mouse embryonic cortex hints at a cooperative function of these proteins during neurodevelopment.

KNOCKDOWN OF DOCK7 BLOCKS RGMA-NEOGENIN-MEDIATED NEURITE OUTGROWTH INHIBITION

Activation of Neogenin signaling by RGMa in cortical neurons induces growth cone collapse and inhibits neurite outgrowth (Hata *et al.* 2009, Schaffar *et al.* 2008). To investigate a potential role for Dock7 in RGMa-Neogenin-induced neurite outgrowth inhibition we tested the effect

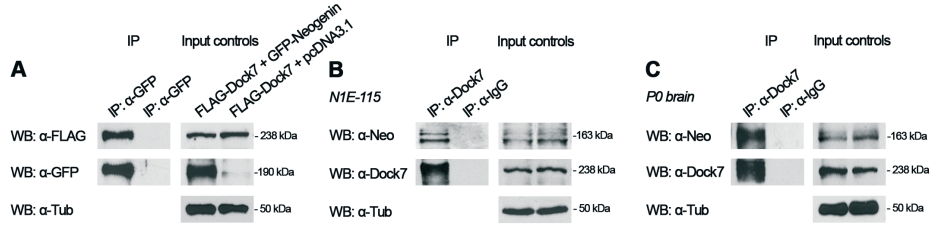

FIGURE 1. Dock7 interacts with Neogenin *in vivo*.

(A) Anti-FLAG immunoblotting detects FLAG-Dock7 in an anti-GFP pull down experiment for GFP-Neogenin, both transiently expressed in HEK293 cells. (B, C) Immunoblotting shows co-immunoprecipitation of Neogenin in an endogenous pull down experiment for Dock7 in N1E-115 neuroblastoma cells (B) or P0 mouse brain lysate (C). Dock7, dedicator of cytokinesis 7; GFP, green fluorescent protein; IP, immunoprecipitation; Neo, Neogenin; Tub, tubulin; WB, Western blot.

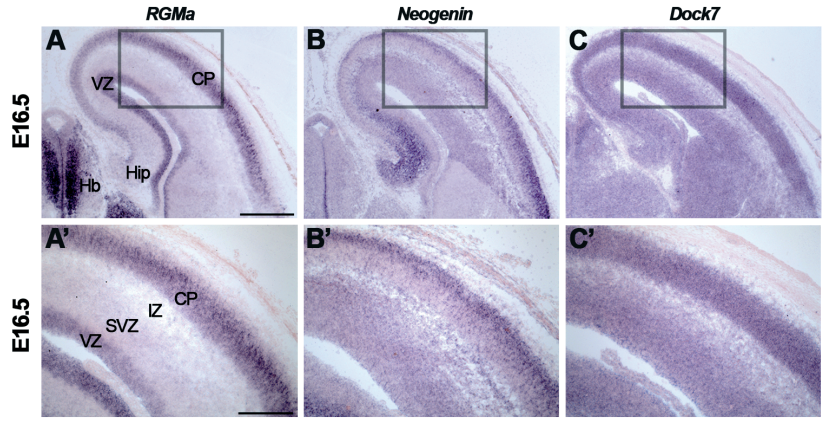

FIGURE 2. *Neogenin* and *Dock7* are strongly expressed in the mouse embryonic cortex.

In situ hybridization on coronal E16.5 mouse brain sections. Panels A'-C' show higher magnifications of the boxed areas in A-C. (A, A') Strong *RGMa* expression is detected in the cortical plate (CP) and ventricular zone (VZ). (B, B') *Neogenin* expression is most prominent in the outer layers of the CP. (C, C') *Dock7* is ubiquitously expressed in the developing cortex with strong expression in the CP. Hb, habenula; Hip, hippocampus; IZ, intermediate zone; SVZ, subventricular zone. Scale bar A-C 500 µm and A'-C' 250 µm.

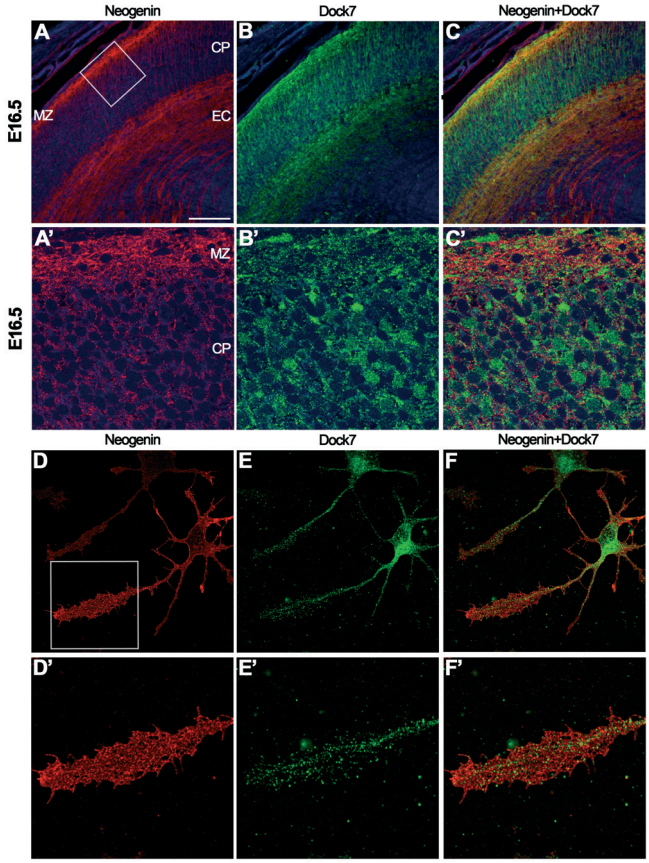

FIGURE 3. Colocalization of Neogenin and Dock7 in E16.5 mouse cortical neurons.

Immunohistochemistry on E16.5 coronal mouse brain sections (A-C') and cultured mouse cortical neurons (D-F'). Confocal microscopy images in panels A'-F'. Panels A'-C' show higher magnifications of the cortical plate (CP) and marginal zone (MZ) in A-C (boxed area in A). Panels D'-F' show higher magnifications of the growth cone in D-F (boxed area in D). Sections A-C' are counterstained with fluorescent Nissl in blue. (A-C') Immunohistochemistry revealed strong expression and colocalization of Neogenin and Dock7 in the MZ and cortical plate CP and in a subset of axons in the external capsule (EC). (D-F') Neogenin and Dock7 immunostaining on dissociated cortical neurons detected strong expression and colocalization of Neogenin and Dock7 in the cell body, axon and in the growth cone. Scale bar A-C: 100 µm.

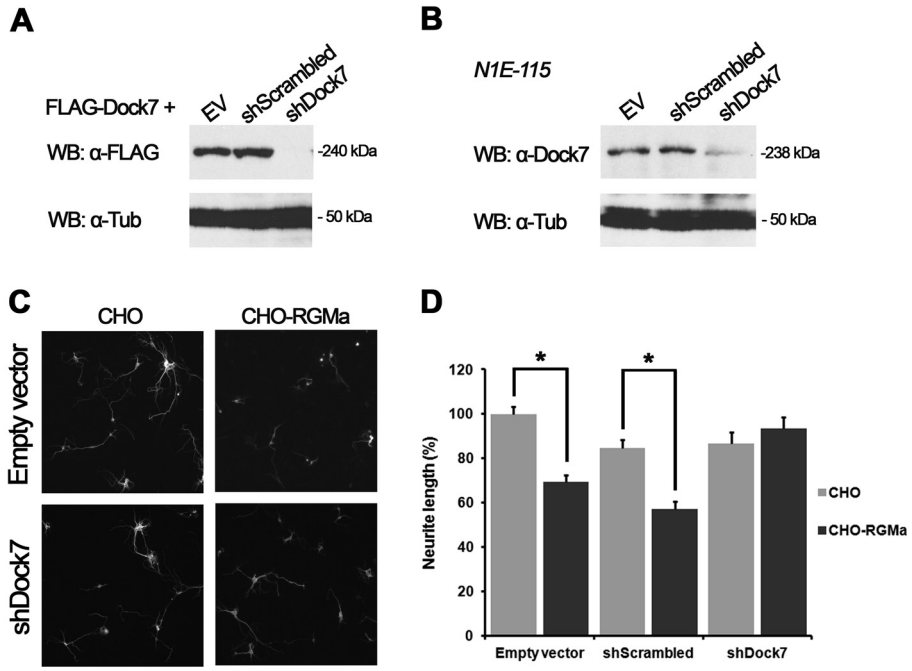

FIGURE 4. Dock7 knockdown blocks RGMa-Neogenin-induced neurite outgrowth inhibition.

(A) Anti-FLAG immunoblotting reveals shRNA-mediated knockdown of FLAG-Dock7 transiently expressed in HEK293 cells, using a Dock7-specific shRNA, compared to scrambled shRNA or pSuper empty vector. Anti-α-Tubulin immunoblotting is used as loading control. (B) Dock7 shRNA induces a strong knockdown of endogenous Dock7 in N1E-115 neuroblastoma cells. (C) Neurite outgrowth of dissociated cortical neurons electroporated with pSuper empty vector is reduced when cultured on a confluent layer of CHO-RGMa cells compared to CHO control cells, as revealed with anti-β-III-Tubulin staining. No reduction in neurite length is observed in dissociated cortical neurons electroporated with Dock7 shRNA. (D) Dissociated cortical neurons are electroporated with pSuper empty vector, pSuper-shScrambled or pSuper-shDock7 and cultured on a confluent layer of CHO control or CHO-RGMa cells for 4 days. Graph shows average length of the longest neurite per neuron ±SEM, *p<0.001, Student T-test. The average neurite length of the empty vector-transfected cells on control CHO cells was set to 100%. EV, empty vector; sh, short hairpin; Tub, tubulin; WB, Western blot.

of Dock7 knockdown in a neurite outgrowth assay of dissociated cortical neurons plated on a confluent layer of either RGMa-expressing CHO cells (CHO-RGMa) or control CHO cells (Hata *et al.* 2006). Dock7 shRNA (Watabe-Uchida *et al.* 2006) used in these experiments induced the specific knockdown of FLAG-Dock7 in HEK293 cells, compared to a scrambled shRNA or an empty vector control, as revealed by anti-FLAG immunoblotting (Fig. 4A). In

addition, Dock7 shRNA induced a strong and specific knockdown of endogenous Dock7 in N1E-115 neuroblastoma cells (Fig. 4B). In the neurite outgrowth assay, dissociated mouse E14.5 cortical neurons were electroporated with Dock7 shRNA, scrambled shRNA or pSuper empty vector and plated on CHO-RGMa or control CHO cells. After four days, images were taken randomly of the cultured neurons using a Cellomics ArrayScan (Thermo Scientific) and neurite length was analyzed with NeuronJ. In these experiments, the length of the longest neurite per neuron was measured. A significant reduction in neurite length was detected in cortical neurons electroporated with the pSuper empty vector or scrambled shRNA when cultured on CHO-RGMa cells compared to control CHO cells (Fig. 4C, D). However, cortical neurons electroporated with Dock7 shRNA did not display a difference in neurite length between neurons cultured on CHO-RGMa or control CHO cells (Fig. 4C, D). These results reveal a requirement for Dock7 in RGMa-Neogenin-induced neurite outgrowth inhibition in cortical neurons.

NO EFFECT OF RGMA STIMULATION ON DOCK7 AND OP18/STATHMIN PHOSPHORYLATION

Phosphorylation of Dock7 at tyrosine 1118 (Tyr^{1118}) is the only regulatory mechanism of Dock7 activity known so far (Yamauchi *et al.* 2008). Dock7 interacts directly with ErB2 in the ErbB2/3 signaling pathway that regulates Schwann cells migration. Schwann cells are myelin-forming glia that migrate along axons and ensheath axons with myelin sheets (Bunge 1993). Upon activation of ErbB2/3 by neuregulin-1, Dock7 becomes phosphorylated at Tyr-1118, which leads to activation of the downstream signaling molecules Rac and Cdc42, and c-Jun N terminal kinase (Yamauchi *et al.* 2008).

To investigate whether RGMa affects Tyr-1118 phosphorylation of Dock7, N1E-115 neuroblastoma cells were stimulated with RGMa-Fc or control Fc protein for 30 min, followed by Dock7 immunoprecipitation. Dock7 pull down samples were analyzed by immunoblotting with a specific antibody recognizing Dock7 phosphorylated at Tyr-1118 (Fig. 5A). No change in Tyr-1118 phosphorylation of Dock7 was detected in N1E-115 cells stimulated with RGMa-Fc as compared to control Fc protein.

Dock7 is also required in the laminin-dependent phosphorylation and inactivation of the microtubule-destabilizing protein Op18/stathmin (Watabe-Uchida *et al.* 2006). Inactivation of Op18/stathmin by Dock7 promotes neuronal polarization and axon formation. In developing neurons, Dock7 and phosphorylated Op18/stathmin are asymmetrically distributed and strongly expressed in the developing axon compared to the future dendrites (Watabe-Uchida *et al.* 2006). To investigate whether RGMa-Neogenin-Dock7 signaling regulates phosphorylation of Op18/stathmin on serine 16 (S16), N1E-115 cells expressing GFP-tagged Op18/stathmin were stimulated with RGMa-Fc or control Fc protein for 30 min. Cell lysates were analyzed with antibodies specific for Op18/stathmin and phosphorylated Op18/stathmin (Op18-S16-P). This experiment did not reveal a difference in Op18/stathmin phosphorylation levels between

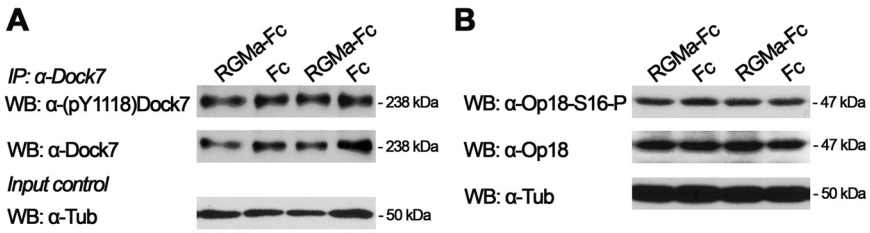

FIGURE 5. RGMa stimulation does not affect phosphorylation of Dock7 and Op18/stathmin.

(A) RGMa treatment (30 min incubation) did not change Dock7 Tyr-1118 phosphorylation in endogenous Dock7 pull down samples from N1E-115 cells. (B) RGMa did not induce a change in Op18/stathmin-GFP S16 phosphorylation levels in N1E-115 cell lysates transiently expressing Op18/stathmin-GFP cDNA. Fc, immunoglobulin Fc tag; IP, immunoprecipitation; Op18; Op18/stathmin; Tub, tubulin; WB, Western blot.

RGMa- or control-stimulated N1E-115 cells (Fig. 5B). In all, these preliminary immunoblotting experiments on Dock7 and Op18/stathmin using phospho-epitope-specific antibodies do not support a role for the phosphorylation of Dock7 and Op18/stathmin downstream of RGMa.

DISCUSSION

DOCK7 AND NEOGENIN SIGNALING IN AXON GUIDANCE

Despite the identification of several components of the Neogenin signaling pathway, our understanding of the RGMa-Neogenin signaling cascade leading to axon repulsion is still rudimentary. In this study we reveal an *in vivo* interaction between Neogenin and Dock7, a novel Neogenin-interacting protein identified in an *in vivo* proteomics screen on Neogenin-interacting proteins using *Syn-GFP-Neogenin* transgenic mouse brains (see Chapter 5). Dock7 belongs to the superfamily of Dock180-related proteins, that function as atypical GEFs for Rac and Cdc42 small GTPases (Cote and Vuori 2002, Miyamoto and Yamauchi 2010). Several Dock180 family members have been implicated in axon and dendrite formation (Kuramoto *et al.* 2009, Ueda *et al.* 2008, Watabe-Uchida *et al.* 2006). Dock7 has also been shown to regulate neuronal polarity and axon formation in hippocampal neurons (Watabe-Uchida *et al.* 2006).

We investigated the role of Dock7 in RGMa-Neogenin-induced neurite outgrowth inhibition, using a neurite outgrowth assay. ShRNA-mediated knockdown of Dock7 blocked the neurite outgrowth-inhibiting effect of RGMa on cortical neurons, revealing the requirement of Dock7 in RGMa-Neogenin-induced neurite outgrowth inhibition. In light of these observations it is interesting that a direct interaction between deleted in colorectal cancer (DCC), a close homologue of Neogenin, and Dock180 is essential to mediate Netrin-1-induced axon attraction, through activation of Rac and Cdc42 (Li *et al.* 2008). Rac and Cdc42 GTPase activity

has been shown to promote axon outgrowth activity in different signaling cascades (Bashaw and Klein 2010). Therefore, RGMa-activated Neogenin signaling may inhibit the activity of these GTPases through its interaction with Dock7 in order to inhibit axon outgrowth. It is currently not known whether RGMa-Neogenin signaling induces changes in Rac and Cdc42 activity. In an experiment in which dorsal root ganglia neurons were stimulated with RGMa, only changes in active Rho GTPase levels were observed but no changes in Rac and Cdc42 activity were reported (Conrad *et al.* 2007).

In addition to its role in axon formation, Dock7 is also involved in signaling mechanisms regulating Schwann cell migration, differentiation and myelination (Torii *et al.* 2012, Yamauchi *et al.* 2008, Yamauchi *et al.* 2011). In Schwann cells, Dock7 Tyr-1118 phosphorylation activates the Rac/Cdc42/JNK signaling cascade which promotes Schwann cell migration. During embryonic and early postnatal stages when Schwann cell migration takes place, Dock7 expression and Tyr-1118 phosphorylation levels are very high. These levels decrease at later postnatal stages when Schwann cell differentiation and myelination occur. In Dock7 shRNA transgenic mice a strong reduction of Dock7 levels results in a decrease in Rac/Cdc42/JNK activity, leading to increased Schwann cell myelination (Torii *et al.* 2012).

We performed an experiment to study the effect of RGMa on Dock7 Tyr-1118 phosphorylation. Immunoblotting experiments did not show an effect of RGMa on Dock7 Tyr-1118 phosphorylation (Fig. 5A). However, further experiments are needed to validate this observation. Apart from Tyr-1118 phosphorylation, Dock7 activity could also be regulated by other signaling proteins that for example change the interaction of Dock7 with Neogenin upon RGMa stimulation. For Dock180 activation of Rac GTPases, Dock180 needs to form a complex with two specific adaptor proteins in order to execute its GEF function for Rac (Kiyokawa *et al.* 1998, Miyamoto and Yamauchi 2010, Valles *et al.* 2004). Further studies are needed to elucidate Dock7 regulation and mechanism-of-action downstream of Neogenin signaling.

NEOGENIN AND DOCK7 IN CORTICAL DEVELOPMENT AND CYTOSKELETON SIGNALING

In this study we revealed strong co-expression and colocalization of Dock7 and Neogenin throughout all layers of the developing E16.5 mouse cortex. Former studies have shown strong expression of Dock7 and Neogenin in zones of active neurogenesis in the developing cortex (Fitzgerald *et al.* 2006, Yang *et al.* 2012, Chapter 3). Interestingly, Yang *et al.* 2012, revealed an important role for Dock7 in neurogenesis and migration during cortex development. Dock7 was shown to regulate the generation of basal progenitors and neurons from radial glial progenitors cells (Yang *et al.* 2012). Furthermore, Dock7 signaling also mediates the switch between proliferation and differentiation of these cells by controlling their apically directed interkinetic nuclear migration (Yang *et al.* 2012). Depletion of Dock7 accelerates apically directed interkinetic nuclear migration, resulting in extended residence and enhanced proliferation of radial glial progenitor cells at apical positions. In contrast, overexpression of Dock7 promotes

the differentiation of radial glial progenitor cells into neurons. Dock7 controls interkinetic nuclear migration by interacting with and antagonizing the microtubule growth-promoting function of TACC3 (Yang *et al.* 2012).

Several other recent studies implicate Dock7 function in the regulation of cytoskeleton dynamics. For example, a requirement for Dock7 in laminin-dependent Op18/stathmin phosphorylation was revealed, through Dock7-mediated activation of Rac. Op18/stathmin is a microtubule-destabilizing protein and its phosphorylation on S16 blocks its activity, resulting in microtubule extension and neurite outgrowth. For RGMa-activated Neogenin signaling, a decrease in Op18/stathmin S16 phosphorylation and increase in Op18/stathmin activity is expected, promoting microtubule instability and neurite retraction. Our preliminary data did not show an effect of RGMa on Op18/stathmin S16 phosphorylation in N1E-115 cells (Fig. 5B).

A recent study revealed that myosin VI, an actin-interacting protein, is a direct interactor of Dock7 and colocalizes with Dock7 in *in vitro* cultures of primary hippocampal neurons (Majewski *et al.* 2012). Myosin VI functions in the organization of actin networks in the cytoplasm and as a motor protein that transports cargos to the minus end of actin filaments (Frank *et al.* 2004, Loubery *et al.* 2012). Another link of Dock7 function to the regulation of the actin cytoskeleton comes from the finding that Dock7 is a putative interactor of molecule interacting with CasL 1 (MICAL-1) (Y. Zhou and R.J. Pasterkamp, unpublished results). *Drosophila* Mical directly binds and modifies the actin cytoskeleton (Hung *et al.* 2010). MICALs can induce disassembly of the actin cytoskeleton through their monooxygenase domain and redox signaling (Hung *et al.* 2011). In addition, MICALs also affect the cytoskeleton indirectly through their interaction with a multitude of signaling proteins, as for example NDR2 kinase, CRMP2 and members of the p130 Cas family (Bouton *et al.* 2001, Suzuki *et al.* 2002, Zhou *et al.* 2011).

In this study we revealed an *in vivo* interaction between Dock7 and Neogenin and its requirement in RGMa-Neogenin-mediated neurite outgrowth inhibition of cortical neurons. For future research, it will be challenging to elucidate the signaling mechanism of Dock7 in the RGMa-Neogenin pathway. Dock7 might mediate repulsive Neogenin signaling through myosin VI, Op18/stathmin or MICALs, all signaling molecules that modulate cytoskeleton dynamics. Both Neogenin and Dock7 function has been related to diverse developmental processes in cortex development, like neurogenesis, differentiation and migration. It will be challenging to elucidate whether RGMa-Neogenin-Dock7 signaling has a role in these neurodevelopmental processes as well.

ACKNOWLEDGEMENT

We are thankful to Toshihide Yamashita for providing us with CHO and CHO-RGMa cell lines, to André Sobel for sharing anti-Op18/stathmin and anti-Op18/stathmin-S16-P antibodies, to Linda van Aelst for her gift of pcDNA3.1/CMV-Flag-Dock7 and to Karin Boekhoorn for

sharing Op18/stathmin-GFP cDNA. This work was supported by HFSP (CDA), NWO (VIDI) and Hersenstichting Nederland grants to R.J.P.

REFERENCE LIST

Andrusiak, M. G., K. A. McClellan, D. Dugal-Tessier, L. M. Julian, S. P. Rodrigues, D. S. Park, T. E. Kennedy, and R. S. Slack. 2011. Rb/E2F regulates expression of neogenin during neuronal migration. Mol. Cell Biol. 31:238-247.

Bashaw, G. J. and R. Klein. 2010. Signaling from axon guidance receptors. Cold Spring Harb. Perspect. Biol. 2:a001941.

Bouton, A. H., R. B. Riggins, and P. J. Bruce-Staskal. 2001. Functions of the adapter protein Cas: signal convergence and the determination of cellular responses. Oncogene 20:6448-6458.

Bradford, D., R. L. Faull, M. A. Curtis, and H. M. Cooper. 2010. Characterization of the netrin/RGMa receptor neogenin in neurogenic regions of the mouse and human adult forebrain. J. Comp Neurol. 518:3237-3253.

Brinks, H., S. Conrad, J. Vogt, J. Oldekamp, A. Sierra, L. Deitinghoff, I. Bechmann, G. Alvarez-Bolado, B. Heimrich, P. P. Monnier, B. K. Mueller, and T. Skutella. 2004. The repulsive guidance molecule RGMa is involved in the formation of afferent connections in the dentate gyrus. J. Neurosci. 24:3862-3869.

Bunge, R. P. 1993. Expanding roles for the Schwann cell: ensheathment, myelination, trophism and regeneration. Curr. Opin. Neurobiol. 3:805-809.

Conrad, S., H. Genth, F. Hofmann, I. Just, and T. Skutella. 2007. Neogenin-RGMa signaling at the growth cone is bone morphogenetic protein-independent and involves RhoA, ROCK, and PKC. J. Biol. Chem. 282:16423-16433.

Conrad, S., F. Stimpfle, S. Montazeri, J. Oldekamp, K. Seid, G. Alvarez-Bolado, and T. Skutella. 2010. RGMb controls aggregation and migration of Neogenin-positive cells *in vitro* and *in vivo*. Mol. Cell Neurosci. 43:222-231.

Cote, J. F. and K. Vuori. 2002. Identification of an evolutionarily conserved superfamily of DOCK180-related proteins with guanine nucleotide exchange activity. J. Cell Sci. 115:4901-4913.

Endo, M. and T. Yamashita. 2009. Inactivation of Ras by p120GAP via focal adhesion kinase dephosphorylation mediates RGMa-induced growth cone collapse. J. Neurosci. 29:6649-6662.

Fitzgerald, D. P., S. J. Cole, A. Hammond, C. Seaman, and H. M. Cooper. 2006. Characterization of neogenin-expressing neural progenitor populations and migrating neuroblasts in the embryonic mouse forebrain. Neuroscience 142:703-716.

Frank, D. J., T. Noguchi, and K. G. Miller. 2004. Myosin VI: a structural role in actin organization important for protein and organelle localization and trafficking. Curr. Opin. Cell Biol. 16:189-194.

Hata, K., M. Fujitani, Y. Yasuda, H. Doya, T. Saito, S. Yamagishi, B. K. Mueller, and T. Yamashita. 2006. RGMa inhibition promotes axonal growth and recovery after spinal cord injury. J. Cell Biol. 173:47-58.

Hata, K., K. Kaibuchi, S. Inagaki, and T. Yamashita. 2009. Unc5B associates with LARG to mediate the action of repulsive guidance molecule. J. Cell Biol. 184:737-750.

Hung, R. J., C. W. Pak, and J. R. Terman. 2011. Direct redox regulation of F-actin assembly and disassembly by Mical. Science 334:1710-1713.

Hung, R. J., U. Yazdani, J. Yoon, H. Wu, T. Yang, N. Gupta, Z. Huang, W. J. van Berkel, and J. R. Terman. 2010. Mical links semaphorins to F-actin disassembly. Nature 463:823-827.

Kiyokawa, E., Y. Hashimoto, T. Kurata, H. Sugimura, and M. Matsuda. 1998. Evidence that DOCK180 up-regulates signals from the CrkII-p130(Cas) complex. J. Biol. Chem. 273:24479-24484.

Kuramoto, K., M. Negishi, and H. Katoh. 2009. Regulation of dendrite growth by the Cdc42 activator Zizimin1/Dock9 in hippocampal neurons. J. Neurosci. Res. 87:1794-1805.

Lah, G. J. and B. Key. 2012. Dual roles of the chemorepellent axon guidance molecule RGMa in establishing pioneering axon tracts and neural fate decisions in embryonic vertebrate forebrain. Dev Neurobiol 72:1458-1470.

Li, X., X. Gao, G. Liu, W. Xiong, J. Wu, and Y. Rao. 2008. Netrin signal transduction and the guanine nucleotide exchange factor DOCK180 in attractive signaling. Nat. Neurosci. 11:28-35.

Loubery, S., C. Delevoye, D. Louvard, G. Raposo, and E. Coudrier. 2012. Myosin VI Regulates Actin Dynamics and Melanosome Biogenesis. Traffic. 13:665-680.

Majewski, L., M. Sobczak, S. Havrylov, J. Jozwiak, and M. J. Redowicz. 2012. Dock7: A GEF for Rho-family GTPases and a novel myosin VI-binding partner in neuronal PC12 cells. Biochem. Cell Biol. 90: 565-574.

Matsunaga, E., H. Nakamura, and A. Chedotal. 2006. Repulsive guidance molecule plays multiple roles in neuronal differentiation and axon guidance. J. Neurosci. 26:6082-6088.

Meijering, E., M. Jacob, J. C. Sarria, P. Steiner, H. Hirling, and M. Unser. 2004. Design and validation of a tool for neurite tracing and analysis in fluorescence microscopy images. Cytometry A 58:167-176.

Metzger, M., S. Conrad, T. Skutella, and L. Just. 2007. RGMa inhibits neurite outgrowth of neuronal progenitors from murine enteric nervous system via the neogenin receptor *in vitro*. J. Neurochem. 103:2665-2678.

Miyamoto, Y. and J. Yamauchi. 2010. Cellular signaling of Dock family proteins in neural function. Cell Signal. 22:175-182.

Monnier, P. P., A. Sierra, P. Macchi, L. Deitinghoff, J. S. Andersen, M. Mann, M. Flad, M. R. Hornberger, B. Stahl, F. Bonhoeffer, and B. K. Mueller. 2002. RGM is a repulsive guidance molecule for retinal axons. Nature 419:392-395.

Pasterkamp RJ, De Winter F, Holtmaat AJ, Verhaagen J (1998) Evidence for a role of the chemorepellent semaphorin III and its receptor neuropilin-1 in the regeneration of primary olfactory axons. J Neurosci 18: 9962-9976.

Rajagopalan, S., L. Deitinghoff, D. Davis, S. Conrad, T. Skutella, A. Chedotal, B. K. Mueller, and S. M. Strittmatter. 2004. Neogenin mediates the action of repulsive guidance molecule. Nat. Cell Biol. 6:756-762.

Reed, S. E., E. M. Staley, J. P. Mayginnes, D. J. Pintel, and G. E. Tullis. 2006. Transfection of mammalian cells using linear polyethylenimine is a simple and effective means of producing recombinant adeno-associated virus vectors. J. Virol. Methods 138:85-98.

Schaffar, G., J. Taniguchi, T. Brodbeck, A. H. Meyer, M. Schmidt, T. Yamashita, and B. K. Mueller. 2008. LIM-only protein 4 interacts directly with the repulsive guidance molecule A receptor Neogenin. J. Neurochem. 107:418-431.

Suzuki, T., T. Nakamoto, S. Ogawa, S. Seo, T. Matsumura, K. Tachibana, C. Morimoto, and H. Hirai. 2002. MICAL, a novel CasL interacting molecule, associates with vimentin. J. Biol. Chem. 277:14933-14941.

Torii, T., Y. Miyamoto, M. Nagao, N. Onami, H. Tsumura, M. Maeda, K. Nakamura, A. Tanoue, and J. Yamauchi. 2012. Knockdown of Dock7 *in vivo* specifically affects myelination by Schwann cells and increases myelin thickness in sciatic nerves without affecting axon thickness. AJMB 2:210-216.

Ueda, S., S. Fujimoto, K. Hiramoto, M. Negishi, and H. Katoh. 2008. Dock4 regulates dendritic development in hippocampal neurons. J. Neurosci. Res. 86:3052-3061.

Valles, A. M., M. Beuvin, and B. Boyer. 2004. Activation of Rac1 by paxillin-Crk-DOCK180 signaling complex is antagonized by Rap1 in migrating NBT-II cells. J. Biol. Chem. 279:44490-44496.

Van den Heuvel, D. M. A., A. J. C. G. M. Hellemons, and R. J. Pasterkamp. 2013. Spatiotemporal expression of repulsive guidance molecules (RGMs) and their receptor Neogenin in the mouse brain. PLOS ONE (in press).

Vielmetter, J., J. F. Kayyem, J. M. Roman, and W. J. Dreyer. 1994. Neogenin, an avian cell surface protein expressed during terminal neuronal differentiation, is closely related to the human tumor suppressor molecule deleted in colorectal cancer. J. Cell Biol. 127:2009-2020.

Watabe-Uchida, M., K. A. John, J. A. Janas, S. E. Newey, and A. L. Van Aelst. 2006. The Rac activator DOCK7 regulates neuronal polarity through local phosphorylation of stathmin/Op18. Neuron 51:727-739.

Wilson, N. H. and B. Key. 2006. Neogenin interacts with RGMa and netrin-1 to guide axons within the embryonic vertebrate forebrain. Dev. Biol. 296:485-498.

Yamauchi, J., Y. Miyamoto, J. R. Chan, and A. Tanoue. 2008. ErbB2 directly activates the exchange factor Dock7 to promote Schwann cell migration. J. Cell Biol. 181:351-365.

Yamauchi, J., Y. Miyamoto, H. Hamasaki, A. Sanbe, S. Kusakawa, A. Nakamura, H. Tsumura, M. Maeda, N. Nemoto, K. Kawahara, T. Torii, and A. Tanoue. 2011. The atypical Guanine-nucleotide exchange factor, dock7, negatively regulates schwann cell differentiation and myelination. J. Neurosci. 31:12579-12592.

Yang, Y. T., C. L. Wang, and A. L. Van Aelst. 2012. DOCK7 interacts with TACC3 to regulate interkinetic nuclear migration and cortical neurogenesis. Nat. Neurosci. 15:1201-1210.

Zhou, Y., Y. Adolfs, W. W. Pijnappel, S. J. Fuller, R. C. Van der Schors, K. W. Li, P. H. Sugden, A. B. Smit, A. Hergovich, and R. J. Pasterkamp. 2011. MICAL-1 is a negative regulator of MST-NDR kinase signaling and apoptosis. Mol. Cell Biol. 31:3603-3615.

CHAPTER 7
General discussion

OUTLINE GENERAL DISCUSSION

During neural development a series of precisely ordered cellular processes functions to establish a functional brain comprising millions of neurons and many more neuronal connections. Neogenin and its repulsive guidance molecule (RGM) ligands contribute to neuronal network formation inducing axon repulsion. Furthermore, RGM-Neogenin signaling controls several other developmental processes in the nervous system including neurogenesis, neuronal differentiation, migration and apoptosis.

The aim of this thesis is to characterize Neogenin function and signaling during neural development. These insights will contribute to a better understanding of situations of perturbed neural development that contribute to the onset of neurodevelopmental disorders. In addition, knowledge of RGM-mediated Neogenin signaling mechanisms may generate novel opportunities for the development of therapies to enhance nerve regeneration after injury. In this thesis we expanded the knowledge on Neogenin function and signaling by performing a detailed expression study for Neogenin, RGM ligands and Unc5 coreceptors during mouse brain development. *In situ* hybridization and immunohistochemistry revealed prominent and specific, but also overlapping, expression of Neogenin, RGMa/b and Unc5A-D. In addition, we conducted *in vitro* and *in vivo* proteomics screens in cell lines and brain lysates of synapsin I-driven *GFP-Neogenin* transgenic mice to identify novel Neogenin-interacting proteins. These screens identified numerous putative novel signaling proteins that can be linked to several cellular processes known to be regulated by Neogenin, including neurite formation, gene transcription and cell survival.

In this chapter, I will first discuss putative roles of Neogenin, RGMs and Unc5s in axon bundle formation and neuron migration, supported by our expression pattern analysis. Next, I will discuss the Neogenin proteomics screens and the potential role of two novel Neogenin-interacting proteins: leucine-rich repeats and immunoglobulin-like domains protein 2 (Lrig2) and dedicator of cytokinesis 7 (Dock7) in RGMa-Neogenin-mediated neurite outgrowth inhibition.

1 RGM AND NEOGENIN IN AXON BUNDLE FORMATION

A putative role for RGMs, Neogenin and Unc5s in the development of axon tracts can be inferred from the expression of these proteins in and around axon bundles. RGMs are known to induce repulsion of axons expressing Neogenin and Unc5 coreceptors (Hata *et al.* 2009). Expression of RGMs around axon bundles expressing Neogenin might therefore act to restrict axon growth to specific brain areas and to fasciculate individual axons into tight bundles, as has been shown for other repulsive guidance proteins (Chedotal and Richards 2010). (Co-) expression of RGMs and Neogenin on axon bundles might mediate axon-axon interactions or contribute to the organization of these bundles. In the next two sections these potential novel

roles in axon bundle formation will be discussed, as well as the functional consequences of the co-expression of RGMs and Neogenin in the same axon or neuron.

1.1 RGM AND NEOGENIN IN AXON BUNDLE ADHESION AND ORGANIZATION

One role of axonal RGMa and Neogenin may be to organize axon bundles into sub-bundles expressing RGMa or Neogenin. For example, RGMa-expressing axons traverse the core of the internal capsule, while Neogenin-positive axons occupy its outer parts (see Chapter 3, Fig. 2G, I). We propose that RGMa expression directs Neogenin-positive axons to the outer region of the internal capsule. Such intra-bundle repulsive mechanisms have been shown for other axon guidance ligand-receptor pairs in the organization of sensorimotor projections (Gallarda *et al.* 2008). RGMa- and Neogenin-positive axons are likely to represent axonal projections from different brain areas. Axons of the corticothalamic, thalamocortical, cortico-collicular and corticospinal tracts all pass through the internal capsule. The Neogenin-expressing axons could represent axonal projections from the cortex, which expresses Neogenin. RGMa-expressing axons could arise from the thalamus which exhibits strong RGMa expression (Figure 1).

In addition to regulating axon bundle formation through repulsive mechanisms, RGMs and Neogenin may act in the adhesion of individual axons within bundles. A role for RGMs as potential adhesive cues was revealed in coculture assays, in which dorsal root ganglia (DRG) neurons that express RGMb and Neogenin, showed increased adhesion to RGMb-expressing HEK293 cells. Furthermore, RGMb has been shown to be able to interact with itself in a homophilic manner when expressed in the same cell (*in cis*). However, exogenous RGMb was also able to bind to RGMb-expressing cells, hinting at *trans* interactions between RGMb molecules as well (Samad *et al.* 2004). This invites the speculation that homophilic RGM or heterophilic RGM-Neogenin interactions may mediate axon adhesive effects (Figure 2A-C). However, a functional role for such interactions *in vivo* remains to be shown.

1.2 *CIS* RGM-NEOGENIN INTERACTIONS

Co-expression of RGMs and Neogenin on axon bundles, as observed for numerous axon bundles in our study, may act to regulate the sensitivity of Neogenin to RGMs in the environment (Figure 2D-F). Studies on several ligand-receptor systems reveal that co-expression of ligands and receptors can block signaling to the same ligands presented in trans. For example, ephrin/Eph *cis* interactions on retinal ganglion axons inhibit Eph responsiveness to ephrin gradients in the tectum (Carvalho *et al.* 2006, Hornberger *et al.* 1999). Similarly, co-expression of semaphorin 6A and plexin-A4 in DRG neurons attenuates the axon repulsive effect that is normally induced by semaphorin 6A (Haklai-Topper *et al.* 2010). Evidence for *cis* interactions between RGMs and Neogenin comes from their role in bone morphogenetic protein (BMP) receptor signaling regulating iron homeostasis and endochondral bone development (Zhang *et al.* 2009, Zhou *et al.* 2010). RGMs function as coreceptors for BMP-2 and BMP-4 and associate *in cis* with Neogenin and BMP receptors, thereby enhancing BMP signaling. During endochondral

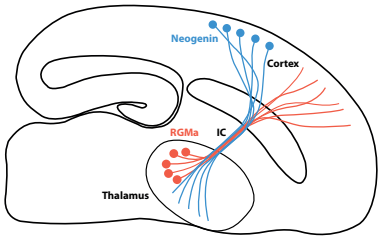

FIGURE 1. RGMa and Neogenin control axon bundle organization.

Schematic model of a putative role for axonal RGMa and Neogenin expression in organizing axonal projections through the internal capsule (IC). RGMa expression on thalamic axons in the core of the IC may direct Neogenin-expressing axons from the cortex projecting to the thalamus to the outer area of the IC.

bone development, *cis* interaction between Neogenin and the RGM-BMP receptor complex is required for the localization of this signaling complex to lipid rafts and activation of Smad signaling (Zhou *et al.* 2010). To test whether *cis* expression of RGMs and Neogenin regulates the sensitivity of axons or neurons to RGM presented *in trans*, RGM expression should be manipulated in neurons that are sensitive to RGM followed by the assessment of the RGMa responsiveness of these neurons. Cerebellar granule neurons (CGNs) represent an excellent model for such experiments. CGNs express high levels of Neogenin and CGN neurite outgrowth is inhibited by RGMa (Hata *et al.* 2006). Dissociated CGNs should be electroporated with an RGMa expression vector and cultured on a confluent layer of RGMa-expressing cells to evaluate the effect of *in cis* neuronal expression of RGMa and Neogenin on the axonal sensitivity to RGMa.

2 RGM-NEOGENIN FUNCTION IN NEURONAL CELL MIGRATION

Functional evidence for a role for RGMs and Neogenin in the regulation of neuronal cell migration comes from *ex vivo* slice culture experiments using RGM or Neogenin overexpression. In hippocampal slice cultures, ectopic expression of RGMb severely disturbs the migration of dentate gyrus precursor cells (Conrad *et al.* 2010). In addition, in slice cultures of the mouse embryonic forebrain, Neogenin overexpression in neuroblasts in the ganglionic eminence (GE) hampers their migration (Andrusiak *et al.* 2011). Interestingly, our detailed expression pattern analysis suggests a more widespread role for RGMs and Neogenin in neuronal cell migration. For example, we and others report prominent expression of RGMa, RGMb and Neogenin in the embryonic cortex and expression of Neogenin in migrating neuroblasts and interneurons (Andrusiak *et al.* 2011, Fitzgerald *et al.* 2006, Gad *et al.* 1997, Oldekamp *et al.* 2004). However, how RGM-Neogenin signaling regulates the migration of these neurons is currently

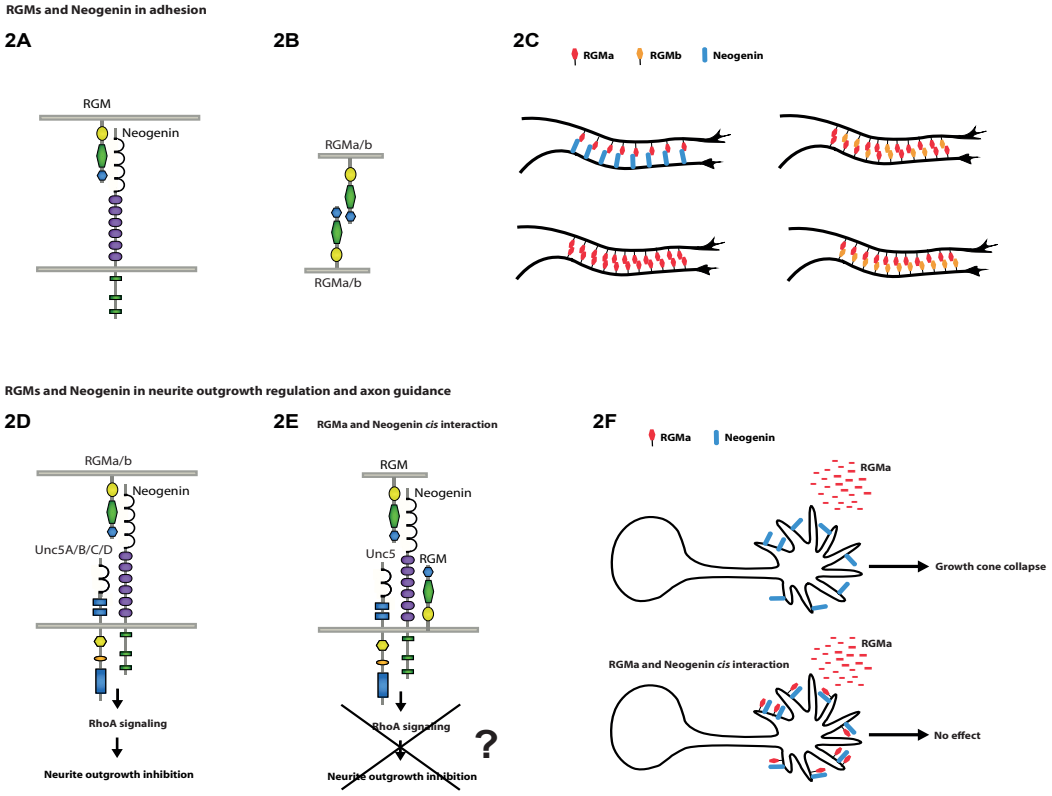

FIGURE 2. RGM, Neogenin and Unc5 interactions during axon bundle development.

Schematic overview of putative interactions between RGMs, Unc5s and Neogenin in neurite outgrowth regulation, axon guidance and adhesion. (A-C) Heterophilic RGM/Neogenin (A) or homophilic RGM/RGM (B) interactions may have adhesive effects (C) during axon bundle development. (D) Binding of RGMa/b to Neogenin mediates activation of RhoA signaling and neurite outgrowth inhibition through association with Unc5 coreceptors. (E, F) *Cis* interactions between RGMa and Neogenin in the same cell could prevent growth cone collapse and axon growth inhibition by RGMa presented *in trans*.

not known. Similar to repulsive signaling by Slits in regulating neuroblast migration (Hu 1999, Nguyen-Ba-Charvet *et al.* 2004, Wu *et al.* 1999), expression of RGMa and RGMb in the cortical VZ/SVZ may direct migrating cortical neurons away from the VZ/SVZ towards the pial surface.

Interestingly, we also detected strong expression of *RGMb* in the striatum at the time of interneuron migration. This observation may help to explain the impaired migration of neuroblasts observed upon overexpression of Neogenin in the GE (Andrusiak *et al.* 2011). Enhanced expression of Neogenin in neuroblasts in the GE might enhance their sensitivity

to the repulsive effects of RGMb and inhibit their migration from the GE. An important future goal is therefore to directly evaluate the effect of RGMb on neuroblast migration *in vitro*, in collagen matrix cell migration assays, and *in vivo*, through the analysis of the *RGMb* knockout mouse (Xia *et al.* 2010). Whether the effects of Neogenin (over)expression in the GE depend on endogenous Unc5 expression is unknown. However, only very weak expression of Unc5A-D was detected in the GE, making their role in GE development doubtful.

3 LRIG2 AND DOCK7 ARE NOVEL COMPONENTS OF THE NEOGENIN SIGNALING CASCADE AND FUNCTION IN RGMA-INDUCED NEURITE OUTGROWTH INHIBITION

Despite the identification of a number of signaling proteins that mediate Neogenin-induced (in) activation of small GTPases and cytoskeletal changes (Conrad *et al.* 2007, Endo and Yamashita 2009, Hata *et al.* 2006, Hata *et al.* 2009, Kubo *et al.* 2008, Zhu *et al.* 2007), our understanding of the RGMa-Neogenin signaling cascade inducing axon outgrowth inhibition and axon repulsion is still incomplete. In addition, the signaling mechanisms in Neogenin-mediated apoptosis signaling and gene transcription are largely unexplored. Neogenin can function as a dependence receptor and in the absence of RGMa activate a signaling pathway which involves death-associated protein (DAP) kinase to induce apoptosis (Fujita *et al.* 2008, Matsunaga *et al.* 2004). Furthermore, RGM binding to Neogenin induces cleavage and release of the Neogenin intracellular domain (NeoICD), which translocates to the nucleus and induces gene transcription (Goldschneider *et al.* 2008). A better understanding of Neogenin signaling mechanisms will not only improve our knowledge of Neogenin functions during neural development, but will also increase our understanding of the role of RGM and Neogenin in injury and disease. Upon injury to the spinal cord, RGM expression is increased around the lesion site and its inhibitory effect on neurite growth blocks effective axonal regeneration (Hata *et al.* 2006). In addition, RGM-Neogenin signaling has recently been implicated in the autoimmune response against myelin causative to multiple sclerosis (Muramatsu *et al.* 2011). Thus, a more complete understanding of RGM-Neogenin signaling mechanisms will contribute to the development of novel therapeutic strategies to treat central nervous system injury and multiple sclerosis.

3.1 NOVEL NEOGENIN SIGNALING PROTEINS

To better characterize Neogenin signaling we performed two proteomics screens to identify novel components of the Neogenin signaling cascade. We conducted an *in vitro* biotin-streptavidin-based Neogenin pull down in HEK293 fibroblast cells (Chapter 4) and an *in vivo* Neogenin pull down on brain lysates of *Syn-GFP-Neogenin* transgenic mice (Chapter 5). In both proteomics screens, mass spectrometry analysis was used to characterize the purified Neogenin signaling complexes. In total, we identified 80 putative novel Neogenin-interacting proteins. Intriguingly, the Neogenin-interacting proteins identified included only one known

Neogenin signaling protein, myosin X. Myosin X was originally identified in a yeast two-hybrid screen using the NeoICD as bait and was also identified as an interactor of NeoICD in our studies (Zhu *et al.* 2007).

The failure to identify any of the other known Neogenin signaling proteins in our proteomics screens may be due to differences in the techniques and material used, i.e. yeast two-hybrid screens versus pull downs in mammalian cells, to identify Neogenin signaling proteins. In experiments following the initial Neogenin pull down experiments, we were able to replicate our findings by combining Neogenin biotin and Neogenin *in vivo* pull down experiments with Western blot analysis using specific antibodies. In addition, the validity of our screens was further confirmed by the identification of 12 proteins that were identified as putative Neogenin-interacting proteins in both Neogenin proteomics screens, but not in unrelated screens in the lab.

In line with the diversity of cell processes in which Neogenin has been implicated, the putative Neogenin-interacting proteins identified in this thesis have been implemented in a broad range of biological functions. A significant number of the Neogenin-interacting proteins are known modulators of the cell cytoskeleton. This is in line with the best-characterized function of Neogenin during neural development, i.e. in neurite outgrowth inhibition and axon repulsion through activation of signaling pathways that act on the cell cytoskeleton (Conrad *et al.* 2007, Endo and Yamashita 2009, Hata *et al.* 2006, Hata *et al.* 2009). Furthermore, modulation of the cell cytoskeleton is also important for other cell processes, like differentiation and migration, in which Neogenin signaling functions (Andrusiak *et al.* 2011, Conrad *et al.* 2010, Lah and Key 2012, Matsunaga *et al.* 2006). In addition to proteins that bind and modulate the actin cytoskeleton, we identified a number of Neogenin-interacting proteins that regulate microtubule cytoskeleton dynamics. For example, CDC42 binding protein kinaseα, dynactin 1, Dock7 and neuron navigator 1 (Culver-Hanlon *et al.* 2006, Harwood and Braga 2003, van Haren *et al.* 2009, Watabe-Uchida 2006, Wilkinson *et al.* 2005). This is intriguing as it is currently unknown whether or how Neogenin regulates the microtubule cytoskeleton.

The role of most novel interactors identified in our proteomics experiments remains to be established. In this thesis we focused on the role of two novel Neogenin-interacting proteins, Lrig2 and Dock7, in RGMa-Neogenin-mediated neurite outgrowth inhibition, as will be reported and discussed in the next two sections.

3.2 LRIG2 MEDIATES REPULSIVE NEOGENIN SIGNALING

Leucine-rich repeats proteins Lrig2 and Lrig3 were identified as Neogenin-interacting proteins in the biotin-streptavidin-based Neogenin pull down in HEK293 fibroblasts (Chapter 4). Lrigs are transmembrane proteins and known modulators of growth factor tyrosine kinase (e.g. ErbB, Met and Ret) receptor signaling (Hedman and Henriksson 2007, Laederich *et al.* 2004, Ledda *et al.* 2008, Shattuck *et al.* 2007, Zhao *et al.* 2008). Despite the identification of Lrig expression in the developing nervous system (Homma *et al.* 2009, Ledda *et al.* 2008, Suzuki *et al.* 1996),

their functions during neural development are largely unexplored. So far the only functional evidence for Lrig function in neural development comes from the observation that Lrig1 inhibits glial cell line-derived neurotrophic factor (GDNF)-activated Ret signaling in neurons. Overexpression of Lrig1 in a culture of primary superior cervical ganglion (SCG) neurons blocks GDNF-Ret-mediated cell differentiation and neurite outgrowth (Ledda *et al.* 2008). Association of Lrig1 to Ret blocks Ret receptor signaling by inhibiting the binding of GDNF ligands and GFRα coreceptors to Ret, thereby blocking the recruitment of Ret to lipid rafts (Ledda *et al.* 2008). Localization of Ret receptors to lipid rafts is essential for the activation of Ret signaling pathway leading to mitogen-activated protein kinase (MAPK) activation.

To explore a role for Lrigs in Neogenin-mediated functions during neural development we analyzed the expression of Neogenin, Lrig1, -2 and -3 in E16.5 mouse brains. *In situ* hybridization experiments revealed that expression of *Lrig*1 and *Lrig*3 was rather weak and restricted to a few brain areas. In contrast, prominent and overlapping expression of *Lrig*2 and *Neogenin* was detected in the cortex and in DRG neurons (see Chapter 4). In addition, immunohistochemistry and immunoprecipitation experiments revealed the *in vivo* colocalization and interaction of Lrig2 and Neogenin, hinting at a cooperative function for Lrig2 and Neogenin during neural development. Indeed, by using a functional neurite outgrowth assay we unveiled a requirement for Lrig2 in RGMa-Neogenin-mediated repulsive signaling in cortical neurons. The mechanisms through which Lrig2 modulates RGMa-Neogenin signaling are currently not known. In the next paragraph we discuss putative roles for Lrig2 in mediating localization of the Neogenin receptor complex to lipid rafts and in terminating Neogenin signaling by mediating Neogenin receptor endocytosis.

3.2.1 Lrig2 in lipid raft localization and signal termination

In GDNF-Ret signaling, association of Lrig1 to Ret receptors affects the localization of the Ret signaling complex on the cell membrane favoring Ret receptor localization outside lipid rafts (Ledda *et al.* 2008). In a similar fashion Lrig2 may regulate the raft localization of Neogenin (Figure 3). Evidence for Neogenin localization to lipid rafts comes from its role in BMP signaling during endochondral bone formation (Zhou *et al.* 2010). Association of Neogenin with the BMP/RGM/BMP receptor complex is essential for the localization of this signaling complex to lipid rafts, required for effective BMP receptor-mediated activation of Smad signaling (Zhou *et al.* 2010). In addition, localization of the Neogenin homologue DCC to lipid rafts is essential for mediating the attractive effects of Netrin-1 (Guirland *et al.* 2004, Herincs *et al.* 2005). However, whether localization of Neogenin to lipid rafts is a requirement for Neogenin functions during neural development remains to be shown.

Lrig2 could also be involved in controlling Neogenin receptor levels. Lrig1 inhibits ErBb and Met receptor signaling by inducing receptor ubiquitylation and degradation (Gur *et al.* 2004, Laederich *et al.* 2004, Shattuck *et al.* 2007). Also, binding of Lrig3 to FGF-1 receptors attenuates FGF-1 signaling by decreasing FGF-1 levels (Zhao *et al.* 2008). In the thesis, we started to

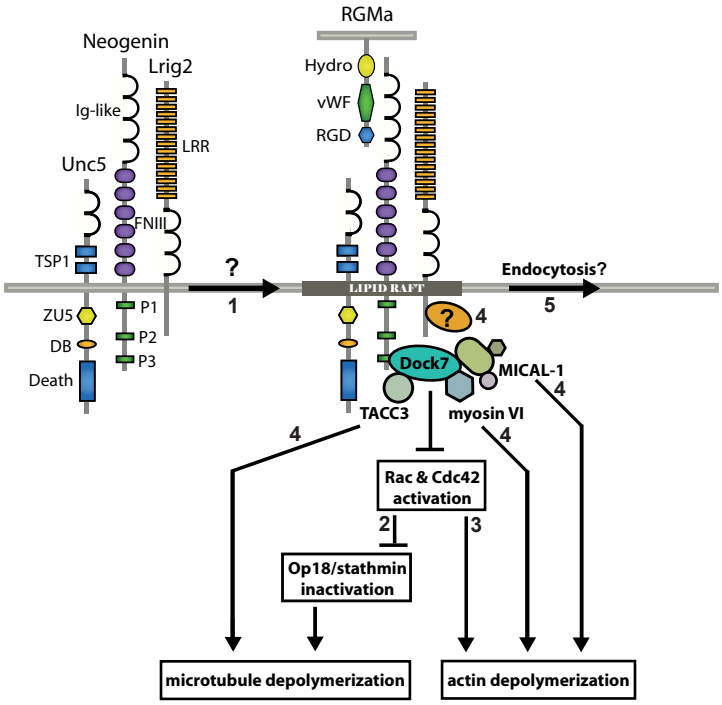

FIGURE 3. Model of the role of Lrig2 and Dock7 during RGMa-Neogenin signaling.

Lrig2 and Dock7 may contribute to RGMa-Neogenin signaling in different ways. 1) Binding of RGMa to Neogenin may induce Lrig2-mediated transport of the Neogenin receptor complex to lipid rafts. 2) Activation of the Neogenin receptor by RGMa may induce dephosphorylation and inactivation of Dock7, thereby blocking Dock7-mediated activation of Rac and Cdc42 GTPases and the inactivation of the microtubule destabilizing protein Op18/stathmin, leading to depolymerization of the microtubule cytoskeleton. 3) Alternatively, RGMa-Neogenin-mediated inactivation of Dock7 may block the actin growth promoting activities of Rac and Cdc42. 4) In addition, both Dock7 and Lrig2 may mediate repulsive RGMa-Neogenin signaling through their association with other cell signaling molecules. No signaling proteins that associate with the Lrig2 intracellular domain have been identified so far. However, the Dock7 binding proteins TACC3, myosin VI and MICAL-1 may induce depolymerization of the microtubule or actin cytoskeleton, respectively. 5) Following activation of the Neogenin signaling cascade by RGMa, Lrig2 may terminate Neogenin signaling by inducing endocytosis of the Neogenin receptor complex. DB, DCC-binding; Dock7, dedicator of cytokinesis 7; Hydro, hydrophobic; FNIII; fibronectin type III; Ig; immunoglobulin; LamNT, laminin N-terminal domain; Lrig2, leucine-rich repeats and immunoglobulin-like domains protein 2; LRR, leucine-rich repeats; MICAL-1, molecule interacting with CasL 1; P, conserved cytoplasmic motif; RGD, Arg-Gly-Asp; RGM, repulsive guidance molecule; TSP1, thrombospondin 1; Unc5, uncoordinated locomotion-5 ; vWF, von Willebrand factor type D; ZU5, ZO-1 and Unc5-like.

evaluate a putative role for Lrig2 in mediating Neogenin receptor degradation. Overexpression of Lrig2 in N1E-115 neuroblastoma or COS-7 cells did not affect endogenous Neogenin levels (see Chapter 4). These preliminary results argue against a role for Lrig2 Neogenin receptor degradation, although further experiments in neurons are needed.

Interestingly, in COS-7 cell binding assays, overexpression of Lrig2 induced a strong reduction in the binding of RGMa to Neogenin. This may indicate that the association of Lrig2 with Neogenin blocks the binding of RGMa to Neogenin. However, this hypothesis is not supported by functional neurite outgrowth assays, in which short hairpin-mediated knockdown of Lrig2 blocks the neurite outgrowth-inhibiting effect of RGMa. If regulation of RGMa ligand binding would be the principal role of Lrig2 in regulating Neogenin function, depletion of Lrig2 in neurons would be predicted to enhance, instead of decrease, neurite outgrowth inhibition upon stimulation with RGMa. Therefore, it seems more likely that the reduction in RGMa ligand binding upon enhanced Lrig2 expression is mediated by the removal of Neogenin from the cell membrane by Lrig2-mediated endocytosis of the Neogenin receptor (Figure 3). Endocytosis is a common mechanism to inactivate ligand-induced receptor signaling in order to keep cells sensitive to signaling cues in the environment (O'Donnell *et al.* 2009). In axon guidance, endocytosis of receptor complexes upon ligand binding is an absolute requirement for ephrins and Sema3s to induce effective axon repulsive signaling (Castellani *et al.* 2004, Cowan *et al.* 2005). Whether activation of the Neogenin receptor by RGMa induces endocytosis of the Neogenin receptor has not been investigated. Thus, it will be interesting to reveal whether endocytosis of Neogenin is important for RGMa-Neogenin signaling and if so, if this process is dependent on Lrig2.

3.3 DOCK7 MEDIATES NEOGENIN-INDUCED NEURITE OUTGROWTH INHIBITION

The *in vivo* Neogenin pull down on *Syn-GFP-Neogenin* transgenic mouse brain lysates identified dedicator of cytokinesis 7 (Dock7) as a putative intracellular Neogenin-interacting protein (Chapter 5). We found that Neogenin and Dock7 are co-expressed in cortical neurons and that knockdown of Dock7 blocks RGMa-induced neurite growth inhibition. Dock7 belongs to the superfamily of Dock180-related proteins that function as activators of Rac and Cdc42 GTPases (Cote and Vuori 2002, Miyamoto and Yamauchi 2010). Dock7 has an important role in axon formation and in the establishment of neuronal polarity in cultured hippocampal neurons (Watabe-Uchida *et al.* 2006). In stage 2 hippocampal neurons Dock7 is selectively localized to the presumptive axon. Overexpression of Dock7 induces the formation of multiple axons, while depletion of Dock7 prevents axon formation (Watabe-Uchida 2006). Dock7 mediates neuronal polarity and axon formation by inducing activation of Rac, which leads to phosphorylation and inactivation of the microtubule destabilizing protein Op18/stathmin (Watabe-Uchida *et al.* 2006). Dock7 also functions in the ErbB2 signaling pathway promoting Schwann cell migration. Upon activation by neuregulin-1, ErbB2 binds and activates Dock7 by Tyr-1118 phosphorylation, thereby inducing activation of Rac1, Cdc42 and c-Jun N-terminal kinase (Yamauchi *et al.* 2008).

In a first attempt to elucidate Dock7 signaling mechanisms downstream of RGMa and Neogenin, we analyzed phosphorylation levels of Dock7 and of Op18/stathmin upon RGMa stimulation. Experiments in N1E-115 neuroblastoma cells did not reveal an effect of RGMa stimulation on Dock7 and Op18/stathmin phosphorylation (see Chapter 5). Although these experiments do not formally exclude the possibility that RGMa-Neogenin signaling in neurons might depend on changes in Dock7 and Op18/stathmin (Figure 3), they hint at the existence of other Dock7-dependent signaling mechanisms in the RGMa-Neogenin pathway.

A recent study showed an important role for Dock7 in neurogenesis and migration in the developing cortex, for which Cdc42 and Rac activation by Dock7 was dispensable (Yang *et al.* 2012). For its function in cortical development, Dock7 was found to interact with and antagonize the microtubule growth-promoting function of TACC3 (Yang *et al.* 2012). Recently two other novel Dock7-interacting proteins have been identified; myosin VI (Majewski *et al.* 2012) and molecule interacting with CasL (MICAL-1) (Y. Zhou and R.J. Pasterkamp, unpublished results), which are both modulators of the actin cytoskeleton. It will therefore be interesting to determine whether Dock7 mediates RGM-Neogenin repulsive signaling by binding to and signaling through TACC3, myosin VI and/or MICAL-1 (Figure 3).

Modulation of RhoA and Ras GTPase activity has been implicated in the RGMa-Neogenin signaling pathway. Activation of Neogenin signaling by RGMa activates RhoA and inhibits Ras (Endo and Yamashita 2009, Hata *et al.* 2006). Dock7 is an activator of two other GTPases: Rac and Cdc42 (Watabe-Uchida *et al.* 2006, Yamauchi *et al.* 2008). In general, activity of Rac and Cdc42 has been implicated in signaling pathways that mediate neurite extension. For example, Netrin-1-induced axon attraction by DCC signaling is mediated through activation of Rac and Cdc42 (Causeret *et al.* 2004, Li *et al.* 2002). Interestingly, a requirement for Dock180 has been revealed in Netrin-1-induced DCC signaling for the activation of Rac and Cdc42 (Li *et al.* 2008). Given the prominent role of small GTPases in RGM-Neogenin signaling it is possible that RGM-Neogenin-Dock7 signaling mediates neurite outgrowth inhibition by blocking Rac and Cdc42 activity (Figure 3). However, experiments in which DRG neurons were stimulated with RGMa did not reveal changes in the activity of Rac and Cdc42 (Conrad *et al.* 2007). Further work is needed to determine how Dock7 mediates the effects of RGMa and Neogenin during axon repulsion and neurite growth inhibition.

4 FINAL WORDS

In this thesis, I characterized the expression of RGMs and their Neogenin/Unc5 receptor complexes during mouse brain development and explored novel mechanisms of Neogenin signaling by characterizing several newly identified Neogenin signaling proteins. The broad, but specific expression patterns of RGMa, Neogenin and Unc5s indicate important and currently unexplored roles in neurogenesis, neuronal differentiation and migration in

different neuronal systems. The elucidation of prominent RGM and Neogenin expression and co-expression on axon bundles suggests a broader function for RGMs and Neogenin in axon guidance and bundle formation than previously shown. The identification of numerous putative Neogenin-interacting proteins with known functions in transcription regulation and apoptotic signaling is a valuable starting point for future studies to unravel the role of these pathways in Neogenin function during neural development. Furthermore, the identification of novel Neogenin signaling proteins that function in Neogenin-mediated neurite outgrowth inhibition, as shown for Lrig2 and Dock in this thesis, generates novel opportunities for the development of therapies to promote axon regeneration.

REFERENCE LIST

Andrusiak, M. G., K. A. McClellan, D. Dugal-Tessier, L. M. Julian, S. P. Rodrigues, D. S. Park, T. E. Kennedy, and R. S. Slack. 2011. Rb/E2F regulates expression of neogenin during neuronal migration. Mol. Cell Biol. 31:238-247.

Carvalho, R. F., M. Beutler, K. J. Marler, B. Knoll, E. Becker-Barroso, R. Heintzmann, T. Ng, and U. Drescher. 2006. Silencing of EphA3 through a *cis* interaction with ephrinA5. Nat. Neurosci. 9:322-330.

Castellani, V., J. Falk, and G. Rougon. 2004. Semaphorin3A-induced receptor endocytosis during axon guidance responses is mediated by L1 CAM. Mol. Cell Neurosci. 26:89-100.

Causeret, F., M. Hidalgo-Sanchez, P. Fort, S. Backer, M. R. Popoff, C. Gauthier-Rouviere, and E. Bloch-Gallego. 2004. Distinct roles of Rac1/Cdc42 and Rho/Rock for axon outgrowth and nucleokinesis of precerebellar neurons toward netrin 1. Development 131:2841-2852.

Chedotal, A. and L. J. Richards. 2010. Wiring the brain: the biology of neuronal guidance. Cold Spring Harb. Perspect. Biol. 2:a001917.

Conrad, S., H. Genth, F. Hofmann, I. Just, and T. Skutella. 2007. Neogenin-RGMa signaling at the growth cone is bone morphogenetic protein-independent and involves RhoA, ROCK, and PKC. J. Biol. Chem. 282:16423-16433.

Conrad, S., F. Stimpfle, S. Montazeri, J. Oldekamp, K. Seid, G. Alvarez-Bolado, and T. Skutella. 2010. RGMb controls aggregation and migration of Neogenin-positive cells *in vitro* and *in vivo*. Mol. Cell Neurosci. 43:222-231.

Cote, J. F. and K. Vuori. 2002. Identification of an evolutionarily conserved superfamily of DOCK180-related proteins with guanine nucleotide exchange activity. J. Cell Sci. 115:4901-4913.

Cowan, C. W., Y. R. Shao, M. Sahin, S. M. Shamah, M. Z. Lin, P. L. Greer, S. Gao, E. C. Griffith, J. S. Brugge, and M. E. Greenberg. 2005. Vav family GEFs link activated Ephs to endocytosis and axon guidance. Neuron 46:205-217.

Culver-Hanlon, T. L., S. A. Lex, A. D. Stephens, N. J. Quintyne, and S. J. King. 2006. A microtubule-binding domain in dynactin increases dynein processivity by skating along microtubules. Nat. Cell Biol. 8:264-270.

Endo, M. and T. Yamashita. 2009. Inactivation of Ras by p120GAP via focal adhesion kinase dephosphorylation mediates RGMa-induced growth cone collapse. J. Neurosci. 29:6649-6662.

Fitzgerald, D. P., S. J. Cole, A. Hammond, C. Seaman, and H. M. Cooper. 2006. Characterization of neogenin-expressing neural progenitor populations and migrating neuroblasts in the embryonic mouse forebrain. Neuroscience 142:703-716.

Fujita, Y., J. Taniguchi, M. Uchikawa, M. Endo, K. Hata, T. Kubo, B. K. Mueller, and T. Yamashita. 2008. Neogenin regulates neuronal survival through DAP kinase. Cell Death. Differ. 15:1593-1608.

Gad, J. M., S. L. Keeling, A. F. Wilks, S. S. Tan, and H. M. Cooper. 1997. The expression patterns of guidance receptors, DCC and Neogenin, are spatially and temporally distinct throughout mouse embryogenesis. Dev. Biol. 192:258-273.

Gallarda, B. W., D. Bonanomi, D. Muller, A. Brown, W. A. Alaynick, S. E. Andrews, G. Lemke, S. L. Pfaff, and T. Marquardt. 2008. Segregation of axial motor and sensory pathways via heterotypic trans-axonal signaling. Science 320:233-236.

Goldschneider, D., N. Rama, C. Guix, and P. Mehlen. 2008. The neogenin intracellular domain regulates gene transcription via nuclear translocation. Mol. Cell Biol. 28:4068-4079.

Guirland, C., S. Suzuki, M. Kojima, B. Lu, and J. Q. Zheng. 2004. Lipid rafts mediate chemotropic guidance of nerve growth cones. Neuron 42:51-62.

Gur, G., C. Rubin, M. Katz, I. Amit, A. Citri, J. Nilsson, N. Amariglio, R. Henriksson, G. Rechavi, H. Hedman, R. Wides, and Y. Yarden. 2004. LRIG1 restricts growth factor signaling by enhancing receptor ubiquitylation and degradation. EMBO J. 23:3270-3281.

Haklai-Topper, L., G. Mlechkovich, D. Savariego, I. Gokhman, and A. Yaron. 2010. *Cis* interaction between Semaphorin6A and Plexin-A4 modulates the repulsive response to Sema6A. EMBO J. 29:2635-2645.

Harwood, A. and V. M. Braga. 2003. Cdc42 & GSK-3: signals at the crossroads. Nat. Cell Biol. 5:275-277.

Hata, K., M. Fujitani, Y. Yasuda, H. Doya, T. Saito, S. Yamagishi, B. K. Mueller, and T. Yamashita. 2006. RGMa inhibition promotes axonal growth and recovery after spinal cord injury. J. Cell Biol. 173:47-58.

Hata, K., K. Kaibuchi, S. Inagaki, and T. Yamashita. 2009. Unc5B associates with LARG to mediate the action of repulsive guidance molecule. J. Cell Biol. 184:737-750.

Hedman, H. and R. Henriksson. 2007. LRIG inhibitors of growth factor signalling - double-edged swords in human cancer? Eur. J. Cancer 43:676-682.

Herincs, Z., V. Corset, N. Cahuzac, C. Furne, V. Castellani, A. O. Hueber, and P. Mehlen. 2005. DCC association with lipid rafts is required for netrin-1-mediated axon guidance. J. Cell Sci. 118:1687-1692.

Homma, S., T. Shimada, T. Hikake, and H. Yaginuma. 2009. Expression pattern of LRR and Ig domain-containing protein (LRRIG protein) in the early mouse embryo. Gene Expr. Patterns. 9:1-26.

Hornberger, M. R., D. Dutting, T. Ciossek, T. Yamada, C. Handwerker, S. Lang, F. Weth, J. Huf, R. Wessel, C. Logan, H. Tanaka, and U. Drescher. 1999. Modulation of EphA receptor function by coexpressed ephrinA ligands on retinal ganglion cell axons. Neuron 22:731-742.

Hu, H. 1999. Chemorepulsion of neuronal migration by Slit2 in the developing mammalian forebrain. Neuron 23:703-711.

Kubo, T., M. Endo, K. Hata, J. Taniguchi, K. Kitajo, S. Tomura, A. Yamaguchi, B. K. Mueller, and T. Yamashita. 2008. Myosin IIA is required for neurite outgrowth inhibition produced by repulsive guidance molecule. J.

Neurochem. 105:113-126.

Laederich, M. B., M. Funes-Duran, L. Yen, E. Ingalla, X. Wu, K. L. Carraway, III, and C. Sweeney. 2004. The leucine-rich repeat protein LRIG1 is a negative regulator of ErbB family receptor tyrosine kinases. J. Biol. Chem. 279:47050-47056.

Lah, G. J. and B. Key. 2012. Novel roles of the chemorepellent axon guidance molecule RGMa in cell migration and adhesion. Mol. Cell Biol. 32:968-980.

Ledda, F., O. Bieraugel, S. S. Fard, M. Vilar, and G. Paratcha. 2008. Lrig1 is an endogenous inhibitor of Ret receptor tyrosine kinase activation, downstream signaling, and biological responses to GDNF. J. Neurosci. 28:39-49.

Li, X., X. Gao, G. Liu, W. Xiong, J. Wu, and Y. Rao. 2008. Netrin signal transduction and the guanine nucleotide exchange factor DOCK180 in attractive signaling. Nat. Neurosci. 11:28-35.

Li, X., M. Meriane, I. Triki, M. Shekarabi, T. E. Kennedy, L. Larose, and N. Lamarche-Vane. 2002. The adaptor protein Nck-1 couples the netrin-1 receptor DCC (deleted in colorectal cancer) to the activation of the small GTPase Rac1 through an atypical mechanism. J. Biol. Chem. 277:37788-37797.

Majewski, L., M. Sobczak, S. Havrylov, J. Jozwiak, and M. J. Redowicz. 2012. Dock7: A GEF for Rho-family GTPases and a novel myosin VI-binding partner in neuronal PC12 cells. Biochem. Cell Biol. 90: 565-574.

Matsunaga, E., H. Nakamura, and A. Chedotal. 2006. Repulsive guidance molecule plays multiple roles in neuronal differentiation and axon guidance. J. Neurosci. 26:6082-6088.

Matsunaga, E., S. Tauszig-Delamasure, P. P. Monnier, B. K. Mueller, S. M. Strittmatter, P. Mehlen, and A. Chedotal. 2004. RGM and its receptor neogenin regulate neuronal survival. Nat. Cell Biol. 6:749-755.

Miyamoto, Y. and J. Yamauchi. 2010. Cellular signaling of Dock family proteins in neural function. Cell Signal. 22:175-182.

Muramatsu, R., T. Kubo, M. Mori, Y. Nakamura, Y. Fujita, T. Akutsu, T. Okuno, J. Taniguchi, A. Kumanogoh, M. Yoshida, H. Mochizuki, S. Kuwabara, and T. Yamashita. 2011. RGMa modulates T cell responses and is involved in autoimmune encephalomyelitis. Nat. Med. 17:488-494.

Nguyen-Ba-Charvet, K. T., N. Picard-Riera, M. Tessier-Lavigne, E. A. Baron-Van, C. Sotelo, and A. Chedotal. 2004. Multiple roles for slits in the control of cell migration in the rostral migratory stream. J. Neurosci. 24:1497-1506.

O'Donnell, M., R. K. Chance, and G. J. Bashaw. 2009. Axon growth and guidance: receptor regulation and signal transduction. Annu. Rev. Neurosci. 32:383-412.

Oldekamp, J., N. Kramer, G. Alvarez-Bolado, and T. Skutella. 2004. Expression pattern of the repulsive guidance molecules RGM A, B and C during mouse development. Gene Expr. Patterns. 4:283-288.

Samad, T. A., A. Srinivasan, L. A. Karchewski, S. J. Jeong, J. A. Campagna, R. R. Ji, D. A. Fabrizio, Y. Zhang, H. Y. Lin, E. Bell, and C. J. Woolf. 2004. DRAGON: a member of the repulsive guidance molecule-related family of neuronal- and muscle-expressed membrane proteins is regulated by DRG11 and has neuronal adhesive properties. J. Neurosci. 24:2027-2036.

Shattuck, D. L., J. K. Miller, M. Laederich, M. Funes, H. Petersen, K. L. Carraway, III, and C. Sweeney. 2007. LRIG1 is a novel negative regulator of the Met receptor and opposes Met and Her2 synergy. Mol. Cell Biol. 27:1934-1946.

Suzuki, Y., N. Sato, M. Tohyama, A. Wanaka, and T. Takagi. 1996. cDNA cloning of a novel membrane glycoprotein that is expressed specifically in glial cells in the mouse brain. LIG-1, a protein with leucine-rich repeats and immunoglobulin-like domains. J. Biol. Chem. 271:22522-22527.

van Haren, J., K. Draegestein, N. Keijzer, J. P. Abrahams, F. Grosveld, P. J. Peeters, D. Moechars, and N. Galjart. 2009. Mammalian Navigators are microtubule plus-end tracking proteins that can reorganize the cytoskeleton to induce neurite-like extensions. Cell Motil. Cytoskeleton 66:824-838.

Watabe-Uchida, M., K. A. John, J. A. Janas, S. E. Newey, and A. L. Van Aelst. 2006. The Rac activator DOCK7 regulates neuronal polarity through local phosphorylation of stathmin/Op18. Neuron 51:727-739.

Wilkinson, S., H. F. Paterson, and C. J. Marshall. 2005. Cdc42-MRCK and Rho-ROCK signalling cooperate in myosin phosphorylation and cell invasion. Nat. Cell Biol. 7:255-261.

Wu, W., K. Wong, J. Chen, Z. Jiang, S. Dupuis, J. Y. Wu, and Y. Rao. 1999. Directional guidance of neuronal migration in the olfactory system by the protein Slit. Nature 400:331-336.

Xia, Y., J. L. Babitt, R. Bouley, Y. Zhang, S. N. Da, S. Chen, Z. Zhuang, T. A. Samad, G. J. Brenner, J. L. Anderson, C. C. Hong, A. L. Schneyer, D. Brown, and H. Y. Lin. 2010. Dragon enhances BMP signaling and increases transepithelial resistance in kidney epithelial cells. J. Am. Soc. Nephrol. 21:666-677.

Yamauchi, J., Y. Miyamoto, J. R. Chan, and A. Tanoue. 2008. ErbB2 directly activates the exchange factor Dock7 to promote Schwann cell migration. J. Cell Biol. 181:351-365.

Yang, Y. T., C. L. Wang, and A. L. Van Aelst. 2012. DOCK7 interacts with TACC3 to regulate interkinetic nuclear migration and cortical neurogenesis. Nat. Neurosci. 15:1201-1210.

Zhang, A. S., F. Yang, J. Wang, H. Tsukamoto, and C. A. Enns. 2009. Hemojuvelin-neogenin interaction is required for bone morphogenic protein-4-induced hepcidin expression. J. Biol. Chem. 284:22580-22589.

Zhao, H., K. Tanegashima, H. Ro, and I. B. Dawid. 2008. Lrig3 regulates neural crest formation in *Xenopus* by modulating Fgf and Wnt signaling pathways. Development 135:1283-1293.

Zhou, Z., J. Xie, D. Lee, Y. Liu, J. Jung, L. Zhou, S. Xiong, L. Mei, and W. C. Xiong. 2010. Neogenin regulation of BMP-induced canonical Smad signaling and endochondral bone formation. Dev. Cell 19:90-102.

Zhu, X. J., C. Z. Wang, P. G. Dai, Y. Xie, N. N. Song, Y. Liu, Q. S. Du, L. Mei, Y. Q. Ding, and W. C. Xiong. 2007. Myosin X regulates netrin receptors and functions in axonal path-finding. Nat. Cell Biol. 9:184-192.

ADDENDUM

CURRICULUM VITAE

LIST OF PUBLICATIONS

SAMENVATTING IN HET NEDERLANDS

DANKWOORD

CURRICULUM VITAE

Dianne van den Heuvel is geboren op 10 september 1983 te Tiel. In 2001 behaalde zij haar VWO diploma (Atheneum met profiel Natuur en Gezondheid) aan het ORS Lek en Linge te Culemborg. In datzelfde jaar begon zij met de studie Biologie aan de Wageningen Universiteit. Na afronding van de bachelor Celbiologie in 2004 (*cum laude*), vervolgde zij haar opleiding met de gelijknamige master. Gedurende deze master heeft Dianne onderzoek gedaan naar de ontwikkeling van een gestandaardiseerde test waarin transgene fruitvlieglarven (*Drosophila*) worden gebruikt om stoffen met antioxidant eigenschappen te identificeren. Dit onderzoek is uitgevoerd bij Plant Research International (PRI, Wageningen Universiteit) onder supervisie van Dr. Maarten Jongsma (PRI) en Dr. Joop van Loon (vakgroep Entomologie, Wageningen Universiteit). Vervolgens deed zij een onderzoeksproject onder begeleiding van Dr. Jeroen Pasterkamp in het Rudolf Magnus Instituut voor Neurowetenschappen (Universitair Medisch Centrum (UMC) Utrecht) naar de signaaltransductie cascade van Plexin-A4. Na afronding van de master Celbiologie in 2006 (*cum laude*) begon zij aan haar promotieonderzoek in de onderzoeksgroep van Dr. Jeroen Pasterkamp, naar de functie en signaaltransductie van Repulsive Guidance Molecule/Neogenin tijdens de neuronale ontwikkeling. De resultaten van dit onderzoek staan beschreven in dit proefschrift. Sinds mei 2012 is Dianne werkzaam als postdoc onderzoeker in het UMC Utrecht en doet zij in de onderzoeksgroep van Prof. Dr. Leonard van den Berg (Experimentele Neurologie) onderzoek naar de motor neuron ziekte amyotrofe laterale sclerose (ALS).

Dianne van den Heuvel was born on September 10th in Tiel, the Netherlands. After graduating secondary school (Atheneum, ORS Lek en Linge, Culemborg) in 2001, she became a Biology student at the Wageningen University. After obtaining her bachelor-degree Cell Biology (*cum laude*) in 2004, she continued with the master Cell Biology at the same university. During her master she performed two scientific research projects. The aim of the first research project was to develop an *in vivo Drosophila*-based screening assay for antioxidant compounds. This study was executed at the research institute Plant Research International (PRI, Wageningen University) under supervision of Dr. Maarten Jongsma (PRI) en Dr. Joop van Loon (Entomology, Wageningen University). During her second research project under supervision of Dr. Jeroen Pasterkamp she investigated the Plexin-A4 signaling cascade at the Rudolf Magnus Institute of Neuroscience (University Medical Center (UMC) Utrecht). After obtaining her master degree (*cum laude*) in 2006, she started as a PhD student in the research group of Dr. Jeroen Pasterkamp studying Repulsive Guidance Molecule/Neogenin function and signaling during neural development. The results of this research project are presented in this thesis. In May 2012, Dianne started working as postdoctoral research fellow in the research group of Prof. Dr. Leonard van den Berg (Experimental Neurology, UMC Utrecht) on the motor neuron disease amyotrophic lateral sclerosis (ALS).

LIST OF PUBLICATIONS

De Backer, M.W., M.A. Brans, M.C. Luijendijk, K.M. Garner, **D.M.A van den Heuvel**, R.J. Pasterkamp and R.A. Adan. 2010. Neuropeptide delivery to the brain: a von Willebrand factor signal peptide to direct neuropeptide secretion. BMC Neuroscience. 11:94.

Kolk, S.M., R.A. Gunput, T. S. Tran, **D.M.A. van den Heuvel**, A.A. Prasad, A.J.C.G.M. Hellemons, Y. Adolfs, D.D. Ginty, A. L. Kolodkin, J.P. Burbach, M.P. Smidt and R.J. Pasterkamp. 2009. Semaphorin 3F is a bifunctional guidance cue for dopaminergic axons and controls their fasciculation, channeling, rostral growth, and intracortical targeting. The Journal of Neuroscience. 29:12542-12557.

Van den Heuvel, D.M.A. and R.J. Pasterkamp. 2008. Getting connected in the dopamine system. Progress in Neurobiology. 85:75-93.

Van den Heuvel, D.M.A., A.J.C.G.M. Hellemons and R.J. Pasterkamp. 2013 Spatiotemporal expression of repulsive guidance molecules (RGMs) and their receptor Neogenin in the mouse brain. PLOS ONE (*in press*).

Groen, E.J.N, K. Fumoto, A.M. Blokhuis, J. Engelen-Lee, Y. Zhou, **D.M.A van den Heuvel**, M. Koppers, F. van Diggelen, J. van Heest, J.A.A. Demmers, J. Kirby, P.J. Shaw, E. Aronica, W.G.M. Spliet, J.H. Veldink, L.H. van den Berg and R.J. Pasterkamp. 2013 ALS-associated mutations in FUS disrupt the axonal distribution and function of SMN1. S*ubmitted to* Human Molecular Genetics.

SAMENVATTING IN HET NEDERLANDS

De ontwikkeling van het zenuwstelsel tot een netwerk van miljoenen zenuwcellen en een veelvoud aan zenuwverbindingen wordt nauwkeurig gereguleerd door verschillende cellulaire processen. Neogenin en Repulsive Guidance Molecules (RGMs) spelen een belangrijke rol in de ontwikkeling van het zenuwstelsel. Neogenin is een receptor die voorkomt op zenuwvezels en de aanwezigheid van RGM signaalstoffen remt de groei van deze zenuwvezels. Op deze manier reguleren RGMs en Neogenin de groei en ontwikkeling van zenuwbanen. Naast de vorming van zenuwbanen zijn Neogenin en RGMs ook betrokken bij andere processen tijdens de neuronale ontwikkeling, zoals neurogenese, neuronale differentiatie, migratie en gereguleerde celdood (zie **hoofdstuk 1**).

Op dit moment is onze kennis over de rol van Neogenin en RGMs tijdens de ontwikkeling van het zenuwstelsel beperkt. Daarnaast is er weinig bekend over de signaaltransductie cascades die door Neogenin worden gebruikt om zenuwgroei te remmen. Het onderzoek beschreven in dit proefschrift is gericht op het vergroten van onze kennis over de functie en signaaltransductie van Neogenin en RGMs tijdens de neuronale ontwikkeling, door 1) een analyse van Neogenin, RGM en Unc5 coreceptor expressie tijdens de ontwikkeling van het muizenbrein, en 2) door het identificeren van Neogenin interactoren die een rol hebben in de Neogenin signaaltransductie cascade.

Een beter inzicht in de regulatie van ontwikkelingsprocessen door Neogenin en RGMs tijdens de ontwikkeling van het zenuwstelsel is belangrijk, omdat verstoring van deze processen kan bijdragen aan het ontstaan van ontwikkelingsstoornissen, zoals autisme en schizofrenie (zie **hoofdstuk 2**). Daarnaast is de regulatie van zenuwgroei door RGMs en Neogenin niet alleen belangrijk voor de ontwikkeling van zenuwbanen, maar heeft ook een belangrijke rol in het blokkeren van zenuwgroei na schade aan het volwassen zenuwstelsel, zoals bijvoorbeeld bij een dwarslaesie. Na ruggenmergletsel neemt de hoeveelheid RGM toe, waardoor zenuwgroei wordt geremd en daarmee het herstel van beschadigde zenuwbanen. Naast een rol voor RGMs en Neogenin in zenuwregeneratie, spelen deze eiwitten ook een rol in ziekten zoals multiple sclerose, de ziekte van Alzheimer en de ziekte van Parkinson (zie **hoofdstuk 1**).

In de expressiestudie beschreven in **hoofdstuk 3** is met behulp van RNA *in situ* hybridisatie en immunohistochemie de expressie van RGMa/b, Neogenin en Unc5A-D tijdens de ontwikkeling van de hersenen in de muis onderzocht. *In situ* hybridisatie detecteerde de expressie van deze eiwitten in cellagen door specifieke aankleuring van RNA in de cellichamen. Immunohistochemie toonde de expressie van deze eiwitten aan in cellichamen en in zenuwuitlopers door middel van specifieke antilichaamkleuringen. In deze studie is gekeken naar de expressie van RGMa/b, Neogenin en Unc5A-D op drie verschillende leeftijden: in muizenembryo's van 16,5 dagen oud (E16.5), in pasgeboren muizen van vijf dagen oud (P5) en in volwassen muizen (adult). De expressie van deze moleculen is in detail bestudeerd

in vijf verschillende hersengebieden: het olfactorisch systeem, de cortex, hippocampus, habenula en het cerebellum. De expressie analyse toonde een brede expressie aan van RGMs, Neogenin and Unc5s op alle onderzochte leeftijden. *In situ* hybridisatie toonde specifieke expressiepatronen van deze eiwitten in cellagen en structuren van de onderzochte hersengebieden. Immunohistochemie detecteerde prominente expressie van RGMa, RGMb en Neogenin op verschillende zenuwbanen. De brede en specifieke expressiepatronen van RGMa/b, Neogenin en Unc5A-D in de verschillende hersengebieden duiden op een rol voor deze eiwitten in neuronale ontwikkelingsprocessen zoals differentiatie en migratie. Daarnaast geven de verschillende, maar ook deels overlappende, expressiepatronen van Unc5A-D aan, dat Neogenin voor specifieke functies tijdens de neuronale ontwikkeling een receptor complex zou kunnen vormen met verschillende Unc5 coreceptoren. De sterke expressie van RGMa en RGMb op zenuwbanen geeft een aanwijzing dat RGMs, naast het reguleren van zenuwgroei als remmende factoren in de omgeving, ook een rol zouden kunnen spelen in de organisatie en adhesie van zenuwbanen.

De gedetailleerde analyse van RGM, Neogenin en Unc5 expressie in deze studie vormt een belangrijke basis voor toekomstig onderzoek naar de rol van deze eiwitten in de ontwikkeling van verschillende hersengebieden.

Onze huidige kennis van de Neogenin signaaltransductie cascade geactiveerd door RGMa is zeer beperkt. Eerder onderzoek heeft laten zien dat de aanwezigheid van Unc5 coreceptoren in het Neogenin receptor complex essentieel is voor de activatie van RhoA en inactivatie van Ras. Om een beter inzicht te krijgen in de signaaltransductie cascade die wordt geactiveerd door Neogenin werden in deze studie Neogenin receptor complexen gezuiverd en geanalyseerd in twee verschillende proteomics screens voor Neogenin interactoren. In **hoofdstuk 4** hebben we in een humane fibroblast (HEK293) cellijn met endogene Neogenin expressie, ook Neogenin met een biotine label tot expressie gebracht en opgezuiverd. Daarnaast hebben we, zoals in **hoofdstuk 5** beschreven, GFP-Neogenin geïsoleerd uit hersenlysaat van jonge *Syn-GFP-Neogenin* muizen. Bij deze transgene muizen brengt de synapsin I promoter GFP-gelabeled Neogenin specifiek in zenuwcellen tot expressie. De analyse van de Neogenin receptor complexen in beide proteomics screens door middel van massaspectrometrie identificeerde 80 nieuwe Neogenin interactoren die een rol kunnen spelen bij de regulatie van zenuwgroei door Neogenin. Daarnaast kunnen deze nieuwe Neogenin interactoren ook onze kennis vergroten van Neogenin functies in andere neuronale processen, gezien de bekende rol van een aantal nieuwe Neogenin interactoren in de organisatie van het cytoskelet, migratie, gereguleerde celdood en gentranscriptie.

In deze studie zijn twee nieuwe Neogenin interactoren, Lrig2 en Dock7, in meer detail onderzocht. Immunohistochemie en immunoprecipitatie experimenten toonden de *in vivo* interactie tussen Neogenin en respectievelijk Lrig2 en Dock7 in hersenweefsel. Met behulp van

functionele uitgroei experimenten van zenuwcellen bewijzen we dat Lrig2 en Dock7 essentieel zijn voor het remmen van zenuwgroei door RGMs (zie **hoofdstuk 4 en 6**).

Lrigs zijn transmembraaneiwitten en vooral bekend als remmers van groeifactor receptor activiteit. Er is op dit moment zeer weinig kennis over de rol van Lrigs tijdens de ontwikkeling van het zenuwstelsel. Met behulp van RNA *in situ* hybridisatie tonen wij aan dat de verschillende Lrig eiwitten, Lrig1, -2 en -3, tot expressie komen in de embryonale muizenhersenen. Lrig2 komt het sterkst tot expressie en er is ook duidelijke co-expressie van Lrig2 en Neogenin in verschillende hersenstructuren, zoals bijvoorbeeld de cortex.

Lrigs remmen groeifactor receptor activiteit door afbraak van deze receptoren te induceren of de lokalisatie van de receptoren naar lipid rafts, signaaltransductie hotspots in het celmembraan, te blokkeren. In experimenten waarin Lrig2 tot overexpressie werd gebracht in een N1E-115 neuroblastoma cellijn vonden wij geen verandering in het expressieniveau van Neogenin. Wel vonden we een reductie in binding van RGMa aan Neogenin in cellen die Lrig2 tot overexpressie brachten (zie **hoofdstuk 4**). Deze resultaten tonen aan dat Lrig2 de binding van RGMs aan Neogenin kan reguleren.

De rol van Lrig2 in RGMa-Neogenin signaaltransductie die leidt tot de inhibitie van zenuwgroei is op dit moment nog onbekend. Lrig2 zou een rol kunnen spelen in de lokalisatie van Neogenin in lipid rafts in het celmembraan, wat een vereiste zou kunnen zijn voor de activatie van de Neogenin signaaltransductie cascade die zenuwgroei blokkeert. Anderzijds zou Lrig2 ook een rol kunnen spelen in de beëindiging van Neogenin signaaltransductie door endocytose van Neogenin te induceren na activatie van Neogenin door RGMa (zie **hoofdstuk 7**).

Dock7 is een activator van Cdc42 en Rac GTPases en heeft een rol in verschillende processen tijdens de ontwikkeling van het zenuwstelsel, zoals neurogenese, celpolariteit, de vorming van zenuwvezels, migratie en myelinisatie. Daarnaast reguleert Dock7 de groei van het microtubuli cytoskelet door de activiteit van het microtubuli destabiliserend eiwit Op18/stathmin te reguleren. In experimenten waarin N1E-115 neuroblastoma cellen gestimuleerd werden met RGMa, vonden we geen effect op de fosforylering van Op18/stathmin als van Dock7 zelf (zie **hoofdstuk 6**). Hoewel de rol van Dock7 in RGMa-Neogenin gereguleerde remming van zenuwgroei op dit moment niet bekend is, zou Dock7 de afbraak van het celcytoskelet kunnen induceren door de activiteit van Cdc42 of Rac, of van de Dock7 interactoren TACC3, myosin VI en MICAL-1, die bekende regulatoren zijn van het cytoskelet, te reguleren (zie **hoofdstuk 7**).

Deze studie laat zien dat twee nieuwe Neogenin interactoren, Lrig2 en Dock7, essentieel zijn voor het remmen van zenuwgroei door RGMs. Meer onderzoek is nodig om de rol van Lrig2 en Dock7 in de RGMa-Neogenin signaaltransductie cascade op te helderen. Daarnaast is de identificatie van talrijke andere Neogenin interactoren in deze studie een waardevol

uitgangspunt voor toekomstige studies naar de functie en signaaltransductie van Neogenin in verschillende neuronale processen. De identificatie van Neogenin interactoren die een rol hebben in het remmen van zenuwgroei door Neogenin, zoals Lrig2 en Dock7, vormt nieuwe aanknopingspunten voor de ontwikkeling van een therapie voor de behandeling van zenuwletsel.

DANKWOORD

En dan is dit de plek waar ik graag een aantal mensen wil bedanken!

Allereerst mijn begeleider en co-promotor **Jeroen Pasterkamp**. Toen ik als MSc student bij jou mijn tweede stage kwam doen grapten een aantal collega's dat de Pasterkamp groep verdubbeld was. Afgelopen jaren is je onderzoeksgroep flink gegroeid en heb ik je leren kennen als een enorm ambitieuze en talentvolle onderzoeker! Ik ben erg blij dat ik de mogelijkheid heb gekregen om in jouw groep een aio-project te kunnen doen. Het was erg uitdagend om een nieuw project te beginnen en ik heb afgelopen jaren heel veel geleerd. Ik had nooit zover kunnen komen zonder jouw enthousiasme, betrokkenheid en motivatie. Je goede begeleiding kenmerkte zich onder andere in een kamerdeur die bijna altijd openstond, presentaties die in het begin best een keer voor jou geoefend mochten worden en de wonderbaarlijke snelheid waarmee jij benodigdheiden voor het onderzoek kon regelen. Het mooie is dat ik je op dit moment weer wekelijks spreek over mijn onderzoeksprojecten in een samenwerkingsverband met de groep van Leonard van den Berg.

Peter Burbach, mijn promotor. Peter, bedankt voor je steun en betrokkenheid afgelopen jaren. Je positieve instelling en rustige persoonlijkheid heb ik erg kunnen waarderen. Bedankt ook voor het kritisch doorlezen van alle hoofdstukken en je steun en advies tijdens het afronden van mijn proefschrift.

De leden van de leescommissie, **Prof. Dr. Burbach, Prof. Dr. Geijsen, Prof. Dr. Klumperman, Prof. Dr. van den Berg en Prof. Dr. Verhaagen**, wil ik graag bedanken voor het beoordelen van mijn manuscript.

Anita Hellemons. Ik weet nog hoe blij ik was toen jij als analist mee ging werken aan mijn project. Er liepen op dat moment veel verschillende projecten en jouw hulp bij *in situ* hybridisatie en immunohistochemie experimenten kwam als een geschenk uit de hemel. Hoewel wij vonden dat de kleuringen best goed lukten in het begin, hebben we in de loop van de tijd de protocollen nog flink kunnen optimaliseren, waardoor ze nog veel mooier zijn geworden! Al die uren coupes snijden, kleuren en fotograferen is beloond met een publicatie in PLOS ONE, waarin veel van onze mooie plaatjes te zien zijn! Naast je hulp bij de expressiepaper heb je aan heel veel andere experimenten in dit proefschrift bijgedragen. En met veel enthousiasme. Je was altijd bereid een extra sample of glaasje mee te nemen, ook al kon ik niet altijd duidelijk uitleggen waarom dat nu echt nodig was. Daarnaast ben je ook nog eens heel kritisch op de kwaliteit van je werk. Het is je niet snel te veel. Naast het doen van allerlei experimenten maak je ook nog tijd voor een praatje of om mij even (naast de cryostaat)

de perfecte schaatstechniek te demonstreren. Sinds september heb je er een uitdaging bij: een deeltijd HBO studie Voeding en Diëtetiek, en zit je weer in de collegebanken en in allerlei werkgroepjes. Ik heb er veel bewondering voor dat je deze uitdaging bent aangegaan en ik ben er van overtuigd dat je het tot een succes zult maken. Voor mij was het niet meer dan vanzelfsprekend om jou als paranimf te vragen voor mijn verdediging.

Iedereen van de Pasterkamp groep. De eerste 'lichting' aio's: Yeping, Rou-Afza en Asheeta. **Asheeta**, thanks for all nice talks and discussions. **Yeping**, your comforting words in the protein lab 'aah that doesn't look too bad' always made me feel better when you found me staring in despair at a difficult to interpret, messy, Western blot film. **Rou-Afza**, wij hebben samen alle facetten van het aio-schap beleefd. Mooie jaren waren het, hoewel er soms ook flinke kuilen in de weg zaten. Met jouw enthousiasme voor de wetenschap, werklust, doorzettingsvermogen en gevoel voor humor heb je alles tot een goed einde weten te brengen! Ik weet zeker dat deze eigenschappen je ook goed van pas komen bij je postdoc baan in Plymouth/Exeter. Echt super dat je overkomt om mij bij te staan tijdens mijn verdediging als paranimf!

Sharon en Alwin, bedankt voor alle nuttige adviezen en support tijdens de eerste jaren!

Fumo, I really enjoyed sharing a bench with you, while both of us were doing IP work.

Youri, bedankt voor alle hulp op zowel de 4e als 5e verdieping!

Eljo, Ewoud, Anna, Koushik, Bart, Ewout, Liset, Francesca, Sara, Max and Vamshi thanks for all the nice talks and discussions about science.

Susan, ik ben erg blij dat jij verder bent gegaan met het Lrig2 project. Jouw talent voor onderzoek heeft ook bij dit project al mooie resultaten opgeleverd!

Ewoud, Amila en Karin. Bedankt voor jullie bijdrage aan dit onderzoek als stagestudenten.

Leo, bedankt voor alle hulp op het lab en ook voor het tot tweemaal toe wegbrengen van gewonde vogels naar de vogelopvang! :-)

Alle kamergenootjes door de jaren heen. **Marijke M.-de B.**, wij hebben in de loop van de jaren een heel goede vriendschap opgebouwd! **Linda**, naast een heel gezellige meid ben je een heel serieuze onderzoeker met een enorm werktempo. Gelukkig ben ik je toch nét voor weten te blijven. ;-) **Myrte**, het werk in het weekend was een stuk leuker als ik jou, vaak in je hardlooptenue, achter de computer aantrof en we tussendoor wat konden kletsen en we alle

etenswaar die we bij ons hadden deelden voor de lunch. Het weekendje in Oxford was super! **Marijke A.**, jij hebt een grote passie voor onderzoek. Veel succes met alle experimenten de komende tijd!

Anup, fridaynight ice skating was great fun and a great relief in the busy final year of my PhD!

Alle analisten van de 4e en 5e verdieping. **Henk, Marina, Marjolein, Keith, Rea, Inge, Lars en Raymond**. Zonder jullie zouden de labs niet zo goed georganiseerd zijn! Daarnaast kan je bij jullie altijd terecht met technische vragen.

Ria, Joke, Krista, Sandra en Vicki, bedankt voor de administratieve ondersteuning!

Netty, heel erg bedankt voor het layouten van mijn proefschrift. Zonder jouw hulp had deze er een heel stuk saaier uitgezien!

Gwen, Fedor, Erica, Minou, Krispijn, Gijs en Kim. Jullie vriendschappen zijn heel waardevol voor me! Naast dat we best ook wel eens serieuze gesprekken voeren, hebben we vooral heel veel lol met zijn allen!

Astrid, laten we snel weer afspreken om binnenkort samen te eten en bij te praten.

Bas, onze goede gesprekken tijdens mooie wandelingen heb ik erg kunnen waarderen afgelopen jaren!

De jaarclub. Fabianne, Roseri, Anne Marie en Ellis. Een jarenlange vriendschap. We zien elkaar niet heel vaak, maar als we afspreken is het altijd super gezellig en heerlijk bijkletsen!

IJmkje, als je over bent uit Engeland hebben we altijd veel bij te praten en dat kan altijd prima gecombineerd worden met een mooie wandeling op de dijk of in de uiterwaarden. Aan de kleine week die we samen in en rond Stockholm hebben doorgebracht, nadat ik naar een congres was geweest in het noorden van Zweden, heb ik goede herinneringen!

Opa en Oma. Ja hoor, de studie is klaar! Heel erg bedankt voor jullie steun door de jaren heen.

Martine, Martin, Tessa en Alex, bedankt voor jullie steun en lieve kaartjes! Een dagje in de Noordoostpolder staat altijd garant voor veel plezier en ontspanning!

Lieve **Rob**, bedankt voor de fijne tijd samen en alle ontspanning!

Mijn ouders. Pap, mam, ik ben heel dankbaar voor de mogelijkheden en vrijheid die jullie mij hebben gegeven om mij te ontwikkelen tot wie ik nu ben. Jullie doorzettingsvermogen, energie en enthousiasme is altijd een voorbeeld voor mij geweest! Bedankt voor jullie onvoorwaardelijke steun en alle goede gesprekken!